Radboud Repository

Radboud University Nijmegen

PDF hosted at the Radboud Repository of the Radboud University Nijmegen

The following full text is a publisher's version.

For additional information about this publication click this link.
http://hdl.handle.net/2066/19147

Please be advised that this information was generated on 2017-12-05 and may be subject to change.

The human RNase MRP complex

Composition, assembly and role in human disease

Hans van Eenennaam

The human RNase MRP complex

Composition, assembly and role in human disease

Hans van Eenennaam, 2002

Cover illustration

Statue of the Dwarf Seneb and his family, painted limestone, height 34 cm, width 22.5 cm, Giza, Tomb of Seneb, Late Fifth - Early Sixth Dynasty.

From: The Cairo museum Masterpieces of Egyptian Art, Francesco Tiradritti, Thames & Hudson Ltd, London, 1998

The human RNase MRP complex

Composition, assembly and role in human disease

een wetenschappelijke proeve op het gebied van de
Natuurwetenschappen, Wiskunde en Informatica

PROEFSCHRIFT

ter verkrijging van de graad van doctor
aan de Katholieke Universiteit Nijmegen,
volgens besluit van het College van Decanen
in het openbaar te verdedigen op
vrijdag 14 juni 2002
des namiddags om 1:30 uur precies
door

Hans van Eenennaam

geboren op 3 november 1973
te Middelburg

Promotor

Prof. Dr. W.J. van Venrooij

Co-promotor

Dr. G.J.M. Pruijn

Manuscriptcommissie

Prof. Dr. L.B.A. van de Putte

Prof. Dr. F.P.J.T. Rutjes

Prof. Dr. H.F. Tabak (Universiteit van Amsterdam)

voor mijn ouders

ISBN 90-9015696-8
© 2002 by Hans van Eenennaam

The research described in this thesis was performed at the Department of Biochemistry, Faculty of Science, University of Nijmegen, the Netherlands. This work was supported in part by the Netherlands Foundation for Scientific Research (NWO-CW).

hoe

als je je

met zorgeloosheid

kon omringen

en dat dat

je ruimte

was

(Bert Schierbeek)

Table of contents

Chapter 1 General introduction 9

Part I

Chapter 2 hPop4: a new protein subunit of the human RNase MRP 25
and RNase P ribonucleoprotein complexes

Chapter 3 hPop5, a protein subunit of the human RNase MRP 39
and RNase P endoribonucleases

Part II

Chapter 4 Basic domains target protein subunits of the RNase MRP 55
complex to the nucleolus independently of complex association

Chapter 5 RNA-protein interactions in the human RNase MRP 71
ribonucleoprotein complex

Chapter 6 Identity of the RNase MRP and RNase P associated..... 91
Th/To-autoantigen.

Part III

Chapter 7 Autoantibodies against small nucleolar ribonucleoprotein 107
complexes and their clinical associations.

Chapter 8 Mutations in the RNA component of the RNase MRP cause a 121
pleiotropic human disease, cartilage-hair hypoplasia.

Part IV

Chapter 9 General discussion..... 137

Samenvatting/Summary..... 151

References..... 155

List of publications..... 162

Dankwoord en acknowledgements 163

Curriculum vitae 167

Chapter 1

General introduction

Adapted from IUBMB Life (2000) 49: 265-272

Nowadays, it is generally assumed that the 'RNA world' was one of the early phases in the evolution of life. At that stage of evolution ribonucleic acids (RNAs) were thought to play a key role in the catalysis of chemical reactions and its own replication. In the current phase of evolution, one of the major functions of RNA is the transfer of information stored in genes, from DNA (deoxyribonucleic acid) to proteins. During this process, a copy of the DNA is made in the form of messenger RNA (mRNA). This messenger RNA is subsequently transported to the site of protein synthesis, where the message is translated and the encoded protein is synthesised. In the latter process, two other classes of RNA are involved. The transfer RNAs (tRNA) delivers the amino acids to the ribosome. This synthesising machinery binds the incoming amino acids to the growing polypeptide chain. The ribosome itself contains numerous proteins and four RNAs, called ribosomal RNAs (rRNA).

Before these different RNAs (mRNA, tRNA and rRNA) can function in the above-described processes, they undergo a maturation process directly after their synthesis. In eukaryotes all these RNAs are cleaved and/or undergo modifications such as ribose-methylation and conversion of a uridine to a pseudouridine. The cleavage generating the mature 5'-end of tRNAs and the cleavages and modifications needed for the complete maturation of rRNAs are mediated by other RNAs that are primarily found in the nucleolus and therefore designated as small nucleolar RNAs or snoRNAs.

In this chapter our knowledge on the structure and function of these small nucleolar RNAs, with emphasis on the RNase MRP and RNase P complexes, will be summarised.

Small nucleolar ribonucleoprotein particles

In eukaryotes the 5.8S, 18S and 25/28S rRNAs are transcribed by RNA polymerase I as one long precursor. The processing of this precursor not only involves endo- and exonucleolytic cleavages, but also ribose methylation and conversion of uridines to pseudouridines (1,2). These processing and modification events are mediated by small nucleolar RNAs and their associated proteins (the so-called small nucleolar ribonucleoproteins or snoRNPs). Although snoRNAs are heterogeneous in size, snoRNAs can be classified in three distinct groups based on conserved sequence elements: box C/D snoRNAs, box H/ACA snoRNAs and RNase MRP/RNase P RNAs ((3), reviewed in ref. (4,5)).

Box C/D snoRNPs

The box C/D snoRNAs contain the conserved C (consensus sequence: RUGAUGA) and D (consensus sequence: CUGA) boxes, which are frequently followed or preceded by a stem structure (see Figure 1A). Imperfect copies of box C/D sequences (referred to as box C' and D') have been described and are located between box C and box D (6-8). Most of the box C/D snoRNAs, e.g. U24-U63, harbour an extended region (10-21 nucleotides) of base complementarity to rRNA, thereby positioning box D and/or D' exactly 5 nucleotides from the nucleotide that has to be modified via 2'-O-ribose methylation (Figure 1A) (6,9).

At present 51 of the 55 ribose methylation sites in yeast ribosomal RNA have been assigned to 41 different guide snoRNAs (10). In mammals 105-107 ribose methylation sites have been mapped and at present only 14 ribose methylations remain without identified cognate guide snoRNA (2,11).

A small group of box C/D snoRNAs lack sequence complementarity to rRNA and these snoRNAs have been demonstrated to function in endonucleolytic processing of pre-rRNA. This group includes U3, U8, U13 and U22 snoRNA (reviewed in ref. (4,5,12))

Three proteins have been shown to be specifically associated with all box C/D snoRNAs: fibrillarin, Nop56 and Nop5/58 (13-15). Although no clear function has been demonstrated for these proteins, sequence and structure homology between known methyltransferases and fibrillarin strongly suggest that fibrillarin is the 2'-O-methyltransferase enzyme (16).

Box H/ACA snoRNPs

The box H/ACA snoRNAs possess 5' and 3' hairpin domains, connected and followed by single-stranded hinge and tail regions that carry the conserved H (AnAnnA) and ACA boxes, respectively (Figure 1B). Two short

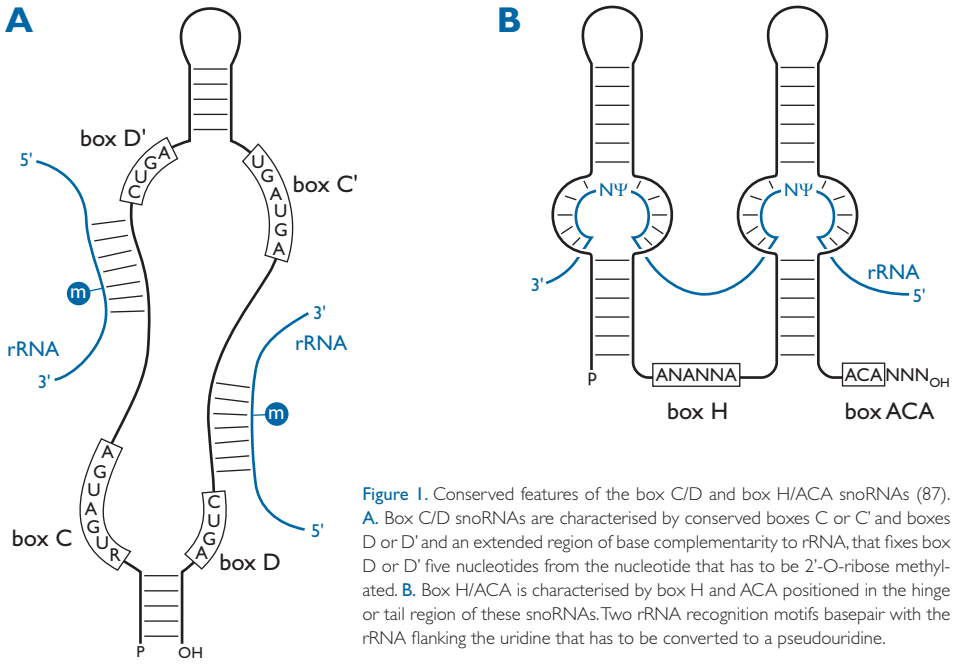

Figure 1. Conserved features of the box C/D and box H/ACA snoRNAs (87). A. Box C/D snoRNAs are characterised by conserved boxes C or C' and boxes D or D' and an extended region of base complementarity to rRNA, that fixes box D or D' five nucleotides from the nucleotide that has to be 2'-O-ribose methylated. B. Box H/ACA is characterised by box H and ACA positioned in the hinge or tail region of these snoRNAs. Two rRNA recognition motifs basepair with the rRNA flanking the uridine that has to be converted to a pseudouridine.

"rRNA recognition motifs" present in the snoRNA are able to base pair with rRNA sequences flanking the uridine to be converted into pseudouridine (Figure 1B) (3,17).

At present, 42 of the 91-93 pseudouridines present in mammalian rRNAs can be explained by the identification of 40 box H/ACA snoRNAs, e.g. U64-U72 ((2,11) and references therein).

Four proteins have been shown to be specifically associated with box H/ACA snoRNAs: hGar1, NAP57/dyskerin, hNHP2 and hNOP10 (18-20). The homology between NAP57/dyskerin and pseudouridine synthases involved in tRNA and bacterial rRNA modifications strongly suggests that NAP57/dyskerin represents the pseudouridine synthase associated with the box H/ACA snoRNPs (21).

RNase MRP/RNase P

The RNase MRP and RNase P complexes are the only known representatives of the third class of small nucleolar RNPs. Both ribonucleoprotein particles function as endonucleases and have been shown to be involved in the processing of pre-rRNA and pre-tRNA, respectively. A more detailed overview of these complexes is given below.

RNase MRP and RNase P ribonucleoprotein particles

Function and subcellular localisation of RNase MRP

The RNase MRP (for Mitochondrial RNA Processing) was originally identified in mouse cells by virtue of its ability to cleave the mitochondrial RNA that functions as a primer for mitochondrial DNA replication *in vitro* (22). Initiation of mitochondrial DNA replication occurs at two origins of replication (O_H and O_L). O_H initiates the replication of the heavy strand of mtDNA, whereas O_L is involved in the replication of the complementary light strand. Initiation of the replication of the heavy strand is a two step process (reviewed in ref. (23)).

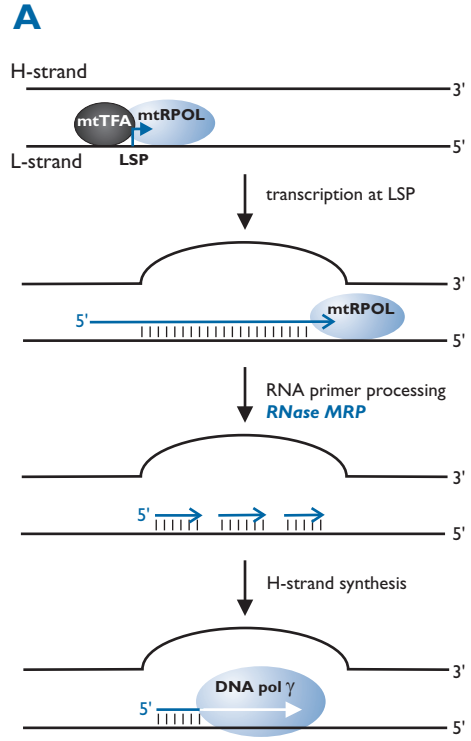

Figure 2. → Function of RNase MRP and RNase P complexes. A. RNase MRP has been shown to function in the processing of mitochondrial RNA that functions as a primer for DNA replication. The parental mtDNA are indicated with H-strand and L-strand, for heavy- and light-strand, respectively. Transcription starts from the Light Strand Promoter (LSP) and is initiated by a mitochondrial transcription factor (mtTFA) and mitochondrial RNA polymerase (mtRPOL). After transcription of the heavy strand origin of replication (O_H), the transcript remains bound to the DNA duplex and is subsequently cleaved by RNase MRP to form primers that function in the inititation of DNA synthesis by DNA polymerase γ (reviewed in ref. (23,88)). (Continued on next page)

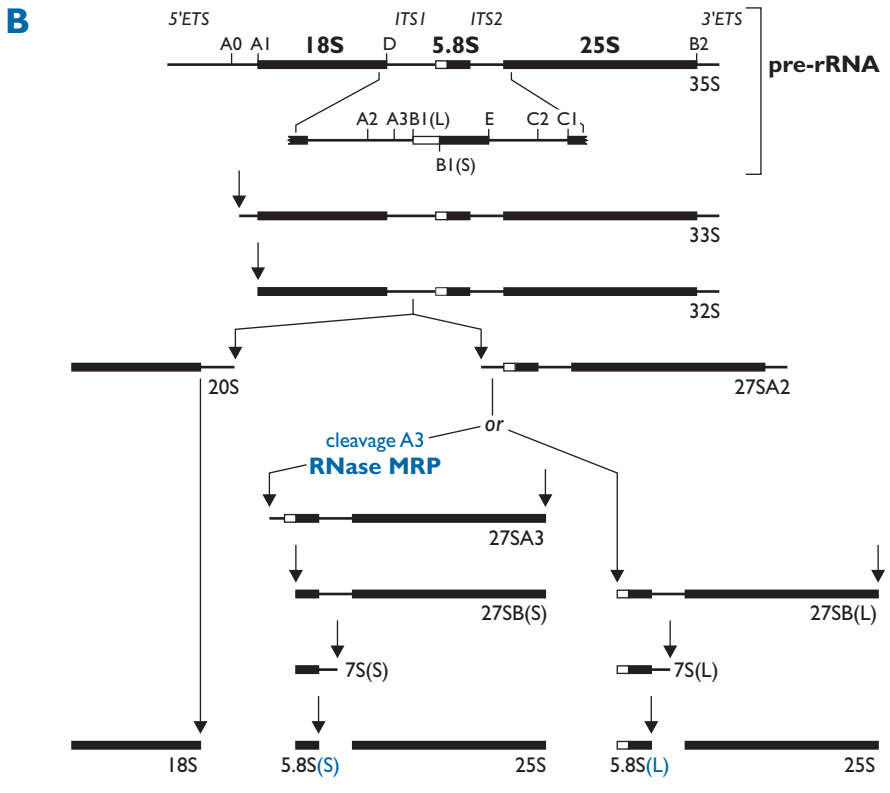

Figure 2 (Continued) B. RNase MRP and RNase P have been shown to function in the processing of precursor rRNA in yeast. The 35S (primary) transcript, as is depicted at the top, is processed to mature 25S, 18S, and 5.8S rRNAs (from (4)). The cleavage sites (A0 through E), the relative positions of the rRNA sequences (black boxes), the external transcribed spacers (5'ETS and 3'ETS), and the internal transcribed spacers (ITS1 and ITS2) are indicated. The small white box marks the sequence in the long form of 5.8S rRNA, 5.8S(L), that is absent in the short form of 5.8S rRNA, 5.8S(S). RNase MRP is involved in the cleavage event at site A3 in ITS1, whereas RNase P might be involved in the processing of ITS2 (reviewed in ref. (89)). (Continued on next page).

First, RNA transcription of the light strand is initiated at the light-strand promoter (LSP) thereby forming a three stranded R-loop (RNA transcript with mitochondrial DNA) (24,25); see Figure 2A. Secondly, the RNA transcript is cleaved by RNase MRP to generate RNA molecules that subsequently function as primers for the DNA synthesis of the heavy strand by DNA polymerase γ.

Biochemical purification of the RNase MRP activity from mitochondria showed that this enzyme is a ribonucleoprotein particle, that the RNA component is essential for its activity and that the RNA component is encoded in the nucleus (26,27).

In addition to its mitochondrial function, evidence for the involvement of the RNase MRP complex in the biogenesis of ribosomes has been obtained in the yeast *Saccharomyces cerevisiae* (28-30). RNase MRP was shown to cleave the precursor of ribosomal RNA at site A3 within the first internal transcribed spacer (ITS1) (see Figure 2B). Under normal growth conditions, two forms of 5.8S rRNA are produced, a long form and a short form, the latter being approximately 10 times more abundant than the former. When the RNase MRP activity is abrogated by mutation or depletion of one of its constituents, cleavage at site A3 of pre-rRNA is inhibited, leading to accumulation of the long form of 5.8S rRNA (28,29,31-38). Although no clear function of the two forms of 5.8S rRNA has been described, it has been shown that inhibition of 5.8S(S) rRNA synthesis thereby enhancing the amount of 5.8S(L) rRNA, results in a change in the expression of several proteins, suggesting that these forms of 5.8S rRNA play a role in the selective translation of (some) proteins (29). The identity of the proteins that are either up- or downregulated has not been investigated, yet.

Genetic depletion of either RNA or protein components of the RNase MRP complex demonstrated that the RNase MRP complex is essential for yeast viability. However, it was shown that cleavage at site A3 in the pre-rRNA is not (39), suggesting that RNase MRP exhibits another, as yet unidentified, function that is essential for viability. The mitochondrial function of RNase MRP is probably also not essential for viability because yeast cells without mitochondrial DNA form *petite* colonies on a fermentable medium and are viable (reviewed in ref. (40)).

Recent findings in yeast suggest that the RNase MRP complex may also play a role in cell cycle control (41). Yeast cells containing mutations in the gene encoding the RNase MRP specific protein subunit Snmlp show defects in plasmid segregation, which is suggested to be caused by telophase arrest. This effect has also been found with an RNase MRP RNA mutant, suggesting some role for RNase MRP in the breakdown of the mitotic spindle and closing steps of mitosis (41). Whether this cell cycle arrest is directly or indirectly caused by the defect of these mutants in pre-rRNA processing is at present unclear.

Subcellular partitioning and in situ hybridisation experiments confirmed the presence of RNase MRP in mitochondria and nucleoli (42,43), with the vast majority being localised in the nucleolus. The central region of the RNase MRP RNA (Figure 3A) is important for its mitochondrial localisation (42), whereas the 5' located P3 domain of the RNase MRP RNA (see below) is necessary for its nucleolar localisation (44). These data suggest that two different structural domains within the RNase MRP RNA, which is transcribed by RNA polymerase III in the nucleoplasm, mediate its transport to these different subcellular compartments.

Function and subcellular localisation of RNase P

The characterisation of the first tRNA precursor soon led to the identification of the enzymatic activity that processed the 5' end of

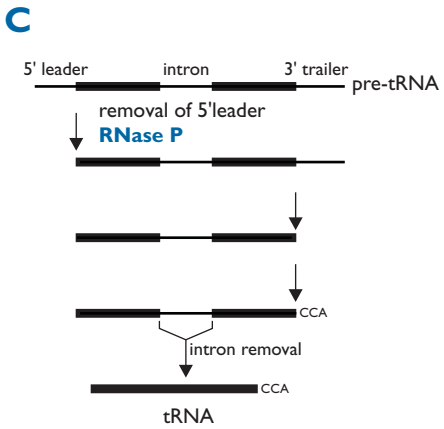

Figure 2. (Continued). C. Processing of precursor tRNA. RNase P mediates the removal of the 5' leader sequence of precursor tRNA. The 5' leader, 3' trailer, and intron elements are indicated (the latter being present in only a subset of pre-tRNAs). Although end maturation precedes intron removal in this representation, the actual order of these events may be reversed (reviewed in ref. (53)).

precursor tRNA in *E. coli* (45). Purification of the RNase P enzyme from *E. coli* showed that the enzyme is a ribonucleoprotein particle (46). The RNA subunit (M1 RNA) of *E. coli* RNase P is encoded by the rnpB gene and is 377 nucleotides long (47). The protein component of the *E. coli* RNase P complex is encoded by the *rnpA* gene, consists of 119 amino acids and is called C5. (48). Although both components of the bacterial RNase P complex are necessary for its pre-tRNA processing activity *in vivo* (49), enzymatic activity of the RNA component alone could be demonstrated *in vitro* under conditions of high ionic strength (50).

Nowadays, RNase P complexes in bacteria, yeast and human have been identified (reviewed in ref. (51,52)) and all are able to process the precursor of tRNA. Processing of pre-tRNA in yeast and human includes multiple steps (Figure 2C). After removal of the 5'-leader and 3'- trailer sequence by either endonuclease or exonuclease activity, the CCA trinucleotide is added to the 3' end and nucleotides are modified (reviewed in ref. (53)). Before export to the cytoplasm can occur intervening sequences (introns), if present, will have to be removed.

Besides the tRNAs encoded in the nucleus, human and yeast cells both contain mitochondrially encoded tRNAs. Although the removal of the 5'-leader sequences of mitochondrial pre-tRNAs initially was appointed to a protein enzyme (54,55), recent data indicate that the mitochondrial RNase P activity is contained in a ribonucleoprotein complex, containing an RNA component identical to the nuclear RNase P RNA (43). At this moment it is unclear whether the same set of proteins is associated with both nuclear and mitochondrial RNase P complexes.

An additional function of the RNase P complex has been reported a few years ago. Yeast cells containing mutations in the RNase P RNA showed, besides accumulation of pre-tRNA, accumulation of an aberrant form of 5.8S rRNA (56). This aberrant form of 5.8S rRNA was shown to have a 35 nucleotide extension at the 3' end of the 5.8S rRNA, indicating that RNase P might also function in the cleavage of pre-rRNA in ITS2 (see Figure 2B).

In situ hybridisation experiments using both anti-sense oligonucleotides and nick-translated DNA probes have revealed that the human RNase P complex is localised throughout the cytoplasm and the nucleus (57,58) as well as in structures at the edge of the nucleolus known as perinucleolar compartments (PNCs) (59). These PNCs have been proposed to function in the biogenesis of RNA polymerase III transcripts and not to reflect active RNase P complexes (reviewed in ref. (53)). Microinjection of rhodamine-labeled RNase P RNA showed an initial localisation of RNase P RNA to the nucleolus followed by a redistribution throughout the nucleus (58). Deletion mutant analyses of the RNase P RNA suggested that the 5' located P3 domain, which displays a predicted secondary structure similar to that of the RNase MRP RNA, is required for its nucleolar localisation (Figure 3B) (58). Furthermore, these experiments demonstrated that the 3'-part of the RNase P RNA is important for the nucleoplasmic localisation observed after the initial nucleolar accumulation. In summary, the human RNase P complex has been shown to function in the processing of pre-tRNAs in both nucleus and mitochondria, which is consistent with the reported subcellular localisations.

In the yeast *Saccharomyces cerevisiae* a different subcellular localisation has been reported for the RNase P complex. In situ hybridisation experiments in yeast indicated that RNase P RNA is predominantly found in the nucleolus (60). A nucleolar localisation has also been reported for some pre-tRNAs, suggesting that the removal of the 5' leader of pre-tRNA in yeast may occur in the nucleolus (60). A nucleolar localisation of RNase P is also consistent with its proposed role in the processing of pre-rRNA in the ITS2 which also proceeds in this compartment (56).

Th/To autoantibodies facilitated the identification of human RNase MRP and P RNAs

The finding that patients with certain connective tissue diseases produce autoantibodies directed against the human RNase P complex resulted in the identification of the RNA component of human RNase P (also called H1 or 8-2 RNA) (61-63). The identified RNA molecule is 340 nucleotides long, is synthesised by RNA polymerase III and has a pppG 5'-end. The same autoimmune sera also immunoprecipitated the RNA component of the human RNase MRP particle (also called Th or 7-2 RNA), which consists of 267 nucleotides, is also synthesised by RNA polymerase III and also has a pppG 5'-end (62,64-66). Patient antibodies that recognise both RNase MRP and RNase P complexes are designated as anti-Th/To. The anti-Th/To specificity has been observed in 4-13% of scleroderma patients (67,68). An analysis of clinical parameters showed that anti-Th/To antibodies are predominantly found in scleroderma patients with limited cutaneous involvement and in certain patients with primary Raynaud's phenomenon whose disease evolved to limited cutaneous involvement (67). The cumulative survival of patients with these antibodies was only 78% at 10 years, compared to 91% for patients that do not have anti-Th/To specificity.

The observation that patient antibodies often recognise both RNase MRP and RNase P complexes, strongly suggested that these complexes are structurally related. Although the RNA components of RNase P and RNase MRP are poorly conserved at the sequence level, both experimental and phylogenetic data suggest that they fold into similar secondary structures, as illustrated in Figure 3 (69,70).

These similar secondary structures are also referred to as cage-shaped structures (69) and correspond to the first three stem-loop structures, designated as P1-P3, and a long-range interaction (P4); see Figure 3. The similarity between the P3 domains of RNase MRP and RNase P RNAs is not restricted to their secondary structures, because experiments with yeast mutants, in which the P3 domains of RNase MRP and RNase P had been swapped, demonstrated that such mutations did not lead to loss of function or specificity (71).

Because the Th/To-patients' sera examined were unable to immunoprecipitate the RNA components of the RNase MRP and RNase P complexes from deproteinised cell extracts, it was concluded that these particles share at least one autoantigenic polypeptide (65). Using ^{35}S-methionine or ^{3}H-leucine labelled HeLa cell extract, the autoantigenic protein was found to have a molecular weight of approximately 40 kDa (68,72,73) and for this reason it was designated Th-40. Crossreactivity of antibodies raised against the *E. coli* RNase P protein with the Th-40 autoantigen strongly suggested that the Th-40 autoantigen represents the human

homologue of this prokaryotic RNase P protein (74). UV-crosslinking analysis showed that the autoantigenic Th-40 polypeptide could be UV-crosslinked to stem-loop P3 of RNase MRP and RNase P RNA (75,76). As described above, deletion of the P3 domain in RNase P and RNase MRP RNA resulted in loss of nucleolar localisation, suggesting an important role for the Th-40 autoantigen in the subcellular localisation of these enzymes (44,58).

RNase MRP and RNase P protein subunits

Screening of a yeast library with temperature-sensitive mutants for strains that contained an altered ratio of 5.8S(L) to 5.8S(S) at the non-permissive temperature, resulted in the identification of the first protein associated with both RNase MRP and RNase P in yeast (37). This protein was designated Pop1 for "Processing of precursor". Subsequently, other protein subunits of the RNase MRP complex were identified as suppressors of temperature-sensitive RNase MRP RNA mutants: Snm1p, Pop3p and Pop4p (32,34,35). Characterisation of these proteins showed that only Snm1p appeared to be specifically associated with the RNase MRP complex, whereas Pop3p and Pop4p were also found to be associated with the RNase P complex. The yeast Rpp1p and Rpp2p proteins were identified as homologues of two human RNase P proteins, but were also found associated with the RNase MRP complex (33,36). Purification of the RNase P complex from yeast resulted in the identification of 4 additional protein subunits (Pop5p, Pop6p, Pop8p and Rpr2p) of which only the Rpr2p protein appeared to associate specifically with the RNase P complex (38).

The characterisation of the first protein shared by RNase MRP and RNase P in yeast (37) facilitated the cloning of the first cDNA encoding a human RNase MRP/RNase P protein subunit: hPop1 (77). More recently, cDNAs encoding several other human protein subunits have been isolated after the biochemical purification of the RNase P complex from HeLa cells: Rpp14, Rpp20, Rpp29, Rpp30, Rpp38, and Rpp40 (78-80). One additional protein copurified with RNase P activity from HeLa cells (Rpp25), which has been recently identified (78, Guerrier-Takada, personal communication).

The identification of protein subunits specific for either RNase MRP or RNase P in yeast (Snm1p and Rpr2p, respectively) suggests that such protein subunits are likely to exist in human cells as well (32,38). Indeed, the human homologue of the RNase P specific protein subunit (Rpr2p) has recently been identified: Rpp21 (81).

Screening of cDNA libraries in a yeast two hybrid system using Rpp14, Rpp20, Rpp21, Rpp29, Rpp30, Rpp38, Rpp40 and hPop1 as bait identified three putative new protein components of the RNase MRP and P complexes: small heat shock protein 27 (Hsp27), human LIM domain-containing protein (LIMD1) and an exoribonuclease (OIP2) (82). It was shown that Hsp27 is able to bind Rpp20 and that addition of Hsp27 stimulates RNase P activity *in vitro*. However, a stable association between Hsp27 and the RNase P holoenzyme could not be demonstrated. The significance of the interactions of LIMD1 and OIP2 with Rpp14 remains to be elucidated.

The protein subunits of RNase MRP and RNase P for which sequence information has been obtained by cDNA analysis lack all of the currently known RNA-binding motifs (38). However, in all yeast RNase MRP and RNase P proteins except Rpp1p, a motif can be discerned in which two neighbouring lysine residues are preceded or followed by an additional lysine at a distance of three to eight intervening residues. Although the relevance of this finding is unclear, this motif has been suggested to be implicated in RNA association, protein-protein interactions, or nuclear localisation (38). In most of the known protein subunits of human RNase MRP and RNase P, similar lysine-rich motifs can be discerned. Most of these proteins are (highly) basic and have predicted pI values between 7.5 and 11. In addition, one single acidic protein has been identified in both human and yeast RNase MRP/RNase P: Rpp40 and Pop8p, respectively (38,80). Recently, the functional significance of sequence elements rich in basic amino acids for some of the RNase P and RNase MRP protein subunits has been demonstrated (83). Muta-

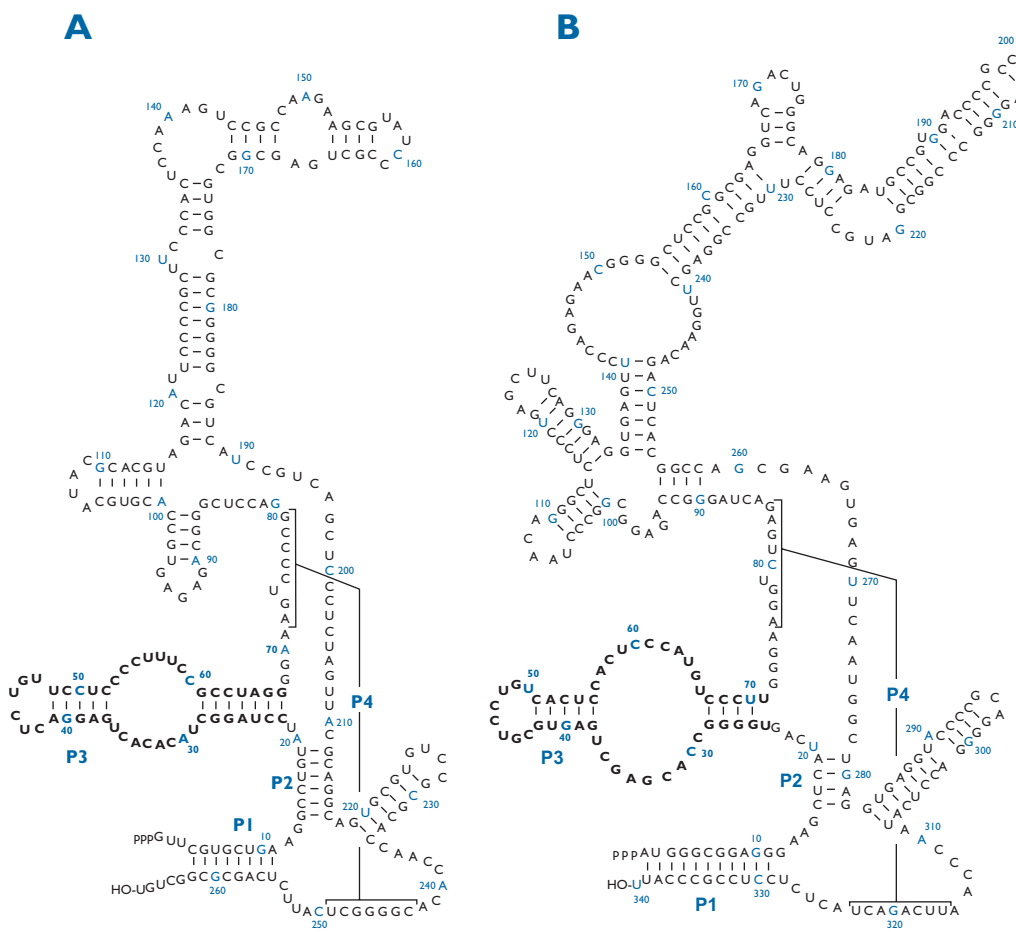

Figure 3. Secondary structures of human RNase MRP RNA (A) and RNase P RNA (B).The secondary structure of RNase MRP RNA is based on phylogenetic comparison and chemical modification data (70).The secondary structure of RNase P RNA is based on phylogenetic comparison of vertebrate RNase P RNAs (90,91).The structurally conserved 5'-located P3 domain is indicated in bold.

tional analysis of the basic domains in the Rpp38 and Rpp29 proteins suggested that they are required for their nucleolar accumulation and that the Rpp14 protein subunit, which lacks such clusters of basic amino acids, is transported to the nucleus and nucleolus by a 'piggyback' mechanism (83).

After purification of the human RNase P from HeLa cells, the purified RNase P complex was shown to contain ATPase activity. Interestingly, the Rpp20 protein subunit has significant homology with a putative ATP binding cassette in an ABC transporter ATPase from *Arabidopsis thaliana*. The recombinant Rpp20 protein appeared to display ATPase activity and deletion of the putative ATP binding cassette resulted in a decreased ATPase activity (84). It is still unknown whether human RNase MRP, which also contains Rpp20, displays ATPase activity as well.

Interactions between RNase MRP and RNase P subunits

UV-crosslinking experiments have provided insight into the intermolecular interactions occurring in the RNase MRP and RNase P particles. Using this technique, in combination with patients' autoantibodies directed to the RNase MRP and RNase P particles, Yuan and coworkers showed that the major autoantigenic polypeptide, Th-40, is bound to the P3 domain of RNase MRP and RNase P RNA (Figure 3) (75). Analysis of randomised mutants of the P3 domain of RNase P RNA in yeast showed that four conserved nucleotides in this domain are important for viability and yeast three-hybrid studies showed that in these mutants the interaction between the P3 domain and Pop1 is abolished (85). Three-hybrid studies using the human RNase P RNA allowed the identification of interactions of Rpp21, Rpp29, Rpp30 and Rpp38 proteins, but not hPop1 with this RNA, suggesting that the latter interaction is not evolutionarily conserved (86). In addition, UV-crosslinking experiments showed that Rpp21, Rpp29 and Rpp30, but not Rpp38, directly interacts with the P3 domain of RNase P RNA (86).

Yeast two-hybrid analyses using Rpp14, Rpp20, Rpp21, Rpp29, Rpp30, Rpp38, Rpp40 and hPop1 indicated that Rpp30 strongly interacts with Rpp14. Similarly, a strong interaction could be demonstrated between Rpp40 and Rpp21. Furthermore, several weak interactions between the other protein components could be detected. The observation that not all of these two-hybrid interactions are reciprocal, i.e. are also detected when the DNA-binding and transcription activation domains are interchanged, complicates the interpretation of these data (82).

Recently, recombinant Rpp14 and Rpp21 proteins were shown to interact with pre-tRNA suggesting that these proteins may be involved in recognition and/or the cleavage of pre-tRNA (81).

Outline of this thesis

The RNase MRP complex has been shown to cleave precursor rRNA and mitochondrial RNA needed for mitochondrial DNA replication. At the start of this project, in 1997, the RNA component and one protein subunit of the human RNase MRP complex had been cloned. Furthermore, a protein of 40 kDa (Th-40), which was recognised by autoantibodies of scleroderma patients, had been reported to be associated with the human RNase MRP complex. The goal of this project was to identify new protein subunits of the RNase MRP complex, to shed more light on the identity of Th-40 autoantigen, to obtain more information on the architecture of the RNase MRP complex and to study the relation between the RNase MRP complex and the related RNase P complex.

The results reported in this thesis are divided into three parts:

- **I** novel protein components of the RNase MRP complex
- **II** assembly of the RNase MRP complex
- **III** RNase MRP and human disease

In **Part I** the identification and cDNA cloning of two novel protein components of the human RNase MRP complex is described. These two novel human protein subunits were identified by virtue of their homology with two yeast RNase MRP proteins. Biochemical analyses showed that these proteins are also shared by the human RNase P complex. The cloning of hPop4 is reported in **Chapter 2** and the cloning of hPop5 in **Chapter 3**.

In **Part II** various data are described which are aimed at the elucidation of the assembly pathway and architecture of the human RNase MRP complex. First (**Chapter 4**) the subcellular localisation and complex association of three protein subunits of the human RNase MRP and RNase P complexes are studied by deletion mutagenesis. In addition, the effects of these deletions on the RNase P activity have been determined. In the next chapter (**Chapter 5**) the development of a reconstitution assay for the RNase MRP complex is described as well as the application of this assay to study the role of structural elements of the RNase MRP RNA in the association of different protein subunits. UV-crosslinking analyses were performed to identify proteins that directly interact with the RNase MRP RNA. In the last chapter of this part (**Chapter 6**) the paradoxical differences between our data presented in Chapter 5 and literature data on the Th-40 autoantigen are studied. The identity of the Th-40 autoantigen is elucidated and an explanation for the apparent controversy is provided.

In **Part III** the relationship between the RNase MRP complex and certain human diseases is studied. The RNase MRP complex has been found to be an autoantigen targeted by autoantibodies in patients suffering from certain connective tissue diseases. In **Chapter 7** a relatively large collection of patient sera was screened for the presence of autoantibodies directed against nucleolar components, including the three classes of small nucleolar ribonucleoprotein complexes (box C/D snoRNPs, box H/ACA snoRNPs and RNase MRP/P). In addition, clinical data were collected by chart review and the relevance of these autoantibodies for diagnosis and prognosis is discussed. In **Chapter 8** the role of the RNase MRP complex in a completely different disease is discussed. Genetic analyses of patients suffering from the inherited disease cartilage hair hypoplasia (characterised by dwarfism) demonstrated that these patients have mutations in the gene encoding the RNA component of the RNase MRP complex.

Finally, the results obtained in this project are discussed in **Chapter 9**. A summary completes this thesis.

Part I

Novel components of the RNase MRP complex

Chapter 2

hPop4: A new protein subunit of the human RNase MRP and RNase P ribonucleoprotein complexes

Hans van Eenennaam
Ger J.M. Pruijn
Walther J. van Venrooij

Nucleic Acids Research (1999) 12: 2465-2472

Abstract

RNase MRP is a ribonucleoprotein particle involved in the processing of pre-rRNA. The RNase MRP particle is structurally highly related to the RNase P particle, which is involved in pre-tRNA processing. Their RNA components fold into a similar secondary structure and they share several protein subunits.

We have identified and characterized human and mouse cDNAs that encode proteins homologous to yPop4p, a protein subunit of both the yeast RNase MRP and RNase P complexes. The human Pop4 cDNA encodes a highly basic protein of 220 amino acids. Transfection experiments with epitope-tagged hPop4 protein indicated that hPop4 is localized in the nucleus and accumulates in the nucleolus. Immunoprecipitation assays using extracts from transfected cells expressing epitope-tagged hPop4 revealed that this protein is associated with both the human RNase MRP and RNase P particles. Polyclonal rabbit antibodies raised against recombinant hPop4 recognized a 30 kDa protein in total HeLa cell extracts and specifically co-immunoprecipitated the RNA components of the RNase MRP and RNase P complexes. Finally we showed that anti-hPop4 immunoprecipitates possess RNase P enzymatic activity. Taken together, these data show that we have identified a protein that represents the human counterpart of the yeast Pop4p protein.

Introduction

In eukaryotes the 5.8S, 18S and the 25S/28S rRNAs are transcribed as one long precursor by RNA polymerase I. The maturation of this precursor not only involves endo- and exonucleolytic cleavages, but also methylation and pseudouridinylation (1). Proper processing of the precursor rRNA requires a group of small nucleolar ribonucleoprotein particles (snoRNPs). These snoRNPs consist of proteins associated with so-called snoRNAs, which are heterogeneous in size and contain structural elements. Based on their structural elements the snoRNAs can be divided into three groups: Box C/D snoRNAs, Box H/ACA snoRNAs and RNase MRP/RNase P (5). While most Box C/D snoRNAs have been demonstrated to function in ribose methylation (92) and Box H/ACA in pseudouridinylation of the rRNAs (93), RNase MRP and RNase P function as endonucleases (56,94).

Originally the RNase MRP has been identified as an endoribonuclease able to cleave, *in*

vitro, mitochondrial RNA that functions as a primer for mitochondrial DNA replication (22). Most of the RNase MRP is, however, not localized in the mitochondria but is found in the nucleolus of cells (26,72). Genetic and biochemical experiments in *Saccharomyces cerevisiae* have shown that the RNase MRP is involved in the formation of the short form of the 5.8S rRNA (5.8S (S)), by catalyzing the cleavage at site A3 in the Internal Transcribed Spacer 1 (ITS1) of pre-rRNA (28-30,37). An involvement of RNase MRP in mitochondrial DNA replication *in vivo* has not been demonstrated yet.

The sensitivity of RNase MRP function to both ribonucleases and proteases demonstrates a requirement for both RNA and protein subunits for catalytic activity (26). The RNA subunit of the RNase MRP has been cloned from several species including human (66), mouse (27), rat (95), cow (96), toad (97), yeast (98), *Arabidopsis* and tobacco (99). The RNA subunit of RNase MRP is related to the RNA subunit of RNase P, an endoribonuclease involved in the processing of the 5'-end of precursor-tRNAs (100,101) and also suggested to be involved in processing of the precursor-rRNA in Internal Transcribed Spacer 2 (ITS2) (56). Both RNA components have similar secondary structure elements, in particular the so-called cage-shaped domain (69,70) which contains many conserved nucleotides, supporting the idea that the RNase MRP and RNase P RNAs have evolved from a common ancestor (102,103). The identification of these RNAs via anti-Th/To sera from patients suffering from the connective tissue diseases systemic lupus erythematosus (SLE) and scleroderma, which immunoprecipitate both RNA components, has led to alternative names for these RNA components: RNase MRP is also referred to as Th or 7-2 RNA and RNase P RNA as H1 or 8-2 RNA (61,62,64,65,104).

The close relationship between the RNase MRP and RNase P is also supported by the fact that both particles contain similar protein subunits. Recently, purification of the RNase P particle from *S. cerevisiae* led to the identification of 9 protein subunits copurifying with the RNase P RNA (38). All these proteins are encoded by genes essential for RNase P activity and for cell viability. Four of these protein subunits: Pop1p (37), Pop3p (35), Pop4p (34) and Rpp1p (33), had been identified before and all four appeared to be components of both the RNase P and RNase MRP particle. Other subunits shared by both particles are Pop5p, Pop6p, Pop7p/Rpp2p and Pop8p. Yeast RNase MRP and RNase P also contain at least one protein subunit specifically associated with each of these particles, which are designated Snm1p (32) and Rpr2p (38), respectively.

The human RNase P particle has also been purified from HeLa cells, which resulted in the cDNA cloning of four RNase P protein subunits (78,80). Rpp20, Rpp30, Rpp38 and Rpp40 have been characterized and sequence comparison revealed that Rpp20 is the human homologue of Pop7p/Rpp2p while Rpp30 is the human homologue of Rpp1p (33,36,38,80). The first human protein subunit characterized was the hPop1 protein (77), the homologue of the yeast Pop1p. For hPop1, Rpp30 and Rpp38 it has been established that they are subunits of both RNase MRP and RNase P (77,105) and this is likely to be the case for Rpp20 as well.

In this report we describe the identification of the human and mouse homologues of the yeast Pop4p. A complete cDNA encoding the human homologue of yPop4 was cloned and characterized. This cDNA encodes a novel nucleolar 30 kDa protein, that is associated with both RNase MRP and RNase P. Polyclonal rabbit antibodies were raised against hPop4, and used to confirm the association of hPop4 with these two ribonucleoprotein complexes.

Results

Identification of putative human and mouse Pop4p homologues

Recently, the cDNA cloning and characterization of Pop4p from *S. cerevisiae* has been described (22). This protein was shown to be a subunit of both the yeast RNase MRP and RNase P particles and to be essential for 5.8S rRNA and pre-tRNA processing. The open reading frame (ORF) of the yeast Pop4 cDNA encodes a protein comprised of 279 codons with a predicted molecular weight of 33 kDa.

The amino acid sequence of yeast Pop4p, hereafter designated yPop4, was compared with protein and 'translated nucleic acid' sequence databases to identify homologous sequences that might represent mammalian homologues of yPop4. Six overlapping nucleic acid sequence entries, corresponding to human Expressed Sequence Tags (ESTs), were retrieved. Using these ESTs a cDNA sequence could be constructed of 1133 nucleotides, containing an ORF encoding a protein of 220 amino acids. For reasons documented below this protein will be referred to as hPop4.

Besides the human ESTs retrieved from the sequence databases using the yPop4 amino acid sequence, five mouse ESTs were selected. The combination of these five ESTs also allowed the derivation of a cDNA sequence, which in this case was comprised of 1433 nucleotides, containing an ORF encoding a protein of 221 amino acids. The latter protein will be referred to as mPop4, since its amino acid sequence is highly homologous to that of hPop4 (see below).

No in-frame stop codon was found upstream of the first ATG in the human cDNA sequence, which might implicate that the cDNA did not represent the complete mRNA. However, since such an in-frame stop codon is present upstream of the first ATG in the mPop4 cDNA sequence and since the amino acid sequences derived from the hPop4 and mPop4 cDNA are highly homologous, it is reasonably to assume that the first ATG in the human cDNA sequence represents the start codon of the hPop4 mRNA.

Cloning of hPop4 cDNA

To clone a cDNA encoding the complete open reading frame of hPop4, two oligonucleotides were designed based on the cDNA sequence derived from the human ESTs. These oligonucleotides were used as PCR primers to amplify the hPop4 ORF using DNA from both human placenta and teratocarcinoma cDNA libraries as template. Sequencing of several clones resulting from this procedure revealed that clones derived from both cDNA libraries were completely identical, thereby ruling out the introduction of PCR artifacts. Nevertheless, in these cDNA clones minor differences were found in comparison to the sequence derived from the human ESTs. Nucleotides 100-104 of the cDNA sequence (numbering according to EMBL/Genbank database entry with accession number Y18863) are 5'-GCGGG-3', while the EST sequence contains an additional nucleotide in this segment 5'-GCGGGG-3'. The resulting frame shift is restored by the presence of an additional C-residue at position 139 in the

cDNA. Finally, a C-residue was found at position 162 of the cDNA rather than a G at this position in the EST sequence, resulting in an alanine codon instead of a glycine at position 46 in the amino acid sequence. Although we can not exclude the possibility that these differences represent genetic polymorphisms, it is more likely that they are due to sequencing errors, which are known to occur relatively frequently in EST sequences. In the complete hPop4 cDNA sequence the coding sequence corresponds to the sequence determined in this study while the UTRs are derived from the EST sequences. At position -20 relative to the start of the poly(A)-tail a putative polyadenylation signal can be found. In conclusion, the combined cDNA is 1133 nucleotides long and encodes a protein of 220 amino acids, with a predicted molecular weight of 25.4 kDa and a predicted pI of 10.9.

To investigate whether the size of the hPop4 cDNA was in accordance with the size of the mRNA, the latter was analyzed by northern blot hybridization using total RNA extracted from a human melanoma cell line. A probe derived from nucleotides 100-590 of the cDNA sequence hybridized to a single mRNA species of about 1.3 kb, which is in good agreement with the length of the cDNA (data not shown).

In Figure 1 an alignment is shown of the amino acid sequences derived from the human, mouse and yeast Pop4 cDNAs. The homology between human and mouse Pop4 proteins is high (83% identity; 90% similarity), while the homology between human and yeast Pop4 is much lower, but still significant (29% identity; 49% similarity). The amino acid conservation between mammalian and yeast Pop4 proteins is most extensive in three blocks in the C-terminal half of the Pop4 protein.

In the hPop4 protein sequence a clustering of basic amino acids is evident between residues 53 and 85, which may contain a functional bipartite nuclear localization sequence (NLS), as in this region three partly overlapping elements matching the bipartite NLS consensus sequence can be discerned.

```
hPop4     1 ---MKSVIYHALSQKEANDSD-------------VQPSGA------QRAEAFVRAFLKRS
mPop4     1 ---MKAAIYHAFSHKEAKDHD-------------VQELGS------QRAEAFVRAFLKQS
yPop4     1 MDRTQTFFIKDCLFTKCLEDPEKPFNENRFQDTLLLLPTDGGLTSRLQRQQRKSKLNLDNL

hPop4    39 TPRMSPQARRDQLQR----------KAVVLEYFTRHK-RKEKKKKAKGLSARQRRELRLF
mPop4    39 IPHMSQEDCESHLQR----------KAVILEYFTRLKPRPRPKKKSKGLSAKQRRDMRLF
yPop4    61 QKVSQLESADKQLEKRDYQRINKNSKIALREYINNCKKNTKKCLKLAYENKITDKEDLLH

hPop4    88 DIKPEQ-------QRYSLFLPLH-ELWKQYIRDLCSGLK--PDTQPQMIQAKLLKADLHG
mPop4    89 DIKPEQ-------QRYSLFLPLH-ELWKQYIRDLCNGLK--PDTQPQMIQAKLLKADLHG
yPop4   121 YIEEKHPTIYESLPQYVDFVPMYKELWINYIKELLNITKNLKTFNGSLALLKLSMADYNG

hPop4   138 AIISVTKSKCPSYVGITGILLQETKHIFKIITKE---DRLKVIPKLNCVFTVET------
mPop4   139 AIISVTKSKCPSYVGVTGILLQETKHVFKIITRE---DHLKVIPKLNCVFTIEI------
yPop4   181 ALLRVTKSKNKTLIGLQGIVIWDSQKFFIMIVKGNIIDEIKCIPKKGTVFQFEIPISDDD

hPop4   189 DGFISY-IYGSKFQLRSSERSAKKFKAKGTIDL------
mPop4   190 DDFISY-IYGSKFQLRASERSAKKFKAKGSIDL------
yPop4   241 DSALRYSILGDRFKYRSVDRAGRKFKSRRCDDMLYYIQN
```

Figure 1. Alignment of amino acid sequences derived from human, mouse and yeast Pop4 cDNAs. Amino acids that are identical in at least two of three proteins are marked by a black box, while amino acids with a conserved character are marked with a gray box. Dashes indicate the absence of corresponding amino acids.

hPop4 accumulates in the nucleoli

To investigate the subcellular localization of hPop4, a VSV-G tag sequence (106) was fused to either the 5'-end or the 3'-end of the hPop4 cDNA and cloned in the mammalian expression vector pCI-neo. The resulting constructs (VSV-hPop4 and hPop4-VSV) were used to transfect HeLa cells and after overnight culturing the localization of the VSV-tagged hPop4 protein was determined via indirect fluorescence confocal microscopy, using a monoclonal anti-VSV-tag antibody. The results, which were identical for both constructs, showed a strong nucleolar and a weak, homogeneous nucleoplasmic staining pattern (Figure 2, panel B). Since the anti-VSV-tag antibody in non-transfected cells generated no signal above background, the observed staining appeared to be specific for the hPop4-VSV protein expressed in transfected cells. To confirm that the nuclear regions most intensely stained by the anti-VSV-tag antibodies represented nucleoli and to investigate whether hPop4 co-localized with hPop1, double immunostaining with affinity-purified anti-hPop1 antibodies (77) was performed (Figure 2, panels A-C). Note that hPop1 is also an RNase MRP and RNase P subunit and therefore co-localization of hPop1, which has previously been shown to accumulate in the nucleolus, and hPop4-VSV would be consistent with an association of hPop4-VSV with these ribonucleoprotein complexes. Indeed a full co-localization of hPop4-VSV and hPop1 was observed (Figure 2, panel C). In conclusion, transiently expressed hPop4-VSV localizes to the nucleus and strongly accumulates in the nucleolar compartment.

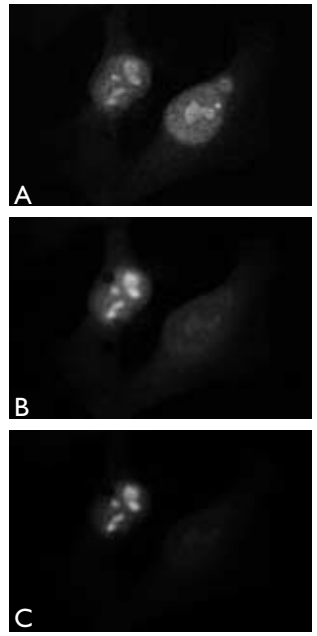

Figure 2. Subcellular localization of hPop4. Double immunofluorescence and confocal microscopy was performed on HeLa cells, which were transiently transfected with hPop4-VSV. Cells were fixed with methanol and stained with affinity-purified anti-hPop1 (77) (A) and anti-VSV (B) antibodies. C. superimposition of panels A and B.

hPop4 is associated with both the RNase MRP and RNase P particles

To determine whether the hPop4 protein is indeed a subunit of the human RNase MRP and the related RNase P particle, immunoprecipitation experiments were performed with epitope-tagged hPop4 protein. HeLa cells were transfected with both VSV-tagged hPop4 constructs and the corresponding empty vector (pCI-neo) as a control. Cell extracts prepared from these cells were used for immunoprecipitation with anti-VSV antibodies, anti-fibrillarin (a protein associated with Box C/D snoRNPs) antibodies, and a patient serum, known to immunoprecipitate both RNase MRP and RNase P complexes (anti-Th/To). RNAs were extracted from immunoprecipitates and from total cell extracts, fractionated by gel electrophoresis and analyzed by northern blot hybridization using probes specific for RNase MRP, RNase P,

U3 (a Box C/D snoRNA) and U1 RNA. As is shown in Figure 3 (lane 3) the RNase MRP and RNase P RNAs are both precipitated by the anti-VSV-tag antibody from a cell extract containing VSV-tagged hPop4 protein. Identical results were obtained for both VSV-tagged hPop4 constructs. The specificity of this result was established by the lack of co-precipitation of U1 and U3 RNA and by the inability of the anti-VSV-tag antibody to co-precipitate RNase MRP or RNase P RNA from extracts of control cells (transfection with pCI-neo vector; Figure 3, lane 7). As expected, the anti-Th/To patient serum immunoprecipitated both the RNase MRP and RNase P RNAs from both types of cell extracts (lanes 2 and 6). The specific immunoprecipitation of U3 RNA by the anti-fibrillarin antibodies (lanes 4 and 8) and the lack of immunoprecipitation of U1 RNA (lanes 2-4 and 6-8) further substantiated the specificity of the assay. Taken together, these results indicate that the VSV-tagged hPop4 protein associates with both the RNase MRP and RNase P particles.

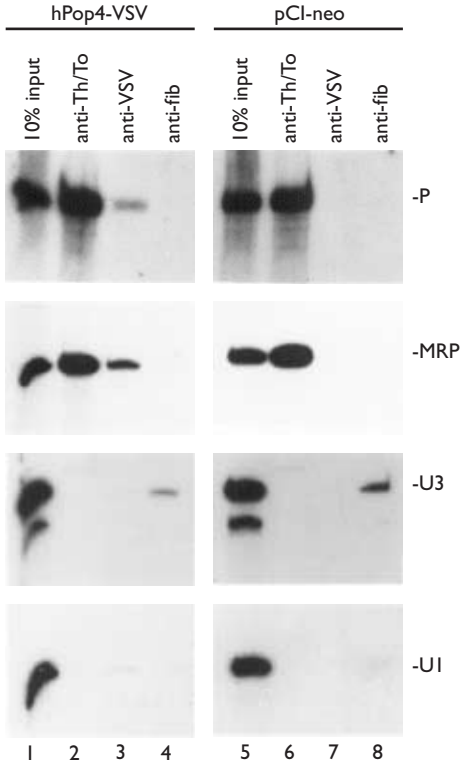

Figure 3. VSV-tagged hPop4 associates with RNase MRP and RNase P. HeLa cells were transfected with hPop4-VSV cDNA construct and the empty vector as a negative control. After overnight culturing, cell extracts used for immunoprecipitation with anti-Th/To, anti-VSV-tag and anti-fibrillarin (anti-fib) antibodies. RNAs were isolated from the immunoprecipitates (lanes 2-4 and 6-8) and from the total cell extracts (lanes 1 and 5) and analyzed by northern blot hybridization using specific probes for RNase P, RNase MRP, U3 and U1 RNA, as indicated on the right. Lanes 1-4, material from cells expressing hPop4-VSV. Lanes 5-8, material from control cells transfected with pCI-neo. The amounts of the RNAs analyzed in lanes 1 and 5 corresponds to 10% of the amounts of extracts used for immunoprecipitations (10% input). The faint U1 snRNA band observed in lane 3 is due to some non-specific co-precipitation with the anti-VSV antibody.

Anti-hPop4 antibodies immunoprecipitate both RNase MRP and RNase P particles

To exclude the possibility that association of hPop4-VSV with the RNase MRP and RNase P particles was due to overexpression of the protein in the transiently transfected HeLa cells, a polyclonal antiserum was raised against recombinant hPop4 to study the endogenous non-tagged hPop4 protein. The hPop4 protein was expressed as a fusion protein with Gluthatione S-Transferase (GST) in *Escherichia coli*, which was designated GST-hPop4. After purification using Gluthathione-Sepharose-4B beads, GST-hPop4 (Figure 4, lane 1) was used to immunize rabbits. Western blot analysis showed that the resulting rabbit antisera, in contrast to the corresponding pre-immune sera, recognized not only the recombinant GST-hPop4, but also the hPop4 protein expressed in HeLa cells (Figure 4). Besides the band representing the GST-hPop4 protein, some faster migrating bands in the recombinant material were recognized by the anti-hPop4 antisera as well. These bands are most probably due to proteolytic degradation of the GST-hPop4 protein during the purification and may in part be stained due to anti-GST activity in the sera. Note that the endogenous hPop4 protein of HeLa cells migrated at approximately 30 kDa in SDS-PAGE gels.

To investigate whether hPop4 is a subunit of both the endogenous RNase MRP and RNase P particles, immunoprecipitations were performed with this anti-hPop4 antiserum using total HeLa cell extracts. The co-precipitating RNAs were isolated and analyzed by northern blot hybridization using probes specific for RNase MRP, RNase P and U3 RNA. As depicted in Figure 5 (lane 4) the anti-hPop4 antiserum efficiently immunoprecipitated both the RNase MRP and RNase P RNA components, while the pre-immune serum did not immunoprecipitate any of the RNAs analyzed (Figure 5, lane 5). The specificity of the antiserum was substantiated by the observations that a control polyclonal rabbit antiserum (lane 3) did not detectably precipitate RNAs, while a patient anti-Th/To antiserum as well as rabbit anti-hPop1 antiserum did co-immunoprecipitate the RNase MRP/RNase P RNAs (lanes 2 and 6).

In conclusion, these results fully support previous findings that hPop4 is a component of both RNase MRP and RNase P.

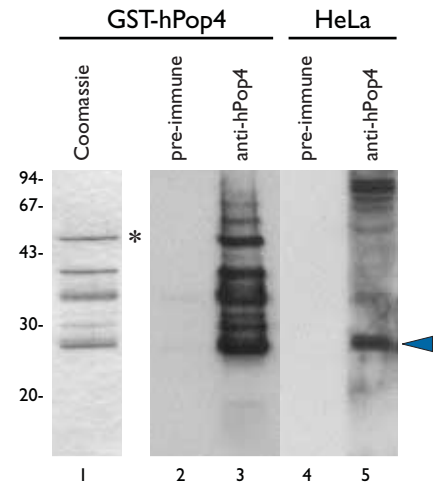

Figure 4. Western blot analysis of rabbit antiserum raised against GST-hPop4. Rabbit antisera were raised against recombinant GST-hPop4 fusion protein expressed in *E. coli*. GST-hPop4 protein (lane 1 shows the recombinant protein preparation stained with Coomassie Brilliant Blue) was separated by 13% SDS-PAGE and transferred to nitrocellulose filters. After incubation with anti-hPop4 antiserum (lane 3) or pre-immune serum (lane 2), bound antibodies were visualized with horseradish peroxidase-conjugated goat anti-rabbit antibodies and chemiluminescence. The reactivity of the antiserum with proteins from a total HeLa extract was analyzed also by western blotting: anti-hPop4 (lane 5) and pre-immune serum (lane 4). On the left, the molecular weights of protein markers are indicated. The full-length GST-hPop4 protein band is indicated with an asterisk, while the blue arrow points to the HeLa hPop4 protein.

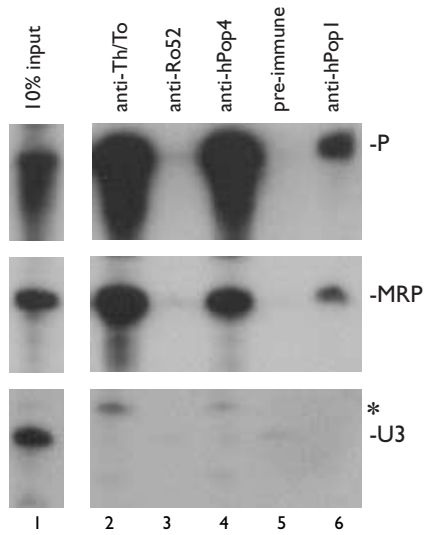

Figure 5. Anti-hPop4 antiserum co-immunoprecipitates the RNA components of RNase MRP and RNase P. RNPs were immunoprecipitated from a total HeLa cell extract using anti-Th/To (lane 2), anti-Ro52 (lane 3), anti-hPop4 (lane 4), pre-immune (lane 5) and anti-hPop1 (lane 6) antisera. Co-precipitating RNAs and RNA from total extract were isolated, resolved by denaturing polyacrylamide gel electrophoresis and analyzed by northern blotting using riboprobes specific for human RNase P, RNase MRP and U3 RNA, as indicated on the right. The signals marked with an asterisk, are due to incomplete removal of the RNase P probe prior to the incubation with the U3 RNA probe.

Anti-hPop4 antibodies immunoprecipitate RNase P enzymatic activity

Having demonstrated that the anti-hPop4 antibodies specifically immunoprecipitate the RNase MRP and RNase P RNAs from total HeLa cell extracts, we analyzed whether the immunoprecipitates contained any RNase P enzymatic activity. Immunoprecipitates were incubated with a ^{32}P-labeled pre-tRNA. The products of this reaction were resolved on a denaturing polyacrylamide gel and visualized using autoradiography. The results in Figure 6 show that the anti-hPop4 antibodies are indeed able to immunoprecipitate the enzymatically active RNase P complexes, as the pre-tRNA is specifically cleaved into mature tRNA and the 5'-leader. The capability to immunoprecipitate this activity was indistinguishable from that of the anti-hPop1 antiserum, which was used as a positive control. In contrast, the pre-tRNA incubated with the immunoprecipitate of either the pre-immune serum or a control antiserum was not processed (lanes 2 and 4). We conclude that the hPop4 protein is associated with a catalytically active form of RNase P.

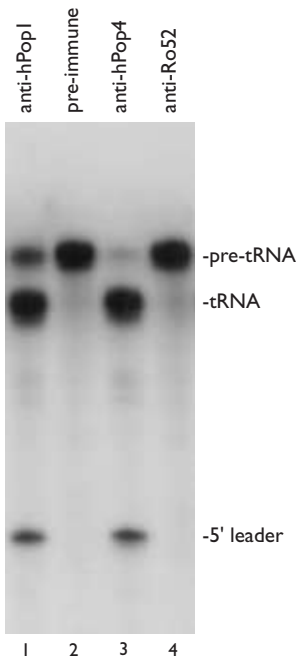

Figure 6. Anti-hPop4 antibodies immunoprecipitate enzymatically active RNase P. Anti-hPop1 (lane 1), pre-immune (lane 2), anti-hPop4 (lane 3) and anti-Ro52 (lane 4) sera were used for immunoprecipitations from total HeLa cell extract. Immunoprecipitates were assayed for RNase P enzymatic activity by incubating with a ^{32}P-labeled pre-tRNA substrate. Subsequently, the RNAs were isolated and resolved by denaturing polyacrylamide gel electrophoresis and visualized by autoradiography. On the right, the positions of the pre-tRNA, the mature tRNA and the 5'-leader sequence are indicated.

Discussion

We have identified and cloned a new subunit of the human RNase MRP particle, which is also associated with the evolutionarily related RNase P particle. The new subunit exhibits homology to the yeast Pop4 protein and was therefore designated hPop4. We showed that the subcellular localization of hPop4 is primarily nucleolar and that this protein is associated with catalytically active RNase P particles.

Amino acid sequence of hPop4

While a high degree of amino acid sequence conservation was observed between the human and putative mouse Pop4 polypeptides, the human and yeast Pop4 sequences are only moderately homologous (29% identity), which is, however, slightly higher than the degree of sequence conservation observed for other RNase MRP/RNase P proteins, like hPop1/Pop1 (22% identity) (77), Rpp30/Rpp1 (23% identity) (33) and Rpp20/Rpp2 (14% identity) (36). Sequence analysis did not reveal the presence of known protein sequence motifs in the mammalian Pop4 polypeptides, apart from putative nuclear localization sequences. The most conserved regions are found in the C-terminal half of the protein. Within this region an evolutionarily conserved cluster of basic amino acids is found near the C-terminus. Recently, Chamberlain *et al*. (38) identified an element consisting of two contiguous lysine residues preceded or followed by an additional lysine at a distance of 3-8 intervening residues, which is found in all known RNase P proteins, except Rpp1p (33,38). Several sequences corresponding to this element are present in hPop4 and mPop4 and a few of such elements are found at an equivalent position in yeast. This element is also found in some ribosomal proteins and might be involved in protein-RNA association or protein-protein interactions.

Interestingly, the phenylalanine at position 207 of yPop4, which has been demonstrated to be mutated in the yeast strain that led to the identification of this protein (34), is not conserved in the human and mouse Pop4 proteins. The substitution of the phenylalanine by either a leucine or a serine in yPop4 enabled the protein to suppress the rrp2-2 phenotype, which is due to a mutation in the RNA component of the RNase MRP. The authors suggested that this amino acid substitution somehow compensated the functional defect of the base substitution in the RNA component of RNase MRP. The proposed direct interaction between the yPop4 protein and the RNase MRP RNA may not be found for the human RNase MRP RNA and hPop4, as the region of the RNase MRP RNA that is mutated in the rrp2-2 strain is not present in the human RNase MRP RNA (28).

The hPop4 sequence described in the present study is further supported by a recent paper, in which the cDNA sequence of a protein called Rpp29 has been described. Rpp29 has been isolated as a protein subunit of the human RNase P particle, which is homologous to yeast Pop4p (79). Sequence comparison revealed that Rpp29 is almost identical to hPop4, as might be anticipated by their mutual homology with yPop4. Only two differences were observed between the hPop4 and Rpp29 protein sequences. Human Pop4 contains a serine at position 38 and a leucine at position 76, while in the sequence of Rpp29 these amino acids are substituted by a threonine and a phenylalanine, respectively. The presence of the serine and the leucine at these positions in hPop4 is supported by the identity of the equivalent amino acids in the predicted sequence for mPop4, which are also a serine and a leucine (Figure 1). Based upon both their sequences (the hPop4 and Rpp29 cDNAs differ only by 6 nucleotides) and biochemical characteristics it is highly likely that hPop4 and Rpp29 represent the same protein. At present, it is unclear whether the small sequence differences between hPop4 and Rpp29 are due to imperfect cDNA sequences or to a genetic polymorphism.

Nucleolar accumulation of hPop4

The nucleolar accumulation observed for VSV-tagged hPop4 is in agreement with the association of the hPop4 protein with the RNase MRP and RNase P particles. Previously, it has been proposed that accumulation of proteins in the nucleoli is a two-step process (107-109). First, a nucleolar protein is transported from the cytoplasm to the nucleoplasm, which is dependent on an NLS, and subsequently functional domains that interact specifically with other nucleolar components mediate nucleolar entry. The subcellular localization of the RNase MRP particle has been determined to be primarily nucleolar, while only a minority of

RNase MRP complexes has been reported to reside in the mitochondria (26,72,110). We could, however, not detect any staining above background in the cytoplasm of HeLa cells, in agreement with biochemical fractionation data which did not show a significant portion of the RNase MRP RNA in the mitochondria of HeLa cells (72). RNase P has been reported to be localized in both the nucleoplasm and nucleolus and recent studies indicate that the majority of RNase P is localized in the nucleolus (60), strongly suggesting that at least some aspects of pre-tRNA processing occur in the nucleolar compartment.

hPop4 is shared by RNase MRP and RNase P

In yeast Pop1p, Pop3p, Pop4p, Pop5p, Pop6p, Pop7p/Rpp2p, Pop8p and Rpp1p are protein subunits associated with both RNase MRP and RNase P (36,38). In addition, two yeast proteins have been identified, which are specifically associated with either RNase MRP (Snm1p) (32) or RNase P (Rpr2p) (38). Presently such particle-specific proteins have not been identified in mammals yet.

In agreement with the association of yeast Pop4 with both particles, we showed that its human counterpart, hPop4, is also a subunit of both RNase MRP and RNase P and is associated with catalytically active RNase P. Also the Rpp29 protein, which is most likely identical to hPop4, has recently been reported to be associated with (catalytically active) RNase P (79). The capability to immunoprecipitate enzymatically active RNase P has been reported before for antibodies directed against the hPop1, Rpp20, Rpp30, Rpp38 and Rpp40 protein subunits of RNase P (77,78,80).

The hPop4 protein is probably not directly bound to the RNase MRP and RNase P RNA components, since recent immunoprecipitation experiments using the anti-hPop4 antiserum failed to detect a radiolabeled polypeptide comigrating in SDS-PAGE with hPop4 after UV-crosslinking of RNase MRP particles reconstituted with radiolabeled RNase MRP RNA (our unpublished observations). With the latter type of experiments we recently identified three human proteins with apparent molecular weights of 20, 25 and 40 kDa, that directly interact with the RNase MRP RNA (105). These data suggest that the association of the hPop4 protein with these ribonucleoprotein particles might be mediated by protein-protein interactions. Further studies will be required to elucidate the molecular interactions that determine RNase MRP architecture.

Acknowledgements

We thank Drs. Helma Pluk and Wiljan Hendriks (Dept. of Celbiology, University of Nijmegen) for useful discussions and suggestions and Ben de Jong and Rolf Janssen for technical assistance. We are grateful to Dr. Winfried Degen and Carla Onnekink for providing the northern blot with total human RNA. The patient sera were kindly provided by Dr. Frank van den Hoogen (Dept. of Rheumatology, University of Nijmegen). We thank Dr. Bertrand Séraphin (EMBL, Heidelberg) for providing us with the pre-tRNA substrate and Dr. Marc Monestier (Department of Microbiology and Immunology, Temple University School of Medicine, Philadelphia) for the anti-fibrillarin monoclonal antibody ASWU1. This work was supported by the Netherlands Foundation for Chemical Research (NWO-CW) with financial aid from the Netherlands Organization for Scientific Research (NWO).

Materials and Methods

Accession number

The hPop4 cDNA described in this report has been deposited in the EMBL database under accession number Y18863.

cDNA cloning and sequence analysis

Database searches were done using the BLASTN 2.0.5 program (111). The accession numbers of the overlapping human Expressed Sequence Tags (ESTs) are N40691, AA134865, W74573, AA308539, AA132996 and AA576911. The accession numbers of the overlapping mouse ESTs are W66853, W46039, AA1990967, AA929907 and W15729.

Oligonucleotides were designed based on the human EST sequences to amplify the open reading frame of hPop4: pop41 [5'-GCG-GAT-CCC-TCG-AGA-TGA-AGA-GTG-TGA-TCT-ACC-ATG-CAT-TG-3'] and pop42 [5'-GCG-GAT-CCC-CCG-GGT-CAT-CTA-GAC-AGG-TCA-ATC-GTT-CCC-TTC-GC-3']. The polymerase chain reaction was performed on 200 ng denatured DNA from λgt11 human placenta (Clontech) and teratocarcinoma cDNA libraries (112). The amplified fragments were ligated in the PCR-II-TOPO vector (Invitrogen) and sequenced using the dideoxynucleotide chain termination method.

Transfection constructs

Vesicular stomatitis virus G epitope (106) (VSV-G)-tagged (hereafter referred to as VSV-tagged) cDNAs were constructed as follows. The VSV-55k and 55k-VSV cDNA constructs, as described in (113), contain a *Xho*I and a *Xba*I-site, respectively, between the 55k open reading frame (ORF) and the VSV-tag sequence, which is positioned either at the N-terminal or at the C-terminal side of the ORF. Digestion by either *Xho*I/*Sma*I or *Xho*I/*Xba*I results in release of the 55k-cDNA from these plasmids. The VSV-tagged constructs of hPop4 were constructed by isolation of the hPop4 ORF from the hPop4/PCR-II-TOPO construct by either *Xho*I/*Sma*I or *Xho*I/*Xba*I digestion and ligation into the *Xho*I/*Sma*I or *Xho*I/*Xba*I digested VSV-55k or 55k-VSV constructs. The integrity of the resulting constructs was checked by DNA sequencing. The pCI-neo plasmid (Promega), which has been used previously to prepare VSV-55k and 55k-VSV, was used as a control in the transfection experiments.

Transient Transfection of HeLa cells

HeLa monolayer cells were grown to 80% confluency by standard tissue culture techniques and subsequently $3x10^6$ cells were transfected with 10 µg plasmid DNAs in a total volume of 400 µl of Dulbecco's modified Eagle's medium containing 10% fetal calf serum. Electroporation was performed at 276 V and a capacity of 950 µF with a Gene Pulser II (BioRad). After electroporation, cells were resuspended in 10 ml of Dulbecco's modified Eagle's medium containing 10% fetal calf serum and grown overnight either on coverslips or in flasks.

Cells grown on coverslips were washed twice with phoshate-buffered saline (PBS), fixed with methanol (5 min at -20°C) and used for immunofluorescence assays.

Cells grown in flasks were harvested, washed once with PBS and used to prepare extracts for immunoprecipitation assays.

Immunofluorescence

Indirect immunofluorescence assays were performed on hPop4-VSV transfected HeLa cells. Fixed cells were incubated with affinity-purified rabbit anti-hPop1 antibodies ((77), diluted 1:100 in PBS) and affinity-purified mouse anti-VSV tag antibodies (Boehringer, diluted 1:50 in PBS) for 1 h at room temperature, washed with PBS and subsequently incubated with swine-anti-rabbit coupled to FITC (diluted 1:50 in PBS) and rabbit-anti-mouse

coupled to TRITC (diluted 1:50 in PBS) for 1 h at room temperature. Cells were mounted with PBS/glycerol containing Mowiol and bound antibodies were visualized by confocal microscopy.

Preparation of HeLa cell extracts

Extracts of HeLa cells were prepared by resuspending cell pellets in buffer A (25 mM Tris-HCl pH 7.5, 100 mM KCl, 1 mM dithioerythritol, 2 mM EDTA, 0.5 mM phenylmethylsulfonyl fluoride, 0.05% NP-40) and lysis by sonification using a Branson microtip (three times 20 s). Insoluble material was removed by centrifugation (12,000 g, 15 min) and supernatants were used directly for immunoprecipitations.

Anti-hPop4 antiserum

To raise a polyclonal anti-hPop4 antiserum, the hPop4 protein was expressed as a fusion protein with Glutathione S-Transferase (GST) in *E.coli* and purified as described previously (114). Rabbits were immunized with this material according to standard procedures (115). For each immunization 200 µg of GST-hPop4 was used.

Western blot analysis

For western blot analysis the anti-hPop4 and pre-immune sera were used in a 500-fold dilution in the presence of 1% normal goat serum. Detection was performed using horseradish peroxidase-conjugated goat-anti-rabbit IgG (Dako Immunoglobulins) as secondary antibody and visualization by chemiluminescence.

Immunoprecipitation and pre-tRNA processing assay

Monoclonal anti-VSV-tag (Boehringer) and anti-fibrillarin ASWU1 (a kind gift of Dr. M. Monestier) antibodies, patient anti-Th/To serum, and rabbit anti-hPop4, anti-hPop1, anti-Ro52 and pre-immune serum from the rabbit immunized with hPop4 protein were coupled to protein A-agarose beads (Biozym) in IPP500 (500 mM NaCl, 10 mM Tris-HCl pH 8.0, 0.05% NP-40) by incubation for 2 h at room temperature. Beads were washed twice with IPP500 and once with IPP150 (150 mM NaCl, 10 mM Tris-HCl pH 8.0, 0.05% NP-40). For each immunoprecipitation cell extract was incubated with the antibody-coupled beads for 2 h at 4°C. Subsequently, beads were washed three times with IPP150.

To analyze co-precipitating RNAs, the RNA was isolated by phenol-chloroform extraction and ethanol precipitation. RNAs were resolved on a denaturing polyacrylamide gel and blotted to a Hybond-N membrane (Amersham). Northern blot hybridizations with riboprobes specific for human RNase P, RNase MRP, U3 and U1 RNAs were performed as previously described (116).

To assay for RNase P enzymatic activity in the immunoprecipitates, an internally ^{32}P-labeled pre-tRNA substrate (*S.pombe* tRNA^{Ser} SupS1; (117)), a kind gift of Dr. B. Séraphin, was transcribed in vitro and gel-purified. This 110 nt-long substrate contains a 5'-end extension of 28 nts in comparison with the mature tRNA. The immunoprecipitates were incubated with equal amounts of substrate in assay buffer (20 mM Tris-HCl pH 8.0, 10 mM $MgCl_2$, 1 mM DTE, 50 mM KCl, 50 mg/ml BSA, 60 U/ml RNasin) for 10 minutes at 37°C under constant agitation. RNA was subsequently isolated by phenol-chloroform extraction and ethanol precipitation and analyzed by denaturing polyacrylamide gel electrophoresis and autoradiography.

Chapter 3

hPop5, a protein subunit of the human RNase MRP and RNase P endoribonucleases

Hans van Eenennaam
Dorien Lugtenberg
Judith H.P. Vogelzangs
Walther J. van Venrooij
Ger J.M. Pruijn

Journal of Biological Chemistry (2001) 276: 31635-31641.

Abstract

The RNase MRP and RNase P particles both function as endoribonucleases. RNase MRP has been implicated in the processing of precursor-rRNA, whereas RNase P has been shown to function in the processing of pre-tRNA. Both ribonucleoprotein particles have an RNA component that can be folded into a similar secondary structure and share several protein components.

We have identified human, rat, mouse, cow and Drosophila homologues of the Pop5p protein subunit of the yeast RNase MRP and RNase P complexes. The human Pop5 cDNA encodes a protein of 163 amino acids with a predicted molecular mass of 18.8 kDa. Polyclonal antibodies raised against recombinant hPop5 identified a 19 kDa polypeptide in HeLa cells and showed that hPop5 is associated with both RNase MRP and RNase P. Using affinity-purified anti-hPop5 antibodies we demonstrated that the endogenous hPop5 protein is localised in the nucleus and accumulates in the nucleolus, which is consistent with its association with RNase MRP and RNase P. Catalytically active RNase P was partially purified from HeLa cells and hPop5 was shown to be associated with it. Finally, the evolutionarily conserved acidic C-terminal tail of hPop5 appeared to be neither required for complex formation nor for RNase P activity.

Introduction

The RNase MRP/RNase P ribonucleoprotein particles form one of the three families of small nucleolar ribonucleoprotein complexes that are involved in the processing of precursor-rRNA to mature 5.8S, 18S and 25/28S rRNA (reviewed in ref. (5)). The RNase MRP ribonucleoprotein particle has originally been identified by virtue of its capacity to cleave a mitochondrial RNA *in vitro* to generate RNA primers for mitochondrial DNA replication (22). However, most of the RNase MRP complex has been shown to reside in the nucleolus (26,72). There it functions in the formation of the short form of the 5.8S rRNA (5.8S(S)) by cleaving at site A3 in the internal transcribed spacer 1 (ITS1) of precursor-rRNA (28-30,37). In many different aspects, the RNase MRP complex is related to the RNase P complex, a ribonucleoprotein complex required for the removal of the 5'-end of the precursor tRNAs. Both function as site-specific endonucleases, contain an RNA component that has been proposed to adopt a similar cage-shaped structure, share several protein subunits and are predominantly

localised in the nucleolus (reviewed in ref. (118)).

The biological importance of the RNase MRP function is substantiated by the recent observations that mutations in the gene encoding the RNA component of the human RNase MRP complex cause an autosomal recessive disease called cartilage-hair hypoplasia (119). In addition, RNase MRP and RNase P play a role in certain autoimmune diseases. Protein components of the RNase MRP and RNase P complexes are targeted by autoantibodies in systemic lupus erythematosus and scleroderma (61,62,64,65,104).

The first identified protein subunit of the human RNase MRP and RNase P complexes is the hPop1 protein, which is a homologue of the yeast Pop1p protein (77). Most of the currently known human protein subunits of the RNase MRP and RNase P complexes have been identified via purification of the RNase P complex from HeLa cells: Rpp14, Rpp20, Rpp29/hPop4, Rpp30, Rpp38 and Rpp40 (78-80,120). In yeast ten proteins have been found to be associated with either RNase MRP, RNase P or with both complexes (reviewed in ref. (118)). Snm1p has been reported to be associated specifically with the RNase MRP complex, whereas the Rpr2p protein is only bound to the RNase P complex (32,38). Other subunits shared by RNase MRP and RNase P in yeast are: Pop1p, Pop7p/Rpp2p, Pop4p, Rpp1p, Pop3p, Pop5p, Pop6p and Pop8p (33-38). Although homologues for several of the yeast proteins are found in human cells (Pop1p, Pop4p, Pop7p/Rpp2p, Rpp1p), until now no homologues have been identified for Snm1p, Pop3p, Pop5p, Pop6p, Pop8p and Rpr2p (reviewed in ref. (118)). In this report we describe the identification, cDNA cloning and characterization of the human Pop5 protein, which, like all human protein subunits identified so far, is associated with both RNase MRP and RNase P RNAs.

Results

Identification of homologues of yeast Pop5p

Purification of the yeast RNase P holoenzyme has resulted in the identification of nine protein subunits (38). Although some of these were shown to have homologues in humans, no human homologues have been reported for Snm1p, Pop3p, Pop5p, Pop6p, Pop8p and Rpr2p. We have searched protein and 'translated nucleic acid' sequence databases to identify sequences that might represent human homologues of these yeast protein subunits.

Four virtually identical nucleic acid entries were found that encode a putative human homologue of the yeast Pop5p protein (hereafter designated yPop5). The latter polypeptide consists of 173 amino acids and has a predicted molecular mass of 19.6 kDa. The corresponding human sequence (database entry AF117232) is 785 nt long and contains an ORF encoding a polypeptide of 162 amino acids with a predicted molecular mass of 18.7 kDa. For reasons documented below this protein will be referred to as hPop5.

Besides the human ESTs retrieved from the sequence databases, two mouse ESTs, two rat ESTs, one cow EST and one *Drosophila melanogaster* entry that encode putative homologues of the yeast Pop5p protein were identified. These entries contain ORFs of 169, 169, 170 and 145 amino acids, respectively.

Cloning of the human Pop5 cDNA

To obtain a cDNA encoding the putative human Pop5 protein, two oligonucleotides were designed based on the identified human EST sequence. These oligonucleotides were used as PCR primers to isolate hPop5 cDNAs from human teratocarcinoma and placenta cDNA libraries. Sequence analysis of several clones obtained by this procedure revealed that cDNAs derived from both sources were identical, thereby ruling out the introduction of PCR artefacts. Two minor differences were found in all sequenced cDNAs in comparison with the corresponding EST described above (AF117232). Nucleotides 154-162 in the cloned cDNA sequence (numbering according to database accession no. AJ306296) are 5'-GCA·GCC·GCC-3', whereas the EST contains 5'-GCA·CCC-3' at this position, resulting in the replacement of a Pro-codon by two Ala-codons in the cloned cDNA in comparison with the EST. Furthermore, a single nucleotide substitution was detected at position 461, where a T residue was found rather than a C residue, which is observed at this position in the human EST.

To determine whether the first ATG present in the human EST represents the translational start codon, we synthesised cDNA from several sources of mRNA. DNA sequencing of the resulting clones revealed that no additional sequence information was obtained (data not shown). The cloned cDNA encodes a protein of 163 amino acids, with a predicted molecular mass of 18.8 kDa and a predicted pI of 7.9.

In Figure 1 an alignment of the amino acid sequences derived from the human, cow, rat, mouse, *Drosophila* and yeast cDNAs/ESTs is shown. This illustrates the high level of homology between the mammalian Pop5 polypep-

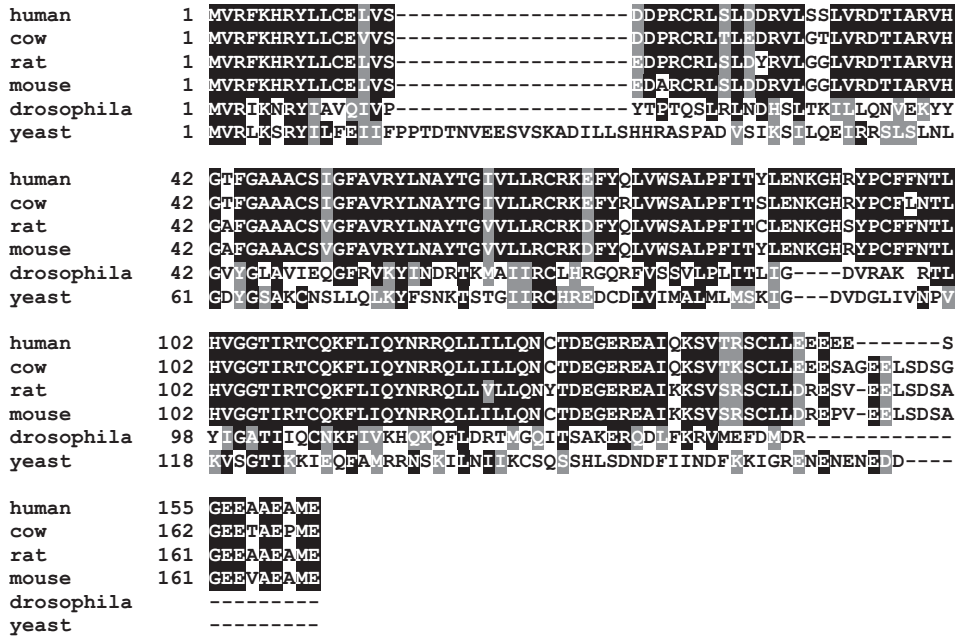

Figure 1. Alignment of amino acid sequences derived from human, cow, rat, mouse, *Drosophila* and yeast (*Saccharomyces cerevisiae*) Pop5 cDNAs. Amino acids that are identical in at least four of six proteins are marked by a black box, whereas related amino acids are marked with a grey box. Dashes indicate the absence of amino acids.

tides (88-91% identity, 93-95% similarity), whereas the homology between the human, Drosophila and yeast proteins is much lower (23-27% identity and 40-43% similarity). The conservation of the yeast and human Pop5 amino acid sequences is most extensive in the N-terminus. Except for the acidic C-terminus, the primary sequence of hPop5 does not reveal established sequence motifs. The acidic nature of the C-terminus is conserved from human to yeast (in hPop5 9 out of 15 residues are acidic), although it it appears to be absent in the *Drosophila* sequence.

Anti-hPop5 antibodies immunoprecipitate both RNase MRP and RNase P particles

To determine whether the hPop5 protein is associated with the human RNase MRP and RNase P ribonucleoprotein particles, a polyclonal antibody was raised against recombinant hPop5. The hPop5 protein was expressed as a fusion protein with GST in *E. coli*. The recombinant GST-hPop5 fusion protein was purified using glutathione-Sepharose 4B beads (Figure 2, lane 2) and used for immunisation of rabbits. Western blot analysis showed that the resulting rabbit serum is reactive with the GST-hPop5 protein (lane 4), whereas the pre-immune serum is not (lanes 3). Because the rabbit serum failed to recognise the hPop5 protein in HeLa extracts (data not shown), anti-hPop5 antibodies were purified by affinity selection with recombinant GST-hPop5 from the rabbit serum. Prior to the GST-hPop5 selection the rabbit serum was depleted of anti-GST activity by performing affinity selection with recombinant GST. Western blot analysis of HeLa cell extracts with the affinity-purified antibodies against hPop5 revealed a single protein with an estimated size of 19 kDa (lane 6), whereas the affinity-purified antibodies against GST failed to detect any protein in HeLa extracts (lane 5).

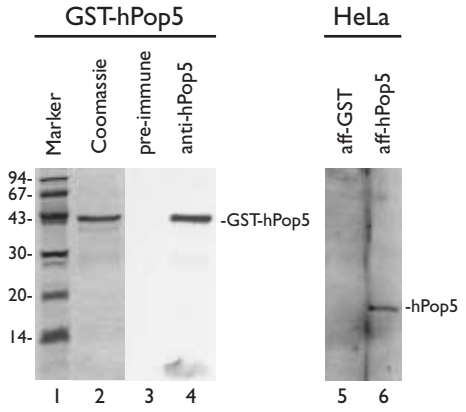

Figure 2. HeLa cells express a 19 kDa hPop5 polypeptide. A rabbit antiserum was raised against recombinant GST-hPop5 fusion protein expressed in *E. coli*. Lane 2 shows the recombinant GST-hPop5 protein preparation stained with Coomassie Brilliant Blue. The GST-hPop5 protein was efficiently recognized by the anti-hPop5 antiserum (lane 4) on western blots. As a control the reactivity of the corresponding pre-immune serum is shown in lane 3. The anti-GST and anti-hPop5 antibodies and their reactivity with proteins from a total HeLa cell extract was analysed by western blotting (lanes 5 and 6, respectively). Lane 1 contains molecular weight marker proteins.

To investigate whether the hPop5 protein is associated with the RNase MRP and RNase P complexes, immunoprecipitations with the anti-hPop5 serum using total HeLa cell extract were performed. The co-precipitating RNAs were isolated and analysed by northern blot hybridisation using riboprobes specific for RNase MRP, RNase P and U3 RNA. As depicted in Figure 3 (lane 6), the anti-hPop5 antiserum efficiently immunoprecipitated both RNase MRP and RNase P RNAs, whereas no detectable precipitation of U3 RNA was observed. The specificity of this assay was demonstrated by the observation that pre-immune serum did not precipitate any of the RNAs analysed (lane 5) and that anti-55K antibodies specifically precipitated U3 RNA (lane 3) in accordance with previous observations (113). In addition, the RNase MRP and RNase P RNAs were co-immunoprecipitated by a patient anti-Th/To antiserum and by anti-hPop4 antibodies (lanes 2 and 4). These results indicate that the 19 kDa hPop5 protein is associated with both RNase MRP and RNase P RNAs in HeLa cells.

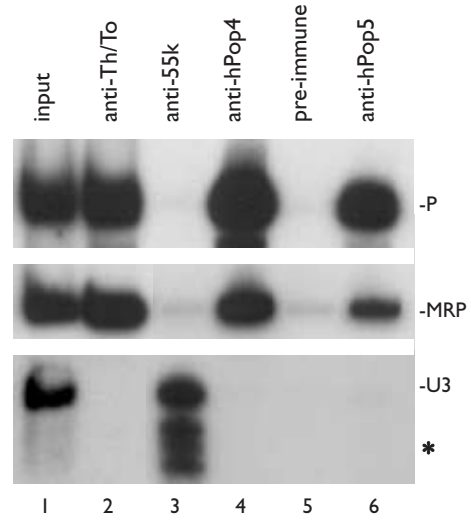

Figure 3. hPop5 is associated with the RNA components of RNase MRP and RNase P. RNPs were immunoprecipitated from a total HeLa cell extract using anti-Th/To (lane 2), anti-55K (lane 3), anti-hPop4 (lane 4), pre-immune (lane 5) and anti-hPop5 (lane 6) antisera. Co-precipitating RNAs and RNAs from total extract (lane 1) were isolated, resolved by denaturing polyacrylamide gel electrophoresis and analyzed by northern blotting using riboprobes specific for human RNase P, RNase MRP and U3 RNA, as indicated on the right. The signals marked with an asterisk represent degradation products of the U3 RNA.

hPop5 accumulates in the nucleoli

To investigate the subcellular localization of the hPop5 protein, the affinity-purified antibodies directed against GST-hPop5 and GST were used for immunolocalisation experiments in HEp-2 cells. The affinity-purified anti-hPop5 antibodies strongly stained the nucleoli and showed in addition a fine-speckled cytoplasmic staining (Figure 4, panel A). Using affinity-purified anti-GST antibodies a similar fine-speckled cytoplasmic staining pattern, but no nucleolar staining was observed (panel C), strongly suggesting that the cytoplasmic staining is caused by anti-GST reactivity. Although these results do not completely rule out a cytoplasmic localization of the hPop5 protein, they clearly show that the hPop5 protein accumulates in the nucleoli, consistent with its association with RNase MRP and RNase P.

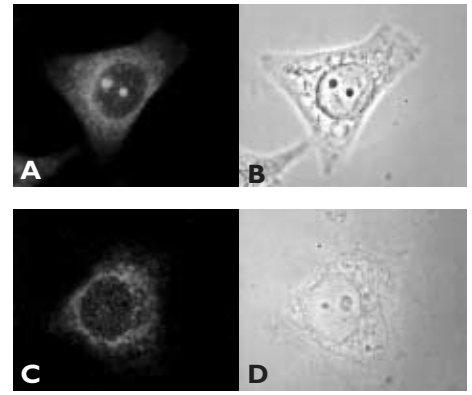

Figure 4. Subcellular localisation of the hPop5 protein. HEp-2 cells were fixed and stained with affinity-purified anti-hPop5 (panel A) or affinity-purified anti-GST (panel C) antibodies. The corresponding phase-contrast images are shown in panels B and D, respectively.

Anti-hPop5 antibodies immunoprecipitate catalytically active RNase P

To obtain further evidence that the hPop5 protein is part of the complete RNase P complex, we tested whether hPop5 is associated with catalytically active RNase P. First, we partially purified the active RNase P complex from a HeLa cell extract by DEAE-Sepharose chromatography and glycerol gradient centrifugation. The fractions of the glycerol gradient were tested for RNase P activity by monitoring

its ability to specifically cleave an internally labelled precursor-tRNA substrate to tRNA and its 5'-leader. Products of this reaction were separated on a denaturing polyacrylamide gel and visualised by autoradiography. In agreement with previous observations (63,78), the RNase P activity was only detected in relatively fast sedimenting fractions (Figure 5A). To study the presence of the hPop5 protein in the active RNase P fractions of the glycerol gradient, these fractions were analysed by immunoblotting. As shown in the lower part of Figure 5A, hPop5 (bottom panel), hPop4 (middle panel) and Rpp38 (top panel) co-fractionated with the RNase P activity, suggesting that hPop5 indeed is associated with catalytically active RNase P. To confirm this, immunoprecipitations were performed on RNase P containing glycerol gradient fractions using affinity-purified anti-hPop5 and anti-GST antibodies and the immunoprecipitates were assayed for RNase P activity. As shown in

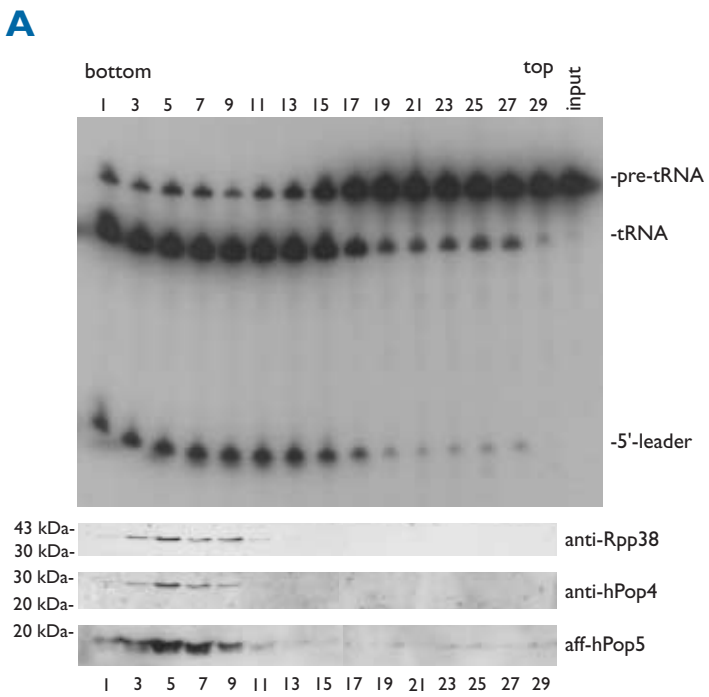

← **Figure 5.** hPop5 associates with catalytically active RNase P. The RNase P holoenzyme was purified from a total HeLa extract by DEAE-Sepharose column chromatography followed by glycerol gradient centrifugation.

A. Top panel: Fractions of the glycerol gradient (1-29) were assayed for RNase P activity by incubation with a ^{32}P-labelled pre-tRNA substrate (input). Subsequently, the reaction products were analysed by denaturing polyacrylamide gel electrophoresis and autoradiography. On the right, the positions of the pre-tRNA, the mature tRNA and the 5'-leader are indicated.

Bottom part: Detection of RNase MRP/RNase P proteins in glycerol gradient fractions. Reactivity with affinity-purified anti-hPop5 (bottom), anti-hPop4 (middle) and anti-Rpp38 (top) antisera with proteins from glycerol gradient fractions was analysed by western blotting. On the left the positions of molecular weight markers are indicated and on the right the antisera that were used.

B. Anti-hPop4 (lanes 1 and 5), affinity-purified anti-GST (lanes 2 and 6) and affinity-purified anti-hPop5 (lanes 3 and 7) antibodies were used for immunoprecipitations using fraction 5 of the glycerol gradient. Immunoprecipitates (IPP) and supernatants were assayed for RNase P activity (lanes 1-3 and lanes 5-7, respectively). On the right, the positions of the pre-tRNA, the mature tRNA and the 5'-leader are indicated.

→ **Figure 6.** The C-terminus of hPop5 is neither required for complex association nor for RNase P activity. HEp-2 cells were transfected with constructs encoding hPop5, hPop5 Δ(145-163) and the corresponding 'empty' vector as a negative control and extracts of these cells were subjected to immunoprecipitation with anti-VSV antibodies.

A. Association of VSV-tagged hPop5 and the C-terminal deletion mutant of hPop5 with RNase MRP and RNase P complexes. Lanes 1 and 4, empty vector; lanes 2 and 5, hPop5; lanes 3 and 6, hPop5 Δ(145-163). RNA isolated from extract (input; lanes 4-6) and immunoprecipitates (IPP; lanes 1-3) was analysed by northern blotting using riboprobes for RNase MRP and RNase P RNA, as indicated on the right.

B. RNase P activity was assayed as described in the legend of Figure 5. Lane 1, material from cells expressing hPop5-VSV; lane 2, hPop5 Δ(145-163); lane 3, empty vector; lane 4, substrate pre-tRNA; lane 5 glycerol gradient fraction 5. On the right, the positions of the pre-tRNA, the mature RNA and the 5'-leader are indicated.

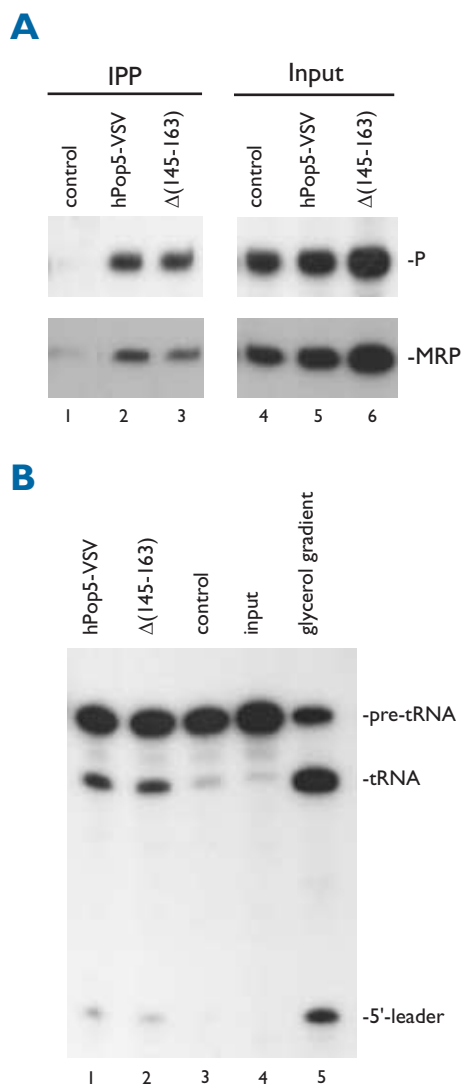

Figure 5B (lanes 2 and 3) the immunoprecipitate obtained with the affinity-purified anti-hPop5 antibodies was able to cleave pre-tRNA into mature tRNA and its 5'-leader, whereas the immunoprecipitate of the affinity-purified anti-GST antibodies was not. The RNase P activity in the anti-hPop5 immunoprecipitate was indistinguishable from that obtained with anti-hPop4 antibodies, which functioned as a positive control (lane 1). These results indicate that the hPop5 protein is part of the catalytically active RNase P complex. Although these data do not show that the hPop5 protein is associated with catalytically active RNase MRP as well, the strong evolutionary relationship between the RNase P and RNase MRP complexes suggests that hPop5 is also associated with RNase MRP.

The acidic C-terminus of hPop5 is not essential for complex association

As described above the only amino acid sequence element that could be detected in the primary structure of hPop5 is its acidic C-terminus. Therefore, we investigated whether this sequence element is required for complex association. A VSV-tag sequence (106) was fused to the 3'-end of the hPop5 ORF and to the 3' end of a truncated cDNA lacking the sequence corresponding to the acidic C-terminus (designated hPop5-VSV and hPop5 Δ(145-163), respectively). HEp-2 cells were transfected with these constructs or with the corresponding 'empty' vector as a negative control. After culturing the cells for 16 h extracts were prepared and used for immunoprecipitation with anti-VSV-tag antibodies. Co-precipitating RNAs were isolated and analysed via northern blot hybridisation using riboprobes for RNase MRP and RNase P RNA. As is shown in Figure 6A (lanes 1 and 2), RNase MRP and RNase P RNA were both immunoprecipitated from a cell extract containing the hPop5-VSV protein, but not from an extract from cells transfected with the empty vector. This result confirms that hPop5 associates with the RNase MRP and RNase P RNAs in human cells and demonstrates that this approach is suitable to analyse hPop5 mutants. As depicted in lane 3, the hPop5 Δ(145-163) mutant was able to associate with both RNase MRP and RNase P RNA, indicating that the evolutionarily conserved acidic C-terminus is not required for association with these ribonucleoproteins.

To investigate whether this element plays a role in the endoribonuclease activity of RNase P, HEp-2 cells were transfected with the VSV-tagged hPop5 and hPop5 Δ(145-163) constructs and immunoprecipitations were performed on extracts prepared from these cells. A ^{32}P-labeled precursor-tRNA was incubated at 37°C with the immunoprecipitates and the resulting products were analysed by denaturing polyacrylamide gel electrophoresis and autoradiography. As shown in Figure 6B, lanes 1 and 2, complexes associated with both hPop5 and the mutant lacking the acidic C-terminus displayed RNase P activity, whereas a control immunoprecipitate did not. Thus the most C-terminal 19 amino acids of hPop5 are neither required for complex association nor for RNase P activity.

Discussion

In this report we describe the cloning of a novel human RNase MRP/RNase P protein subunit. Based upon its homology with the yeast Pop5p protein we have designated this protein hPop5. We showed that the human protein, like the yeast Pop5p protein is associated with both RNase MRP and RNase P ribonucleoprotein particles and that the latter particle is catalytically active *in vitro*.

hPop5 is evolutionarily conserved

Besides the human homologue of Pop5p, our database searches identified two ESTs (accession no. AI751395 and AA534933) encoding a putative homologue of the RNase P specific protein subunit: Rpr2p (118). No homologues were identified for the Snm1p, Pop3p, Pop6p and Pop8p protein, suggesting that only 6 of the 10 yeast RNase MRP/RNase P protein subunits have human counterparts. A high degree of sequence conservation was observed among the mammalian Pop5 proteins, whereas only a moderate level of conservation exists between human, yeast and *Drosophila* Pop5 (23-27% identity). A similar level of sequence conservation has been reported for other RNase MRP and RNase P protein subunits: hPop1/Pop1p (22% identity), Rpp30/Rpp1p (23% identity), Rpp20/Rpp2p (14% identity) and hPop4/Pop4p (29% identity) (77-80,120). Recently, the analysis of the genomes of archae bacteria allowed the detection of hPop5 and Rpp30 counterparts also in these organisms (121) and in addition showed that the secondary structures of Pop5 and Rpp14 are related. A similar conservation from humans to archaea has been suggested for the Rpp29/hPop4 and Rpp21 subunits (51). A comparison of the secondary structures of RNase MRP RNA and RNase P RNA from various organisms has led to the hypothesis that RNase MRP evolved from RNase P in an early eukaryote (122). The association of the four highly conserved proteins with MRP RNA would be explained by the hypothesis that proteins associated with RNase P RNA have the capacity to bind MRP RNA as well.

Nucleolar accumulation of hPop5

We showed that the hPop5 protein is localised in the nucleus and accumulates in the nucleolus (Figure 4). Previously, it has been proposed that nucleolar entry is a two-step mechanism (107-109). First, a nucleolar protein is transported to the nucleus and subsequently it accumulates in the nucleolus. Recently, we demonstrated that clusters of basic amino acids are important for the localisation of protein subunits of RNase MRP and RNase P in the nucleolus (123). The absence of a nuclear localisation signal as well as clusters of basic residues in the hPop5 amino acid sequence suggests that hPop5 is targeted to the nucleus/nucleolus in a different manner. The hPop5 protein might be transported to the nucleus and nucleolus by a piggyback mechanism. In that case hPop5 binds in the cytoplasm to another (RNase MRP/RNase P) protein, which carries the hPop5 protein to the nucleus and subsequently to the nucleolus. Transport of the hPop5 protein from the nucleoplasm to the nucleolus might also be dependent on its association with the (partially assembled) RNase MRP/RNase P ribonucleoprotein complexes. A similar situation has been proposed for the Rpp14 protein (83).

hPop5 is the sixth protein subunit shared by the human RNase MRP and RNase P complexes

The results in Figures 3 and 6 demonstrate that the hPop5 protein subunit, like its yeast counterpart, is associated with both RNase MRP and RNase P. The association of protein subunits with both RNase MRP and RNase P has

been previously reported for hPop1, Rpp30, Rpp38 and hPop4/Rpp29 (reviewed in ref. (118)) and has been observed for the Rpp20 protein subunit as well (our unpublished observations). The sharing of protein subunits by these endoribonuclease complexes might be explained at least in part by the conservation of the secondary structure of their RNA components and the suggestion that the RNase MRP RNA has evolved from the RNase P RNA in early eukaryotes (see above). In yeast two protein subunits have been described to be specifically associated with either the RNase MRP complex or the RNase P complex (32,38). Such complex-specific protein subunits have not been described for the human enzymes yet.

An alternative explanation for extensive subunit sharing is the possibility that RNase MRP and RNase P assemble into a single complex in human cells. This possibility is supported by the finding that a subset of the cellular RNase MRP and RNase P complexes has been shown to exist in such a macromolecular complex (57). However, in yeast the majority of the RNase MRP and RNase P complexes can be physically separated and they function separately from each other (30,38,78,80). The exact function and architecture of this human macromolecular complex and its relation to the individual RNase MRP and RNase P complexes remain to be elucidated and provide interesting topics for further research.

Acknowledgements

We would like to thank Drs. Cecilia Guerrier-Takada and Sidney Altman for sharing their knowledge on the purification of the RNase P holoenzyme and for their kind gift of anti-Rpp38 antibodies and Dona Wesolowski for technical assistance (Dept. of Molecular, Cellular and Developmental Biology, Yale University). The patient serum was kindly provided by Dr. Frank van den Hoogen (Dept. of Rheumatology, University of Nijmegen). This work was supported in part by the Netherlands Foundation for Chemical Research (NWO-CW) with financial aid from the Netherlands Organization for Scientific Research (NWO).

Materials and Methods

Accession number

The hPop5 cDNA described in this report has been deposited in the EMBL database: accession number AJ306296.

cDNA cloning and sequence analysis

Database searches were performed using the BLASTN 2.0.10 program (111). The accession numbers of the human Expressed Sequence Tags (ESTs) are AF117232, XM-012126, NM-015918 and AF070660. The accession numbers for the overlapping mouse ESTs are BF121181 and BF583365, for rat ESTs BF567090 and AW918527, for cow BF075658 and for *Drosophila melanogaster* AAF49372.

The following oligonucleotides (based on the human EST sequence) were used to isolate the open reading frame of hPop5 by a PCR-based approach: pop51 [5'-GCG-GAT-CCC-TCG-AGA-TGG-TGC-GGT-TCA-AGC-ACA-GG-3'] and pop52 [5'-GCG-GAT-CCC-CCG-GGT-CAT-CTA-GAC-TCC-ATT-GCT-TCT-GCA-GCC-TCC-TC-3']. The polymerase chain reaction was performed with 200 ng denatured DNA from λgt11 human placenta (Clontech) and teratocarcinoma cDNA libraries as starting material (112). The amplified fragments were ligated in the PCR-II-TOPO vector (Invitrogen) and sequenced using the dideoxynucleotide chain termination method.

Anti-hPop5 antiserum

To raise a polyclonal anti-hPop5 antiserum, the hPop5 protein was expressed as a fusion protein with Glutathione S-Transferase (GST) in *E. coli* and purified by glutathione affinity chromatography (114). Rabbits were immunised with this material following standard procedures (115). For each injection 200 µg of GST-hPop5 was used.

Affinity purification of hPop5 antibodies

To obtain anti-hPop5 and anti-GST antibodies, two affinity columns were prepared by immobilising either 1.25 mg of GST-hPop5 or 4.8 mg of GST protein to 1.5 g of CNBr-activated Sepharose-4B (Amersham-Pharmacia) according to the manufacturer's instructions. Rabbit serum raised against GST-hPop5 was first depleted of anti-GST activity by chromatography on the GST affinity column equilibrated with Buffer A (350 mM NaCl, 0.05% NP-40, 1 x PBS). Anti-GST antibodies were eluted from the column using Buffer B (0.1 M Glycine-HCl pH 2.5, 0.5 M NaCl, 0.05% NP-40). This procedure was repeated until no detectable anti-GST activity could be measured in the flow-through using ELISA methods. Subsequently, the flow-through was loaded on the GST-hPop5 column in Buffer A. After washing with Buffer A, the anti-hPop5 antibodies were eluted with Buffer B.

Western blot analysis

For western blot analysis the rabbit anti-hPop5 and pre-immune sera were used in a 500-fold dilution, whereas affinity-purified anti-GST and anti-hPop5 antibodies were used in a 100-fold dilution. Detection was performed using horseradish peroxidase-conjugated goat-anti-rabbit IgG (Dako Immunoglobulins) as secondary antibody and visualisation by chemiluminescence.

Preparation of HEp-2 cell extracts

Extracts of HEp-2 cells were prepared by resuspending cell pellets in buffer A (25 mM Tris-HCl pH 7.5, 100 mM KCl, 1 mM dithioerythritol, 2 mM EDTA, 0.5 mM phenylmethylsulfonyl fluoride, 0.05% NP-40) and lysis by sonication using a Branson microtip (three times 20 s). Insoluble material was removed by centrifugation (12,000 g, 15 min) and supernatants were used directly for immunoprecipitations.

Immunoprecipitation

A monoclonal anti-VSV-tag antibody (Roche), an anti-55K (113) antiserum, a patient anti-Th/To serum, the rabbit anti-hPop5 antiserum, an anti-hPop4 antiserum (120) and pre-immune serum from the rabbit immunised with hPop5 protein were coupled to protein A agarose beads (Biozym) in IPP500 (500 mM NaCl, 10 mM Tris-HCl pH 8.0, 0.05% NP-40) by incubation for 1 h at room temperature. Beads were washed twice with IPP500 and once with IPP150 (150 mM NaCl, 10 mM Tris-HCl pH 8.0, 0.05% NP-40). For each immunoprecipitation a cell extract was incubated with the antibody-coupled beads for 2 h at 4°C. Subsequently, beads were washed three times with IPP150.

To analyse co-precipitating RNAs, the RNA was isolated by phenol-chloroform extraction and ethanol precipitation. RNAs were resolved on a denaturing polyacrylamide gel and blotted to a Hybond-N membrane (Amersham). Northern blot hybridisations with riboprobes specific for human RNase P, RNase MRP and U3 RNAs were performed as previously described (116).

Immunofluorescence

Indirect immunofluorescence assays with affinity-purified rabbit anti-hPop5 antibodies and affinity-purified rabbit anti-GST antibodies were performed on HEp-2 cells. Fixed cells were incubated with affinity-purified antibodies (diluted 1:20 in PBS) for 1 h at room temperature, washed with PBS and subsequently incubated with Alexa Fluor® 488 goat-anti-rabbit IgG conjugate

(Molecular Probes, diluted 1:75 in PBS) for 1 h at room temperature. Bound antibodies were visualised by epi-fluorescence microscopy.

RNase P purification from HeLa cells

Purification of the human RNase P enzyme was performed as described before (63,78). HeLa S3 cells (National Cell Culture Center, Minneapolis, Minnesota) were pelleted, disrupted, and the cell lysate was centrifuged at 10,000 g followed by another centrifugation at 100,000 g. The extract was loaded on a DEAE-Sepharose column and bound material was eluted with a linear 100-500 mM KCl gradient. Fractions containing RNase P activity were pooled, concentrated and further fractionated by centrifugation in a 15-30% glycerol gradient.

pre-tRNA processing assay

To assay for RNase P activity in the immunoprecipitates and column fractions, an internally ^{32}P-labeled pre-tRNA substrate (*S. pombe* $tRNA^{Ser}$ SupS1), was transcribed *in vitro* and gel-purified. This 110 nt-long substrate contains a 5'-end extension of 28 nts in comparison with the mature tRNA. The immunoprecipitates or fractions were incubated with equal amounts of substrate in assay buffer (20 mM Tris-HCl pH 8.0, 10 mM $MgCl_2$, 1 mM DTE, 50 mM KCl, 50 µg/ml BSA, 60 U/ml RNasin) for 10 minutes at 37°C. Reaction products were analysed by denaturing polyacrylamide gel electrophoresis and autoradiography.

Transfection constructs

Vesicular stomatitis virus G epitope (106) (VSV-G)-tagged (hereafter referred to as VSV-tagged) cDNAs were constructed as follows. 55k-VSV cDNA constructs (113), containing either a *Xho*I or a *Xba*I-site between the 55k open reading frame (ORF) and the VSV-tag sequence (positioned at the N- and C-terminal sides, respectively) were cleaved with *Xho*I and *Xba*I releasing the 55k-cDNA from this plasmid. The VSV-tagged constructs of hPop5 were constructed by isolation of the hPop5 ORF from the hPop5/PCR-II-TOPO construct by *Xho*I/*Xba*I digestion and ligation into the *Xho*I/*Xba*I digested 55k-VSV constructs.

A construct expressing deletion mutant hPop5 Δ(145-163) was generated by a PCR-based approach. Besides the deletion introduced by the PCR strategy, an *Xho*I site was introduced at the 5'-end of the translational start codon, whereas an *Xba*I site was introduced at the 3'-end of the coding sequence. The transfection construct was generated by ligating the *Xho*I/*Xba*I fragment into the *Xho*I/*Xba*I digested 55k-VSV constructs. The integrity of the resulting construct was confirmed by DNA sequencing. The pCI-neo vector (Promega), which has been used to prepare 55k-VSV previously, was used as a control in the transfection experiments.

Transient transfection of HEp-2 cells

HEp-2 monolayer cells were grown to 70% confluency by standard tissue culture techniques in either culture flasks or on coverslips. HEp-2 cells were transfected with the VSV-tagged constructs (3-4 µg) using LipofectAmine 2000 (Gibco-BRL) according to the manufacturer's instructions. After overnight growth in flasks, cells were harvested, washed once with PBS and used to prepare extracts for immunoprecipitation assays.

Part II

Assembly of the RNase MRP complex

Chapter 4

Basic domains target protein subunits of the RNase MRP complex to the nucleolus independently of complex association

Hans van Eenennaam
Annemarie van der Heijden
Rolf J.R.J. Janssen
Walther J. van Venrooij
Ger J.M. Pruijn

Molecular Biology of the Cell (2001) 12:3680-3689.

Abstract

The RNase MRP and RNase P ribonucleoprotein particles both function as endoribonucleases, have a similar RNA component and share several protein subunits. RNase MRP has been implicated in pre-rRNA processing and mitochondrial DNA replication, whereas RNase P functions in pre-tRNA processing. Both RNase MRP and RNase P accumulate in the nucleolus of eukaryotic cells.

In this report we show that for three protein subunits of the RNase MRP complex (hPop1, hPop4 and Rpp38) basic domains are responsible for their nucleolar accumulation and that they are able to accumulate in the nucleolus independently of their association with the RNase MRP and RNase P complexes. We also show that certain mutants of hPop4 accumulate in the Cajal bodies, suggesting that hPop4 traverses through these bodies to the nucleolus. Furthermore, we characterised a deletion mutant of Rpp38 that preferentially associates with the RNase MRP complex, giving a first clue about the difference in protein composition of the human RNase MRP and RNase P complexes. Based upon all available data on nucleolar localisation sequences we hypothesise that nucleolar accumulation of proteins containing basic domains proceeds by diffusion and retention rather than by an active transport process. The existence of nucleolar localisation sequences is discussed.

Introduction

The endoribonuclease MRP (Mitochondrial RNA Processing) complex is a member of the large family of small nucleolar ribonucleoprotein particles shown to be involved in precursor-rRNA processing. Three classes of snoRNPs can be distinguished based on structural elements: Box H/ACA snoRNPs, Box C/D snoRNPs and RNase MRP/RNase P (5).

RNase MRP and RNase P ribonucleoprotein particles are related in many aspects. Both complexes function as site-specific endonucleases: RNase P is involved in the generation of the mature 5′ end of tRNAs, whereas RNase MRP has been shown to be involved in the processing of pre-rRNA. The RNA components of both enzymes adopt a similar cage-shaped secondary structure. Furthermore, it became clear that most of the currently known human protein subunits of RNase MRP and RNase P are shared by both enzymes (see for review ref. (118)).

Besides the reported function of RNase MRP in the processing of pre-rRNA, *in vitro* experiments have shown that RNase MRP is also involved in the processing of mitochondrial RNA that functions as a primer for mitochondrial DNA replication (22). Only a relatively small amount of RNase MRP has been reported to reside in the mitochondria, whereas the majority (99%) of RNase MRP is located in the nucleolus (110). By genetic depletion in yeast it has been shown that the nucleolar RNase MRP is involved in the formation of the short form of the 5.8S rRNA [5.8S(S)], by catalysing the cleavage at site A3 in the first internal transcribed spacer (ITS1) of pre-rRNA (28, 30,29). Although none of these functions have been demonstrated to apply to the human system as yet, they are thought to be evolutionarily conserved. Recently, it was demonstrated that mutations in the human gene coding for the RNase MRP RNA cause an autosomal recessive disease called cartilage-hair hypoplasia, suggesting that the RNase MRP complex and/or its substrates play an important role in embryogenesis (119).

The first identified element important for the targeting of RNase MRP to the nucleolus is the 5'-terminal region of the RNase MRP RNA (referred to as P3 domain or Th/To binding site) (44). The RNase P complex has been detected in both nucleolus and nucleoplasm (58,60) and it has been determined that the evolutionarily conserved P3 domain of RNase P RNA functions in nucleolar localisation as well (58). Recently, a domain in two protein subunits, Rpp29 (identical to hPop4) and Rpp38, of RNase MRP and RNase P has been reported to be involved in the nucleolar localisation of these protein subunits (83). In both cases the highly basic nature of these domains rather than a distinct amino acid sequence appeared to be important.

In this study we analysed several deletion mutants of three protein subunits associated with both RNase MRP and RNase P: hPop1 (77), hPop4 (120) and Rpp38 (78,105) and examined the accumulation of these mutants in the nucleolus, complex association and RNase P enzymatic activity.

Results

To learn more about the nucleolar targeting of the human RNase MRP and RNase P complexes, three of their protein subunits (hPop1, Rpp38 and hPop4) were mutated and the effects of the mutations on their subcellular localisation was analysed by fluorescence microscopy. Figure 1 shows the main characteristics of the hPop1, Rpp38 and hPop4 protein subunits, including putative nuclear localisation signals, identified nucleolar localisation signals and conserved sequence elements.

Because the nucleolar accumulation of these protein subunits might be dependent on their association with the particles, the association of the mutants with the RNase MRP and RNase P RNAs was analysed by northern blot hybridisation and their assembly into functional particles was analysed in an in vitro pre-tRNA processing assay.

Basic domains of the hPop1 protein are required for its nucleolar targeting

DNA molecules encoding wildtype hPop1 and deletion mutants of hPop1 were cloned into the mammalian expression vector pCI-neo, in combination with a sequence encoding a VSV-G tag (106) fused to the 5'-end of the coding sequences, and transiently expressed in HEp-2 cells. After overnight culturing, the cells were fixed and the subcellular localisation of the VSV-tagged hPop1 (mutants) was determined by indirect immunofluorescence using anti-VSV-tag antibodies.

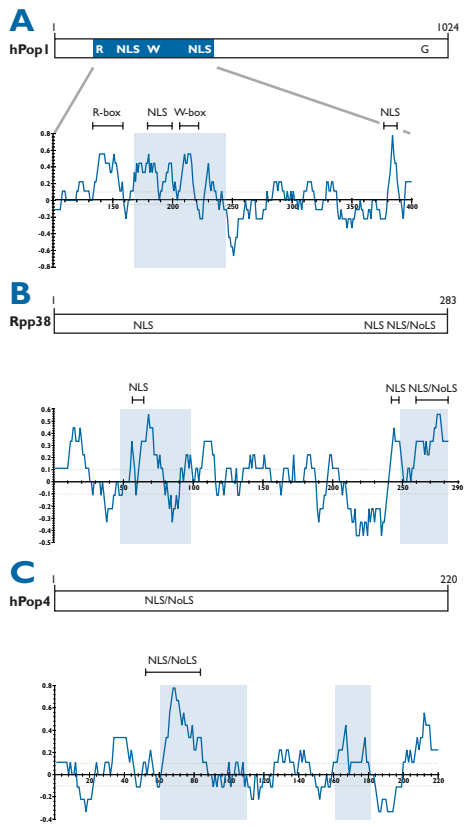

Figure 1. Schematic representation of the hPop1, Rpp38 and hPop4 proteins. The length, putative nuclear localisation signals (NLS) and nucleolar localisation signals (NoLSs) as established by Jarrous and coworkers (83) for the hPop1 (A), Rpp38 (B) and hPop4 (C) protein subunits are depicted in the upper parts. The lower parts represent charge plots of these proteins. Values on the vertical axis represent positively charged and negatively charged regions respectively. These values were calculated using a window of 9 amino acids. Light blue regions in the charge plots represent the regions of the proteins important for their nucleolar localisation. For the hPop1 protein (A) the charge plot of only amino acids 100-400 is depicted (blue area in upper part). The R-, W- and G-box refer to conserved sequence elements observed in the hPop1 protein (77).

The results in Figure 2A, panels 1 and 2, show that the VSV-hPop1 construct expressed a protein that accumulated in the nucleoli, in accordance with previous observations (77). A similar nucleolar staining pattern was found for VSV-tagged hPop1 deletion mutants Δ(711-1024), Δ(558-1024) and Δ(339-1024) (see Table I), indicating that the N-terminal region plays an important role in the nucleolar accumulation of the hPop1 protein. This was confirmed by the finding that a mutant in which most of these amino acids had been deleted, VSV-hPop1 Δ(1-318), was targeted to the nucleoplasm and did not accumulate in the nucleoli (Figure 2A, panels 3 and 4).

These results were further detailed by the finding that a deletion mutant containing only the N-terminal 128 amino acids, Δ(129-1024), was found uniformly distributed throughout the cell (Figure 2A, panels 5 and 6). Taken together, these results suggest that amino acids 129-318 are important for the nucleolar accumulation of the hPop1 protein.

To study whether a hPop1 fragment comprising amino acids 128-319 was able to accumulate in the nucleolus, we fused this part of the hPop1 protein to EGFP and analysed its localisation. This fragment of hPop1 indeed proved to be sufficient for nucleolar targeting of EGFP (Figure 2B, panels 1 and 2). In this region one of the two putative nuclear localisation sequences, a highly conserved arginine-rich motif (R-box) and a tryptophan-rich domain (W-box) have been identified (77). In the same way, three subfragments of the aa 128-319 region were analysed. Constructs were made that encode only the R-box (aa 128-167), the NLS and W-box together (aa 168-319) and the R-box, NLS and W-box (aa 128-245), each fused to EGFP. Surprisingly, these fusion

proteins all localised to the nucleolus (see Figure 2B, panels 3-6 for 128-167 and 128-245 and Table I for 168-319), although the efficiency of nucleolar accumulation for the 168-319 and 128-245 fusion proteins was much higher than that for the 128-167 fragment. The latter was also detected in the cytoplasm and nucleoplasm (panel 3).

Rpp38 harbours two regions important for nucleolar accumulation

Recently, Jarrous and collaborators have identified a so-called nucleolar localisation sequence (referred to as NoLS) near the C-terminus of the Rpp38 protein subunit of the RNase MRP and RNase P complexes (83). To investigate whether this NoLS was sufficient for the nucleolar localisation of the Rpp38 protein we made several deletion mutants of the Rpp38, fused them to ECFP and expressed them transiently in HEp-2 cells. As is depicted in Figure 3, panel 1, the wild type Rpp38-ECFP fusion protein was localised in both nucleoli and nucleoplasm. This distribution is very similar to that reported before for a GFP-Rpp38 fusion protein (83). Although this distribution deviates from what has been described for the endogenous Rpp38 protein (localisation to the nucleolus and Cajal bodies (83)), cells with a lower level of expression of this construct showed more prominent nucleolar staining, suggesting that the strong nucleoplasmic staining is caused by overexpression.

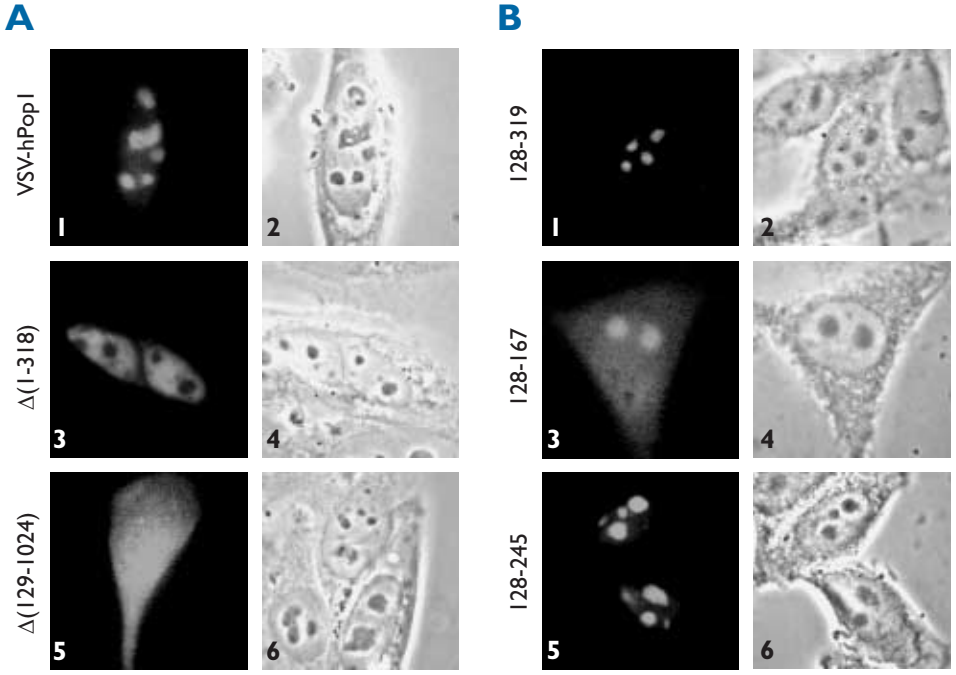

Figure 2. Subcellular localisation of deletion mutants of hPop1. **A.** VSV-hPop1 constructs were transiently transfected into HEp-2 cells. Cells were fixed with paraformaldehyde and the expressed proteins were visualised using anti-VSV antibodies (panels 1,3 and 5). A phase-contrast image of the same cells is shown in panels 2, 4 and 6. Panels 1 and 2:VSV-hPop1 construct, panels 3 and 4:VSV-hPop1 Δ(1-318), panels 5 and 6:VSV-hPop1 Δ(129-1024). **B.** EGFP-hPop1 constructs were transiently transfected into HEp-2 cells. Cells were fixed with methanol/aceton and the fluorescent proteins were visualised by direct fluorescence microscopy (panels 1, 3 and 5). Phase-contrast images of the same cells are shown in panels 2, 4 and 6. Panels 1 and 2: EGFP-hPop1 128-319, panels 3 and 4: EGFP-hPop1 128-167, panels 5 and 6: EGFP-hPop1 128-245.

A construct that encodes Rpp38 lacking the N-terminal 40 amino acids showed an identical subcellular localisation (Table I). Surprisingly, deletion of the N-terminal 98 amino acids resulted in staining of only the nucleoplasm (Figure 3, panel 3), which suggests that in spite of the presence of the complete NoLS (amino acids 246-283), this mutant is not able to enter the nucleoli. Further truncation of the N-terminus of the Rpp38 protein (Rpp38 Δ(1-141)) resulted in a cytoplasmic accumulation and a weak nuclear staining (see Figure 3, panel 5). Finally, we showed that deletion of the C-terminus (Rpp38 Δ(246-283) and Rpp38 Δ(181-283)) results in nucleoplasmic staining, loss of nucleolar accumulation and staining of the cytoplasm (Figure 3, panel 7 and Table I).

Taken together, these results indicate that two domains appear to be necessary for the nucleolar accumulation of the Rpp38 protein subunit and that each of these domains (amino acids 40-98 and 246-283) alone is not sufficient for nucleolar targeting.

The amino-terminus of Rpp38 differentiates between RNase MRP and RNase P complexes

Because differences in the subcellular localisation of various Rpp38 deletion mutants might be dependent on its ability to associate with the RNase MRP and/or RNase P particle, complex association was studied by immunoprecipitation using anti-ECFP antibodies and extracts of transiently transfected cells. Complex association was monitored by the isola-

Construct	Subcellular localisation	Complex association with RNase MRP/P	Association with RNase P activity
hPop1 protein			
wild type	No	–	–
Δ(711-1024)	No	nd	nd
Δ(558-1024)	No	nd	nd
Δ(339-1024)	No	nd	nd
Δ(1-318)	Np	nd	nd
Δ(129-1024)	No + Np + Cy	nd	nd
128-319	No	nd	nd
128-167	No + Np + Cy	nd	nd
168-319	No	nd	nd
128-245	No	nd	nd
Rpp38 protein			
wild type	No + Np	+	+
Δ(1-40)	No + Np	only MRP	–
Δ(1-98)	Np	–	–
Δ(1-141)	No + Np + Cy	–	–
Δ(181-283)	Np + Cy	–	–
Δ(246-283)	Np	+	+
hPop4 protein			
wild type	No	+	+
Δ(1-10)	No	+	+
Δ(1-47)	No	+	+
Δ(61-109)	No + CB	–	–
Δ(162-220)	No + CB	–	–
Δ(181-220)	No	–	–
Δ(210-220)	No	+	+

Table I. Summary of subcellular localisation, complex association with RNase MRP and RNase P and RNase P activity of deletion mutants of hPop1, Rpp38 and hPop4 protein subunits.

Abbreviations:
No = Nucleolus;
Np = Nucleoplasm;
Cy = Cytoplasm;
CB = Cajal Bodies;
– = no association with RNase MRP and RNase P/no association with RNase P activity;
+ = association with RNase MRP and RNase P/association with active RNase P;
nd = not determined

tion of RNA from the immunoprecipitates and visualisation of RNase MRP and RNase P RNA by northern blot hybridisation. As indicated in Figure 4A, lane 9, the wild type Rpp38-ECFP fusion protein effectively associated with both RNase P and RNase MRP, in accordance with previously published data (105). Surprisingly, the Rpp38 Δ(246-283) mutant also associated with both the RNase MRP and the RNase P complex (Figure 4A, lane 14), despite the loss of its ability to enter the nucleolus. Moreover, an N-terminal deletion mutant, which displayed a wild type subcellular distribution, Rpp38 Δ(1-40), appeared to associate preferentially with the RNase MRP particle (Figure 4A, lane 10). With this mutant only a very inefficient co-precipitation of RNase P RNA was reproducibly observed, which suggests that the N-terminus of the Rpp38 is involved in its stable association with the RNase P complex but not with the RNase MRP complex.

In contrast, no complex association was observed for the remaining deletion mutants of Rpp38, Rpp38 Δ(1-98), Δ(1-141) and Δ(181-283), which was not due to lack of expression as demonstrated by western blotting (our unpublished results).

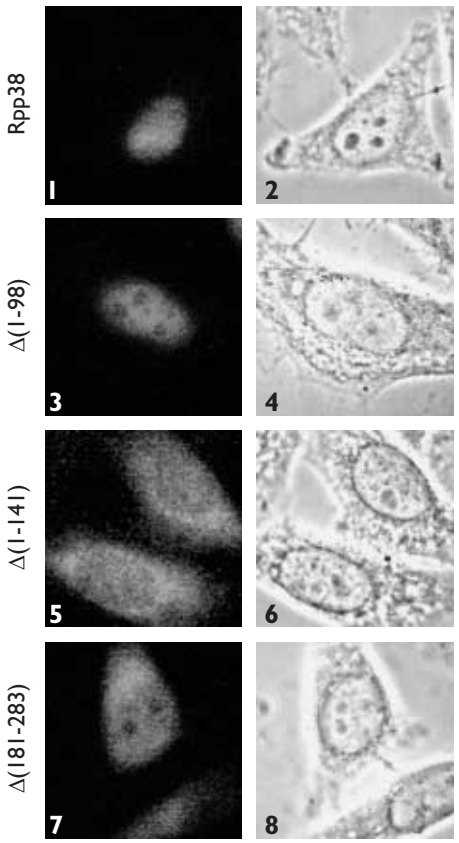

Figure 3. Subcellular localisation of deletion mutants of Rpp38. ECFP-Rpp38 constructs were transiently transfected into HEp-2 cells. Cells were fixed with methanol/aceton and the fluorescent proteins were visualised by direct fluorescence microscopy (panels 1, 3, 5 and 7). Phase-contrast images of the same cells are shown in panels 2, 4, 6 and 8. Panels 1 and 2: ECFP-Rpp38, panels 3 and 4: ECFP-Rpp38 Δ(1-98), panels 5 and 6: ECFP-Rpp38 Δ(1-141) and panels 7 and 8: ECFP-Rpp38 Δ(181-283).

The carboxy-terminus of Rpp38 is dispensable for RNase P function

To investigate whether the complexes bound by the Rpp38 deletion mutants were functionally active, we analysed the immunoprecipitated complexes in an *in vitro* precursor-tRNA processing assay. A ^{32}P-labeled precursor-tRNA was incubated at 37°C with the anti-ECFP immunoprecipitates and the resulting products were analysed by denaturing polyacrylamide gel electrophoresis and autoradiography.

Particles associated with either the wild type ECFP-Rpp38 fusion protein or the C-terminal deletion mutant Δ(246-283) displayed RNase P enzymatic activity (Figure 4B, lanes 2 and 7, respectively), whereas control material obtained from extracts of cells expressing ECFP alone did not (lane 1). As expected, no RNase P activity was detected with the remaining deletion mutants of Rpp38, including Δ(1-40), in agreement with the lack of stable association

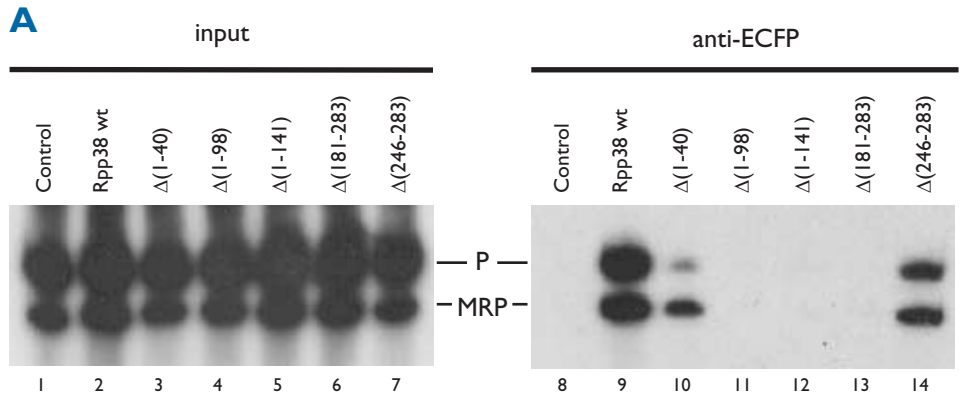

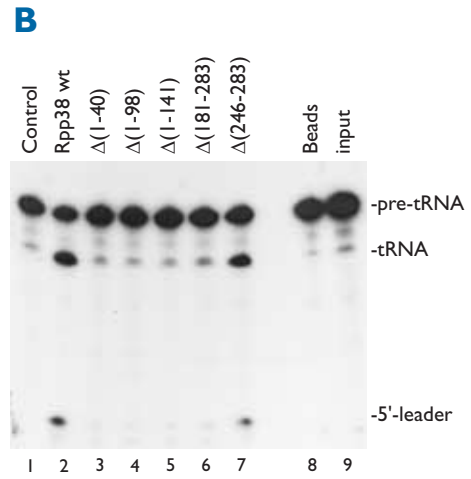

Figure 4. Association of ECFP-Rpp38 (mutants) with RNase MRP and RNase P ribonucleoprotein particles and RNase P activity associated with ECFP-Rpp38 deletion mutants.
A. Constructs encoding (deletion mutants of) ECFP-Rpp38 were transiently transfected in HEp-2 cells. Extracts from these cells used for immunoprecipitations with anti-ECFP antibodies. RNA isolated from total cell extracts (lanes 1-7) and immunoprecipitates (lanes 8-14) was analysed by northern blot hybridisation using riboprobes specific for RNase MRP and RNase P RNA. Lanes 1 and 8, material from control cells expressing ECFP alone; lanes 2 and 9, ECFP-Rpp38; lanes 3 and 10, ECFP-Rpp38 Δ(1-40); lanes 4 and 11, ECFP-Rpp38 Δ(1-98); lanes 5 and 12, ECFP-Rpp38 Δ(1-141); lanes 6 and 13, ECFP-Rpp38 Δ(181-283) and lanes 7 and 14, ECFP-Rpp38 Δ(246-283). The positions of RNase P and RNase MRP RNA are indicated.
B. RNase P activity assay associated with anti-ECFP immunoprecipitates from extracts of cells transiently transfected with ECFP-Rpp38 (deletion mutants). Lane 1, material from control cells expressing ECFP alone; lane 2, ECFP-Rpp38; lane 3, ECFP-Rpp38 Δ(1-40); lane 4, ECFP-Rpp38 Δ(1-98); lane 5, ECFP-Rpp38 Δ(1-141); lane 6, ECFP-Rpp38 Δ(181-283); lane 7, ECFP-Rpp38 Δ(246-283); lane 8, beads alone and lane 9, substrate RNA. On the right, the positions of the pre-tRNA, the mature tRNA and the 5'-leader are indicated.

with the RNase P complex (Figure 4B, lanes 3-6).

hPop4 contains two regions important for nucleolar localisation

Next, the subcellular localisation and the association with the RNase MRP and (catalytically active) RNase P complexes were studied for six deletion mutants of the hPop4 protein subunit, following the procedures described above.

Indirect immunofluorescence showed that the VSV-tagged hPop4 protein subunit is localised in the nucleoli as has been established previously (120), (Figure 5, panel 1). The subcellular localisation of the Δ(1-10), Δ(1-47), Δ(181-220) and Δ(210-220) deletion mutants (all VSV-tagged) showed that deletion of either the N- or the C-terminal regions of the hPop4 does not affect the localisation of this protein as they all accumulated in the nucleoli (see Table I).

Two different subcellular localisation patterns were observed for two other deletion mutants, one lacking an internal region (Δ(61-109)) and another in which a relatively

large part of the C-terminus had been deleted (Δ(162-220)). As shown in Figure 5, panels 3 and 7, both mutants do have the ability to accumulate in the nucleolus. However, in addition to strong nucleolar staining observed in a subset of cells, for both mutants cells with weaker or no nucleolar staining were present as well. In many of these cells the fluorescent staining was concentrated in nucleoplasmic foci, as is depicted in Figure 5, panel 5, for Δ(61-109). These foci appeared to be Cajal bodies (formerly designated coiled bodies), which was established by co-localisation experiments using anti-p80 coilin antibodies (our unpublished results).

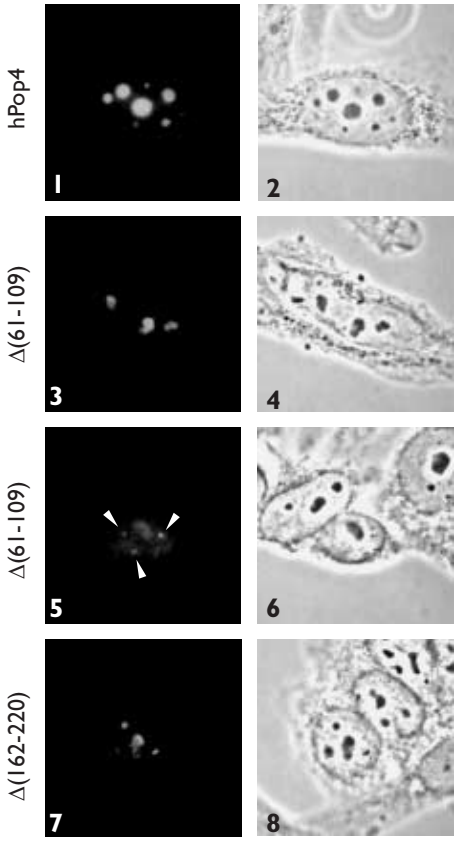

Figure 5. Subcellular localisation of deletion mutants of hPop4. VSV-hPop4 constructs were transiently transfected into HEp-2 cells. Cells were fixed with methanol/aceton and the expressed proteins were visualised by indirect fluorescence microscopy using anti-VSV antibodies (panels 1, 3, 5 and 7). Phase-contrast images of the same cells are shown in panels 2, 4, 6 and 8. Panels 1 and 2: VSV-hPop4, panels 3 and 4: VSV-hPop4 Δ(61-109), nucleolar accumulation, panels 5 and 6: VSV-hPop4 Δ(61-109), accumulation in the Cajal bodies and panels 7 and 8: VSV-hPop4 Δ(162-220), nucleolar pattern.

To investigate whether the subcellular distribution of these deletion mutants was somehow correlated with the ability to associate with RNase MRP and RNase P ribonucleoprotein particles, co-immunoprecipitation experiments were performed with anti-VSV-tag antibodies using extracts from transiently transfected cells. As described previously (120), the wild type hPop4 protein was found to be associated with both RNase MRP and RNase P complexes (Figure 6A, lane 10), whereas control precipitations did not display RNase MRP and RNase P RNA (lane 9). Deletion of the N-terminus of the hPop4 protein subunit did not abolish the association with both complexes, because deletion mutants Δ(1-10) and Δ(1-47) coprecipitated wild type levels of both RNAs (lanes 11-12). Also deletion of 11 amino acids from the C-terminus did not affect the association with both particles (lane 14). In contrast, the internal deletion mutant and the mutants having more than 10 amino acids deleted from the C-terminus of the hPop4 protein did not detectably associate with RNase MRP and RNase P RNA, as demonstrated by the results in lanes 13 and 15-16 (Figure 6A). Control experiments (western blotting) showed that this was not due to lack of expression (our unpublished results).

Finally, to investigate the association of the hPop4 deletion mutants with catalytically active RNase P complexes the immunoprecipitates were analysed in the pre-tRNA processing assay. As demonstrated in Figure 6B, lanes

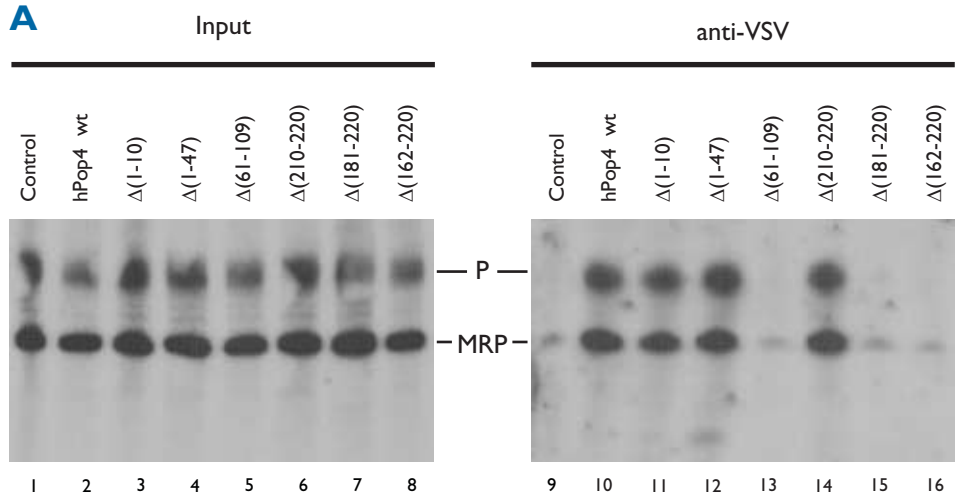

Figure 6. Association of VSV-hPop4 (mutants) with RNase MRP and RNase P ribonucleoprotein particles and RNase P activity associated with VSV-hPop4 deletion mutants.
A. Constructs encoding (deletion mutants) of VSV-hPop4 were transiently transfected into HEp-2 cells. Extracts from these cells were used for immunoprecipitation with anti-ECFP antibodies. RNA isolated from total cell extracts (lanes 1-8) and immunoprecipitates (lanes 9-16) was analysed by northern blot hybridisations using riboprobes specific for RNase MRP and RNase P RNA. Lanes 1 and 9, material from cells transfected with empty vector alone; lanes 2 and 10, VSV-hPop4; lanes 3 and 11, VSV-hPop4 Δ(1-10); lanes 4 and 12, VSV-hPop4 Δ(1-47); lanes 5 and 13, VSV-hPop4 Δ(61-109); lanes 6 and 14, VSV-hPop4 Δ(210-220); lanes 7 and 15, VSV-hPop4 Δ(181-220) and lanes 8 and 16, VSV-hPpop4 Δ(162-220). The positions of RNase MRP and RNase P RNA are indicated on the right.
B. RNase P activity assay associated with immunoprecipitates from extracts of cells transiently transfected with VSV-hPop4 (deletion mutants). Lane 1, material from cells transfected with empty vector alone; lane 2, material from cells expressing VSV-hPop4; lane 3 VSV-hPop4 Δ(1-10); lane 4, VSV-hPop4 Δ(1-47); lane 5, VSV-hPop4 Δ(61-109); lane 6, VSV-hPop4 Δ(162-220); lane 7, VSV-hPop4 Δ(181-220); lane 8, VSV-hPop4 Δ(210-220); lane 9, input. On the right, the positions of the pre-tRNA, the mature tRNA and the 5'-leader are indicated.

1 and 2, particles containing the wild type VSV-tagged hPop4 protein displayed enzymatic activity. The analysis of the deletion mutants showed a complete correlation between the capacity to associate with the RNase P particle and the enzymatic activity (lanes 3-8). This result implies that neither the N-terminal 47 nor the C-terminal 11 amino acids of hPop4 are required for RNase P activity.

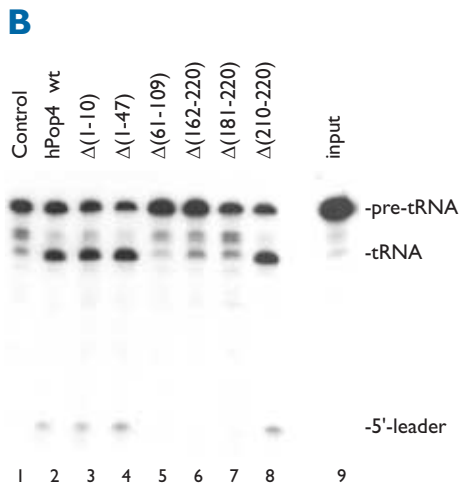

Discussion

We have analysed the effects of deletions in the hPop1, hPop4 and Rpp38 protein subunits of RNase MRP and RNase P on their subcellular localisation, on their association with RNase MRP and RNase P and on the enzymatic activity of RNase P (see Table I for a summary). The results identified regions in each of these

proteins important for their nucleolar accumulation. The nucleolar localisation of hPop1 appeared to be dependent on a region near the N-terminus of this protein. The Rpp38 protein subunit needs two distinct regions to accumulate in the nucleolus. Although none of the hPop4 deletion mutants analysed failed to enter the nucleolus two mutants of this protein accumulated in the Cajal bodies in a subset of the cells. Importantly, complex association did not appear to be a requirement for nucleolar accumulation. All deletion mutants of Rpp38 and hPop4 that retained the capacity to associate with the RNase MRP and P complexes were bound to enzymatically active RNase P, suggesting that the deleted amino acids are dispensable for this activity. Finally, the N-terminus of Rpp38 appeared to be required for a stable association with RNase P but not with RNase MRP.

The N-terminus of Rpp38 discriminates between RNase P and RNase MRP

The RNase MRP and RNase P ribonucleoprotein complexes show a high degree of similarity. Their RNA components can be folded in similar cage-shaped structures, and most of the currently known protein subunits have been shown to be associated with both complexes (for review see ref. (118)). In yeast only a single protein subunit has been reported to be specifically associated with either RNase MRP (98) or RNase P (38), whereas the other seven proteins are common to both particles. So far no human orthologues of the particle-specific yeast proteins have been found.

The N-terminal deletion mutant Δ(1-40) of Rpp38 appeared to associate preferentially with the RNase MRP complex. This implicates that the N-terminus of this protein plays an important role in the association with the RNase P complex. Whether the lack of binding of this mutant to RNase P is due to the loss of interactions with the RNA component (105) or with another, most likely particle-specific protein subunit is presently not known.

The selective interaction of Rpp38 Δ(1-40) with the RNase MRP complex in combination with the lack of RNase P activity associated with this complex implies that the RNase MRP particle is unable to cleave the precursor-tRNA (substrate for RNase P), unless the N-terminus of Rpp38 is required for this activity.

Basic domains in the protein subunits of RNase MRP and P are involved in their nucleolar accumulation

A comparison of the regions in the three proteins that affect their nucleolar accumulation showed that all were highly enriched in basic amino acids (see Figure 1), suggesting that basic regions are important for nucleolar localisation. Basic sequence elements have been implicated in nucleolar localisation of the Rpp38 and Rpp29/hPop4 protein subunits before (83). Jarrous and co-workers proposed that nucleolar localisation sequences (referred to as NoLS) are present at positions 260-283 in Rpp38 and 63-85 in hPop4, respectively (83). They showed that these elements are able to direct a reporter protein to the nucleolus. Our data confirm that these elements are required for nucleolar targeting of these proteins but also show that in the case of Rpp38 an additional element (aa 40-98) is required, whereas in the case of hPop4 a deletion of the previously identified NoLS (Δ(61-109)) does not abrogate its transport to the nucleolus. Apparently, the NoLS of Rpp38 identified previously is required but not sufficient for nucleolar accumulation, and hPop4 contains more than one functional NoLS.

The wild type Rpp29/hPop4 has been reported to be present in the Cajal bodies previously (83). Surprisingly, two deletion mutants of hPop4 appeared to be retained in the Cajal bodies in a subset of the transfected cells. Transport of the Rpp29/hPop4 protein subunit through the Cajal bodies on its way to the nucleolus fits very well in the model proposing that snoRNPs assemble into larger complexes in the Cajal bodies and are subsequently transported to the nucleolus (124). A defect in this assembly process caused by the deletions in our mutants might lead to their retention in the Cajal bodies. However, in addition to the retention in the Cajal bodies both mutants did enter the nucleoli in some cells. More importantly, all three proteins studied in this report have the capacity to enter the nucleus and nucleolus independent of an association with the cognate RNAs strongly suggesting that the association with the cognate particles is not an absolute requirement for transport of these proteins to the nucleoli.

Does a NoLS exist?

The involvement of regions rich in basic amino acids in nucleolar localisation has been found by others as well. For the poly(A)-binding protein II (PABP2) it has been shown that the basic C-terminal region of this nucleoplasmic protein directs a reporter protein to the nucleolus (125) and more recently it was shown that a basic element in p80-coilin, a marker protein for Cajal bodies, when uncovered by the deletion of an acidic region, also leads to a nucleolar localisation (126). In addition, two viral proteins, herpesvirus MEQ protein and PRRSV nucleocapsid protein (127,128), and two cellular proteins, rat spermatidal protein TP2 and human I-mfa domain containing protein HICp40 (129,130) have been reported to contain NoLSs consisting of stretches of basic residues as well. Comparison of these various basic sequence elements does not reveal a consensus sequence. Taken together, our results and the work of others indicate that stretches of basic residues, even when these are derived from proteins that normally do not reside in the nucleoli, may target proteins to the nucleolus independently of functionality (e.g. complex association).

A prerequisite for nucleolar accumulation is translocation of a protein from the cytoplasm to the nucleoplasm. In the nucleoplasm proteins may bind to their functional entities. Nucleolar accumulation can subsequently proceed by two mechanisms: one in which the translocation to the nucleolus is an active process (either mediated by a signal in the protein which directs it to the nucleolus or mediated by its association with other molecules/complexes which are actively transported to the nucleolus); another in which nucleolar entry is a passive process mediated by diffusion. In the latter case accumulation in the nucleolus may be due to retention by binding to nucleolar components.

The existence of a specific signal that directs proteins to the nucleolus is not supported by the data discussed above. The deletion of the previously described NoLS in hPop4 does not block nucleolar localisation (hPop4 Δ(61-109)) and a mutant that does contain the NoLS identified in Rpp38 is not localised to the nucleolus (Rpp38 Δ(1-98)). Moreover, the NoLS identified in PABP2 is not able to direct this protein to the nucleolus (125). In conclusion, these data strongly suggest that the identified

basic domains are not functioning in an active nucleolar transport pathway. Transport to the nucleolus via assembly into functional complexes is also not supported by our data. Mutants of all three proteins studied (hPop1, hPop4 and Rpp38) are able to localise to the nucleolus independently of complex association. This is substantiated by the finding that different proteins composed of 10-20 basic amino acids fused to EGFP are able to localise to the nucleolus as well (83,125,130). Nucleolar accumulation by diffusion and retention is consistent with all available data. Whether nucleolar retention is caused by the specific binding to nucleolar components, is not clear at present. Most likely the RNase MRP complex is bound in the nucleolus because it is involved in the processing of the precursor-rRNA and it associates with either pre-rRNA or the processing-machinery. However, such a mechanism does not explain the nucleolar localisation mediated by small stretches of basic amino acids. This type of nucleolar accumulation might be explained by the high concentration of negatively charged molecules in the nucleolar compartment (e.g. precursor-rRNA, rDNA) to which these basic elements may non-specifically bind. Thus, in our opinion data obtained by these kind of experiments should be interpreted with great care.

In conclusion, we suggest that nucleolar localisation signals that mediate active transport to the nucleolus may not exist and that the previously identified basic elements localise proteins to the nucleolus by virtue of their nucleolar retention capacity after diffusion into the nucleolus.

Acknowledgements

We thank Dr. Bertrand Seraphin (EMBL, Heidelberg) for providing us with the pre-tRNA construct, Dr. Sidney Altman (Yale University, New Haven) and Dr. C. Liew (University of Toronto) for their kind gift of Rpp38 cDNA and Dr. Wiljan Hendriks (Department of Cell Biology, University of Nijmegen) for providing us with anti-EGFP/ECFP antibodies.

This work was supported in part by the Netherlands Foundation of Chemical Research (NWO-CW) with financial aid from the Netherlands Organisation for Scientific Research (NWO).

Materials and Methods

hPop1 deletion mutant constructs

hPop1 cDNA (77) was mutated by PCR to introduce a *Xho*I site before the translational start codon. The PCR product was digested with *Xho*I/*Eco*RI and ligated into an *Xho*I/*Eco*RI digested pCI-neo vector (Promega) that contains a 5' VSV-G tag encoding sequence inserted between the original *Nhe*I-*Xho*I sites of pCI-neo (113), resulting in a construct referred to as VSV-hPop1.

Partial digestion of VSV-hPop1 with *Hpa*I and *Xba*I results in the release of a DNA fragment of 900 bp. The vector with the remaining hPop1 cDNA sequence was treated with Klenow polymerase and religated, generating a construct encoding the VSV-hPop1 Δ(711-1024) deletion mutant. Constructs encoding VSV-hPop1 Δ(558-1024) and VSV-hPop1 Δ(339-1024) were obtained by partial *Eco*RV digestion of VSV-hPop1, followed by religation to the filled-in *Sal*I-site of pCI-neo. The later constructs contain a vector-encoded translational stop codon, thus encoding 8 additional amino acids at the C-terminus.

Digestion with *Sma*I of VSV-hPop1 releases a DNA fragment with a length of 2100 bp, which was ligated in filled-in *Xho*I/*Sma*I digested VSV-pCI-neo, resulting in a construct designated VSV-hPop1 Δ(1-318). VSV-hPop1 Δ(129-1024) was obtained by cleavage of VSV-hPop1 with *Eco*RI/*Sma*I and subsequent religation of the vector-containing fragment. Synthesis of the mutant encoded by this construct is terminated by a vector-encoded translational stop codon, leading to 6 additional C-terminal amino acids.

A construct encoding hPop1 (128-319) was obtained by ligation of the *Eco*RI/*Sma*I DNA fragment of VSV-hPop1 in *Eco*RI/*Sma*I digested pEGFP-C1 (Clontech). Ligation of the *Eco*RI/*Rsa*I fragment of VSV-hPop1 in *Eco*RI/*Sma*I digested pEGFP-C1 results in a construct designated hPop1 (128-167). Digestion of VSV-hPop1 with *Rsa*I/*Sma*I and subsequent ligation of the resulting fragment in *Sma*I digested pEGFP-C1 generates the hPop1 (168-319) construct. The *Eco*RI/*Pst*I digested fragment of VSV-hPop1 was ligated in *Eco*RI/*Pst*I digested pEGFP-C1 resulting in hPop1 (128-245).

The integrity of all DNA constructs described above was confirmed by DNA sequencing.

hPop4 deletion mutant constructs

Wildtype hPop4 cDNA was subcloned in pCI-neo containing a DNA sequence coding for either an N-terminal or a C-terminal VSV-G tag as described (120); the resulting constructs were designated VSV-hPop4 and hPop4-VSV, respectively.

A DNA fragment of hPop4/pCR-II-Topo obtained by digestion with *Dde*I/*Sma*I (120) was treated with Klenow polymerase to fill in the overhangs and was ligated in VSV-hPop4 digested with *Xho*I/*Sma*I and treated with Klenow polymerase, resulting in the VSV-hPop4 Δ(1-10) construct. Ligation of a Klenow polymerase treated DNA fragment resulting from digestion of hPop4/pCR-II-Topo with *Nco*I/*Xba*I in hPop4-VSV treated with Klenow polymerase after *Xho*I/*Xba*I digestion, generated a construct encoding hPop4-VSV Δ(1-47).

Two DNA fragments generated by *Xho*I/*Rsa*I and *Rsa*I/*Xba*I digestion of hPop4/PCR-II-Topo were ligated in *Xho*I/*Xba*I digested VSV-hPop4, resulting in the VSV-hPop4 Δ(61-109) construct.

Three C-terminal deletion mutants were generated using PCR-based approaches. Besides the mutations introduced by PCR, a *Xba*I-site was introduced after the most 3' codon, followed by an in-frame stop-codon and a *Sma*I-site in the oligonucleotides used. Using this strategy DNA fragments were produced and digested with *Xho*I/*Sma*I and ligated in *Xho*I/*Sma*I digested VSV-hPop4, generating VSV-hPop4 Δ(162-220), Δ(181-220) and Δ(210-220), respectively.

The integrity of these constructs was confirmed by DNA sequencing.

Rpp38 deletion mutant constructs

Wildtype Rpp38 cDNA was subcloned in the pECFP-C3 vector (Clontech) containing a DNA sequence encoding an N-terminal ECFP tag.

Constructs encoding deletion mutants of Rpp38 were generated by PCR-based approaches. Besides the deletions introduced by the PCR strategy, an *Xho*I site was introduced in-frame at the 5'-end of the translational start codon, whereas an *Xba*I site was introduced at the 3'-end of the coding sequence. Digestion with *Xho*I/*Xba*I of the PCR products and ligation in *Xho*I/*Xba*I digested pECFP-C3, generated the following constructs; Rpp38 Δ(1-40), Δ(1-98), Δ(1-141), Δ(181-283) and Δ(246-283).

The integrity of the constructs described above was confirmed by DNA sequencing.

Transient transfection of HEp-2 cells

HEp-2 monolayer cells were grown to 70% confluency by standard tissue culture techniques in either culture flasks or on coverslips. pCI-neo derived constructs (3-4 μg) were transfected in HEp-2 cells using LipofectAmine 2000 reagent (Gibco-BRL) according to the manufacturer's instructions. pEGFP/pECFP derived constructs (10 μg) were transfected into $3x10^6$ HEp-2

cells by electroporation in a total volume of 400 µl of Dulbecco's modified Eagle's medium containing 10% fetal calf serum. Electroporation was performed at 276 V and a capacity of 950 mFa with a Gene Pulser II (BioRad).

Transfected cells were grown overnight in Dulbecco's modified Eagle's medium supplemented with 10% fetal calf serum.

Cells grown on coverslips were washed twice with phosphate buffered saline (PBS), fixed with either methanol (5 min at -20ºC) or with 4% paraformaldehyde (20 min at room temperature) and permeabilised using 0.2% Triton-X-100 (5 min at room temperature).

Cells grown in flasks were harvested, washed once with PBS and used to prepare extracts for immunoprecipitation assays (see below).

Immunofluorescence

Indirect immunofluorescence assays were performed on transfected HEp-2 cells. Fixed cells were incubated with affinity-purified mouse anti-VSV tag antibodies (Roche, diluted 1:50 in PBS) for 1 h at room temperature, washed with PBS and subsequently incubated with rabbit-anti-mouse immunoglobulins coupled to FITC for 1 h at room temperature. Cells were mounted with PBS/glycerol and bound antibodies were visualised by fluorescence microscopy.

Preparation of HEp-2 cell extracts

Extracts of HEp-2 cells were prepared by resuspending cell pellets in buffer A (25 mM Tris-HCl pH 7.5, 100 mM KCl, 1 mM dithioerythritol, 2 mM EDTA, 0.5 mM phenylmethylsulfonyl fluoride, 0.05% NP-40) and lysis by sonication using a Branson microtip (three times 20 s). Insoluble material was removed by centrifugation (12,000 g, 15 min) and supernatants were used directly for immunoprecipitation.

Immunoprecipitation and pre-tRNA processing assay

Monoclonal anti-VSV-tag (Roche) or anti-EGFP antibodies were coupled to protein A-agarose beads (Biozym) in IPP500 (500 mM NaCl, 10 mM Tris-HCl pH 8.0, 0.05% NP-40) by incubation for 1 h at room temperature. Beads were washed twice with IPP500 and once with IPP150 (150 mM NaCl, 10 mM Tris-HCl pH 8.0, 0.05% NP-40). For each immunoprecipitation the cell extract was incubated with the antibody-coupled beads for 2 h at 4°C. Subsequently, beads were washed three times with IPP150.

To analyse co-precipitating RNAs, the RNA was isolated from the beads by phenol-chloroform extraction and ethanol precipitation. RNAs were resolved on a denaturing polyacrylamide gel and blotted to a Hybond-N membrane (Amersham). Northern blot hybridisations with riboprobes specific for human RNase P and RNase MRP RNAs were performed as previously described (116).

To assay for RNase P enzymatic activity in the immunoprecipitates (i.e. the beads), an internally ^{32}P-labeled pre-tRNA substrate (*S. pombe* tRNA^{Ser} SupS1 (117)) was transcribed *in vitro* and gel-purified. This 110 nt-long substrate contains a 5'-extension of 28 nts in comparison with the mature tRNA. The immunoprecipitates were incubated with substrate RNA in assay buffer (20 mM Tris-HCl pH 8.0, 10 mM $MgCl_2$, 1 mM DTE, 50 mM KCl, 50 µg/ml BSA, 60 U/ml RNasin) for 10 min at 37ºC. The products were analysed by denaturing polyacrylamide gel electrophoresis and autoradiography.

Chapter 5

RNA-protein interactions in the human RNase MRP ribonucleoprotein complex

Helma Pluk
Hans van Eenennaam
Saskia A. Rutjes
Ger J.M. Pruijn
Walther J. van Venrooij

RNA (1999) 5: 512-524

Abstract

The eukaryotic nucleolus contains a large number of small RNA molecules which, in the form of small nucleolar ribonucleoprotein complexes (snoRNPs), are involved in the processing and modification of pre-rRNA. One of the snoRNPs which has been shown to possess enzymatic activity is the RNase MRP. RNase MRP is an endoribonuclease involved in the processing of the 5' end of 5.8S rRNA.

In this study the association of the hPop1 protein with the RNase MRP complex was investigated. The hPop1 protein seems not to be directly bound to the RNA component, but requires nucleotides 1-86 and 116-176 of the MRP RNA to associate with the RNase MRP complex via protein-protein interactions. UV crosslinking followed by ribonuclease treatment and immunoprecipitation with anti-Th/To antibodies revealed that in addition to hPop1, three human proteins of about 20, 25 and 40 kDa can associate with the RNase MRP complex. The 20 and 25 kDa proteins appear to bind to stem-loop I of the MRP RNA while the 40 kDa protein requires the central part of the MRP RNA (nt 86-176) for association with the RNase MRP complex. In addition, we show that the human RNase P proteins Rpp30 and Rpp38 are also associated with the RNase MRP complex. Expression of VSV-tagged versions of these proteins in HeLa cells followed by anti-VSV immunoprecipitation resulted in co-precipitation of both RNase P and RNase MRP complexes. Furthermore, UV-crosslinking followed by anti-Th/To and anti-Rpp38 immunoprecipitation revealed that the 40 kDa protein we detected in UV crosslinking is probably identical to Rpp38.

Introduction

Eukaryotic cells contain a large number of small nucleolar RNAs (snoRNAs) which, in the form of small nucleolar ribonucleoprotein complexes (snoRNPs), are involved in the various steps of ribosome synthesis. Several snoRNPs have been shown to be required for pre-rRNA processing, and a large set of snoRNPs is involved in ribose methylation and pseudouridinylation of rRNA (reviewed in ref. (5,12,93,131)). Although many snoRNPs might be part of catalytic complexes involved in the cleavage and modification reactions, sofar only one snoRNP has been shown to possess enzymatic activity on a pre-rRNA substrate *in vitro*: RNase MRP (30).

RNase MRP was originally identified as an endoribonuclease able to cleave *in vitro* an RNA substrate derived from the mitochondrial origin of DNA replication (22,26). The vast majority of RNase MRP is, however, localized in the nucleolus (42,44,72,99), where it is involved in the processing of the 5' end of 5.8S rRNA (reviewed in ref. (94,132)). RNase MRP cleaves the yeast pre-rRNA at site A3 within ITS1 *in vivo* (28,29,37) and *in vitro* (30), giving rise to the 5.8S(S) rRNA. RNase MRP is related to the RNase P endoribonuclease since both RNPs contain several identical protein subunits (see below) and their RNA subunits, referred to as MRP (or Th) and P (or H1) RNA, respectively, have common structural features (76,103). Although the nucleotide sequences of the RNase MRP RNA and the RNase P RNA are not highly homologous, they can be folded into very similar cage-shaped secondary structures (29,69). RNase P cleaves precursor tRNA molecules to remove the 5' leader sequence and to generate the correct 5' end of mature tRNA (reviewed in ref. (100,101,133)). Recently, RNase P has also been implicated in the processing of the ITS2 region of pre-rRNA; its exact role in pre-rRNA processing is, however, unclear (5,101). Human RNase P RNA was shown to be localized in the nucleoplasm of cells, but in addition transiently localizes to the nucleolus (58). Recently, yeast RNase P RNA as well as early pre-tRNA processing events were localized primarily to the nucleolus (60). These findings suggest that, in contrast to what generally has been assumed, both RNase MRP and RNase P may primarily function in the nucleolus of cells.

Several protein subunits of the *Saccharomyces cerevisiae* RNase MRP complex have been characterized: Pop1p, Pop3p, Pop4p, Pop5p, Pop6p, Pop7p/Rpp2p, Pop8p and Rpp1p (33-38). These proteins are not only components of the RNase MRP particle but are also associated with the RNase P ribonucleoprotein complex. In addition, one RNase MRP specific protein has been identified in *S. cerevisiae*: Snm1p (32). One human RNase MRP and RNase P associated protein, i.e. hPop1, has been characterized (77). hPop1, which was identified via its homology to the yeast Pop1p protein, is a 115 kDa autoantigenic protein that is predominantly localized in the nucleolus. Recently, four human RNase P associated proteins were characterized: Rpp20, Rpp30, Rpp38 and Rpp40 (78,80). It is likely that (some of) these proteins, as in yeast, are associated with the human RNase MRP complex as well.

Sera from patients suffering from systemic autoimmune diseases, such as scleroderma and systemic lupus erythematosus (SLE), often contain autoantibodies directed to a variety of cytoplasmic, nuclear and nucleolar proteins. A group of patient sera, referred to as anti-Th/To, contain antibodies directed to the RNase MRP and RNase P ribonucleoprotein complexes. Antibodies in these sera were shown to immunoprecipitate the RNase MRP and RNase P RNPs from a HeLa cell extract (61,62,64,65,104). The RNA components of these complexes were not precipitated by these antibodies (65), indicating that anti-Th/To antibodies recognize at least one common or antigenically related protein that is associated with both the RNase MRP and RNase P ribonucleoprotein complexes.

Anti-Th/To sera immunoprecipitate a number of proteins ranging in molecular mass from 18 to 120 kDa from a HeLa cell extract, the most commonly observed one being a protein of 40 kDa, mostly referred to as the Th40 antigen (68,72,75,134-136). It has been suggested that the RNase P associated Rpp38 protein, which is recognized by at least some anti-Th/To sera (80), might be identical to the Th40 autoantigen. In addition to Th40, also hPop1 is a frequent target of anti-Th/To serum antibodies (77).

In this study we investigated the association of the hPop1 protein with the RNase MRP complex. Via *in vitro* reconstitution and immunoprecipitation it was shown that the hPop1 protein requires nucleotides 1-86 and 116-176 of MRP RNA to associate with the MRP complex. UV-crosslinking followed by immunoprecipitation with anti-Th/To antibodies identified three proteins of about 20, 25 and 40 kDa which are able to bind to the RNase MRP RNA. Furthermore, we show that the human RNase P proteins Rpp30 and Rpp38 are also associated with the RNase MRP complex. The 40 kDa protein observed by UV-crosslinking is probably identical to Rpp38. The binding sites of the crosslinked proteins on the RNase MRP RNA were studied and a model in which the hPop1 protein is bound indirectly via these MRP proteins to the RNase MRP complex is proposed.

Results

MRP RNA domains required for association of hPop1 to the RNase MRP complex

To investigate the association of the hPop1 protein with the RNase MRP complex we incubated *in vitro* transcribed ^{32}P-labeled MRP RNA with HeLa cell extract and analyzed reconstituted complexes by immunoprecipitation using anti-hPop1 antibodies. As shown in Figure 1 (lane 1), rabbit antibodies raised against bacterially expressed hPop1 protein (77) were able to immunoprecipitate reconstituted MRP RNA-protein complexes. In contrast, reconstituted U1 and U3 RNP complexes were not immunoprecipitated by anti-hPop1 antibodies, and control antibodies (rabbit anti-Ro52; Figure 1, lane 2) were not able to precipitate the MRP RNA. No MRP RNA was precipitated by anti-hPop1 antibodies when HeLa cell extract was omitted from the incubation (data not shown), confirming that the precipitation of the MRP RNA is due to association of hPop1 and possibly other MRP proteins with the *in vitro* transcribed MRP RNA. In addition, a patient serum containing anti-Th/To antibodies was also able to specifically immunoprecipitate the reconstituted MRP complex (Figure 1, lane 3). These results show that an *in vitro* reconstituted MRP complex can be

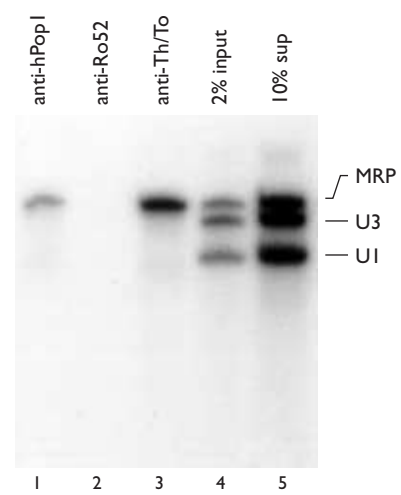

Figure 1. *In vitro* reconstitution of MRP RNA complexes. ^{32}P-labeled MRP, U3 and U1 RNAs were incubated in HeLa cell extract and reconstituted complexes were immunoprecipitated with rabbit anti-hPop1 antibodies (lane 1), rabbit anti-Ro52 antibodies (lane 2) and human anti-Th/To serum antibodies (lane 3). RNAs were extracted from immunoprecipitates, immune supernatants and the input RNA mixture, resolved by denaturing polyacrylamide gel electrophoresis and visualized by autoradiography. Lanes 1-3, RNA isolated from the immunoprecipitates; lane 4, RNA isolated from 2% of the input RNA mixture; lane 5, RNA isolated from 10% of the immune supernatant of the anti-hPop1 immunoprecipitation.

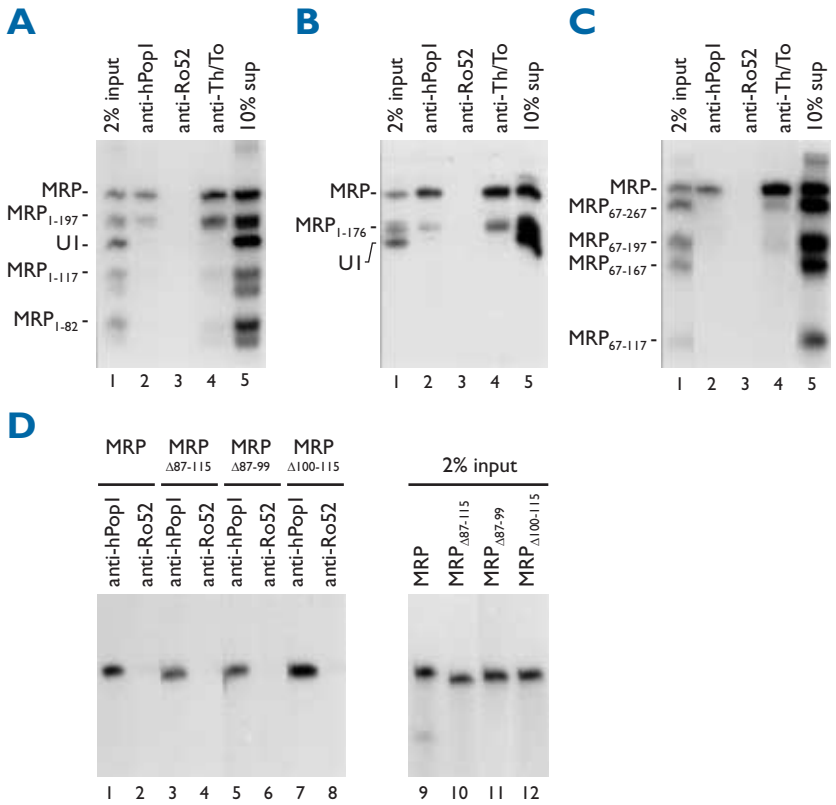

Figure 2. MRP domains required for hPop1 association. ^{32}P-labeled MRP RNAs, full-length as well as deletion mutants, were incubated in HeLa cell extract and reconstituted complexes were immunoprecipitated with rabbit anti-hPop1 antibodies, rabbit anti-Ro52 antibodies and anti-Th/To serum antibodies. RNAs were extracted from immunoprecipitates, immune supernatants and the input RNA mixture, resolved by denaturing polyacrylamide gel electrophoresis and visualized by autoradiography. **A.** Reconstitution using ^{32}P-labeled MRP, $MRP_{1\text{-}197}$, $MRP_{1\text{-}117}$, $MRP_{1\text{-}82}$ and U1 RNAs. Lane 1: RNA isolated from 2% of the input RNA mixture; lane 2: RNA isolated from the anti-hPop1 immunoprecipitate; lane 3: RNA isolated from the anti-Ro52 immunoprecipitate; lane 4: RNA isolated from the anti-Th/To serum immunoprecipitate; lane 5: RNA isolated from 10% of the immune supernatant of the anti-hPop1 immunoprecipitation. **B.** Reconstitution using ^{32}P-labeled MRP, $MRP_{1\text{-}176}$ and U1 RNAs. **C.** Reconstitution using ^{32}P-labeled MRP, $MRP_{67\text{-}267}$, $MRP_{67\text{-}197}$, $MRP_{67\text{-}167}$ and $MRP_{67\text{-}117}$ RNAs. **D.** Reconstitution using ^{32}P-labeled MRP, $MRP_{\Delta 87\text{-}115}$, $MRPD_{87\text{-}99}$ and $MRP_{\Delta 100\text{-}115}$ RNAs. Lanes 1, 3, 5, 7: RNA isolated from the anti-hPop1 immunoprecipitates; lanes 2, 4, 6, 8: RNA isolated from the anti-Ro52 immunoprecipitates; lanes 9-12: RNA isolated from 2% of the input RNA mixture. **E** → *top of next page.* Schematic representation of the MRP RNA deletion mutants and a summary of their ability to be immunoprecipitated by anti-hPop1 antibodies after incubation in HeLa cell extract. Nucleotide numbers are indicated, and the domains of MRP required for association of hPop1 are shaded in dark blue.

immunoprecipitated by anti-hPop1 and anti-Th/To antibodies.

To study the domain(s) of MRP RNA required for association of the hPop1 protein with the RNase MRP complex, we incubated *in vitro* transcribed ^{32}P-labeled MRP RNA deletion mutants with HeLa cell extract and immunoprecipitated reconstituted complexes with anti-hPop1 antibodies. The results of these experiments are shown in Figures 2A-D, and are summarized in Figure 2E. Deletion of the 3' terminal 70 or 91 nucleotides of MRP RNA ($MRP_{1\text{-}197}$ (Figure 2A) and $MRP_{1\text{-}176}$ (Figure 2B), respectively) has a minor effect on the association of the hPop1 protein with the MRP complex, since these mutant MRP RNAs were still, although somewhat less efficiently than full-length MRP RNA, precipitated by anti-hPop1 antibodies (Figure 2A-B, lane 2). Further deletion of the 3' end of MRP RNA to nucleotide 117, resulting in mutant $MRP_{1\text{-}117}$, resulted in loss of precipitation by anti-hPop1 antibodies, indicating that the hPop1 protein is unable to associate with the $MRP_{1\text{-}117}$ RNA (Figure 2A, lane 2). In addition, MRP RNA deletion mutants in which 5' terminal nucleotides are deleted, e.g. $MRP_{67\text{-}267}$ (Figure 2C, lane 2) or $MRP_{86\text{-}267}$ and $MRP_{127\text{-}267}$ (data not shown), were not immunoprecipitated by anti-hPop1 antibodies after incubation with HeLa cell extract. These results suggest that the hPop1 protein needs nucleotides 1 to 176 of MRP RNA for association with the MRP complex. To define this region in more detail we constructed deletion mutants in which stemloops II and/or III of MRP RNA (Figure 3) are deleted: $MRP_{\Delta 87\text{-}115}$, $MRP_{\Delta 87\text{-}99}$ and $MRP_{\Delta 100\text{-}115}$, respectively. After reconstitution in HeLa cell extract, these internal deletion mutants were all three efficiently precipitated by anti-hPop1 antibodies (Figure 2D, lanes 3, 5 and 7).

Reconstituted mutant MRP RNA complexes were also immunoprecipitated using an anti-Th/To patient serum containing anti-hPop1 antibodies. The precipitation results obtained with the serum were similar to the results obtained using rabbit anti-hPop1 antibodies; full-length MRP, $MRP_{1\text{-}197}$, $MRP_{1\text{-}176}$ and MRP RNA lacking stemloop II and/or III were efficiently precipitated (Figure 2A-B, lanes 4 and data not shown). In addition $MRP_{1\text{-}117}$, $MRP_{1\text{-}82}$, $MRP_{67\text{-}267}$ and $MRP_{67\text{-}197}$, which could not be precipitated by anti-hPop1 antibodies, were weakly precipitated by the anti-Th/To serum (Figure 2A, lane 4 and Figure 2C, lane 4, respectively), suggesting that this serum in addition to anti-hPop1 antibodies contains antibodies directed to other MRP protein(s) which are able to associate with these mutant MRP RNAs.

Taken together, these results indicate that the hPop1 protein requires nucleotides 1-86 and 116-176 of MRP RNA to associate with the

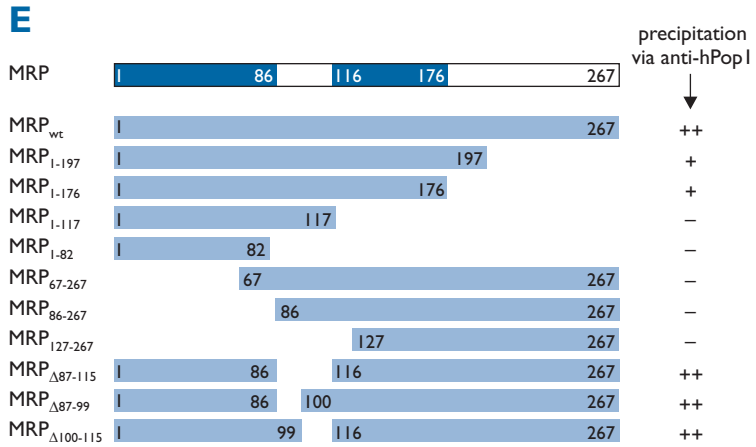

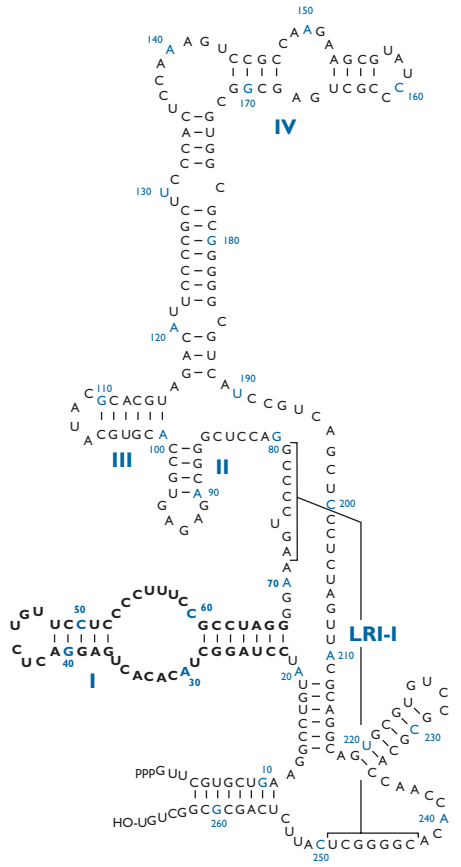

Figure 3. Human RNase MRP RNA. Secondary structure model of human MRP RNA adapted from Schmitt *et al.* (1993). Stemloop structures mentioned in the text are numbered (I-IV) and the proposed long range interaction ('*pseudoknot*') responsible for the '*cage*' structure of MRP RNA is indicated (LRI-I).

RNase MRP complex (Figure 2E). These parts of the MRP RNA include the predicted stemloop structures I and IV, but lack stemloops II and III. Furthermore, the predicted pseudoknot structure which involves the 5′ and 3′ regions of MRP RNA is not required for binding of hPop1 to the MRP complex since 3′ deletion mutants of MRP RNA lacking the ability to form this structure could be immunoprecipitated by anti-hPop1 antibodies.

Identification of MRP RNA binding proteins by UV crosslinking

To investigate if the hPop1 protein is associated directly or indirectly with the MRP RNA, we performed reconstitution experiments with *in vitro* translated ^{35}S-labeled hPop1 protein and in vitro transcribed biotinylated MRP RNA, followed by precipitation using streptavidin agarose beads. The results of these experiments strongly suggested that hPop1 is unable to bind to the MRP RNA directly, since no hPop1 protein could be detected in the precipitate (data not shown). In addition, we were unable to detect a mobility shift of MRP RNA after incubation of ^{32}P-labeled MRP RNA with purified bacterially expressed hPop1 protein and analysis by native gel electrophoresis (data not shown). Next, the binding of hPop1 to the RNase MRP complex was studied using UV-crosslinking. ^{32}P-labeled MRP RNA and control RNAs (U3 and U1 RNA) were incubated with HeLa cell extract, UV irradiated and RNase A treated. The ribonuclease treatment is essential because it removes most of the labeled RNA resulting in a complex of protein crosslinked to a short labeled oligonucleotide that can be immunoprecipitated by antibodies and analyzed by SDS-PAGE.

As shown in Figure 4A (lane 5), rabbit anti-hPop1 antibodies were unable to precipitate a ^{32}P-labeled protein, suggesting that the hPop1 protein was not in close contact with the MRP RNA during UV-crosslinking and thus probably not directly bound to the MRP RNA. Also anti-Th/To patient sera containing anti-hPop1 antibodies were unable to immunoprecipitate a ^{32}P-labeled protein of approximately 115 kDa, i.e. hPop1 (Figure 4A, lanes 3-4). However, these sera were able to immunoprecipitate ^{32}P-labeled polypeptides of approximately 20, 25 and 40 kDa, hereafter referred to as MRP20, MRP25 and MRP40, respectively (Figure 4A, lanes 3-4). These three proteins were precipitated by several anti-Th/To sera, although the efficiency of precipitation varied depending on the patient serum used. The specificity of UV crosslinking and precipitation was confirmed by the observation that MRP20, MRP25 and MRP40 were only detected if MRP RNA was used for UV-crosslinking. UV-crosslinking of control RNAs such as U3 and U1 RNA followed by anti-Th/To immunoprecipitation did not result in the detection of radiolabeled polypeptides (Figure 4A, lanes 9-10 and 15-16). In addition normal human serum did not precipitate the MRP20, MRP25 and MRP40 proteins (Figure 4A, lane 2). As shown in Figure 4A (lane 6), not only MRP20, MRP25 and MRP40 were UV-crosslinked to MRP RNA, a large number of ^{32}P-labeled proteins was detectable after UV-crosslinking of MRP RNA and RNase A treatment followed by SDS-PAGE. However, the use of U3 and U1 RNAs also resulted in a large number of ^{32}P-labeled proteins after UV-crosslinking (Figure 4A, lanes 12 and 18), which makes it rather difficult to distinguish between MRP specific and non-specific proteins and thus stresses the need for immunoprecipitation after UV-crosslinking.

The specificity of the MRP20, MRP25 and MRP40 crosslinking was further established by competition experiments in which an excess of

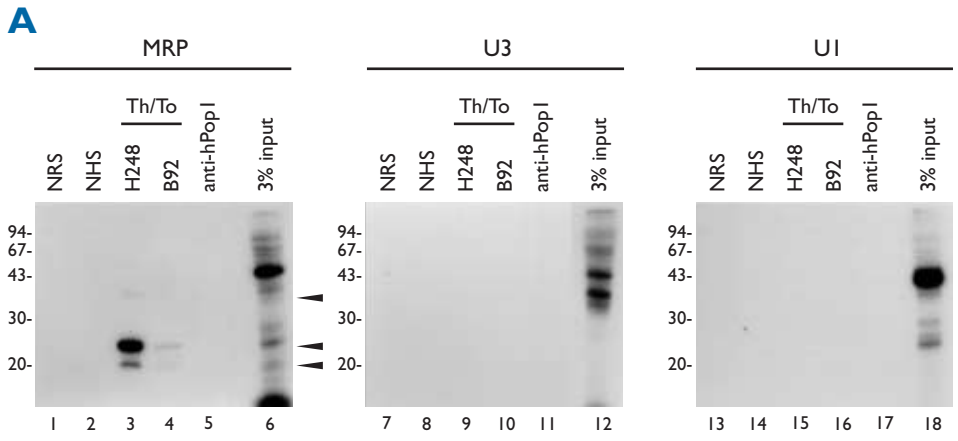

Figure 4. UV crosslinking analysis of MRP RNA. **A.** ^{32}P-labeled MRP RNA (lanes 1-6), U3 RNA (lanes 7-12) and U1 RNA (lanes 13-18) were incubated in HeLa cell extract and exposed to UV light to achieve crosslinking of RNA-protein complexes. Crosslinked complexes were treated with RNase A and subsequently immunoprecipitated by rabbit anti-hPop1 antibodies (lanes 5, 11 and 17), normal rabbit serum (lanes 1,7 and 13), anti-Th/To serum antibodies (lanes 3-4, 9-10 and 15-16) and normal human serum (lanes 2, 8 and 14). Precipitated proteins were analyzed by 13% SDS polyacrylamide gel electrophoresis and visualized by autoradiography. Lanes 6, 12 and 18 represent 3% of the crosslinked proteins used for immunoprecipitation. The MRP20, MRP25 and MRP40 proteins are indicated by arrows. Protein molecular weight markers are shown at the left. **B.** ^{32}P-labeled MRP RNA and nonradioactive competitor RNA (10-fold excess) were incubated in HeLa cell extract and exposed to UV light to achieve crosslinking of RNA-protein complexes. Crosslinked complexes were treated with RNase A and subsequently immunoprecipitated by anti-Th/To serum antibodies. Precipitated proteins were analyzed by 13% SDS polyacrylamide gel electrophoresis and visualized by autoradiography. Lane 1: no competitor RNA present; lane 2: cold MRP RNA as competitor; lane 3: cold U1 RNA as competitor; lane 4: cold U3 RNA as competitor.

nonradioactive competitor MRP, U3 or U1 RNA was co-incubated with ^{32}P-labeled MRP RNA in HeLa cell extract. Following UV-crosslinking and anti-Th/To serum immunoprecipitation, only competitor MRP RNA was able to compete for the crosslinking of the MRP20, MRP25 and MRP40 proteins (Figure 4B, lane 2). Incubation with competitor U1 or U3 RNA had no influence on the crosslinking of these proteins to the MRP RNA.

The MRP25 protein was reproducibly the most strongly labeled protein after UV-crosslinking and anti-Th/To immunoprecipitation. However, methylene-blue mediated photocrosslinking (137) decreased the MRP25 signal and increased the MRP20 signal, thus reversing the intensity of the protein bands (data not shown). Also, the use of [α-^{32}P]CTP instead of [α-^{32}P]UTP for the in vitro transcription of labeled RNAs had some influence on the relative intensities of the observed protein bands after crosslinking. MRP40 was more efficiently labeled when [α-^{32}P]CTP was used (data not shown), possibly due to the presence of more C residues at the MRP40 crosslinking site.

Taken together our results suggest that the hPop1 protein is unable to bind directly to the MRP RNA, but associates with the complex via other MRP associated proteins. In addition, the UV-crosslinking data indicate that at least three proteins, MRP20, MRP25 and MRP40, are able to bind directly to the MRP RNA.

Identification of crosslinked MRP proteins

Recently, two human RNase P RNA associated proteins which are recognized by anti-Th/To serum antibodies, have been characterized: Rpp30 and Rpp38 (78,80). It is likely that, similar to the situation in yeast where most of the RNase P associated proteins are also associated with the RNase MRP complex (38), Rpp30 and Rpp38 are also components of the human RNase MRP complex. Therefore, the MRP20, MRP25 and/or MRP40 proteins identified by UV-crosslinking followed by anti-Th/To immunoprecipitation might correspond to the Rpp30 and/or Rpp38 proteins.

Since it had not been fully established whether Rpp30 and Rpp38 are associated with both the human RNase P and RNase MRP complexes, we performed immunoprecipitation experiments with VSV-G (Vesicular Stomatitis

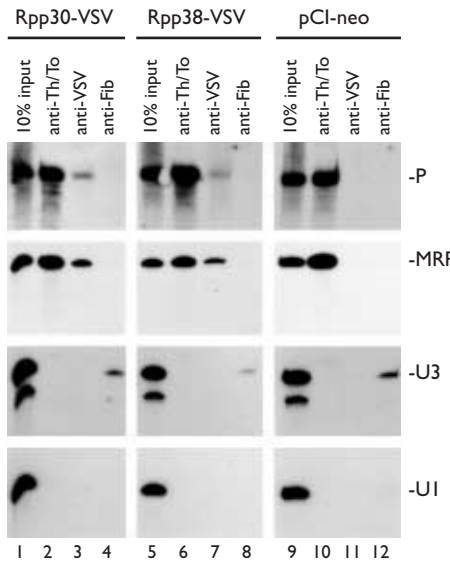

Figure 5. Rpp30 and Rpp38 are RNase P and RNase MRP complex associated proteins. Rpp30-VSV, Rpp38-VSV and pCI-neo were transiently expressed in HeLa cells. Two days after transfection, cells were lysed and used for immunoprecipitation with anti-VSV, anti-fibrillarin and anti-Th/To serum antibodies. RNAs were extracted from immunoprecipitates (lanes 2-4, 6-8 and 10-12) and total cell extracts (lanes 1, 5 and 9), resolved by denaturing polyacrylamide gel electrophoresis and transferred to a northern blot. Specific antisense RNA probes were used to detect human RNase P, RNase MRP, U3 and U1 RNAs, as indicated on the right. Lanes 1-4: cells expressing Rpp30-VSV; lanes 5-8: cells expressing Rpp38-VSV; lanes 9-12: control cells transfected with pCI-neo vector. Lanes 2, 6 and 10: anti-Th/To serum immunoprecipitation; lanes 3, 7 and 11: anti-VSV immunoprecipitation; lanes 4, 8 and 12: anti-fibrillarin immunoprecipitation; lanes 1, 5 and 9: RNA isolated from 10% of total cell extract used for immunoprecipitations.

Virus; (106)) tagged Rpp30 and Rpp38 proteins. Rpp30 and Rpp38 cDNAs (78) were subcloned in the mammalian expression vector pCI-neo containing a VSV-G tag sequence followed by a stop codon in the multiple cloning site (see Material and Methods). The resulting VSV tagged Rpp30 and Rpp38 encoding cDNAs (Rpp30-VSV and Rpp38-VSV, respectively) were transfected into HeLa cells. Two days after transfection, cells were lysed and the resulting total cell extracts were used for immunoprecipitation with anti-VSV and anti-fibrillarin monoclonal antibodies, and anti-Th/To serum antibodies. As a control the pCI-neo vector without insert (pCI-neo) was also used for transfection and the resulting cell extracts for immunoprecipitation experiments. RNAs were extracted from both immunoprecipitates and total cell extracts, fractionated by gel electrophoresis and analyzed by northern blot hybridization with probes specific for RNase P RNA, RNase MRP RNA, U3 RNA and U1 RNA.

As shown in Figure 5, RNase P RNA as well as RNase MRP RNA were co-precipitated by anti-VSV antibodies from cell extracts containing VSV-tagged Rpp30 (Rpp30-VSV (lane 3)) or VSV-tagged Rpp38 (Rpp38-VSV (lane 7)) protein, showing that Rpp30 and Rpp38 are indeed associated with both the human RNase MRP and RNase P complexes. The specificity of this result was established by the lack of RNase MRP and RNase P RNA co-precipitation with (i) anti-VSV antibodies from a control cell extract (pCI-neo) (Figure 5, lane 11) and (ii) anti-fibrillarin antibodies (Figure 5, lanes 4, 8 and 12). RNase P and MRP RNAs were immunoprecipitated from all extracts using anti-Th/To serum antibodies (Figure 5, lanes 2, 6 and 10). No U3 or U1 RNA could be detected in the anti-VSV and anti-Th/To serum immunoprecipitates.

To investigate whether some of the crosslinked MRP proteins are identical to the Rpp30 or Rpp38 proteins, UV-crosslinked complexes reconstituted with ^{32}P-labeled MRP RNA as described above were immunoprecipitated (after RNase A treatment) with rabbit anti-Rpp30 and rabbit anti-Rpp38 antibodies (80). As shown in Figure 6 (lane 3), anti-Rpp38 specific antibodies immunoprecipitated a ^{32}P-labeled polypeptide with an electrophoretic mobility indistinguishable from that of MRP40 (Figure 6, lane 1). This strongly suggests that MRP40 is identical to the Rpp38 protein. In contrast anti-Rpp30 antibodies did not detectably immunoprecipitate a ^{32}P-labeled protein, suggesting that Rpp30 is not identical to any of the crosslinked MRP proteins.

Taken together, these results show that both Rpp30 and Rpp38 are associated with the

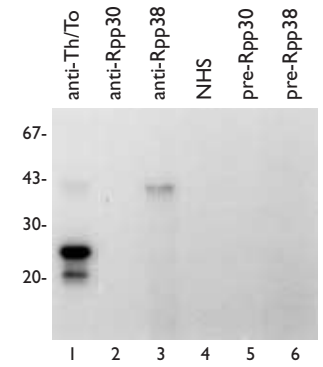

Figure 6. Identification of crosslinked MRP proteins as Rpp30/Rpp38. ^{32}P-labeled MRP RNA was incubated in HeLa cell extract and exposed to UV light to achieve crosslinking of RNA-protein complexes. Crosslinked complexes were treated with RNase A and subsequently immunoprecipitated by anti-Th/To serum antibodies (lane 1), rabbit anti-Rpp30 antibodies (lane 2), rabbit anti-Rpp38 antibodies (lane 3), normal human serum (lane 4) and rabbit pre-immune serum (pre-Rpp30 (lane 5) and pre-Rpp38 (lane 6)). Precipitated proteins were analyzed by 13% SDS polyacrylamide gel electrophoresis and visualized by autoradiography.

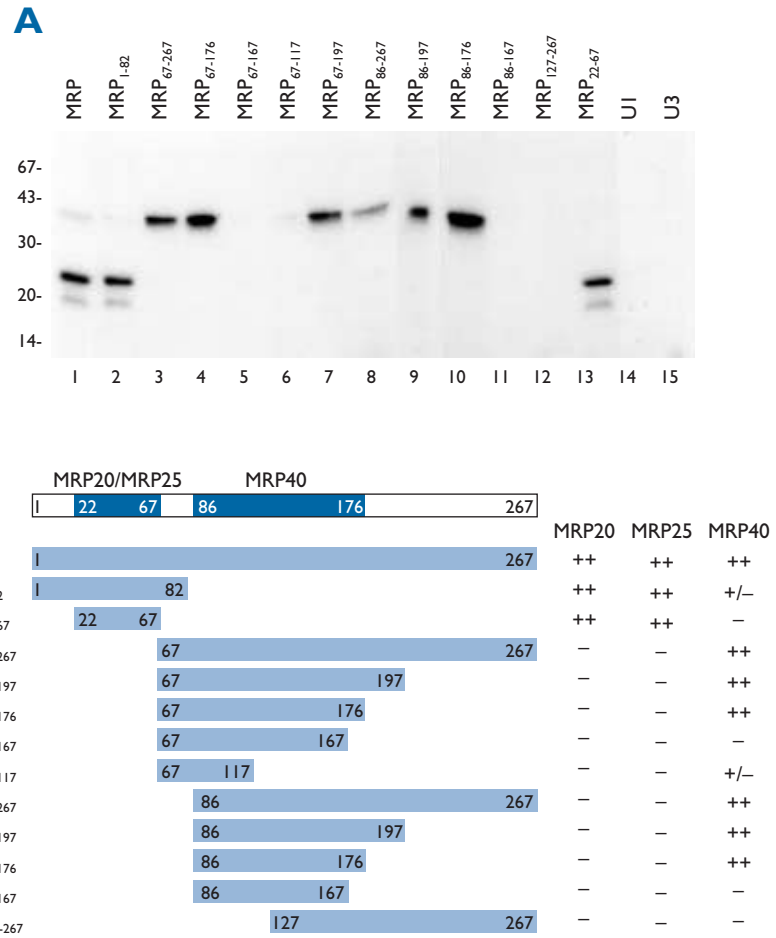

Figure 7. Domains of MRP RNA required for binding of MRP20, MRP25 and MRP40. **A.** ^{32}P-labeled MRP RNA, full-length (lane 1) and deletion mutants (lanes 2-13), U1 RNA (lane 14) and U3 RNA (lane 15) were incubated in HeLa cell extract and exposed to UV light to achieve crosslinking of RNA-protein complexes. Crosslinked complexes were treated with RNase A and subsequently immunoprecipitated by anti-Th/To serum antibodies. Precipitated proteins were analyzed by 13% SDS polyacrylamide gel electrophoresis and visualized by autoradiography. Protein molecular weight markers are shown at the left. **B.** Schematic representation of the MRP RNA deletion mutants and a summary of the ability of the MRP20, MRP25 and MRP40 proteins to be crosslinked to these RNAs (indicated on the right). Nucleotide numbers are indicated, and the domains of MRP required for association of MRP20, MRP25 and MRP40 are shaded in dark blue.

human RNase P as well as the human RNase MRP complexes. In contrast to Rpp30, Rpp38 appears to be in close contact with MRP RNA in the complex. These results are in agreement with the observation that *in vitro* translated Rpp38 protein but not *in vitro* translated Rpp30 protein can be specifically precipitated by streptavidin beads after incubation with biotinylated MRP RNA (data not shown). Furthermore, the MRP40 protein we detected via UV-crosslinking and anti-Th/To immunoprecipitation is probably identical to the Rpp38 protein.

MRP20, MRP25 and MRP40 bind to different domains of the MRP RNA

To study the regions of MRP RNA which are required for binding of the MRP20, MRP25 and MRP40 proteins to the RNase MRP complex, we performed UV-crosslinking experiments with MRP RNA deletion mutants. After incubation of *in vitro* transcribed ^{32}P-labeled MRP RNA deletion mutants in a HeLa cell extract, UV irradiation and RNase A treatment, proteins were immunoprecipitated with anti-Th/To patient serum and analyzed by SDS-PAGE followed by autoradiography. The results of these UV crosslinking experiments are shown in Figures 7A-B. Deletion of the 5' terminal 66 nucleotides, thus removing the first stemloop structure of MRP RNA, abolished the binding of MRP20 and MRP25, while MRP40 was still able to bind to this MRP RNA fragment (MRP_{67-267}) (Figure 7A, lane 3). Strikingly, when MRP_{67-267} was used, MRP40 appeared to be much more efficiently crosslinked than when full-length MRP RNA was used. Further deletion of the 5' end up to nucleotide 86 (MRP_{86-267}) gave similar results (Figure 7A, lane 8). However, a deletion up to nucleotide 127 ($MRP_{127-267}$) resulted in loss of MRP40 crosslinking (Figure 7A, lane 12). 3' end deletions of MRP_{86-267}, resulting in mutants MRP_{86-176} and MRP_{86-167} (Figure 7A, lanes 10 and 11, respectively), showed that MRP40 requires nucleotides 86 to 176 in order to be efficiently crosslinked to the MRP RNA. In addition, MRP40 might have a weak affinity for other parts of the MRP RNA since MRP_{1-82} and MRP_{67-117} produced a weak signal of MRP40 after UV-crosslinking (Figure 7A, lanes 2 and 6). Similar results were obtained when the crosslinked complexes were precipitated with anti-Rpp38 antibodies, again suggesting that MRP40 is identical to Rpp38 (data not shown).

Deletion of the 5' end of MRP RNA to nucleotide 67 (MRP_{67-267}) abolished the binding of MRP20 and MRP25 (Figure 7A, lane 3). However, deletion of most of the 3' end of MRP RNA, resulting in MRP_{1-82}, did not have any effect on MRP20 and MRP25 crosslinking (Figure 7A, lane 2). In addition, MRP20 and MRP25 were still efficiently crosslinked to an MRP RNA deletion mutant containing only the first stemloop structure, MRP_{22-67} (Figure 7A, lane 13). These results indicate that both the MRP20 and MRP25 proteins bind to the same domain of MRP RNA, that is stemloop I.

Discussion

Association of hPop1 with the RNase MRP complex

Via incubation of ^{32}P-labeled MRP RNA, full-length as well as deletion mutants, in a HeLa cell extract followed by immunoprecipitation with anti-hPop1 antibodies, the hPop1 protein was shown to be dependent on nucleotides 1-86 and 116-176 for binding to the RNase MRP complex. However, hPop1 appeared not to bind directly to the MRP RNA since a stable interaction between *in vitro* translated or recombinant hPop1 protein and *in vitro* transcribed MRP RNA could not be detected, and UV-crosslinking of ^{32}P-labeled MRP RNA in a HeLa cell extract, followed by RNase A treatment and immunoprecipitation with anti-hPop1 antibodies did not result in detection of a crosslinked 115 kDa protein. These observations indicate that the hPop1 protein most likely associates with the MRP complex via protein-protein interactions and

the RNase MRP associated protein(s) necessary for hPop1 association require nucleotides 1-86 and 116-176 of the MRP RNA for efficient complex formation.

Three proteins of 20, 25 and 40 kDa can be crosslinked to the MRP RNA

UV-crosslinking experiments led to the identification of three proteins of about 20, 25 and 40 kDa, respectively, which can directly bind to the MRP RNA. Thus, in addition to hPop1, at least three other proteins, MRP20, MRP25 and MRP40, are presumably associated with the human RNase MRP complex. These results are in agreement with previous data, showing that proteins with similar molecular weights can be immunoprecipitated by anti-Th/To serum antibodies and thus were thought to be associated with the RNase MRP complex (68,136). Yuan *et al*. identified a protein of about 40 kDa by UV-crosslinking using RNase MRP RNA which was immunoprecipitable by anti-Th/To serum antibodies (75). However, in contrast to our results, the 20 and 25 kDa proteins were not detected in the latter study. This difference might be due to variations in the crosslinking conditions, HeLa cell extract preparation or MRP RNA transcripts used. For example, the use of [α-^{32}P]CTP instead of [α-^{32}P]UTP for *in vitro* transcription did have a positive effect on the MRP40 signal in UV-crosslinking, possibly due to the presence of more C residues at the MRP40 crosslinking site.

Rpp30 and Rpp38 are associated with the human RNase MRP complex

Recently, four human RNase P associated proteins have been characterized: Rpp20, Rpp30, Rpp38 and Rpp40 (78,80). Two of these human RNase P protein subunits, Rpp30 and Rpp38, were shown to be recognized by anti-Th/To serum antibodies and may, as has been found in the yeast system (38), be part of the human RNase MRP complex as well (78,80). Expression of VSV-tagged Rpp30 and Rpp38 proteins in HeLa cells followed by anti-VSV immunoprecipitation and northern blot analysis of co-precipitating RNAs showed that Rpp30 and Rpp38 are indeed associated with both the human RNase MRP and RNase P complexes. UV-crosslinking of ^{32}P-labeled MRP RNA in a HeLa cell extract followed by immunoprecipitation with anti-Rpp30, anti-Rpp38 and anti-Th/To antibodies indicated that the MRP40 protein, observed after UV-crosslinking, most probably is identical to the Rpp38 protein. Although anti-Th/To and anti-Rpp38 antibodies immunoprecipitated a crosslinked protein of the same molecular mass using both wild-type and deletion mutants of MRP RNA, we cannot exclude the unlikely possibility that MRP40 and Rpp38 are different proteins with similar molecular masses which both can bind directly to the same region of the MRP RNA and are recognized by different antibody populations in the anti-Th/To serum. Rpp30 appears not to be identical to any of the crosslinked MRP proteins since this protein seems unable to associate directly with the MRP RNA. Sequence analysis of the crosslinked MRP proteins will give definitive information about their precise identity.

The MRP20 and MRP25 proteins bind to stemloop I of MRP RNA

Using MRP RNA deletion mutants as the substrate in the UV-crosslinking experiments it could be shown that the MRP20 and MRP25 proteins require nucleotides 22-67 of MRP RNA for efficient binding. Both proteins thus appear to bind to stemloop I of the MRP RNA. Although we cannot rigorously exclude the possibility that MRP20 is a degradation product of MRP25, several observations argue against this possibility. First, the use of different HeLa cell extracts, which probably contain different levels of protease activities, did not have any effect on the relative intensities of the crosslinked MRP20 and MRP25 protein bands. Secondly, methylene blue mediated photo-crosslinking, which has been reported to favour crosslinking to dsRNA regions (137), increased the MRP20 signal concomitant with a decrease of the MRP25 signal. This result of the methylene bleu mediated crosslinking may even indicate that the MRP20 and MRP25 proteins bind to different regions of the stemloop I structure, i.e. that MRP20 possibly binds to one of the stem structures of stemloop I while MRP25 might prefer a single stranded region. Further experiments with detailed stemloop I mutants have to be performed to reveal the precise binding sites of MRP20 and MRP25.

The MRP40 protein: the Th40 autoantigen?

Our analyses showed that MRP40 requires nucleotides 86-176 of MRP RNA for efficient binding. This region encompasses stemloops II, III and IV, but lacks the proposed pseudoknot structure of MRP RNA. Interestingly, the MRP40 protein was much stronger labeled when mutants in which the 5' end was deleted (e.g. MRP_{67-267}) were used compared to full-length MRP RNA, suggesting that the MRP40 binding site may be more readily accessible in these mutant RNAs. As mentioned above, the MRP40 protein is probably identical to the previously described Rpp38 protein (78) because they exhibit similar molecular masses and bind directly to the same region of the MRP RNA.

Previously, a 40 kDa autoantigenic protein, mostly referred to as the 40 kDa Th/To autoantigen (Th40) has been UV-crosslinked to human MRP RNA. It was shown that this protein required nucleotides 21-64, i.e. stemloop I of MRP RNA for binding to the RNase MRP complex (75). In addition, this protein was reported to bind to a similar stemloop structure in human RNase P RNA (134). It seems unlikely that the autoantigenic MRP40 protein described by us is the Th40 autoantigen since the binding site of MRP40 appears to be located in a different part of the MRP RNA. In contrast to a 40 kDa protein binding to stemloop I of MRP RNA, we found 20 and 25 kDa autoantigenic proteins crosslinked with stemloop I of MRP RNA. At present we have no satisfying explanation for these contradictory results.

A model for the RNase MRP complex

Our results strongly suggest that the association of the hPop1 protein with the RNase MRP complex is mainly mediated by protein-protein interactions, and that the RNase MRP associated protein(s) necessary for hPop1 binding require nucleotides 1-86 and 116-176 of MRP RNA for binding. Most interestingly, similar regions of the MRP RNA were found to be required for binding of the MRP20, MRP25 and MRP40 proteins. Therefore, it is not unlikely that the proteins involved in hPop1 association are the MRP20 and/or MRP25 proteins medi-

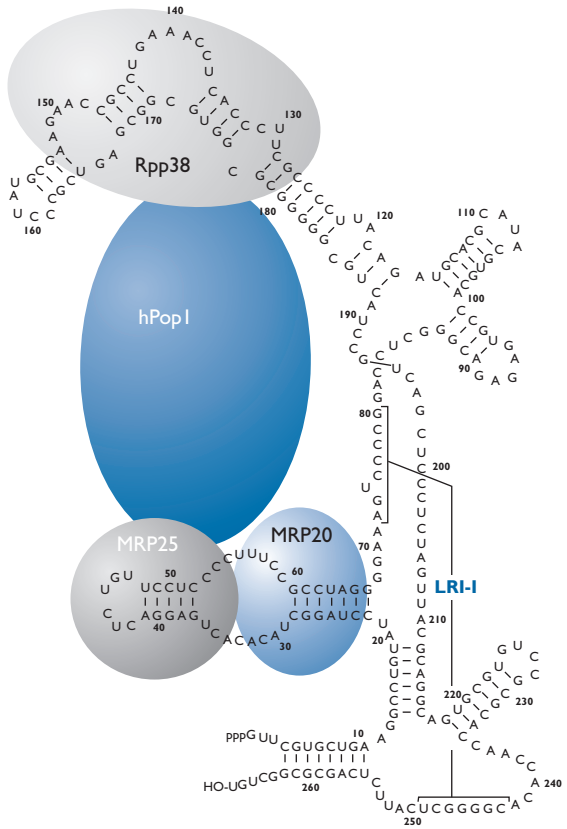

Figure 8. Model for the human RNase MRP complex. Schematic representation of the presence of the MRP20, MRP25, Rpp38 and hPop1 proteins in the human RNase MRP complex. The MRP20 and MRP25 proteins bind directly to the MRP RNA between nucleotides 22 and 67. The exact manner in which they bind to this region is unclear and the idea depicted is just one of the possibilities. Rpp38 binds directly to a region of MRP RNA from nucleotides 86-176. hPop1 binds indirectly via protein-protein interactions to the RNase MRP complex, possibly by binding the MRP20 and/or MRP25 proteins and Rpp38.

ating the interaction with stemloop I of MRP RNA and the MRP40 protein, mediating the interaction with the central part of the MRP RNA. A model of the RNase MRP complex that results from these presumptive protein-protein interactions is depicted in Figure 8. In addition to the depicted proteins, also Rpp30 which could not be crosslinked to the MRP RNA appears to associate via protein-protein interactions to the RNase MRP complex. Furthermore, it is likely that also other not yet identified proteins bind to the RNase MRP complex via protein-protein and/or protein-RNA interactions. Additional experiments designed to reveal the putative protein-protein interactions between hPop1 and MRP20, MRP25 and/or MRP40 are necessary to establish the validity of the model.

Our data do not exclude the possibility that conformational changes occur in the MRP RNA upon binding of MRP20, MRP25 and/or MRP40, which might help in creating a proper binding site for hPop1 and possibly other proteins. In fact, the much more efficient interaction of MRP40 with mutant MRP_{67-267} might be indicative of changes in the RNA structure upon binding of this protein. Interestingly, all the proteins found to be associated with the RNase MRP complex bind directly or indirectly to the 5′ and/or central part of the RNase MRP RNA. Neither hPop1, nor MRP20, MRP25 and MRP40 require regions in the 3′ part of the RNA for association with the MRP complex.

It is therefore possible that the predicted conserved pseudoknot structure of MRP RNA is not involved in protein binding but might be required for the catalytic reactivity of the RNase MRP complex. Stemloop I of MRP RNA has previously been shown to be required for nucleolar localization of MRP RNA (44). It will thus be interesting to find out if the stemloop I binding proteins, MRP20 and MRP25, are involved in the nucleolar targeting of the RNase MRP complex.

This study is a further step in resolving the complexity of the human RNase MRP particle. Detailed knowledge on the proteins associated with the RNase MRP RNA and their interactions may give more insight in the pre-rRNA processing steps in which RNase MRP is involved. Furthermore, detailed information of the RNase MRP complex may simultaneously lead to a better understanding of the related RNase P particle and its function in pre-tRNA and pre-rRNA processing.

Acknowledgements

We are grateful to Drs. S. Altman and N. Jarrous (Yale University, New Haven) for kindly providing Rpp30 cDNA, rabbit anti-Rpp30 and rabbit anti-Rpp38 antibodies and to Dr. C. Liew (University of Toronto) and Dr. S. Altman for Rpp38 cDNA. This work was supported in part by the Netherlands Foundation for Chemical Research (SON) with financial aid from the Netherlands Organization for Scientific Research (NWO).

Materials and methods

Oligonucleotides

The following oligonucleotides were used for obtaining MRP RNA constructs: MRP-0: GCG-AAT-TCG-TTC-GTG-CTG-AAG-GCC-TAG-ATC; MRP-1: GCG-AAG-CTT-ACA-GCC-GCG-CTG-AGA-ATG-AG; MRP-2: GCG-AAT-TCT-AAT-ACG-ACT-CAC-TAT-AGG-GAA-AGT-C-CC-CGG-ACC-T; MRP-3: GCG-AAT-TCT-AAT-ACG-ACT-CAC-TAT-AGG-GCA-GAG-AGT-GCC-ACG-T; MRP-4: GCG-AAT-TCT-AAT-ACG-ACT-CAC-TAT-AGG-CTT-CCC-ACT-CCA-AAG-TCC-G; MRP-5: GAA-AGT-CCC-CGG-ACC-TCG-AGA-CAT-TCC-CCG-CTT-CCC-AC; MRP-6: GAA-AGT-CCC-CGG-ACC-TCG-ACG-TGC-ATA-CGC-ACG-TAG-ACA-TTC; MRP-7: ACC-TCG-GGC-AGA-GAG-TGC-CAG-ACA-TTC-CCC-GCT-TCC-CAC; MRP-8: GCG-AAT-TCT-AAT-ACG-ACT-CAC-TAT-AGG-CCT-AGG-CTA-CAC-ACT-GAG-GAC-T; MRP-9: CGA-AGC-TTC-CTA-GGC-GAA-AGG-GGA-GGA-AC.

MRP constructs and in vitro transcription

A cDNA clone containing the full-length MRP RNA (116) was subcloned into the *Eco*RI/*Hind*III sites of vector pGEM-3Zf(+) and linearized with *Hind*III, giving rise to full-length MRP RNA after *in vitro* transcription. 3′ terminally truncated mutants of MRP, i.e. MRP_{1-197}, MRP_{1-176}, MRP_{1-117} and MRP_{1-82} were obtained by linearization of the full-length MRP construct prior to *in vitro* transcription with restriction enzymes *Alu*I, *Hha*I, *Acc*I and *Ava*II, respectively. 5′ terminally truncated mutants of MRP were obtained by PCR amplification of the wild-type MRP construct using oligonucleotides MRP-2/MRP-1, MRP-3/MRP-1 and MRP-4/MRP-1 giving rise to MRP_{67-267}, MRP_{86-267} and $MRP_{127-267}$, respectively. The PCR products were digested with *Eco*RI/*Hind*III, cloned into pUC19 and linearized with *Hind*III prior to in vitro transcription. 3′ terminal truncations of these mutants were obtained by linearization of the plasmids prior to *in vitro* tran-

scription with restriction enzymes *Alu*I, *Hha*I, *Dde*I and *Acc*I resulting in MRP_{67-197}, MRP_{67-176}, MRP_{67-167}, MRP_{67-117}, MRP_{86-197}, MRP_{86-176}, MRP_{86-167}, MRP_{86-117}, $MRP_{127-197}$, $MRP_{127-176}$ and $MRP_{127-167}$, respectively.

MRP_{22-67} was obtained by PCR amplification of the wild-type MRP construct using oligonucleotides MRP-8/MRP-9. The resulting PCR product was digested with *Eco*RI/*Hind*III, cloned into pUC19 and linearized with *Hind*III prior to *in vitro* transcription. MRP mutants lacking stemloop II and/or III ($MRP_{\Delta 87-115}$, $MRP_{\Delta 87-99}$ and $MRP_{\Delta 100-115}$) were constructed using a two step PCR reaction. In the first step wild-type MRP was used as template in PCR using oligonucleotides MRP-5/MRP-1, MRP-6/MRP-1 and MRP-7/MRP-1. The resulting PCR products were gel purified and used as primer, together with oligonucleotide MRP-0, in a second PCR with wild-type MRP as template. The products of this second PCR were digested with *Eco*RI/*Hind*III, cloned in pGEM-3Zf(+) and linearized with *Hind*III prior to *in vitro* transcription. The integrity of each construct was checked by sequence analysis. MRP constructs lacking stemloop II and/or III contained some additional mutations due to PCR. In $MRP_{\Delta 87-115}$, G68 and C145 were mutated into T68 and T145, in $MRP_{\Delta 87-99}$ T165 was replaced by G165 and in $MRP_{\Delta 100-115}$, G80 and C126 were mutated into T80 and G126, respectively.

For *in vitro* transcription 0.5 µg linearized MRP template was incubated for 1 h at 37°C in 25 µl of buffer containing 40 mM Tris-Cl pH 7.9, 6 mM $MgCl_2$, 2 mM spermidine, 10 mM NaCl, 10 mM dithiothreitol, 0.1 mg/ml bovine serum albumin, 40 U RNasin, 1 mM ATP, 1 mM CTP, 1 mM GTP, 2.5 µM UTP, 20 µCi [α-^{32}P]UTP and 15 U T7 RNA polymerase. After transcription, unincorporated nucleotides were removed by a Sephadex G50 spin column and the RNA was phenol/chloroform extracted and ethanol precipitated. The integrity of the ^{32}P-labeled transcripts was checked by denaturing polyacrylamide gel electrophoresis.

In vitro reconstitution and immunoprecipitation

Twenty-five µl rabbit serum (anti-hPop1 (77) or anti-Ro52 (138)) or 10 µl patient serum (anti-Th/To (H248) or normal human serum) were incubated with 20 µl of a 50% suspension of protein A agarose beads in IPP500 (500 mM NaCl, 10 mM Tris-Cl pH 8.0, 0.05% NP-40) for 1 h at room temperature. Beads were washed twice with IPP500 and once with buffer A (200 mM KCl, 10 mM Hepes pH 7.9, 2 mM $MgCl_2$, 0.05% NP-40). *In vitro* transcribed ^{32}P-labeled MRP RNA, full-length and deletion mutants, were incubated for 45 min. at room temperature with 10 µl of total HeLa cell extract (116) in a volume of 20 µl containing 200 mM KCl, 10 mM Hepes pH 7.9, 2 mM $MgCl_2$, 0.05% NP-40 and 5 mg yeast RNA. Protein A agarose coupled antibodies in 500 µl buffer A were added, and the mixture was incubated for 1 h at 4°C. Beads were washed three times with buffer A, and co-precipitating RNAs were isolated by phenol/chloroform extraction and ethanol precipitation. RNAs were separated on a 8% denaturing polyacrylamide gel and visualized by autoradiography.

UV-crosslinking

In vitro transcribed ^{32}P-labeled MRP RNA, full-length or deletion mutants (4 pmol), were incubated for 45 min. at room temperature with 30 µl of total HeLa cell extract (116) in a total volume of 60 µl containing 150 mM KCl, 12.5 mM Tris-Cl pH 7.4, 1 mM $MgCl_2$ and 0.05% NP-40. For competition experiments 40 pmol of nonradioactive competitor RNA was included in the incubation of ^{32}P-labeled MRP RNA with HeLa cell extract. The mixture was exposed to UV light (254 nm wavelength) with an energy of 1 J/cm^2 for 20 min. on ice in an Amersham UV crosslinker (RPN2500) to achieve crosslinking of RNA to protein. Subsequently, 20 µg of RNase A was added and the mixture was incubated for 1 h at 37°C. Protein A agarose coupled antibodies (rabbit anti-hPop1 (77), normal rabbit serum, anti-Th/To (H248) or normal human serum or rabbit anti-Rpp30, rabbit anti-Rpp38 ((80), kind gifts of Drs. S. Altman and N. Jarrous (Yale University)) in 500 µl IPP150 (150 mM NaCl, 10 mM Tris-Cl pH 8.0, 0.05% NP-40) were added, and the mixture was incubated for 1 h at 4°C. Beads were washed three times with IPP150 and resuspended in SDS-sample buffer. Precipitated proteins were analyzed by 13% SDS polyacrylamide gel electrophoresis and visualized by autoradiography.

Rpp30 and Rpp38 transfection and immunoprecipitation

Rpp30 cDNA ((78), a kind gift of Drs. S. Altman and N. Jarrous (Yale University)) was mutated by PCR to introduce a *Xho*I site before the translational start codon and a *Xba*I site before the stop codon. The PCR product was digested with *Xho*I/*Xba*I and ligated in a *Xho*I/*Xba*I digested pCI-neo vector which contains a 3' VSV-G tag encoding sequence (YTDIEMNRLGK-stop) inserted between the original *Xba*I-*Sal*I sites of pCI-neo. The resulting construct (Rpp30-VSV) contains the VSV-G tag sequence in frame directly behind the last codon of Rpp30 and is terminated by the stop codon introduced after the tag sequence.

Rpp38 cDNA ((78), a kind gift of Dr. C. Liew (University of Toronto) and Dr. S. Altman (Yale University)) was mutated and cloned in pCI-neo containing the 3' VSV tag in the same way, resulting in construct Rpp38-VSV. The integrity of both constructs was checked by sequence analysis.

Transient transfection of HeLa cells with Rpp30-VSV, Rpp38-VSV and pCI-neo DNA followed by immunoprecipitation using anti-VSV, anti-fibrillarin and anti-Th/To serum (H248) antibodies was performed essentially as described (113). Northern blot hybridization with antisense riboprobes specific for P, MRP, U3 and U1 RNAs was performed as previously described (116).

Chapter 6

Identity of the RNase MRP and RNase P associated Th/To-autoantigen

Hans van Eenennaam[1]
Judith H.P. Vogelzangs[1]
Dorien Lugtenberg[1]
Frank H.J. van den Hoogen[2]
Walther J. van Venrooij[1]
Ger J.M. Pruijn[1]

[1] *Department of Biochemistry, University of Nijmegen, Nijmegen, The Netherlands*
[2] *Department of Rheumatology, University Medical Centre St. Radboud, Nijmegen, The Netherlands*

Submitted for publication

Abstract

The RNase MRP and RNase P complexes function as endonucleases and cleave the precursors to rRNA and tRNA, respectively. It has been shown that patients suffering from certain systemic autoimmune diseases produce autoantibodies directed to both complexes (designated anti-Th/To autoantibodies). Anti-Th/To positive patient sera have been shown to co-precipitate a protein of 40 kDa from cell extracts (Th-40), which was suggested to bind to the P3 domain of the RNase MRP and RNase P RNAs.

Here we show that Th-40 is identical to the Rpp38 protein. Paradoxically, Rpp38 does not bind to the P3 domain and only half of the anti-Th/To sera contain anti-Rpp38 reactivity. Two other RNase MRP/RNase P subunits Rpp20 and Rpp25, were found to interact with the P3 domain. The previously reported 40 kDa species associated with this domain appeared to consist of Rpp20 and/or Rpp25 associated with a nuclease resistant RNA fragment. Finally, we demonstrate that almost all tested anti-Th/To patient sera contain autoantibodies to Rpp25 and hPop1, indicating that these proteins harbour the most frequently targeted Th/To determinants. Taken together, our data unequivocally define the identity of the Th/To autoantigen and demonstrate that Th/To autoepitopes are found on several protein subunits of RNase MRP/RNase P.

Introduction

Intracellular macromolecular complexes are important targets of autoantibodies found in the sera of systemic autoimmune disease patients. Autoantibodies directed against components of the nucleolus are often found in patients suffering from scleroderma or scleroderma overlap syndromes (139). Examples of such nucleolar autoantigens are RNA polymerase I, fibrillarin, PM/Scl-100 and Th/To (reviewed in ref. (139)).

Anti-Th/To antibodies have been reported to occur in 4-13% of scleroderma patients (67,68) and are defined as autoantibodies that are able to immunoprecipitate the human RNase MRP and RNase P ribonucleoprotein particles (61,64,68).

The RNase MRP ribonucleoprotein particle has originally been identified by virtue of its capacity to cleave a mitochondrial RNA *in vitro* to generate RNA primers for mitochondrial DNA replication (22). In addition, RNase MRP has been shown to cleave at site A3 within the

first internal transcribed spacer of the precursor of ribosomal RNA in *Saccharomyces cerevisiae* (28-30). In many respects, the RNase MRP complex is related to the RNase P complex. The RNase P complex is required for the removal of the 5'-end of precursor tRNAs and is suggested to be involved in the processing of the precursor rRNA in internal transcribed spacer 2 (reviewed in ref. (118)). The RNase MRP and RNase P complexes both function as site-specific endonucleases, contain an RNA component that has been proposed to adopt a similar secondary structure and share several protein subunits (reviewed in ref. (118)).

At present, nine proteins have been reported to be associated with the human RNase MRP and/or RNase P complexes: hPop1, Rpp14, Rpp20, Rpp21, Rpp29/hPop4, Rpp30, Rpp38, Rpp40 and hPop5 (77-81,120,140). A tenth protein subunit of these ribonucleoprotein particles, Rpp25, has recently been identified and cloned in the laboratory of Dr. S. Altman (personal communication)

The first autoantigenic polypeptide associated with RNase MRP/RNase P was identified via immunoprecipitations with patient sera using ^{35}S-methionine or ^{3}H-leucine labeled HeLa cell extracts (68,72,73,135,136) and has been designated Th-40, referring to its apparent molecular weight of 40 kDa. Yuan and coworkers subsequently showed that a protein with a molecular weight of 40 kDa could be UV-crosslinked to the P3 domain of RNase P and MRP RNA (75), suggesting that Th-40 is bound to this domain. In a previous study we showed that two proteins with apparent molecular weights of 20 and 25 kDa, respectively, can be UV-crosslinked to the P3 domain of RNase MRP RNA (nucleotides 22-67, see Figure 1) and that a protein with a molecular weight of about 40 kDa, Rpp38, is bound to a centrally located region of the RNase MRP RNA (nucleotides 86-176, see Figure 1) (105).

In this study we have determined the identity of the Th-40 autoantigen and have identified the proteins carrying Th/To determinants as well as their binding sites on RNase MRP RNA.

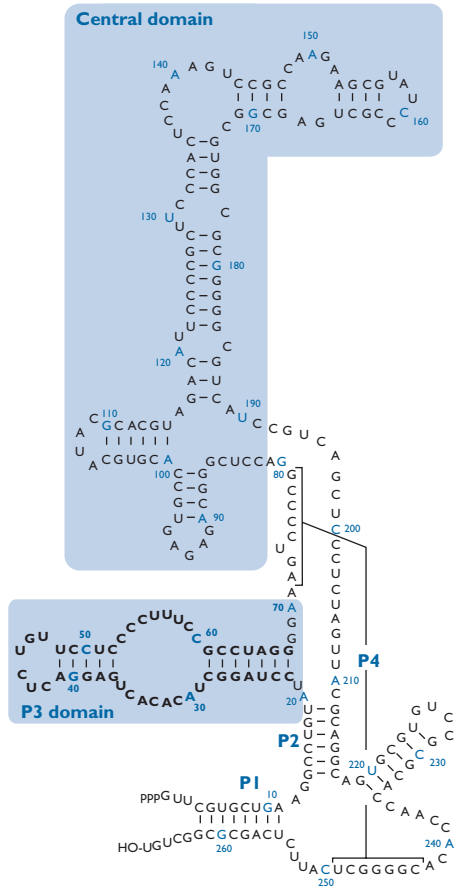

Figure 1. Secondary structure of the human RNase MRP RNA. The secondary structure of RNase MRP RNA is based on phylogenetic comparison and chemical modification data and is adapted from ref. (70).The P3 domain (nucleotides 22-67) and the central domain (nucleotides 86-176) are shaded in blue.

Results

The Th-40 autoantigen is identical to Rpp38

One hundred and seventy two patient sera displaying anti-nucleolar reactivities were screened for their capacity to co-immunoprecipitate RNase MRP RNA, RNase P RNA, U3 snoRNA, U8 snoRNA, U22 snoRNA, U1 snRNA and Y1 scRNA (Van Eenennaam *et al.*, manuscript submitted for publication). Sera that immunoprecipitated RNase MRP and RNase P RNA were designated anti-Th/To sera. To study the polypeptides precipitated by these anti-Th/To sera, immunoprecipitations with biotinylated total HeLa cell extracts were performed. Co-precipitating proteins were analyzed by western blot analysis and visualization using horseradish peroxidase-conjugated streptavidin. As shown in Figure 2A, lanes 1 and 2, anti-Th/To sera co-precipitated several polypeptides, the most prominent one being a 40-kDa protein. This 40-kDa protein was not precipitated by control patient sera (lanes 3-12), which displayed other patterns of co-precipitating proteins.

To determine whether the 40 kDa protein that was co-precipitated by these anti-Th/To sera (lanes 1 and 2) is identical to the previously described Th-40 autoantigen, similar immunoprecipitation experiments were performed with three reference anti-Th/To sera (designated P3 (68), Th-ref and Fu). As shown in Figure 2B, the precipitation patterns of these reference sera (lanes 1, 2 and 3, respectively) were indistinguishable from those obtained with the anti-Th/To sera described above (lanes 4 and 5). We conclude that the 40-kDa band co-precipitated by anti-Th/To sera by definition represents the Th-40 autoantigen.

To shed more light on the identity of the co-precipitating proteins, the western blot depicted in Figure 2A was stripped and reprobed with antibodies directed against Rpp40, Rpp38 and hPop4 (protein subunits of the RNase MRP and RNase P complexes), against the La protein (component of the Ro RNPs) and against the U1A protein (component of the U1 snRNPs). As shown in Figure 2C, lanes 1 and 2, Rpp40, Rpp38 and hPop4 were specifically co-precipitated by the anti-Th/To sera. The specific immunoprecipitation of the La protein by the anti-Ro RNP RNA sera (lanes 5 and 6) and of U1A by the anti-U1 snRNP sera (lanes 11 and 12) further substantiated the specificity of the assay. Overlays of the total protein signals (Figure 2A, lanes 1 and 2) and the immunoblotting signals (Figure 2C, lanes 1 and 2) indicated that the Th-40 autoantigen is identical to the Rpp38 protein.

Th-40/Rpp38 does not interact with the P3 domain of RNase MRP RNA

Paradoxically, Yuan and coworkers have previously demonstrated that the putative Th-40 autoantigen could be UV-crosslinked to the P3 domain of RNase MRP and P RNA (75), whereas we have mapped the binding site for Rpp38 to another region of these RNAs (105). To clarify this issue, the association of Rpp38 with different domains of RNase MRP was further investigated. *In vitro* transcribed ^{32}P-labeled RNase MRP RNA and U3 snoRNA as a control were incubated with a HeLa cell extract and reconstituted complexes were analyzed by immunoprecipitation using anti-Rpp38 antibodies. As shown in Figure 3A, lane 1, these anti-Rpp38 antibodies were able

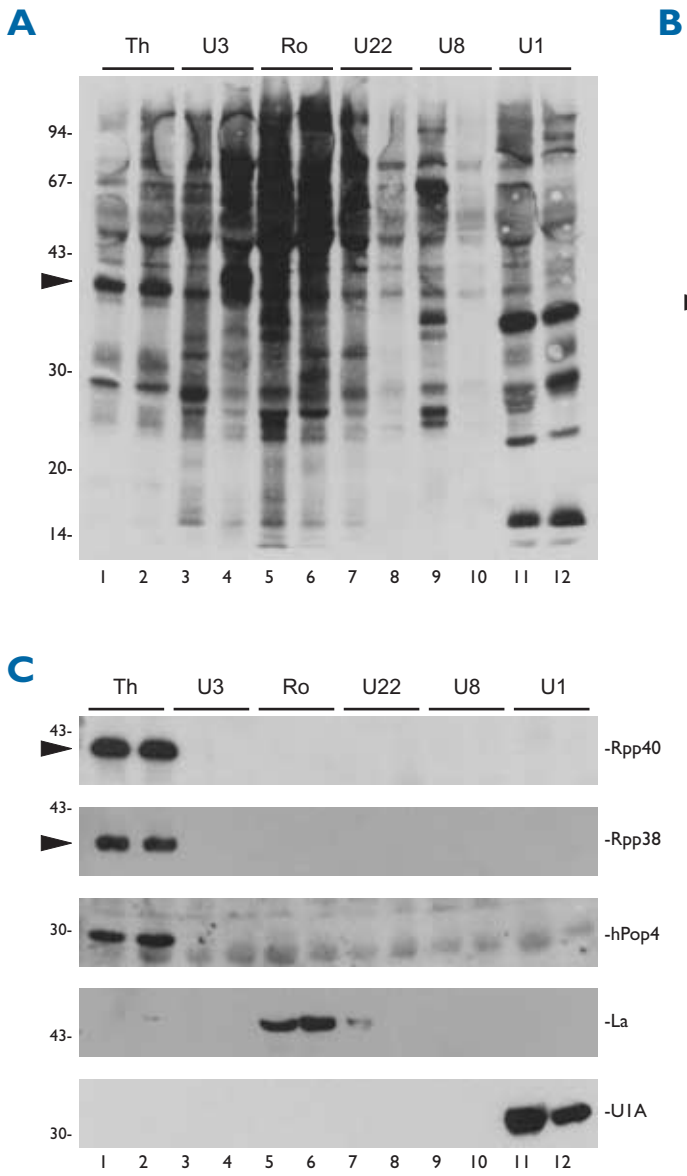

Figure 2. The Th-40 autoantigen is identical to Rpp38. A. Autoantigens were immunoprecipitated from a biotinylated HeLa cell extract using patient sera containing the following reactivities: anti-Th/To (lanes 1 and 2, sera designated Th4 and Th8, respectively), anti-U3 snoRNP (lanes 3 and 4), anti-Ro RNP (lanes 5 and 6), anti-U22 snoRNP (lanes 7 and 8), anti-U8 snoRNP (lanes 9 and 10) and anti-U1 snRNP (lanes 11 and 12). Co-precipitating proteins were resolved on a 13% SDS-PAGE gel, blotted onto nitrocellulose and visualized by HRP-conjugated streptavidin. At the left the positions of molecular weight markers are indicated and the arrow points to the band designated Th-40. B. Immunoprecipitation using three anti-Th/To reference patient sera (P3 (lane 1), Th-ref (lane 2) and Fu (lane 3)) performed as described above. The arrow points to the band designated Th-40. C. The blot shown in panel A was probed with antibodies specific for Rpp40, Rpp38, hPop4, La and U1A. Bound antibodies were visualized by incubation with HRP-conjugated secondary antibodies followed by chemiluminescence. The arrows point to the position of the band designated Th-40 (see panel A).

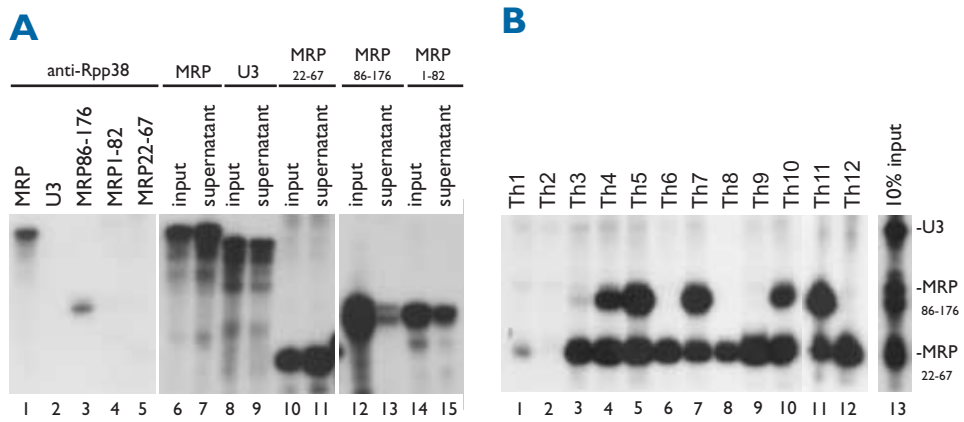

Figure 3. In vitro reconstitution of RNase MRP complexes. A. ^{32}P-labeled RNase MRP RNA, U3 snoRNA and RNase MRP RNA mutants (MRP_{86-176}, MRP_{1-82} and MRP_{22-67}) were incubated in HeLa cell extracts and reconstituted MRP complexes were immunoprecipitated using a rabbit anti-Rpp38 antiserum. RNAs isolated from the immunoprecipitates, the input fractions (10%) and from the supernatants (10%) were analyzed by gel electrophoresis and autoradiography. RNase MRP RNA (lanes 1, 6 and 7), U3 snoRNA (lanes 2, 8 and 9), MRP_{86-176} (lanes 3, 12 and 13), MRP_{1-82} (lanes 4, 14 and 15) and MRP_{22-67} (lanes 5, 10 and 11). B. ^{32}P-labeled U3 snoRNA, MRP_{86-176} and MRP_{22-67} RNAs were incubated in HeLa cell extracts and reconstituted complexes were immunoprecipitated using 12 anti-Th/To patient sera (Th1-Th12, lanes 1-12). Co-precipitating RNAs were isolated from the immunoprecipitates and analyzed by gel electrophoresis and autoradiography. In lanes 13, RNA isolated from 10% of the input fraction from the Th7 precipitation was loaded. C. Anti-Rpp38 reactivity present in the anti-Th/To patient sera (Th1 - Th12) was determined by western blot analysis using recombinant Rpp38 protein (lanes 1-12).

to immunoprecipitate the reconstituted RNase MRP complexes, whereas the U3 control RNA was not co-precipitated (lane 2). Deletion of the 3' terminal 185 nt of RNase MRP RNA resulted in loss of precipitation by anti-Rpp38 antibodies, which confirmed that the Th-40/Rpp38 protein does not associate with the P3 domain (MRP_{1-82} and MRP_{22-67}, see Figure 3A, lanes 4 and 5). In contrast, efficient binding of the Th-40/Rpp38 protein to an RNase MRP RNA mutant comprising the central domain (MRP_{86-176}) was observed (Figure 3A, lane 3). The lack of precipitation of U3 RNA and the P3 containing RNase MRP RNA mutants was not due to instability of these RNAs under the experimental conditions used, as evidenced by the analysis of the supernatants (Figure 3A, lanes 9, 11 and 15). Rpp38 directly binds to the central part of the RNA, because the Rpp38 protein can be UV-crosslinked to this domain (105).

To investigate the specificity of anti-Th/To patient sera in this reconstitution assay, reconstituted complexes were immunoprecipitated with twelve anti-Th/To sera (referred to as Th1-Th12). As shown in Figure 3B, almost all anti-Th/To sera co-immunoprecipitated the P3 domain of RNase MRP RNA (mutant MRP22-67), whereas none of them immunoprecipitated the U3 control RNA. Only five of the sera efficiently immunoprecipitated the central domain of RNase MRP RNA (lanes 4, 5, 7, 10

and 11), which would be consistent with the presence of anti-Rpp38 reactivity in these five patient sera. The presence of anti-Rpp38 autoantibodies in these sera was indeed confirmed by western blot analysis using recombinant Rpp38 protein (Figure 3C).

Taken together, our results show that the Th-40/Rpp38 protein binds to the central domain of RNase MRP RNA, comprised of nucleotides 86-176, and not to the P3 domain. The fact that most of the anti-Th/To sera immunoprecipitated the reconstituted P3 domain strongly suggested that another more frequently targeted autoantigenic component interacts with the P3 domain.

Rpp20 and Rpp25 interact with the P3 domain of RNase MRP RNA

Our previous UV-crosslinking experiments showed that two polypeptides with molecular weights of 20 and 25 kDa associate with the P3 domain of the RNase MRP RNA (105). To investigate whether these two proteins are identical to the recently identified Rpp20 (80) and Rpp25 (C. Guerrier-Takada and S. Altman, personal communication) protein subunits, reconstituted RNase MRP complexes were immunoprecipitated with rabbit antisera raised against Rpp20 or Rpp25. As shown in Figure 4, lanes 7 and 12, both Rpp20 and Rpp25 efficiently reconstituted with the RNase MRP RNA, but not with the U3 control RNA (lanes 6 and 11). Similar analyses using mutant RNAs $MRP_{22\text{-}67}$, $MRP_{1\text{-}82}$ and $MRP_{86\text{-}176}$ showed that Rpp20 is able to associate with both the P3 domain and the central domain (lanes 8-10), whereas Rpp25 associated only with the P3 domain (lanes 13-15). A control pre-immune serum showed only background levels of precipitation (lanes 1-5) and the stability of the RNAs analyzed was again established by the comparison of the supernatants from the anti-Rpp25 precipitations with the input RNAs (lanes 16-25). These results indicate that Rpp20 and Rpp25 are identical to the two proteins that were identified by UV-crosslinking to bind to the P3 domain.

UV-crosslinking experiments using ^{32}P-labeled MRP22-67 RNA (the P3 domain), followed by immunoprecipitations using Th-7 and control patient antibodies and analysis on a high resolution SDS-PAGE gel, showed that in addition to the band previously designated MRP20 (105), the band referred to as MRP25 (105) actually is composed out of three bands (Figure 5A, lane 4). Both anti-Rpp20 and anti-Rpp25 antibodies immunoprecipitated these four bands, confirming that Rpp20 and Rpp25 represent the previously identified crosslinked proteins (lanes 2 and 3). The multiple bands observed in this experiment probably represent the Rpp20 and Rpp25 proteins covalently attached to different nuclease resistant RNA fragments. Pre-immune rabbit sera and control patient sera did not immunoprecipitate any UV-crosslinked proteins (lanes 1 and 5).

The fact that Th40/Rpp38 does not and Rpp20 and Rpp25 do bind to the P3 domain of RNase MRP RNA raised the question why other investigators previously observed a 40-kDa species after UV-crosslinking using the P3 domain (75). To clarify this issue, we performed a UV-crosslinking experiment under the conditions applied by Yuan and coworkers. The main difference with the experimental conditions of our analyses is the use of RNase T1 rather than RNase A to degrade the RNA after UV-irradiation. RNase T1 cleaves single-stranded regions of RNA after a G-residue, while RNase A cleaves single-stranded RNAs preferentially after a C- or U-residue. As shown in Figure 5B, lanes 5 and 6, the RNase T1 digestion resulted in a doublet migrating at approximately 40 kDa, similar to the previously reported results (75). UV-crosslinking followed by RNase A treatment, which was performed in parallel, resulted in the immunoprecipitation of the 20 and 25 kDa species (lanes 2 and 3), confirming our previous results (105). A similar result was obtained with rabbit anti-Rpp20 and

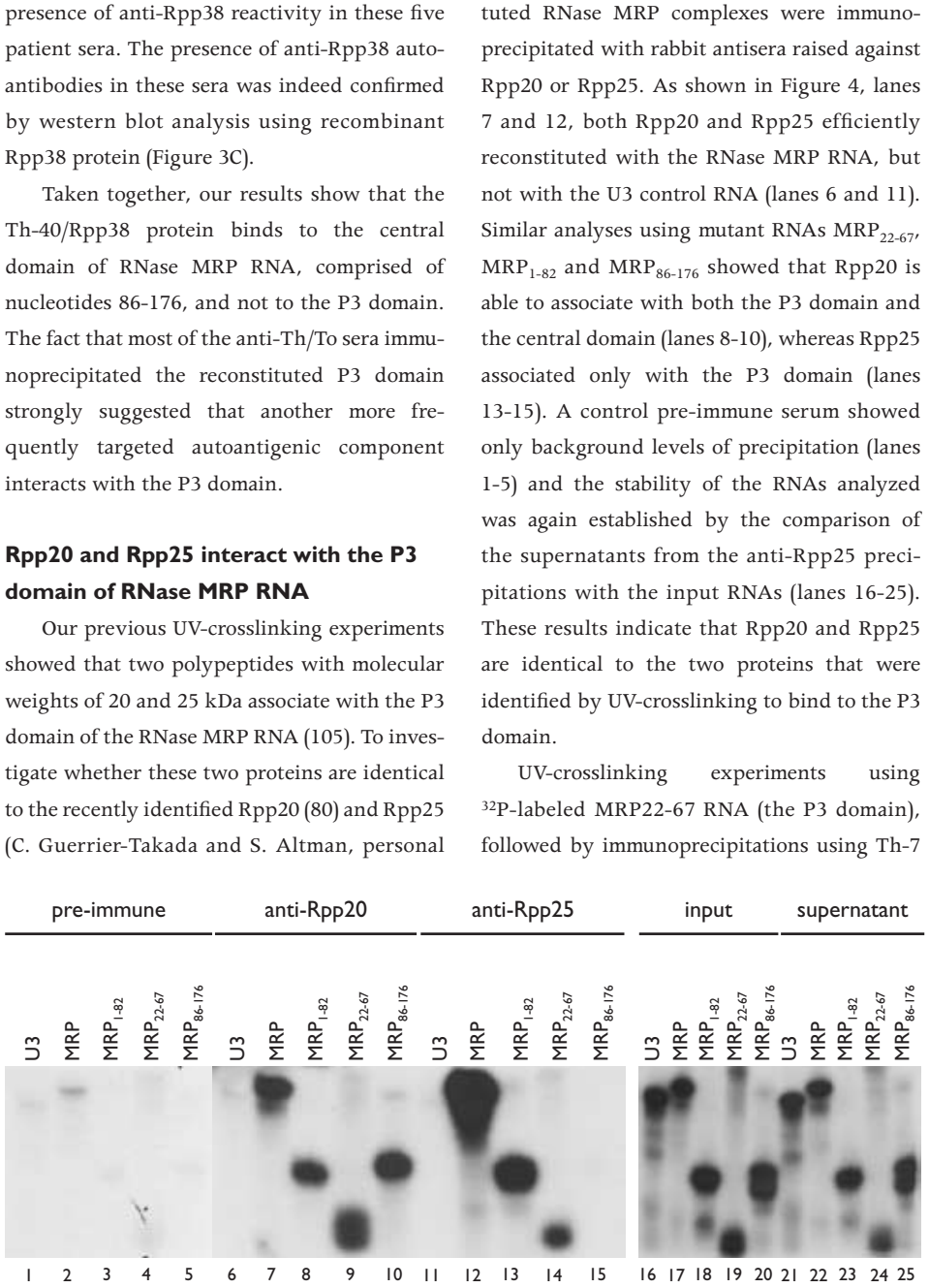

Figure 4. Association of Rpp20 and Rpp25 with the P3 domain of RNase MRP RNA. ^{32}P-labeled U3 snoRNA, RNase MRP, $MRP_{1\text{-}82}$, $MRP_{22\text{-}67}$ and $MRP_{86\text{-}176}$ RNAs were incubated in a HeLa cell extract and reconstituted complexes were immunoprecipitated with pre-immune (lanes 1-5), anti-Rpp20 (lanes 6-10) and anti-Rpp25 (lanes 11-15) antibodies. Co-precipitating RNAs, and RNA from 10% of the input fractions (lanes 16-20) and from 10% of the supernatants from the anti-Rpp25 precipitations (lanes 21-25) were isolated and analysed by denaturing polyacrylamide gel electrophoresis and visualised by autoradiography.

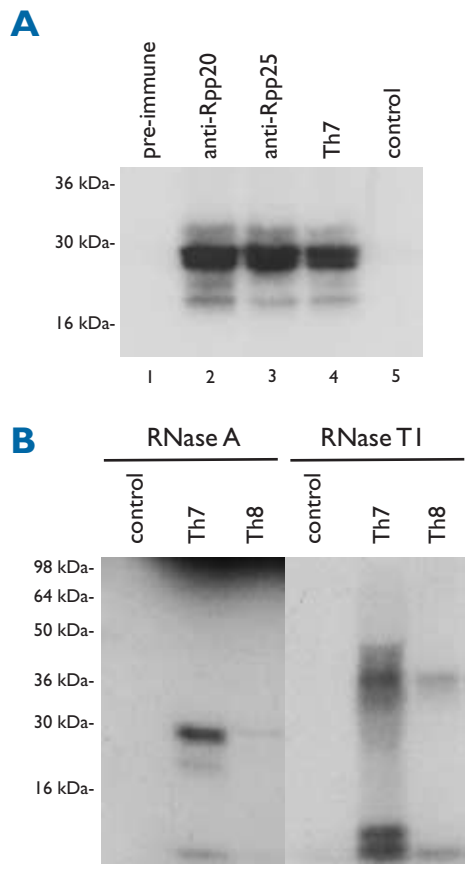

Figure 5. Rpp20 and Rpp25 can be UV-crosslinked to the P3 domain of RNase MRP RNA. **A.** Reconstituted complexes containing ^{32}P-labeled $MRP_{22\text{-}67}$ RNA were subjected to UV-crosslinking and RNase A treatment, followed by an immunoprecipitation using pre-immune rabbit serum (lane 1), anti-Rpp20 serum (lane 2), anti-Rpp25 serum (lane 3), patient serum Th7 (lane 4) and control patient serum (lane 5). Co-precipitating proteins were resolved on a 15% SDS-PAGE gel and crosslinked proteins were visualized by autoradiography. **B.** ^{32}P-labeled $MRP_{22\text{-}67}$ RNA was incubated in HeLa cell extracts and exposed to UV irradiation to induce crosslinking between RNA and cellular proteins. Crosslinked complexes were treated with either RNase A (lanes 1-3) or RNase T1 (lanes 4-6) and subsequently immunoprecipitated with patient sera Th7 (lanes 2 and 5) and Th8 (lanes 3 and 6) or control sera (lanes 1 and 4). Co-precipitating proteins were analysed by 13% SDS-PAGE and visualized by autoradiography. Note that the resolution of the gel shown in panel B is lower than that of the gel in panel A. The positions of molecular weight markers are shown at the left.

anti-Rpp25 as precipitating antibodies instead of patient antibodies (data not shown). From these data we conclude that the difference in apparent molecular weights of the crosslinked species is due to the use of different ribonucleases. In the case of RNase T1 the protein(s) remain(s) most likely covalently bound to a relatively large part of the $MRP_{22\text{-}67}$ RNA, whereas in the case of RNase A only a few nucleotides remain bound to the protein(s).

The resistance of the P3 domain to RNase T1 digestion was confirmed by incubating in vitro transcribed $MRP_{22\text{-}67}$ in a HeLa cell extract, followed by treatment with either RNase A or RNase T1, immunoprecipitation with anti-Th/To sera and RNA analysis by gel electrophoresis. While the size of $MRP_{22\text{-}67}$ was hardly affected by RNase T1 treatment, RNase A degraded $MRP_{22\text{-}67}$ to small (oligo)nucleotides (data not shown).

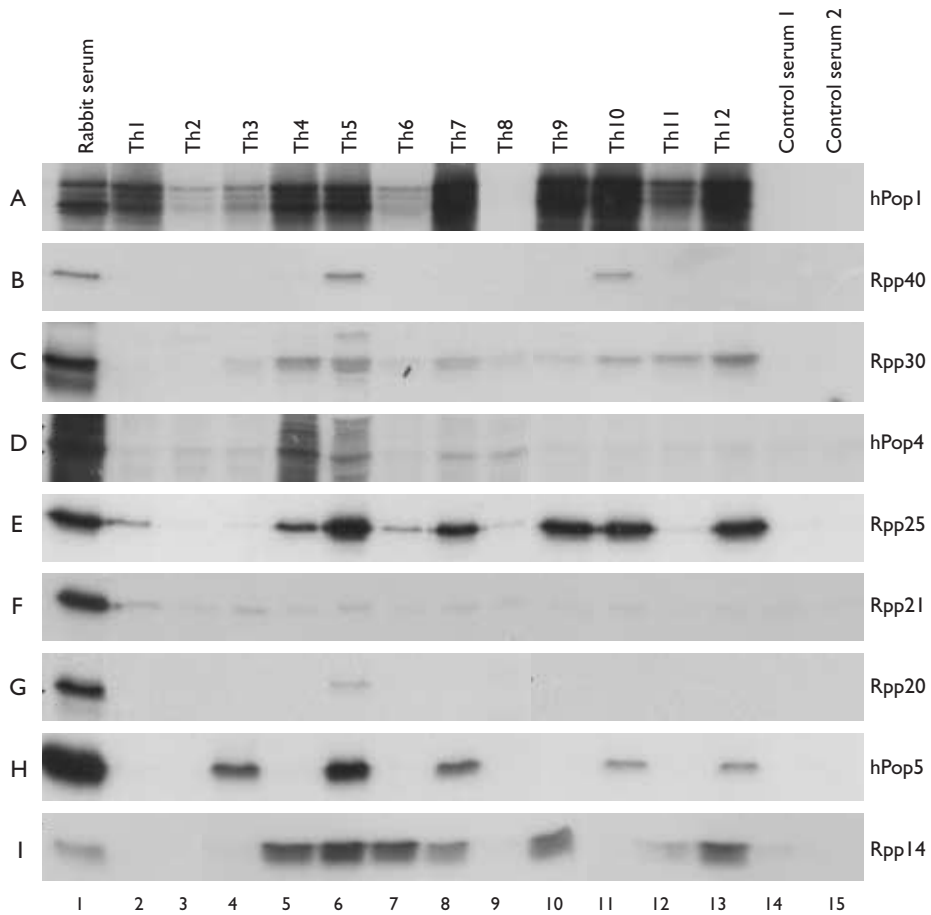

Figure 6. Immunoprecipitation of RNase MRP proteins by anti-Th/To patient sera. ^{35}S-labeled in vitro translated hPop1 (panel A), Rpp40 (panel B), Rpp30 (panel C), hPop4 (panel D), Rpp25 (panel E), Rpp21 (panel F), Rpp20 (panel G), hPop5 (panel H) and Rpp14 (panel I) were subjected to immunoprecipitation with patient sera Th1-Th12 (lanes 2-13), two control patient sera (lanes 14 and 15) and rabbit antisera that were raised against each of these proteins (lane 1). Co-precipitating proteins were visualized by SDS-PAGE and autoradiography.

hPop1 and Rpp25 are the most frequently targeted autoantigenic RNase MRP components

The results described above demonstrate that anti-Th/To sera are frequently reactive with proteins associated with the P3 domain and that Rpp20 and Rpp25 bind to this fragment of RNase MRP RNA. To investigate the antigenicity of these proteins, *in vitro* translated, ^{35}S-labeled Rpp20 and Rpp25 were subjected to immunoprecipitations with anti-Th/To patient sera and two human control sera. As shown in Figure 6, panel G, Rpp20 was only detectably immunoprecipitated by Th5 and not by the other 11 anti-Th/To sera. In contrast, the majority of the anti-Th/To patient sera immunoprecipitated *in vitro* translated Rpp25 (panel E), indicating that Rpp25 represents an important Th/To autoantigen bound to the P3 domain of RNase MRP RNA.

In addition, all other protein subunits, except Rpp38, of the RNase MRP and/or RNase P complexes were tested in similar immunoprecipitation assays using Th1-Th12. As shown in Figure 6, panels A-D, F and H-I, these proteins were recognized with variable frequencies. Almost all anti-Th/To sera recognized hPop1 (panel A), about half of the sera recognized Rpp30 (panel C), hPop5 (panel H) and Rpp14 (panel I), and reactivity with Rpp40, hPop4 and Rpp21 was observed only in a minority of these sera (panels B, D, F).

In conclusion, these data indicate that patient sera precipitating RNase MRP and RNase P complexes (anti-Th/To) most frequently recognize the hPop1 and Rpp25 proteins contained in these complexes.

Discussion

The results of previous studies demonstrated that patient sera containing reactivity directed to both the RNase MRP and RNase P complexes were able to immunoprecipitate a protein of about 40 kDa, named Th-40 (68,72,73,136). Here, we demonstrate that Th-40 is identical to the Rpp38 protein. Although almost all anti-Th/To patient sera were able to (co-) immunoprecipitate the Th-40 autoantigen, only approximately half of the anti-Th/To sera actually contain reactivity directed to the Rpp38 protein. The immunoprecipitation, even under relatively stringent conditions, of Th-40/Rpp38 by patient sera that do not recognize the Rpp38 protein is apparently caused by the recognition of other autoantigenic components in the RNase MRP and RNase P complexes. The RNase P holoenzyme has been shown to be stable up to salt concentrations of 500 mM KCl (78), suggesting that under these conditions the intact complexes rather than individual protein subunits are co-precipitated.

The use of either patient sera recognizing Rpp38 or polyclonal rabbit sera raised against Rpp38 allowed the mapping of the binding-site of Rpp38. Rpp38 binds to the region between nucleotides 86-176 of the RNase MRP RNA, which is in agreement with our previous observations (105). The binding of Rpp38 to this part of the RNase MRP RNA has been suggested to be mediated by a so-called two-stranded, helix-internal loop-helix motif (or Kink-turn motif) between nucleotides 145 and 170 (141,142). The interaction of Rpp38 with the corresponding domain of the RNase P RNA is suggested by the observation that Rpp38 was able to interact with the intact RNase P RNA but not

with a fragment comprising nucleotides 1-74 (86).

The observation that Th-40/Rpp38 binds to the central domain and not to the P3-domain of RNase MRP RNA seemed to be in contradiction to what has been reported by Yuan and coworkers (75,134). However, we demonstrated that the 40-kDa species that both in our and the previous study results from UV-crosslinking to the P3 domain of RNase MRP RNA when RNase T1 is used represents Rpp25 and/or Rpp20 covalently linked to the (almost) complete P3 domain of RNase MRP RNA. Our observation that the P3 domain is protected against or resistant to RNase T1 cleavage is supported by RNase protection experiments as described by Liu and coworkers (134) and is not surprising in view of the almost complete absence of single-stranded guanosines in this part of RNase MRP RNA (see Figure 1).

The results of the deletion mutant analyses demonstrated that Rpp20 is able to bind both to the P3 domain and to an RNase MRP RNA fragment comprised of nucleotides 86-176. A simultaneous interaction (either directly or indirectly) with both the P3 domain and the region 86-176 has been suggested for the hPop1 protein as well (105), although for the efficient association of hPop1 both domains seem to be required. Taken together, these results suggest that these two RNA regions are positioned close to each other in the three-dimensional structure of RNase MRP RNA, which may be stabilized by Rpp20 and/or hPop1 binding.

RNA-protein interactions in the structurally related human RNase P complex have been studied using yeast three-hybrid and UV-crosslinking experiments. The results indicated that Rpp21, Rpp29/hPop4 and Rpp30 interact with the P3 domain of RNase P RNA, whereas the Rpp38 protein interacts with a more 3' located domain (86). Using our reconstitution assay we tried to detect these interactions in the reconstituted RNase MRP complex as well. However, no detectable reconstitution was observed when Rpp14, hPop5, Rpp21, Rpp29/hPop4, Rpp30 and Rpp40 were studied (our unpublished observations). The RNase P reconstitution experiments also indicated that no interaction of Rpp20 and hPop1 proteins with the RNase P RNA could be demonstrated (86). Whether the interactions described for the individual RNase P and RNase MRP complexes can be extrapolated to the other complex is at present not clear. A direct interaction of Rpp25 with the P3 domain of RNase P RNA has been observed as well (C. Guerrier-Takada, personal communication).

The observations that almost no anti-Th/To serum contains reactivity directed to the Rpp20 protein and that the majority of the anti-Th/To sera contain autoantibodies against Rpp25 (Figure 6), suggest that Rpp20 is most probably co-precipitated with anti-Rpp25 when anti-Th/To patient sera are used in reconstitution and UV-crosslinking experiments.

The ability of patient sera that are able to immunoprecipitate the RNase MRP and RNase P complexes has been designated anti-Th/To reactivity (61,64,68). The availability of cDNA clones encoding most, if not all protein subunits of these complexes now allowed a more detailed analysis of the anti-Th/To autoantibody specificities present in patient sera. Our study demonstrates that all protein components may be targeted by anti-Th/To autoantibodies, albeit some of them only rarely. In this study we showed that this reactivity can now be subclassified according to the presence of autoantibodies against each of the identified RNase MRP/RNase P protein subunits or according to the recognition of a specific combination of these. The analysis of a larger collection of anti-Th/To sera will be required to investigate the potential clinical relevance of this subclassification and to determine whether such a classification may aid in establishing the diagnosis and/or prognosis of patients showing anti-Th/To reactivity.

Acknowledgements

We are thankful to Tim Welting for technical assistance and Drs. H. Pluk and R. Hoet for the development of procedures to biotinylate cell extracts. We thank Drs. Cecilia Guerrier-Takada, Sidney Altman (Yale University, New Haven) and Nayef Jarrous (Hebrew University-Hadassah Medical School, Jerusalem) for their kind gifts of rabbit antisera raised against the RNase P proteins and cDNAs encoding these protein subunits. We are grateful to Dr. R. Karwan† (Vienna University Institute of Tumor Biology), Dr. J. Craft (Yale University, New Haven, CT) and Dr. T. Mimori (Kyoto University, Kyoto) for providing us with anti-Th/To reference patient sera. This research has been financially supported by the Council for Chemical Sciences of the Netherlands Organization for Scientific Research (CW-NWO).

Materials and Methods

Immunoprecipitation using biotinylated HeLa cell extracts

Total HeLa cell extract was prepared as described before (116). After dialysis against 50 mM $NaHCO_3$ pH 8.3, 0.5 mM DTE, 0.5 mM PMSF, 1 mg NHS-LC-biotin (Pierce) was added per 20 mg of total protein. After incubation on ice for 2 hours, the reaction was stopped with 50 mM Tris-HCl, pH 8.0. Finally, the buffer was changed to 10 mM Tris-HCl, pH 8.0, 0.5 mM DTE, 0.5 mM PMSF, 0.1 M KCl, 0.01% NP-40 and 20% glycerol by dialysis.

For each immunoprecipitation 20 µl patient serum was incubated with 20 µl of a 50% suspension of protein A-agarose beads in IPP500 (500 mM NaCl, 10 mM Tris-HCl, pH 8.0, 0.05% NP-40) for 1 h at room temperature. Beads were washed two times with IPP500 and once with IPP150 (150 mM NaCl, 10 mM Tris-HCl, pH 8.0, 0.05% NP-40). Biotinylated HeLa extract was added and incubated for 2 hours at 4°C. After 4 washes with IPP150, co-precipitating proteins were eluted with SDS-sample buffer, resolved by 13% SDS-PAGE and blotted onto nitrocellulose membranes.

Detection of biotinylated proteins was performed using horseradish peroxidase-conjugated streptavidin (Dako Immunoglobulins) and visualization by chemiluminescence.

In vitro reconstitution

In vitro transcribed ^{32}P-labeled RNase MRP RNA (full length and deletion mutants MRP_{22-67}, MRP_{1-82} and MRP_{86-176}), and U3 snoRNA were allowed to associate with their protein components in an *in vitro* reconstitution assay and analyzed as described previously (105).

UV-crosslinking

UV-crosslinking experiments to study RNA-protein interactions were performed as described previously (105). After reconstitution and UV-irradiation the reconstituted complexes were treated with either 10 µg of RNase A for 1 hour at 37 °C or 100 units RNase T1 for 30 minutes at 30°C per immunoprecipitation. The protein-RNA complexes were subjected to immunoprecipitation, analyzed by SDS-PAGE and visualized by autoradiography.

Immunoblotting analysis

Patient sera were used in a 5000-fold dilution, polyclonal rabbit sera were used in a 100-fold dilution and mouse monoclonal antibodies SW5 (anti-La) and 9A9 (anti-U1A and anti-U2B''; Euro-Diagnostica, Arnhem, The Netherlands) were used in a 50-fold and 100-fold dilution, respectively. Detection was performed using horseradish peroxidase-conjugated rabbit-anti-human IgG or swine-anti-rabbit IgG or rabbit-anti-mouse IgG (Dako Immunoglobulins) as secondary antibodies and visualization by chemiluminescence.

Recombinant His_6-tagged Rpp38 was obtained by expression of Rpp38 cDNA in pQE-30 (Qiagen) in M15[pREL4] cells according to the manufacturer's instructions.

In vitro translation

For *in vitro* transcription-translation of hPop1, hPop4, hPop5 the hPop1-pT7-7TT, VSV-hPop4 and VSV-hPop5 DNA constructs (77,120,140) were linearized using *Sal*I and *Fsp*I, respectively. The cDNA of Rpp30 (78) was subcloned in pGEM-3Zf(+) and linearized using *Xba*I. The open reading frames of Rpp14, Rpp20, Rpp21, Rpp25 and Rpp40 were subcloned using a PCR based strategy on cDNA constructs as templates (79-81) in pCR4-TOPO (Invitrogen) and linearized using *Sma*I digestion. *In vitro* transcription was performed as described previously using either T7 or T3 RNA polymerase (105). *In vitro* translation of these transcripts was performed in the presence of [^{35}S]-methionine using rabbit reticulocyte lysates (Promega) or wheat germ extracts.

Antisera

Polyclonal rabbit sera against hPop1, hPop4, hPop5 have been described previously (77,120,140). Polyclonal rabbit antibodies raised against Rpp14, Rpp20, Rpp21, Rpp25, Rpp30, Rpp38 and Rpp40 (78-81) were kindly provided by Dr. S. Altman.

The Th/To reference sera designated P3, Th-ref and Fu were kindly provided by Dr. R. Karwan, Dr. J. Craft and Dr. T. Mimori, respectively.

Part III

RNase MRP and human disease

Chapter 7

Autoantibodies against small nucleolar ribonucleoprotein complexes and their clinical associations

Hans van Eenennaam[1]
Judith H.P. Vogelzangs[1]
Laurens Bisschops[2]
Liane C.J. te Boome[2]
Hans P. Seelig[3]
Manfred Renz[3]
Dirk-Jan de Rooij[4]
Rick Brouwer[1]
Helma P. Pluk[1]
Ger J.M. Pruijn[1]
Walther J. van Venrooij[1]
Frank H.J. van den Hoogen[2]

[1] *Department of Biochemistry, University of Nijmegen, Nijmegen, The Netherlands*
[2] *Department of Rheumatology, University Medical Centre St. Radboud, Nijmegen, The Netherlands*
[3] *Institute of Immunology and Molecular Genetics, Karlsruhe, Germany*
[4] *Department of Rheumatology, Sint Maartens Hospital Nijmegen, Nijmegen, The Netherlands*

Submitted for publication

Abstract

Sera from patients suffering from systemic autoimmune diseases such as systemic lupus erythematosus (SLE) and systemic sclerosis (SSc) have been shown to contain reactivities to nuclear components. Autoantibodies specifically targeting nucleolar antigens are most frequently found in patients suffering from SSc or SSc overlap syndromes.

We determined the prevalence and clinical significance of autoantibodies directed to nucleolar RNA-protein complexes, the so-called small nucleolar ribonucleoprotein complexes (snoRNPs). A total of 172 patient sera with anti-nucleolar antibodies were analysed by immunoprecipitation. From 100 of these patients clinical information was obtained by chart review. Autoantibodies directed to snoRNPs were not only detected in patients suffering from SSc and primary Raynaud's phenomenon, but also in patients suffering from SLE, rheumatoid arthritis (RA) and Sjögren's syndrome (SS). Antibodies against box C/D small snoRNPs can be subdivided in anti-fibrillarin positive and anti-fibrillarin negative reactivity. Anti-fibrillarin positive patient sera were associated with a poor prognosis in comparison with anti-fibrillarin negative (reactivity with U3 or U8 snoRNP only) patient sera. Anti-Th/To autoantibodies were associated with SSc, primary RP and SLE and were predominantly found in patients suffering from decreased co-diffusion and esophagus motility and xerophthalmia. For the first time autoantibodies that recognise box H/ACA snoRNPs are described, identifying this class of snoRNPs as a novel nucleolar autoantigen. Taken together, our data show that anti-nucleolar patient sera directed to small nucleolar ribonucleoprotein complexes are frequently found in other diseases than SSc and that categorisation of diagnoses and clinical manifestations based on autoantibody profiles seems particularly informative in patient sera recognising box C/D snoRNPs.

Introduction

Antinuclear antibodies (ANA) have been demonstrated to occur frequently in systemic autoimmune diseases such as systemic lupus erythematosus (SLE), systemic sclerosis (SSc), Sjögren's syndrome (SS), polymyositis (PM) and dermatomyositis (DM). Antibodies targeted to nucleolar autoantigens such as fibrillarin, Th/To, PM-Scl, NOR-90/UBF, RNA

polymerase I, Ku and DNA topoisomerase I (Scl-70) are most frequently found in patients suffering from SSc or SSc overlap syndromes (reviewed in ref. (68,139,143,144)). The occurrence of these antibodies in patient sera is helpful in establishing the diagnosis and prognosis of the disease. For example, autoantibodies directed against DNA topoisomerase I identify a subgroup of SSc with early diffuse disease and pulmonary involvement (reviewed in ref. (139)) and autoantibodies against fibrillarin identify a subgroup of SSc with a poor prognosis (145).

In the past decade, our understanding of nucleolar processes, the most prominent of which is the biogenesis of ribosomes, and the macromolecular complexes involved increased dramatically. It has been shown that the precursor ribosomal RNA, encoding mature 18S, 5.8S and 25S rRNA is extensively processed and modified (reviewed in ref. (4,5,89)). The most important trans-acting factors in these processes are the small nucleolar ribonucleoprotein particles (snoRNPs). These snoRNPs can be divided in three groups based on conserved sequence elements in their RNA components: box C/D snoRNPs, box H/ACA snoRNPs and RNase MRP/RNase P (3), reviewed in ref. (4,5), see Figure 1.

Most of the box C/D snoRNPs have been demonstrated to function in the 2'-O-ribose methylation of pre-rRNA, whereas U3, U8, U13 and U22 box C/D snoRNPs have been demonstrated or suggested to function in the cleavage of pre-rRNA at the 5'- and 3'-end of mature 18S rRNA (reviewed in ref. (4,5)). Up to now three proteins have been identified that are shared by this class of snoRNPs: fibrillarin, Nop56 and Nop5/58 (13-15). The box H/ACA snoRNPs have been implicated in the conversion of uridine residues in pre-rRNA to pseudouridines (3,17) (see Figure 1). At present, four proteins have been shown to specifically associate with this class of snoRNPs: hGar1, Nap57/dyskerin, hNHP2 and hNOP10 (18-20). The RNase MRP and RNase P complexes contain the still uncharacterised Th/To autoantigen (61,63,64)) and are the only representatives of the third class of snoRNPs. Both ribonucleoprotein particles function as endoribonucleases and have been shown to function in the cleavage of pre-rRNA to mature rRNA and the processing of pre-tRNA, respectively (reviewed in ref. (118)) (see Figure 1).

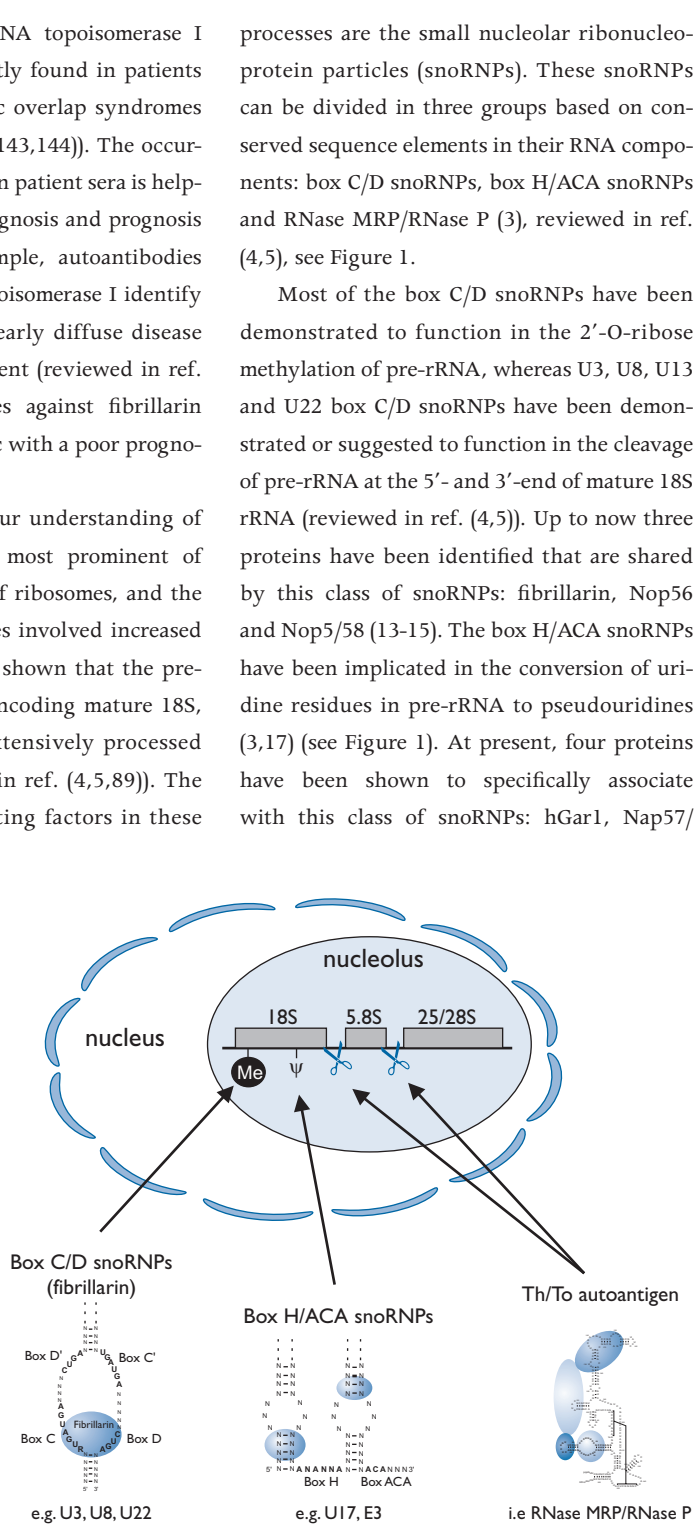

Figure 1. Schematic representation of the structure and function of autoantigenic small nucleolar ribonucleoprotein complexes. In the nucleolus (light blue) the biogenesis of ribosomes takes place. Three of the four ribosomal RNAs (18S, 5.8S and 25/28S) are synthesised as one large precursor. This precursor rRNA is modified at specific positions by 2'-O-ribose methylation (Me) and conversion of uridines to pseudouridines (Ψ). Ribose methylation is mediated by box C/D snoRNPs (bottom left), whereas pseudouridylation is mediated by box H/ACA snoRNPs (bottom middle). The Th/To autoantigen (RNase MRP and RNase P) cleaves the precursor rRNA between the 18S and 5.8S and between the 5.8S and 25/28S rRNA sequences, respectively (bottom right). For a more complete overview see (5,12,89,162).

The aim of this study was to assess whether these three classes of small nucleolar ribonucleoprotein complexes are targeted by autoantibodies present in sera of patients suffering from systemic autoimmune diseases. The clinical relevance of the occurrence of these autoantibodies was investigated using chart reviews of these patients.

Results

Anti-nucleolar patient sera recognise various small nucleolar RNPs

To determine the presence of autoantibodies directed against small nucleolar ribonucleoprotein complexes a random serum collection was tested for the presence of anti-nucleolar antibodies by immunofluorescence using HEp-2 cells as described previously (146). The 172 anti-nucleolar sera obtained were further analysed by immunoprecipitation using a total HeLa cell extract. Co-precipitating RNAs were isolated and analysed by northern blot hybridisation for the presence of RNase MRP/RNase P RNA, U3, U8 and U22 (box C/D) snoRNAs and U17 and E3 (box H/ACA) snoRNAs. We also analysed for reactivities directed to the U1 snRNP complex (probing for U1 snRNA) and the Ro RNPs (probing for Y1 scRNA) since these activities are common in mixed connective tissue disease and Sjögren's syndrome/SLE, respectively.

A typical example of a northern blot analysis is depicted in Figure 2. The upper two panels show that in most cases sera that immunoprecipitate RNase MRP RNA also precipitate RNase P RNA (lanes 2, 4, 13 and 14), although one serum appeared to specifically recognise RNase MRP (lane 17). The recognition of both the RNase MRP and RNase P complexes is generally referred to as Th/To specificity. Lane 11 shows an example of a serum recognising U3, U8 and U22 box C/D snoRNPs, suggesting

Small nucleolar ribonucleoprotein complexes	Total group n=172 (100%)	Diagnosed patient data group n=100 (100%)
Box C/D snoRNPs •	16 (9%)	8 (8%)
U3 snoRNP only	17 (10%)	5 (5%)
U8 snoRNP only	8 (5%)	6 (6%)
Box H/ACA snoRNPs	1 (0.5%)	1 (1%)
Th/To (RNase MRP/RNase P)	14 (8%) ••	7 (7%)
other specificities		
U1 snRNP specific	15 (9%)	9 (9%)
U1/Y1 overlap	8 (5%)	5 (5%)
Y1 scRNP specific	23 (13%)	15 (15%)
PM/Scl-100	44 (26%)	14 (14%)
no activities found	61 (35%)	47 (47%)

Table 1. Summary of northern blot hybridisation data
• A patient is referred to as Box C/D snoRNP specific, when U3, U8 and U22 snoRNA are immunoprecipitated by the patient serum
•• In addition to the 14 patient sera that recognise both RNase MRP and RNase P, one serum has been found that appears to recognise RNase MRP only.

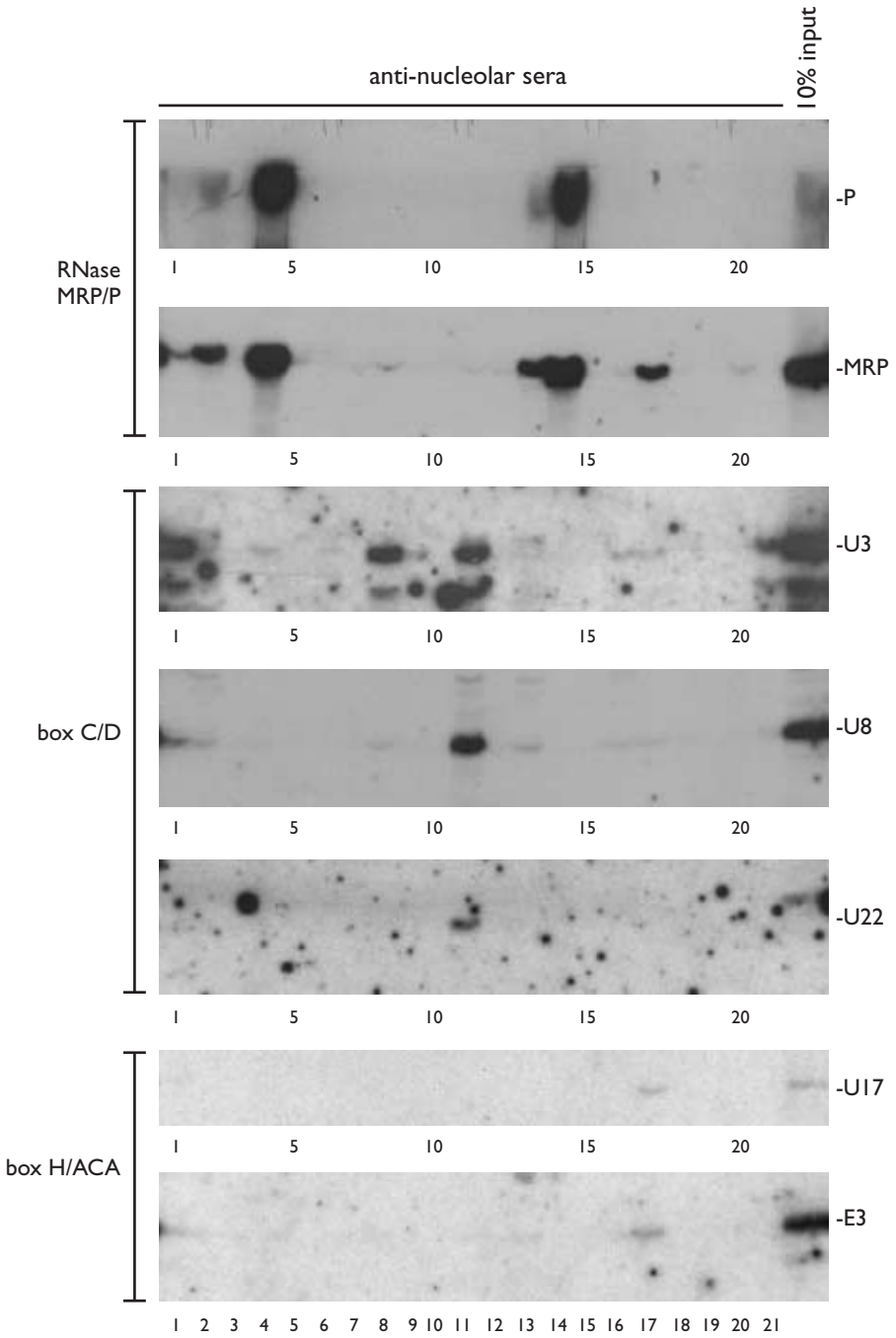

Figure 2. Northern blot analysis of anti-nucleolar sera. Immunoprecipitations using total HeLa cell extract with 21 patient sera (lanes 1-21) are shown. Co-precipitated RNAs were isolated and analysed by northern blot hybridisation with probes specific for RNase P RNA, RNase MRP RNA, U3 snoRNA, U17 snoRNA, E3 snoRNA, U8 snoRNA and U22 snoRNA as indicated on the right of each panel. RNA isolated from total cell extracts (10% input) was analysed in the left and right lanes.

that a polypeptide that is common to this class of snoRNPs is autoantigenic. Lane 17 suggests that a protein common to the box H/ACA snoRNPs is autoantigenic as well, because both box H/ACA snoRNPs E3 and U17 are immunoprecipitated by this patient serum.

Table I summarises the results of the northern blot analyses and the occurrence of autoantibodies against PM/Scl-100, as detected by ELISA analyses of this group of 172 anti-nucleolar patient sera. These data will be described below in more detail for each of the snoRNPs.

Anti-nucleolar activity is found in patients suffering from SLE, SSc, RA and primary RP

Clinical information of 100 patients with anti-nucleolar activity was obtained by chart review. The recognition of nucleolar complexes by autoantibodies in this patient group is specified in Table I. A comparison of the occurrence of these autoantibodies in this group (n=100) with that in the total group (n=172) shows that the patient data group is a good representation of the total group.

Table II shows the diagnoses of the patients in this group. As expected, based on literature data, patients with anti-nucleolar antibodies suffer from SSc (n=14), PM (n=2), DM (n=2), primary RP (n=10) and SSc-overlap syndromes (n=2). Surprisingly, anti-nucleolar antibodies were also found in patients diagnosed with SLE (n=11), SS (n=4), RA (n=20), MCTD (n=4) and a group of different other diseases (n=27), including gout, M. Buerger, M. Kahler, M. Reiter, Crohn's disease, ankylosing spondylitis.

Fibrillarin is autoantigenic in patient sera recognising box C/D snoRNPs

In 9% of the anti-nucleolar patient sera (see Table I), autoantibodies co-precipitating box C/D snoRNAs were found (a serum is designated anti-box C/D snoRNP, when U3, U8 and U22 snoRNAs are all immunoprecipitated).

	Total	Box C/D	U3 only	U8 only	Box H/ACA	Th/To (RNase MRP/P)
	n=100	n=8	n=5	n=6	n=1	n=7
Syndromes						
SLE	11	3				1
SSc	14	1				2
SS	4					
PM	2			1		1
DM	2		1			
RA	20	1	2	2		
MCTD	4					
primary RP	10	2				2
Overlap syndromes						
RA/SLE	1					
RA/SS	2					
SLE/SS	1					
SSc/SS	1					
DM/SSc	1					
Other	27	1	2	3	1	1

Table II. Diagnoses of patients with anti-nucleolar autoantibodies

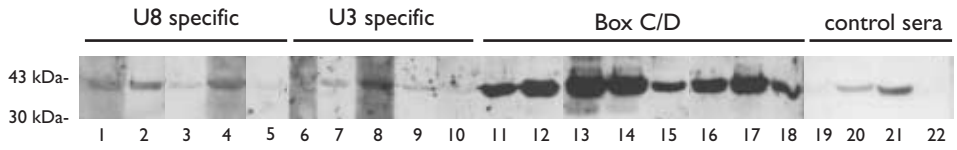

Figure 3. Recognition of fibrillarin by anti-nucleolar sera. Recombinant fibrillarin was separated by SDS-PAGE and transferred to nitrocellulose membranes. Strips of these membranes were incubated with patient sera that co-immunoprecipitate either U8 snoRNA (lanes 1-5) or U3 snoRNA (lanes 6-10) or all box C/D snoRNAs analysed (U8, U3 and U22 snoRNAs) (lanes 11-18) or control sera (lanes 19-22). The position of molecular weight markers is indicated on the left.

Three proteins have been reported to be associated with all box C/D snoRNPs (fibrillarin, Nop56 and Nop5/58) suggesting that one or more of these proteins is targeted by these sera. Previous studies indicated that sera with anti-nucleolar activity frequently contain autoantibodies against fibrillarin (145,147). To investigate the recognition of fibrillarin by the patient sera precipitating the box C/D snoRNPs, western blot analyses were performed using recombinant fibrillarin. As shown in Figure 3, lanes 11-18, all patient sera that are able to immunoprecipitate box C/D snoRNPs efficiently recognise fibrillarin, whereas with sera that recognise merely U8 or U3 snoRNP only background levels of reactivity were observed (lanes 1-10). The former group will now be referred to as anti-fibrillarin positive patient sera.

Anti-fibrillarin antibodies have been reported to occur in patients suffering from primary RP, SSc and SSc-overlap syndromes (68,145). Chart review confirmed that anti-fibrillarin positive sera (n=8) can be found in SSc (n=1) and primary RP (n=2), see Table II. In addition, anti-fibrillarin positive sera were found in patients suffering from SLE (n=3), RA (n=1) and UCTD (n=1). Clinical manifestations of anti-fibrillarin positive patients were studied in more detail, see Table III. Anti-fibrillarin positive patient sera appeared to be particularly associated with manifestations suggesting a more poor prognosis, such as pleuritis, pericarditis, renal failure and myocarditis.

Identification of reactivity to U3 and U8 snoRNPs only

The analyses of this cohort of anti-nucleolar sera showed for the first time that 5-10% of these sera contained reactivity to either U3 snoRNP only or to U8 snoRNP only, see Table I. These sera do not show detectable reactivity to fibrillarin, as illustrated in Figure 3, lanes 1-10. The anti-U3 snoRNP only antibodies (n=5) were found to be present in patients suffering from DM (n=1), RA (n=2), RA with sicca complaints (n=1) and fibromyalgia (n=1), see Table II. Anti-U8 snoRNP only antibodies (n=6) are found in patients suffering from similar diseases, i.e. PM (n=1), RA (n=2), deforming osteoarthritis (n=1), arthralgies (n=1) and JCA (n=1). In more detail, the patient sera that recognise U3 or U8 snoRNP only (n=11) are associated with arthritis (n=7), polymyositis (n=2), RP (n=2) and sicca complaints (n=4, e.g. xerostomia and xerophthalmia), see Table III. In addition, anti-U8 snoRNP only patient sera associate with pleuritis (n=1), anemia (n=3) and lymphopenia (n=3), diabetes (n=1) and vasculitis (n=1).

In summary, anti-fibrillarin positive and negative anti-box C/D snoRNP patient sera appear to be associated with two patients groups with different manifestations. The group of anti-fibrillarin positive sera seems to be associated with a more poor prognosis than the anti-fibrillarin negative patient sera, suggesting that such analyses may contribute to a more reliable prognosis for these patients.

Identification of box H/ACA snoRNPs as a new nucleolar autoantigen

One anti-nucleolar patient serum was found to co-immunoprecipitate both U17 and E3 box H/ACA snoRNAs, indicating that also components of this class of snoRNPs (albeit with low frequency) can be autoantigenic in patients suffering from connective tissue diseases (see Figure 2, lane 17, and Table I). At this moment, four proteins have been identified that are known to associate with all box H/ACA snoRNPs: hGar1, NAP57/dyskerin, hNHP2 and hNOP10 (18-20). Immunoprecipitation of these four proteins, translated *in vitro*, did not generate conclusive data on the direct target of the autoantibodies (our unpublished observations). It is possible that the autoantibodies in this serum react with another, yet unidentified, common subunit of box H/ACA snoRNPs. Chart review of this patient learned that this patient suffered from gout and polyarticular non-erosive arthritis.

Anti-Th/To autoantibodies are associated with different connective tissue diseases

The Th/To autoantigen (RNase MRP/RNase P) has been reported to be recognised by SSc patients with a frequency of 10-14% (62,67,68,139,148). In this population of random

Clinical manifestations	Total	Box C/D	U3 only	U8 only	Box H/ACA	Th/To (RNase MRP/P)
	n=100	n=8	n=5	n=6	n=1	n=7
Butterfly rash	9	1				
discoid lupus	3	1				1
increased photosensitivity	6					
arthritis	44	3	3	4	1	
pleuritis	5	2		1		
pericarditis	5	2				
renal disease	13	2				
neurologic disorders	5					
anemia	33	3		3		1
lymphopenia	20	2		3		2
prox scleroderma	6					
bilat basale longfibrose (X-thorax)	9	1				1
pulmonal hypertension	2					
Raynaud's phenomenon	45	4	1	1		5
decreased co-diffusion	17	2		1		4
decreased esophagus motility	16	2				4
decreased intestine motility	4					
sclerodactyly	16	2				2
digital pitting scars	17	4				3
sicca complaints	48	4	3	1		6
polymyositis	8		1	1		2
diabetes mellitus	3			1		
vasculitis	18			1		2
myocarditis	3	1				

Table III. Clinical manifestations per group of anti-nucleolar patient sera

anti-nucleolar sera, we detected autoantibodies with anti-Th/To specificity in 8% of the cases (n=14). Co-precipitation of RNase MRP and RNase P RNAs was also observed in 15 other anti-nucleolar patient sera, but these sera precipitated Ro RNP complexes as well. This strongly suggests that anti-La antibodies are responsible for the precipitation of the RNase MRP and RNase P RNAs by these sera, because the La autoantigen is known to associate (transiently) with all RNA polymerase III products, including the RNAs associated with RNase MRP, RNase P and Ro RNPs.

The well known association of the anti-Th/To specificity with SSc (n=2) and primary RP (n=2) is supported by our data. In addition, anti-Th/To antibodies were found in one patient with SLE, one patient with PM and one patient with severe weight loss. Chart review of these seven patients showed that the Th/To autoantigen is primarily associated with manifestations of RP (n=5), decreased co-diffusion (n=4), esophagus hypomotility (n=4) and with sicca complaints (n=6, of which 5 suffered from xerophthalmia).

40% of anti-nucleolar reactivity remains uncharacterised

In addition to antibodies targeted to small nucleolar ribonucleoprotein complexes, antibodies to the PM/Scl-100 autoantigen, which are also known to result in nucleolar staining in immunofluorescence, were detected as well (n=44, see Table I). PM/Scl-100 reactivity was found in patients suffering from DM, PM, SSc and DM/SSc overlap syndromes, as has been reported before ((149) and references therein). In addition, reactivity against PM/Scl-100 was detected in sera from patients suffering from RA, SLE, SS and MCTD, see Table I.

All anti-nucleolar patient sera were further tested for the presence of reactivity against the non-nucleolar U1 snRNP and Ro RNPs. Antibodies directed against U1 snRNP were detected in 23 sera, whereas 31 contained anti-Ro RNP reactivity. The presence of these antibodies associated with SLE, MCTD and SLE, SSc and SS, respectively. However, in 61 of the anti-nucleolar sera none of the tested activities could be detected, suggesting that these sera recognise other (possibly yet uncharacterised) autoantigens.

Discussion

This study describes the analysis of a group of 172 anti-nucleolar sera from autoimmune patients for the presence of autoantibodies directed against small nucleolar ribonucleoprotein particles. Other investigators have previously reported that the existence of anti-nucleolar reactivities is particularly associated with SSc (68,139,143,145). In the present study a random collection of patient sera was screened for the presence of anti-nucleolar reactivities and chart review of 100 of these patients indicated that the occurrence of anti-nucleolar reactivity is not restricted to SSc, but is also found in patients suffering from other diseases. The association of anti-nucleolar reactivities with SLE, PM/DM and RA has not been reported before and thus lowers the relevance of anti-nucleolar autoantibody detection for diagnostic purposes.

Autoantibodies precipitating U3 snoRNA and possibly other box C/D snoRNPs have been reported in 5-10% of sera from patients suffering from primary RP, SSc and SSc-overlap syndromes (68). Anti-fibrillarin autoantibodies have been reported not only in SSc, but also in MCTD, SLE, RA and SS (145,147). Our data indicate that two types of anti-box C/D snoRNP autoantibodies exist, one that recognises fibrillarin (i.e. precipitating the whole group of box C/D snoRNPs) and another that recognises individual box C/D snoRNPs such as U3 and U8 snoRNP (this group is also referred to as U3 only or U8 only). This distinction may be important for the diagnosis and prognosis of these patients. Our data and the work of Arnett and coworkers (145) indicate that antibodies directed to fibrillarin are associated with severe SSc, whereas antibodies directed to individual box C/D snoRNPs appear to be associated with arthritis and polymyositis.

The presence of autoantibodies against fibrillarin in the group of sera targeting box C/D snoRNPs does not implicate that autoantibodies directed to other protein subunits shared by all box C/D snoRNPs do not exist. These putative autoantigens include Nop5/58 and Nop56 (14,15). Possible targets of patients sera directed against U3 snoRNP only include U3-55K, Mpp10 and human homologues of IMP3 and IMP4 (113,150,151). Other patient sera could be identified as U8 snoRNP only. At this moment, only one protein is known that specifically binds U8 snoRNP: X29 (152). The X29 protein has been identified in *Xenopus laevis*, but a homologous human protein is likely to exist as well. The identification of the primary targets of box C/D snoRNP specific autoantibodies awaits a better and more complete characterisation of the composition of these ribonucleoprotein complexes.

Autoantibodies against box H/ACA snoRNPs were detected in one patient suffering from gout and arthritis. The existence of autoantibodies against this class of snoRNPs has never been reported before. Four proteins are known to specifically associate with this class of box H/ACA snoRNPs: hGar1, NAP57/dyskerin, hNHP2 and hNOP10 (18-20). We were unable to obtain conclusive data on which of these proteins is autoantigenic. We also can not exclude the possibility that post-translational modifications are important for the recognition of (one of) these proteins by autoantibodies. Post-translational modifications (e.g. methylation or deimination of arginines) have been shown to be of critical importance for the efficient recognition of Sm proteins and RA-specific autoantigens (153,154). Alternatively, a yet unidentified box H/ACA snoRNP associated protein may be targeted by these autoantibodies. The generation of autoantibodies directed to box H/ACA snoRNPs appears to be a rare phenomenon. Northern blot analysis, however, may not be sensitive enough to detect low-titered autoantibodies in anti-nucleolar sera, because box H/ACA snoRNPs are much less abundant than for example U3 and U8 snoRNPs. Both the further characterisation of the composition of box H/ACA snoRNPs and the identification of more patient sera with anti-box H/ACA snoRNP reactivities will be required to shed more light on the specificity of this new class of autoantibodies.

The observed prevalence of autoantibodies directed against the Th/To-autoantigen in SSc patients is in accordance with reported frequencies (8-14%) ((67,145,148,149), reviewed in ref. (139,143)). Because we analysed anti-nucleolar patient sera rather than SSc sera, the present results demonstrate that anti-Th/To antibodies are also present in other autoimmune diseases: e.g. SLE and PM. Both Yamane and coworkers and Okano and coworkers showed that anti-Th/To antibodies are associated with

localised SSc (67,148). In our study, anti-Th/To antibodies are associated with Raynaud's phenomenon, decreased co-diffusion, esophagus hypomotility and xerophthalmia, supporting the previous findings. The major autoantigen associated with the Th/To antigen is referred to as Th-40. This 40 kDa protein has been identified using immunoprecipitation of proteins from radioactively labelled cell extracts and UV-crosslinking analysis (42,72,75). Although three proteins (hPop1, Rpp30 and Rpp38) of the RNase MRP and RNase P complexes have been reported to be recognised by Th/To-sera, none of them seems to represent the Th-40 autoantigen ((77,78), reviewed in ref. (118)), leaving the question on the identity of this autoantigen unanswered.

Surprisingly, a large group of patient sera (35-47%) did not recognise any of the tested small (nucleolar) ribonucleoprotein complexes. It seems likely to assume that in these sera autoantibodies are present directed to other nucleolar autoantigens such as Ku, NOR-90/UBF, RNA polymerase I or DNA topoisomerase I. These proteins/complexes have been reported to be autoantigenic in 10-25% of SSc sera (reviewed in ref. (139,143)). Future research will have to evaluate whether these or other as yet unidentified autoantigens are recognised by patient sera that do no recognise small nucleolar ribonucleoprotein complexes.

Acknowledgements

We would like to thank Ben de Jong and Eugenie Terwindt for technical assistance. We would like to thank Femke van Karnebeek and Iris Ketel for assisting in the chart review. We thank Vanda Pogacic and Dr. Filipowicz (Friedrich Miesher Institute, Basel, Switzerland) for the kind gift of the cDNAs of hGar1, dyskerin, hNHP2 and hNOP10.

This work was supported in part by the Netherlands Organisation for Scientific Research (NWO-CW).

Patients and methods

Patients

Most patient sera were obtained from the department of Rheumatology of the University Medical Centre St. Radboud, Nijmegen and the St. Maartens Hospital, Nijmegen and routinely tested for the presence of anti-nucleolar autoantibodies by indirect immunofluorescence on HEp-2 cells in a 40-fold dilution (146).

A total of 172 sera that displayed anti-nucleolar reactivity were collected. From 100 patients clinical information could be obtained by chart review (26 from the St. Maartens Hospital and 74 from the University Medical Centre St. Radboud). The patients' age and sex were recorded along with clinical findings, which include all signs, symptoms and serology contributing to the classification criteria of RA (155), SLE (156), SSc (157), SS (158) and diagnostic criteria of DM and PM by Peter and Bohan (159,160). Also often occurring non-specific signs such as RP, sicca complaints, pulmonary function test abnormalities, pulmonary hypertension, motility abnormalities of esophagus and gut, myocarditis and other (autoimmune) diseases such as diabetes, vasculitic disorders, thyreoiditis, spondyalarthropathies and gout were recorded.

snoRNP immunoprecipitation analysis

Total HeLa cell extracts were prepared as described previously (116). For each immunoprecipitation with patient serum, 20 µl serum was incubated with 20 µl of a 50% suspension of protein A-agarose beads in IPP500 (500 mM NaCl, 10 mM Tris-HCl pH 8.0, 0.05% NP-40) for 1 h at room temperature. Beads were washed two times with IPP500 and once with IPP150 (150 mM NaCl, 10 mM Tris-HCl pH 8.0, 0.05% NP-40). HeLa extract was added, the mixture was incubated for 2 hours at 4°C and the beads were washed three times with IPP150. To analyse co-precipitating RNAs, the RNA was isolated by phenol-chloroform extraction and ethanol precipitation. RNAs were resolved on a denaturing polyacrylamide gel and blotted onto Hybond-N membranes (Amersham Pharmacia Biotech). Northern blot hybridisations with ^{32}P-labeled oligonucleotides was performed as described by Sambrook *et al.* (161). The following oligonucleotides were used to analyse the following RNAs: RNase P: 5'-GGG-AGA-GCC-CTG-TTA-GGG-CCG-CCC-3'; RNase MRP: 5'-CCC-CGT-GTG-GTT-GGT-GCG-CGG-ACA-C-3'; U3: 5'-CGA-AGC-TTG-TAC-CAC-TCA-GAC-CGC-GTT-CTC-3'; U8: 5'-CAT-GTT-CTA-ATC-TGC-CCT-CCG-GAG-GAG-G-3'; U22: 5'-ACA-GGC-TCT-GGG-ACT-AGG-ACA-GAG-AG-3'; U17: 5'-AGA-GCC-CTA-TGC-TCC-CCT-ACG-CCA-C-3'; E3: 5'-GCA-GGG-GGA-ACG-ACA-ACA-CAG-CAC-3'; U1: 5'-GCG-CGA-ACG-CAG-TCC-CCC-ACT-ACC-AC-3'; Y1: 5'-CTA-AGC-TTA-AAA-GAC-TAG-TCA-AGT-GCA-GT-3'.

Western blot analysis of hFib

Recombinant His_6-tagged human fibrillarin was expressed in and purified from Sf-9 cells using the Bac-to-Bac baculovirus expression system according to the manufacturer's protocol (Gibco-BRL). For western blot analysis approximately 1 ng of recombinant protein was loaded on a 13% SDS-PAGE and transferred to nitrocellulose. Patient sera were used in a 5000-fold dilution. Detection was performed using horseradish peroxidase-conjugated rabbit-anti-human IgG (Dako Immunoglobulins) as secondary antibody and visualisation by chemiluminescence.

Anti PM/Scl-100 autoantibodies

Reactivity with PM/Scl-100 was determined by ELISA as described previously (149).

Chapter 8

Mutations in the RNA Component of RNase MRP cause a Pleiotropic Human Disease, Cartilage-Hair Hypoplasia

Maaret Ridanpää[1,2]
Hans van Eenennaam[3]
Katarina Pelin[1,2]
Robert Chadwick[4]
Cheryl Johnson[4]
Bo Yuan[4]
Walther van Venrooij[3]
Ger Pruijn[3]
Riika Salmela[1,2]
Susanna Rockas[1,2]
Outi Mäkitie[5]
Ilkka Kaitila[6]
Albert de la Chapelle[4]

[1] *Folkhälsan Institute of Genetics, Helsinki, Finland*
[2] *Department of Medical Genetics, University of Helsinki, Finland*
[3] *Department of Biochemistry, University of Nijmegen, Nijmegen, The Netherlands*
[4] *Human Cancer Genetics Program, The Ohio State University, Columbus, Ohio, USA*
[5] *Hospital for Children and Adolescents, Helsinki University Hospital, Helsinki, Finland*
[6] *Department of Clinical Genetics, Helsinki University Hospital, Helsinki, Finland*

Cell (2001) 104: 195-203

Abstract

The recessively inherited developmental disorder, cartilage-hair hypoplasia (CHH) is highly pleiotropic with manifestations including short stature, defective cellular immunity, and predisposition to several cancers. The endoribonuclease RNase MRP consists of an RNA molecule bound to several proteins. It has at least two functions, namely, cleavage of RNA in mitochondrial DNA synthesis and nucleolar cleaving of pre-rRNA.

We describe numerous mutations in the untranslated RMRP gene that cosegragate with the CHH phenotype. Insertion mutations immediately upstream of the coding sequence silence transcription while mutations in the transcribed region do not. The association of protein subunits with RNA appears unaltered. We conclude that mutations in RMRP cause CHH by disrupting a function of RNase MRP RNA that affects multiple organ systems.

Introduction

Pleiotropy, that is, multiple phenotypic manifestations of a single genetic defect, is a hallmark of McKusick-type metaphyseal chondrodysplasia or cartilage-hair hypoplasia (CHH) [MIM #250250] (163). The most prominent characteristic of this recessively inherited disorder is disproportionate short stature with adult heights ranging from 104 to 149 cm. Other common features include hypoplastic hair, ligamentous laxity, defective immunity, hypoplastic anemia, and neuronal dysplasia of the intestine. Manifestations occurring in a smaller proportion of affected individuals include congenital megacolon (Hirschsprung's disease), and predisposition to lymphoma and other cancers. The variation in clinical severity is remarkable both between and within sibships (163-165). CHH was first described in the Old Order Amish where it is a common cause of short-limbed short stature (163,166). The incidence among the Amish was calculated as 1 in 1340 implicating a carrier frequency as high as 1:19 (167). Another founder population, the Finns, displays a similar gene enrichment with a calculated carrier frequency of 1:76 (164). Cases have been described in numerous other populations; however, there is no precise measure of its worldwide incidence (164). A locus responsible for CHH was mapped to a region on the short arm of chromosome 9 eight years ago (168), and subsequently shown to account for most or all CHH (locus homogeneity) (167,169). The critical region has been reduced to less than 1 Mb of DNA by linkage and linkage dis-

equilibrium analysis (170) and physical mapping (171). However, in spite of intensive study of candidate genes in the critical region ((172); unpublished data by the present authors) the gene has been elusive (166). Here we describe mutations in the RMRP gene causing CHH. This study describes disease-causing mutations in a nuclear gene encoding a structural RNA molecule. The untranslated RMRP gene is transcribed by RNA polymerase III, encodes the RNA component of a ribonucleoprotein endoribonuclease (66), and is located in the CHH critical region ((173), and results shown here). Normally the RNase MRP complex is involved in multiple cellular and mitochondrial functions. In the nucleolus this endonuclease partakes in the processing of pre-rRNA whereas in the mitochondrion it cleaves the RNA primers responsible for DNA replication ((27,174), reviewed in ref. (118)). As we did not find any disturbances in the association of specific proteins with RNase MRP RNA from CHH patients, the disease-causing functional impairment of the RMRP gene product remains to be characterized. The existence of one or more elusive additional substrates for this endonuclease has been postulated (5,41). Our findings provide a first step toward an improved understanding of these processes leading to the pleiotropic phenotypic manifestations of CHH.

Name	Location	Type of Polymorphism	PCR Primer Sequences (5'-3')	PCR Product Size (bp)	SSCP Conditions
16P1	Centromeric to *AB002373*	dup TGCATGCA	AAGGATCCTCGCAGCTTTC GCACCCTGGTCAATGTTTTC	182/190	6% Sequagel
AB12GS	AB002373	A/G	AGTGGGCCCATATGAAACAC CCCCTTTGAGTGGTTGCTTAC	118	0.7 x MDE 4 W 15 hr
Del13	CD72	13 nt deletion	GAGGCATGGGGAGTCCAG GTGGAGGAACTTTCATCCCAG	103/90	2% SeaKem
SIT45S	SIT *intron 3*	T/C	GGCTGTGACGCTGCTATTTC AATGCAGGTTCCCATACAGC	223	0.5 x MDE 3 W 17 hr
TP2A	*TPM2* exon 2A	G/A	CGCTTCTCTCCCCTACAATAG GACAGAGGGGACTTGGTCAG	270	0.7 x MDE 5 W 18 hr
TA13S	nt 3806 in *TLN* cDNA	C/T	CTGTGTCAGCTGCCTACCTG AGAGGCCTGGCATTCTTTG	143	1 x MDE 6 W 18 hr
D4S	*KIAA0582*	G/A	CATCCTCCTCCAAGAATGGAC AAACCTCAGCCCTGGCAC	187	0.8 x MDE 6 W 18 hr
D6S	*KIAA0582*	G/A	AATCAGGATCCATTACACCCTC CAGCTTCTCCCTCCCAATC	137	0.7 x MDE 4 W 17 hr
CA1	Between 37D7T7 and Z38966	AC repeat	TTCCTTCTGTGTTGGGTGTG TTCCTATTGAGCCCGATTTG	~140	6% Sequagel
XL6S	Telomeric to EST-C	G/A	AAGGCTGAGTCTGGGTGATTC AAGGCAAACAGGGGATTTTC	152	0.8 x MDE 5 W 17 hr
XL2S	Telomeric to EST-C	G/A	AGACTGAGGTCAGAGGGGGAAG CGCAAGGCTGGTTCTCTGAG	145	0.8 x MDE 5 W 17 hr
XL1S	Telomeric to EST-C	T/C	CAAAAGCCCGTGTTGTTCATC GGTGGAGACAGAGGAGCTGTC	166	0.8 x MDE 5 W 18 hr
CCS	EST-C	G/A	CATTCGGCACATGAGATACG CAGGACTGTGACGTGGAGAG	145	1 x MDE 6 W 17 hr
TG2S	T64224	C/T	CAGAACCAGCATCATAG GGATCCTTGTTATTGGGACAG	187	1 x MDE 5 W 17 hr

Table 1. The new polymorphic markers used in genetic mapping. The order is from the telomere to the centromere.

Results

Genetic map of the CHH region

To refine the genetic map of the CHH region in chromosome 9p13 beyond our previous map (171), we developed new polymorphic markers (Table 1). Haplotypes were constructed of 116 affected chromosomes from 16 multiplex and 42 uniplex Finnish CHH families using 23 polymorphic markers. Among the 116 haplotypes, 96 (83%) shared alleles with the presumptive ancestral haplotype, suggestive of a prevalent shared founder mutation. A graphic representation of those 78 haplotypes in which all alleles could be unequivocally assigned to the 23 markers is shown in Figure 1A. The "ancestral" haplotype shown uppermost was observed in 18 chromosomes, whereas all other chromosomes showed a reduction in the length of the shared haplotype as evidence of historical recombinations. These historical recombinations allowed us to tentatively narrow the critical CHH region to the interval between the TESK1 A/G and D4S markers. This region was later shown to represent 145 kilobases of DNA. The degree of linkage disequilibrium between markers and the disease phenotype can give a hint about the precise location of the sought gene (175) and has proven a powerful tool in the positional cloning of numerous genes in the Finnish population (176). The higher the P_{excess} value, the stronger is the linkage disequilibrium and the closer is the marker to the disease gene (177). Within the above critical region, P_{excess} varied between 0.70 and 0.92 being highest at the adjacent markers TP2A and TA13S (Figure 1A).

Genomic and transcript map of the CHH region

The CHH critical region as defined above was contained in three overlapping BAC clones, 468J10, 199G9, and 497J14 as determined previously (Figure 2 in (171)). The region was known to contain several genes and transcripts; however, in an effort to study all genes, we shotgun-sequenced the three BAC clones and assembled the middle part of the sequence into three contigs, 71.6 kb, 187.6 kb, and 122.7 kb in length (accession nos. AF334828 to AF334830). The 145 kb CHH critical region was fully covered by the largest contig and contained at least 11 genes as shown in Figure 1B.

Mutational analysis in CHH patients

Using available bioinformatics tools and existing databases, we mapped and assembled 11 genes in the critical region that we had sequenced (Figure 1B). We analyzed all 11 genes by a combination of reverse transcriptase PCR cDNA sequencing, single-strand conformational polymorphism (SSCP), and direct genomic PCR sequencing in a panel of 7 CHH patients and one noncarrier control. No potentially disease-causing mutations were found in the coding regions of TESK1, CD72, SIT, AK001187, MN/CA9, TPM2, TLN, LZIP, AAF53384 homolog, and KIAA0258 genes (data not shown). However, the finding of an insertion in the RMRP gene in one CHH patient focused our attention on RMRP.

Mutations in the RMRP gene

The primary transcript of RMRP (accession no. M29916) comprises 267 nucleotides and

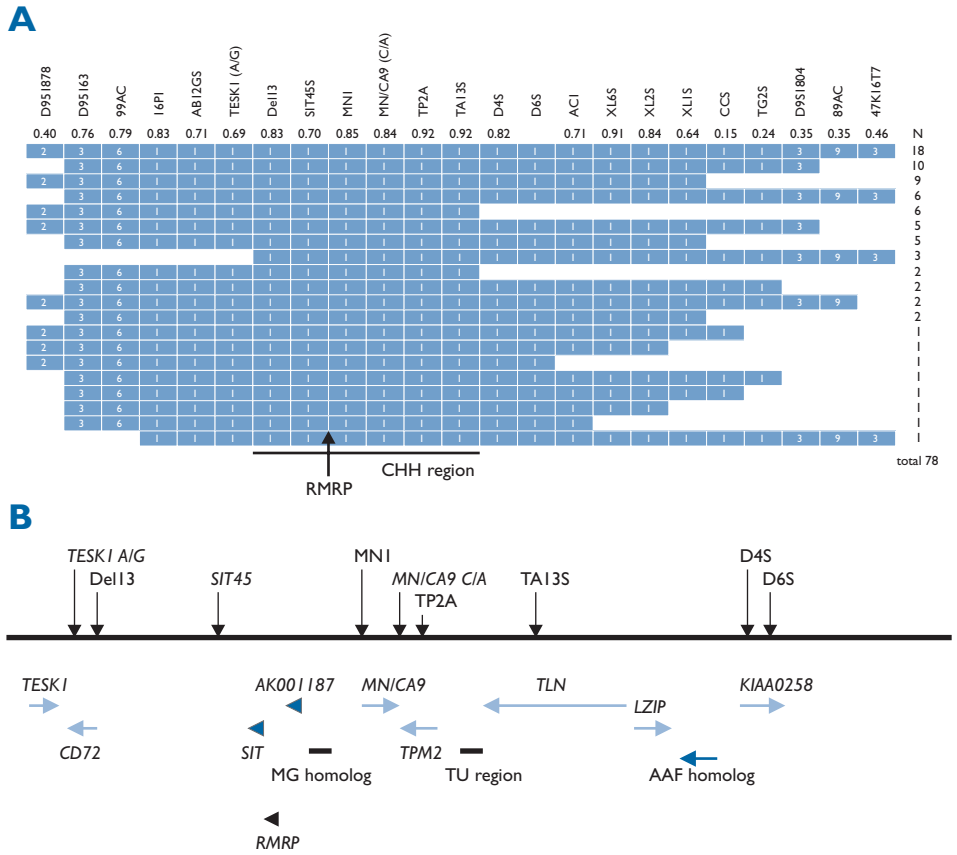

Figure 1. Genetic, physical, and transcript map of the chh region. **A.** Haplotypes of 78 affected chromosomes from Finnish CHH patients are shown. Alleles of the polymorphic markers are arbitrarily numbered. The uppermost haplotype encountered in 18 chromosomes is considered "ancestral." Portions of this haplotype that are shared on the remaining 60 chromosomes are shown in blue. The region shared by all haplotypes extends between markers *TESK1 A/G* and *D4S* and is depicted as the "*CHH region*." The telomere is to the left. On top are shown the P_{excess} values depicting the degree of linkage disequilibrium between each marker and the disease phenotype. A peak at markers *TP2A* and *TA13S* is seen. An arrow indicates the location of the *RMRP* gene. **B.** Shown here is the middle region of the genetic map depicted in (A). Above the line are the 9 polymorphic markers; below the line are the transcripts. Among the genes in the CHH critical region the ones that were mapped there before the genomic sequence was obtained are marked in light blue, whereas the ones marked in dark blue were localized there based on the sequence we generated. RMRP is depicted in black. In addition to these genes, exon prediction and homologies to human and mouse coding sequences suggested one novel gene immediately centromeric to *AK001187 (MG homolog)*. A promoter region near the 3' end of *TLN* and several *non-TLN* ESTs were found to overlap the 3' end of *TLN*. These findings may suggest an unknown gene overlapping *TLN (TU region)*. After repeats were masked, exons of the putative genes were searched using FGENES and GRAIL-1.3 programs. Four exons were predicted for the *MG homolog* whereas three exons were predicted for the *TU region*. Using reverse transcription PCR, we determined that *AK001187* and *MG homolog* belong to the same gene.

is present in the genome as a single copy (27). RMRP is transcribed by RNA polymerase III, which is active within the nucleoplasm (178). The RMRP promoter is a type III promoter lacking intragenic promoter elements (178,179). A TATA box is located between -33 and -25, and additional type III promoter elements are found between -67 and -57 (PSE element), -215 and -208 (octamer element), and between -231 and -225 (SP1 binding site) (180). We PCR amplified the entire ~1 kb RMRP region in four overlapping fragments, and searched for sequence variants by direct sequencing. The mutations are of two distinct types. The first category consists of insertions or duplications between 6 and 30 nucleotides long residing in the region between the TATA box and the transcription initiation site. As shown below, these mutations interfere with the transcription of RMRP. The second category consists of single nucleotide substitutions and other changes involving at most two nucleotides. These reside in highly conserved residues of the transcribed sequence. Table 2 summarizes the mutations found in those CHH patients and families in which a mutation of both alleles has been identified so far. Figure 2 summarizes the location of these mutations. Of note is that while the insertion mutations are of somewhat different length and location, they all result in a lengthening of the important distance between the TATA box and the transcription initiation site. Regarding the 4 different mutations in the transcribed sequence, we note that all are located at sites that are conserved in human, cattle, mouse, rat, and some even in *Xenopus*, *Arabidopsis*, or *Saccharomyces* suggesting that they are functionally important (70,181). Moreover, nucleotides 98 and 262 reside in positions predicted to show double-stranded structure (70) whereas position 98 can be important for MRP40 (recently shown to be identical to Rpp38) protein binding (105). These features suggest that the mutations are extremely likely to cause functional disturbances. Among 70 CHH patients that have been studied for mutations so far, 55 harbor a mutation in both alleles of the RMRP gene. In all instances where samples from several family members were available, the mutations cosegregated with the disease phenotype assuming recessive inheritance. In 13 families with more than one affected child, all affected individuals had identical mutations. All 26

Patient Number	Nationality	Mutation in the Paternal Allele	Mutation in the Maternal Allele
1 •[a]	Finnish	70A→G •[b]	70A→G
2 •[a]	Finnish	•[c]	70A→G
3	Finnish	70A→G	262G→T •[d]
4	Finnish	262G→T •[d]	70A→G
5	Finnish	70A→G	dupTACTCTGTGA at –13 •[e]
6	Finnish	dupTACTCTGTGA at –13 •[e]	70A→G
7 •[a]	Swiss	Two times dupACTACTCTGTGAAGC at -10 •[f]	98dupTG •[f]
8 •[a]	German	70A→G	insCCTGAG at –6 •[f]
9	Canadian	98dupTG •[f]	70A→G
10	English	dupTCTGTGAAGCTGAGGAC at –3 •[f]	193G→A •[g]

Table 2. Mutations in the RMRP gene in CHH patients. •[a] Patients 1, 2, 7, and 8 refer to the ones described in Figures 3 and 4. •[b] Homozygosity for the 70A→G mutation has been diagnosed in a total of 42 Finnish CHH families, including 12 with more than one affected child and 30 with a single affected child. All of these carry modifications of the "ancestral" haplotype described in Figure 1. The 70A→G mutation has been detected in heterozygosity in 1 Finnish control sample out of 120 and in 2 out of 160 non-Finnish control samples. •[c] This patient has uniparental disomy for chromosome 9 with two copies of the maternal, mutation-carrying chromosome, and no paternal chromosome 9. •[d] The 262G→T mutation has been found in compound heterozygosity (with 70A→G) in a total of 6 Finnish CHH families, one of which has two affected children. The chromosomes carrying 262G→T share a haplotype that differs from that of the main "ancestral" one. The 262G→T mutation has not been detected in any of 120 Finnish and 160 non-Finnish control individuals. •[e] The 10-nucleotide TACTCTGTGA duplication at position –13 occurs in heterozygosity in two Finnish families (patients 5 and 6). The chromosomes carrying this mutation share a haplotype that differs from the "ancestral" one. This and all other duplication-insertions have been searched for in 120 Finnish and 160 non-Finnish controls and not found. •[f] None of these mutations have been found in 120 Finnish and 160 non-Finnish controls. •[g] The 193G→A mutation has not been found in any of 112 Finnish and 93 non-Finnish controls.

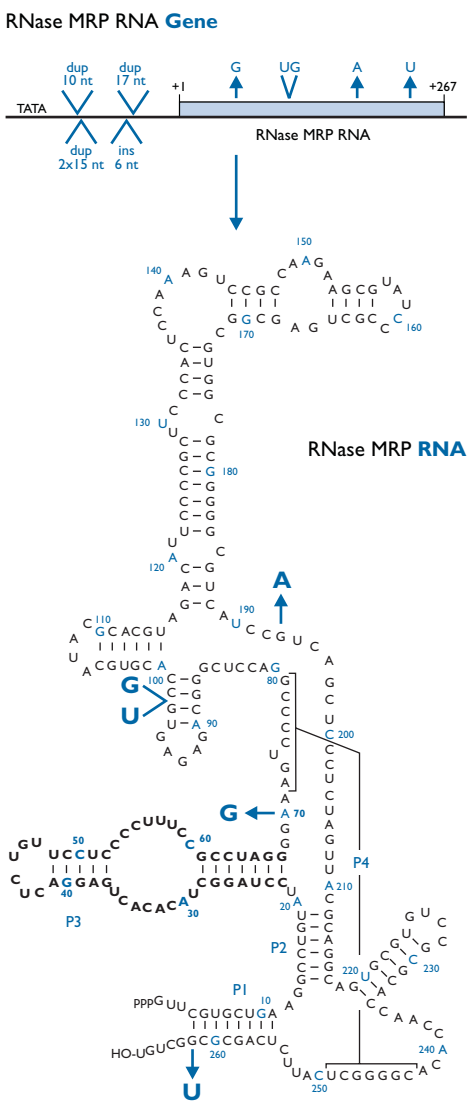

Figure 2. Localization of the RMRP mutations in CHH patients. Depicted in the upper part is the RNase MRP RNA gene as published in ref. (66). Shown is the TATA box at position –33 to –25 and the transcription initiation site (represented by +1). Depicted in the box is the transcribed region of the RNase MRP gene. All mutations listed in Table 2 are shown. The lower part depicts the secondary structure of the RNase MRP RNA shown as adapted from ref. (70). The mutations are shown in dark blue.

parents studied so far were heterozygous for one of the mutations found in the affected child(ren). Among 6 unaffected siblings of affected individuals either heterozygosity for a mutation (n=1) or homozygosity for the wild type sequence (n=5) was seen. Notably, in Finnish patients and parents the chromosomes carrying the main 70A→G mutation all had the main "ancestral" haplotype or modifications thereof (n=110). All 6 chromosomes carrying the 262G→T mutation shared a haplotype that differed from the main one, and both chromosomes carrying the 10 bp duplication had another, "private" haplotype. In searching for these mutations in control individuals comprising 120 anonymous blood donors from Finland, a panel of 61 non-Finnish controls representing various nationalities, and 99 Centre d'Etude du Polymorphisme Humain (CEPH; http://www.cephb.fr) grandparents were screened. A single case of a control sample with one of these mutations was detected in Finland; a blood donor was heterozygous for 70A→G. As the carrier frequency of CHH in Finland is of the order of 1:76 (164), this finding was expected. Among 160 non-Finnish controls, it was found in two samples. These were grandparents of a CEPH family in which kinship between grandparents is likely. None of the other mutations were found in any control sample.

Reduced expression levels of RNase MRP

RNA expressed in some CHH patients cells derived from two patients with single nucleotide mutations in the transcribed region (patients 1 and 2; Table 2) and two patients with insertions (patients 7 and 8) were studied. As is shown in Figure 3, expression of RNase MRP RNA was found in all CHH patients. Using the level of expression of U3 snoRNA and U1 snRNA as references, RNase MRP RNA was less abundantly present in patients 7 and 8 as compared to control cells. Quantitative analysis using a phosphorimager showed that the level of expression of RNase MRP RNA in patients 7 and 8 was reduced to 35-40% of the level expression in control cells. By contrast, MRP RNA was expressed in patients 1 and 2 at a level comparable to that in the controls. In conclusion, these results suggest that the level of expression of RNase MRP RNA is reduced in the CHH patients with 5′ region insertions but not in CHH patients with merely intragenic mutations.

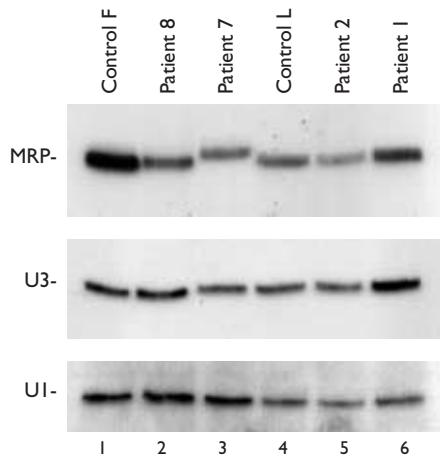

Figure 3. Expression of rnase MRP RNA in cells derived from CHH patients. Total RNA was analyzed by northern blotting using riboprobes directed against RNase MRP RNA, U3 snoRNA and U1 snRNA. Note the slightly larger band expressed in patient 7. Control-F, fibroblasts from a normal control; Patients 8 and 7, fibroblasts from these patients; Control-L, lymphoblasts from a normal control; Patients 2 and 1; lymphoblasts from these patients.

The reduced kevel of RNase MRP RNA is caused by silencing of one RMRP allele

Next we investigated whether the reduced expression seen in patients 7 and 8 was due to the silencing of one allele or a lower activity of both alleles. Both patients are compound heterozygous for mutations (Table 2). In patient 7, the transcript was noted to be slightly larger than in the other CHH patients and the controls, as seen in lane 3 of Figure 3. As the slight increase in transcript size suggested an addition of ~2 nucleotides, we hypothesized that the transcript emanated from the maternal allele that has a 2 bp duplication at position 98 (Table 2). To further study this phenomenon, we reverse transcribed RNA from patients 7 and 8 and a healthy control and then cloned and sequenced the cDNAs. The sequence of RMRP RNA in control cells was identical to that published by Topper and Clayton (66) (accession no. M29916). In patient 7, all 10 clones analyzed showed the duplication of TG at position 98, while in patient 8, all 10 clones sequenced showed the 70A→G mutation. Thus, in these two patients, the alleles with 5′ region insertions were not expressed. Taken together with the fact that total expression levels in these two patients were only 35-40% of the controls (Figure 3), it follows that only the alleles with intragenic mutations were expressed.

RNase MRP protein subunits associate with RNase MRP RNA in CHH patients

To study protein binding to MRP RNA, we performed immunoprecipitations on cell extracts derived from the four CHH patients described in the preceding paragraph, and two controls. As shown in Figure 4, hPop1 and hPop4 were clearly associated with the RNase MRP complex in patients 1, 2, 7, and 8. Similar experiments were done using antibodies against the Rpp30 and Rpp38 protein subunits (78) yielding similar results (data not shown).

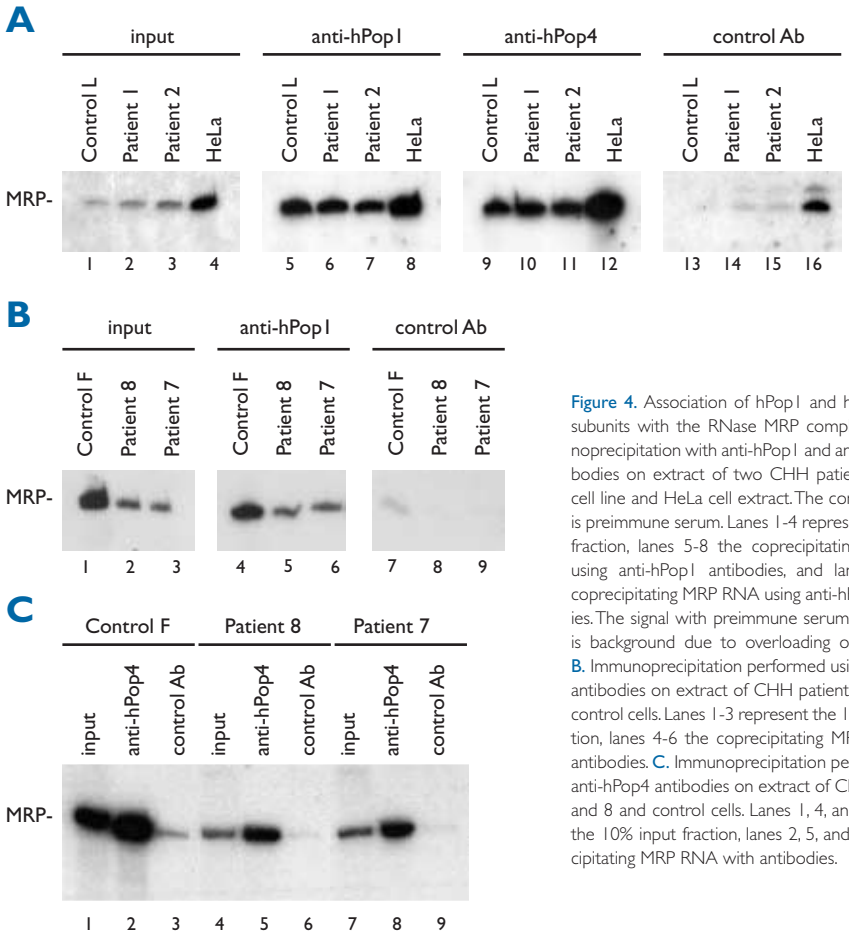

Figure 4. Association of hPop1 and hPop4 protein subunits with the RNase MRP complex. A. Immunoprecipitation with anti-hPop1 and anti-hPop4 antibodies on extract of two CHH patients, a control cell line and HeLa cell extract. The control antibody is preimmune serum. Lanes 1-4 represent 10% input fraction, lanes 5-8 the coprecipitating MRP RNA using anti-hPop1 antibodies, and lanes 9-12 the coprecipitating MRP RNA using anti-hPop4 antibodies. The signal with preimmune serum in HeLa cells is background due to overloading of cell extract. B. Immunoprecipitation performed using anti-hPop1 antibodies on extract of CHH patients 7 and 8 and control cells. Lanes 1-3 represent the 10% input fraction, lanes 4-6 the coprecipitating MRP RNA with antibodies. C. Immunoprecipitation performed using anti-hPop4 antibodies on extract of CHH patients 7 and 8 and control cells. Lanes 1, 4, and 7 represent the 10% input fraction, lanes 2, 5, and 8 the coprecipitating MRP RNA with antibodies.

In summary these immunoprecipitation data suggest that none of the mutations analyzed abolish the association of these four protein subunits with the MRP RNA.

Discussion

As shown here, mutations in RMRP can lead to CHH. Genetic evidence suggests the following model for the effect of RMRP mutations. Duplications and insertions in the region between the TATA box and the point of transcription initiation cause a lengthening of this interval and, at least in two cases, silencing of the corresponding RMRP allele. These we may call "null" promoter mutations. By contrast, mutations in the transcribed part of the gene do not cause inhibition of transcription, and may well be "leaky". These assumptions are based on the fact that no patients have been found that are homozygous for the putative null mutations, and therefore this condition might be lethal as could be deduced from studies in yeast (98). By contrast, patients who are homozygous "leaky" and others who are heterozygous do occur. It might not be surprising if CHH patients with a leaky/leaky genotype were less severely affected than patients who are null/leaky. Both mild and severe cases occur among the numerous patients who are homozygous for the main 70→G mutation ("leaky/ leaky"). However, it is too early to firmly assess any genotype-phenotype correlations. Indeed, we (165) and others (163) are impressed with the great phenotypic variability seen even within sibships. This suggests that other factors than (or in addition to), the RMRP mutation status contribute to the phenotype. These questions may best be addressed by studying experimental mutations in animal models. The first description of CHH by Victor McKusick *et al*. (163) established its major characteristics: recessive inheritance of a condition characterized by disproportionate, short-limbed dwarfism associated with numerous other manifestations. The multi-organ, multi-tissue manifestations of CHH, including cancer stimulated speculations about the nature of the mutated gene (164,182-184). In the largest series of CHH patients studied for cancer, a significant excess of cancer was seen, and it was mainly attributable to non-Hodgkin's lymphoma (185). Our results are compatible with the hypothesis that the basic defect may involve many cellular functions. The RNase MRP complex is one of a large population of small nucleolar ribonucleoproteins (reviewed in ref (5)). In yeast the RNase MRP complex cleaves pre-rRNA (28). The RNA gene that is mutated in CHH was first described as a nuclear gene whose RNA product contributes to the endonuclease activity needed for mitochondrial DNA replication (22,26,27). By immunoprecipitation we showed that the association of four protein subunits with RNase MRP RNA was undisturbed. We have attempted to measure the RNase MRP activity in CHH cells but available methods developed in yeast (28) do not appear to be sensitive enough for human cells (data not shown). In yeast, inhibition of RNase MRP results in the accumulation of a long form of precursor 5.8S rRNA (28). We used primer extension and northern blot hybridization in search of this precursor in CHH cells but found none (data not shown). As far as we know, such long forms have not been documented in humans.

Thus a clear-cut disturbance of one of the two known functions of RNase MRP has not yet been documented in CHH cells. It may even be that the RNA product of RMRP has other functions in addition to the ones characterized so far, and that the mutations found in CHH patients disrupt these. The fact that mutations in the transcript were found only in the highly conserved positions may eventually yield clues in this regard. In analogy with other small nuclear and small nucleolar ribonucleoprotein particles, these residues might be located in regions that are involved in substrate RNA recognition by direct base pairing interactions (5). Alternatively, they might be part of the catalytic center of the enzyme, a possibility supported by the structural homology with RNase P, one of the first RNAs for which a catalytic activity has been identified (50). Interestingly phylogenetic comparison of RNase MRP and RNase P RNA between human and *E. coli* supports this idea. The sequence element 68-GGAA-71 in human RNase MRP RNA is found to be fully conserved (69). The functional significance of these residues is suggested by recent studies on the *E. coli* RNase P complex, in which the two adenosine residues at comparable positions (70 and 71) in RNase MRP RNA

are important for substrate binding and catalysis (reviewed in ref. (186)). Thus, it is tempting to speculate that the A→G substitution at position 70 found in the major haplotype of CHH interferes with the optimal activity of the RNase MRP enzyme. An unknown function has been previously alluded to by Tollervey and Kiss (5) who suggested the existence of yet undetected additional substrates for RNase MRP. As reviewed in ref. (118), a function in cell cycle control is possible. In yeast cells having RMRP mutations, defects in plasmid segregation believed to be caused by telophase arrest have been documented (41). Disturbances in the mitotic process would seem to fit the T cell deficiency described in CHH patients. The immune deficiency, together with the hypoplastic anemia, and the failure of skeletal growth in CHH, would seem to be logical effects of, for example, mitotic arrest.

Acknowledgements

We dedicate this paper to Dr. Victor A. McKusick. We thank our colleagues Teresa Costa, M.D., (Halifax, Canada), Peter Freisinger, M.D., (München, Germany), Andrea Superti-Furga, M.D., (Zürich, Switzerland), and Robin M. Winter, M.D. (London, England) for giving us an opportunity to study their patients. We are grateful to Drs. S. Altman and C. Guerrier-Takada (Yale University) for kindly providing rabbit anti-Rpp30 and anti-Rpp38 antibodies, and to Dr. Pertti Sistonen and Dr. C. L. Harteveld for control samples. Niina Ali-Varpula, Miina Ollikainen, Eija Rintala, Johanna Tommiska, and Reetta Vierumäki are acknowledged for laboratory assistance. Supported by grants CA16058, and CA67941 from the National Institutes of Health, and the Academy of Finland, the Ulla Hjelt Fund, the Sigrid Juselius Foundation, The March of Dimes Birth Defects Foundation (1-FY98-32 and 1-FY99-586), and the Helsinki University Central Hospital Research Fund. The work of H.v.E., W.v.V. and G.P. was supported in part by the Netherlands Foundation for Chemical Research with financial aid from the Netherlands Organization for Scientific Research (NWO-CW).

Materials and Methods

Genetic mapping of the CHH region

Only Finnish CHH patients with a carefully verified diagnosis were studied for the purpose of refining the genetic map. There were 16 families with more than one affected individual (multiplex), and 42 families with one affected individual (uniplex). Several individuals per family were genotyped for 23 polymorphic markers. From each family only 2 affected haplotypes (one maternal, one paternal) were considered in the analysis. Haplotypes were constructed manually. The presumptive ancestral founding haplotype was reconstructed assuming the minimum number of historical recombinations. A measure of linkage disequilibrium between a marker and the disease phenotype (P_{excess}) is calculated using the formula

$$P_{excess} = (P_{affected} - P_{normal})/(1 - P_{normal}),$$

where $P_{affected}$ is the frequency of the allele in affected chromosomes and P_{normal} is the frequency of the allele in unaffected chromosomes (177). For these calculations most of the 116 affected haplotypes were used that were judged to descend from the putative shared major founder mutation. The corresponding normal haplotypes (n > 100 at each marker) were taken from the unaffected maternal and paternal chromosomes. The number of haplotypes (affected and normal) varied slightly between markers because of occasional uncertainty in allele assignment.

Analysis of polymorphic markers

Most of the novel polymorphic markers were found during SSCP analyses or sequencing of candidate genes in patient samples. 16P1 and AC1 were found based on the genomic BAC sequence. Primers for the SSCP markers and the genomic 13 nt deletion (Del13) were designed using the Primer 3 program at the Whitehead Institue for Biomedical Research/MIT Center for Genome Research at http://www.genome.wi.mit.edu (Table 1). Primers 5'-TCC-TTG-GAC-AAG-TAC-CAA-CA-3' and 5'-GGG-AAA-CACA-GTG-CCT-CT-3' were used for D9S1878 (http://www.cephb.fr/mail.html). Primers for the other polymorphisms were listed in Table 2 in ref (171). For the SSCP analyses, the PCR products were loaded on MDE (FMC BioProducts) gels and run overnight at room temperature (Table 1). Markers D9S1878, D9S163, D9S1804, 99AC, 89AC, and AC1 were separated in 6% Sequagel (National Diagnostics) gels at 50°C. Bands on the polyacrylamide gels were visualized by silver staining as described in detail in ref. (187).

Genomic sequencing of the CHH region

Three BAC clones (497J14, 199G9, and 468J10) from the previously assembled contig (171) covering the CHH critical region were shotgun sequenced. Libraries were prepared in pCR-BluntII-Topo vector (Invitrogen) using the GATC GmbH service (Konstanz, Germany). Forty 96-well plates were sequenced, in both directions, using the BigDye Terminator AmpliTaq FS Cycle Sequencing Kit (PE Applied Biosystems). Cycle Sequencing was performed using the PE9700 Thermal Cycler (Perkin Elmer). The cycling protocol was 30 cycles of 95°C for 30 s, 50°C for 20 s, and 60°C for 4 min. Cycling was performed using 10 µl reactions and reactions were purified by filtration plate. Custom vector primers TOPO2 5'-AGATG CATGCTCGAGCGG-3' and TOPO1 5'-TCGGATCCACTAGTAACG-3' designed by GATC GmbH, were used. Sequences were processed through a series of programs in UNIX. After quality assessment using Phred, 72% of subclone sequences were passed for use in assembling contigs using Phrap. Gap filling was performed using a combination of primer walking from the contig ends and PCR across the gaps. Primer sequences and PCR conditions are available on request. Finishing was facilitated by using MIT's Finish program (http://www.genome.wi.mit.edu). The genomic sequence of the 187.6 kb CHH region was analyzed using the Genotator program package.

Patients and controls

Mutational analyses have so far been done on 51 CHH families from Finland and 4 families from other countries. With few exceptions both parents and all affected children have been studied. In addition a small number (n=7) of unaffected children have also been studied. The diagnostic criteria were as outlined previously (165). To search for the observed sequence variants in controls, 120 anonymous blood donors from Finland, a panel of 61 control individuals of various ethnicities (Chinese, Iranian, Indian, Indonesian, South European, British, German, Danish, Dutch) and 99 grandparents of CEPH families were studied. The number of controls studied is shown for each sequence variant (Table 2).

Mutation detection in RMRP

The RMRP gene (accession no. M29916) was sequenced in four PCR fragments RM1-RM4.

The primers were: RM1F: 5'-CTG-GCA-CCC-TCA-TGG-GAG-3'; RM1R: 5'-GCA-CAC-CCA-GGT-ACC-AGC-TAG-3'; RM2F: 5'-GGA-GGA-TAC-AGG-CGA-GTC-AG-3'; RM2R: 5'-GCA-GAA-TAG-CTA-ATA-GAC-ACG-AAA-TG-3'; RM3F: 5'-GGC-CAG-ACC-ATA-TTT-GCA-TAA-G-3'; RM3R: 5'-CGG-ACT-TTG-GAG-TGG-GAA-G-3'; RM4F: 5'-AGA-GAG-TGC-CAC-GTG-CAT-AC-3'; RM4R: 5'-CTT-CAT-AGC-AAG-GCC-AAG-AAC-3'.

Primers for RM3I fragment inside RM3 were 5'-CTT-AGA-AAG-TTA-TGC-CCG-AAA-AC-3' and 5'-GAA-

AGG-GGA-GGA-ACA-GAG-TC-3'; 5% Sequagel (National Diagnostics) gels were used for separation. Deletions and insertions in the 5' region of RMRP were searched for within 1.5 kb from the M29916 sequence by running PCR fragments in 5% Sequagel (National Diagnostics) and LongRanger (FMC BioProducts) gels at 50°C. The primer sequences and PCR conditions are available on request from the authors.

Extraction and analysis of total RNA

Lymphoblast (Control-L, patient 1 and patient 2) and fibroblast (Control-F, patient 7 and patient 8) cells were pelleted and total RNA isolated using Trizol (Gibco-BRL) as suggested by the manufacturer. RNAs were resolved on 5% denaturing polyacrylamide gels and blotted to Hybond-N+ membranes (Amersham). Northern blot hybridizations with riboprobes specific for human RNase MRP, U3 snoRNA, and U1 snRNA were performed as previously described (116). Quantitative analysis of the levels of transcription was done with a Phosphorimager (Biorad).

Synthesis and Analysis of cDNA

First strand cDNA synthesis and 5' RACE were performed using a SMART RACE cDNA amplification kit (Clontech) as described by the manufacturer. For first strand synthesis MRP-1 oligo 5'-GCG-AAG-CTT-ACA-GCC-GCG-CTG-AGA-ATG-AG-3' was used. RACE was done using MRP-1 and MRP-0 5'-GCG-AAT-TCG-TTC-GTG-CTG-AAG-GCC-TAG-ATC-3') and products were cloned using the TOPO-TA cloning kit (Invitrogen) and sequenced using the dideoxynucleotide chain termination method.

Immunoprecipitation

Anti-hPop1 (77) and anti-hPop4 (120) antibodies were coupled to protein A-agarose beads (Biozym) in IPP500 (500 mM NaCl, 10 mM Tris-HCl pH 8.0, 0.05% NP-40) by incubation for 2 hr at room temperature. Beads were washed twice with IPP500 and once with IPP150 (150 mM NaCl, 10 mM Tris-HCl pH 8.0, 0.05% NP-40). For each immunoprecipitation the cell extract was incubated with the antibody-coupled beads for 2 hr at 4°C. Subsequently, beads were washed three times with IPP150. To analyze coprecipitating RNAs, the RNA was isolated by phenol-chloroform extraction and ethanol precipitation. RNAs were analyzed by northern blot hybridization as described above.

Part IV

Chapter **9**

General discussion

Abstract

The human RNase MRP complex is an RNA-protein complex functioning in the cleavage of RNA. Two substrates of this endoribonuclease have been identified sofar. The cleavage of a mitochondrial transcript into small RNA primers needed for mitochondrial DNA replication was the function by which this enzyme was first identified. A few years later it was shown that the RNase MRP complex was involved in the cleavage of precursor ribosomal RNA. The RNase MRP complex was shown to be related to the RNase P complex, an RNA-protein complex involved in the processing of precursor tRNA.

The aim of the project underlying this thesis was to characterise the composition of the RNase MRP complex, to study its assembly and to investigate its relation to certain human diseases. The results obtained in this project are described in Part I, II and III, respectively. In this Chapter, the contribution of the studies described in this thesis to our knowledge on the human RNase MRP complex will be discussed.

Novel protein components of the RNase MRP complex

In the last decade, ten proteins were shown to be associated with the RNase MRP and/or RNase P complex in yeast *Saccharomyces cerevisiae*: Pop1p, Snm1p, Pop3p, Pop4p, Rpp1p, Rpp2p/Pop7p, Pop5p, Pop6p, Pop8p and Rpr2p (32-38). Biochemical and genetic analyses have shown that all of these proteins, except Snm1p and Rpr2p, are associated with both RNase MRP and RNase P. The Snm1p protein was shown to be specifically associated with the RNase MRP complex, whereas the Rpr2p protein was found to be specifically associated with the RNase P complex (32,38).

The first protein subunit of the human RNase MRP complex was identified by virtue of its homology with the Pop1p protein component of the yeast RNase MRP/P complex (77). In Part I of this thesis the identification of two additional protein components of the human RNase MRP and RNase P complexes is described (Chapters 2 and 3, (120,140)). These two proteins, referred to as hPop4 and hPop5, were identified as the human homologues of yeast Pop4p and Pop5p, respectively. Simultaneously, the human RNase P complex has been purified in the laboratory of Dr. S. Altman, resulting in the identification and characterisation of seven additional protein subunits: Rpp14, Rpp20, Rpp25, Rpp29, Rpp30, Rpp38 and Rpp40 ((78-80), Guerrier-Takada, personal

communication). Sequence comparison showed that Rpp29 is identical to the hPop4 protein and therefore this protein will be referred to as Rpp29/hPop4 (79,120). Rpp20 represents the human homologue of Rpp2p/Pop7p and Rpp30 is homologous to Rpp1p (33,36). Recently, the human homologue of the yeast protein component that was shown to be specifically associated with the RNase P complex was identified: Rpp21 (81). Four of the identified proteins have been shown to have homologues in archae bacteria as well: hPop4, hPop5, Rpp21 and Rpp30, suggesting that these eukaryotic and archaeal proteins share a common ancestor (51,121).

To elucidate whether the recently identified human RNase P proteins are also associated with the RNase MRP complex, immunoprecipitations using rabbit antibodies raised against the RNase P proteins were performed. As shown in Figure 1, at least eight of the currently identified proteins are shared by the RNase MRP and RNase P complexes (lanes 3, 5-10, 13). Surprisingly, these results also indicate that the human homologue of the yeast protein that was found to be specifically associated with the RNase P complex (Rpr2p) is associated with both RNase P and RNase MRP (lane 9). The failure of the rabbit antisera against Rpp14 and Rpp40 to co-precipitate RNase P RNA implies that no conclusions can be drawn on their association with the RNase MRP complex. In conclusion, up to date no human proteins that are specifically associated with either RNase MRP or RNase P have been identified.

The currently described protein components of the human and yeast RNase MRP and RNase P complexes are summarised in Table I.

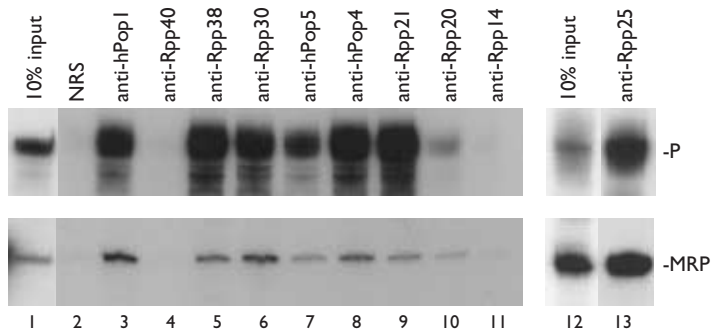

Figure 1. Association of protein subunits with RNase MRP and RNase P complexes. Immunoprecipitations were performed using antibodies raised against hPop1 (lane 3), Rpp40 (lane 4), Rpp38 (lane 5), Rpp30 (lane 6), hPop5 (lane 7), hPop4 (lane 8), Rpp21 (lane 9), Rpp20 (lane 10), Rpp14 (lanes 11) and Rpp25 (lane 13) with partially purified RNase MRP and RNase P (lanes 1-11) ((140) and our unpublished observations) or a HeLa cell extract (lanes 12 and 13). Co-precipitating RNAs and RNAs from 10% of the input fractions (lanes 1 and 12) were isolated, resolved by denaturing gel electrophoresis and analysed by northern blotting using riboprobes specific for RNase MRP and RNase P RNA (116).

The RNase MRP and P complexes in human cells differ from their yeast counterparts

Our current knowledge on the composition of the human and yeast RNase MRP and P complexes and the results from biochemical and genetic analyses of both complexes indicate that the human complexes are not simply homologues of the yeast complexes. A major difference between the human and yeast complexes concerns their protein composition. Although most of the human and yeast proteins are homologous, homologues of some of the yeast proteins do not appear to exist in human cells (i.e. Snm1p, Pop3p, Pop6p and Pop8p). Vice versa, counterparts of some human RNase MRP/RNase P proteins are not evident in yeast (e.g. Rpp14, Rpp25, Rpp38 and Rpp40). Although it can not be completely excluded that homologues of these proteins are present, but have not been identified yet, scanning of the yeast and human genomes (which have been completely sequenced) did not reveal obvious homologues, strongly suggesting that they do not exist.

Another difference between the yeast and human complexes is the existence in yeast of proteins specifically associated with either RNase MRP or RNase P, whereas these have not been identified in human. Moreover, as described above, it was found that the human homologue of the RNase P specific protein in yeast is also associated with the human RNase MRP complex and no human homologue of the yeast RNase MRP specific protein could be identified.

Furthermore, the human and yeast complexes show a different behaviour during biochemical purification. It yeast, it has been shown that the RNase MRP and RNase P activities can be physically separated using classical biochemical purification methods (30,38). In humans, separation of the majority of the RNase MRP and RNase P complexes can also be achieved, when the RNA component was used to monitor their fractionation ((80), our unpublished observations). However, a small part of the RNase MRP complex co-fractionated with the RNase P complex and RNase MRP activity could only be detected in these fractions (our unpublished observations). This suggests that active RNase MRP might exist in one large complex together with RNase P. However, our data are contradicted by the results of Karwan and co-workers, who published that both fractions of RNase MRP contained endonuclease activity (135). On the other hand, our results are supported by the findings of Lee and co-workers who showed, using RNA selections with antisense oligonucleotides, that a small fraction of the RNase MRP complex

Protein	Molecular weight (cal/app)	Predicted pI	Yeast homologue	RNase MRP •[a]	RNase P •[a]	Reference
hPop1	115/115	9.8	Pop1p	+	+	(37,77)
Rpp40	34/40	5.3		nd	+	(80)
Rpp38	32/38	9.9		+	+	(78,105, this thesis)
Rpp30	30/30	9.4	Rpp1p	+	+	(78,33,105, this thesis)
Rpp29/hPop4	25/30	10.9	Pop4p	+	+	(34,79,120, this thesis)
Rpp25	21/25	9.7		+	+	(78, Guerrier-Takada, pers. comm.)
Rpp21	18/21	9.6	Rpr2p	+/– •[b]	+	(38,81)
Rpp20	16/20	8.7	Rpp2p/Pop7p	+	+	(80,38,36)
hPop5	19/19	7.9	Pop5p	+	+	(38,140, this thesis)
Rpp14	14/14	7.6		nd	+	(79)
			Snm1p	+	–	(32)
			Pop3p	+	+	(35)
			Pop6p	+	+	(38)
			Pop8p	+	+	(38)

Table I. Composition of human RNase MRP and RNase P complexes. •[a] Association with complex is indicated by + ; no association with – ; nd: not determined. •[b] The yeast homologue of Rpp21 (Rpr2p) has been shown to associate specifically with RNase P.

forms higher order structures with the RNase P complex (57). Because the only obvious difference between the human RNase MRP and RNase P complex is the RNA component, a purification strategy based on an RNA-tag fused to the RNase MRP RNA, rather than purifications based on the biochemical features of these complexes, may solve this paradox. The RNA-tag approach will not only shed more light on whether the RNase MRP is associated with the RNase P complex but also on whether the currently identified protein subunits are associated with each individual complex or with a combined RNase MRP/RNase P complex.

Finally, recent experiments indicated that components of the RNase MRP and RNase P complexes have co-evoluted. Swapping of the P3 domain from human RNase MRP RNA with that from the yeast RNase MRP RNA showed that this hybrid RNA is not functional, suggesting that for a proper function of this complex human proteins are required (71).

In conclusion, all these data suggest that the human RNase MRP and RNase P complexes are at least partially different from the yeast enzymes.

Assembly of the human RNase MRP complex

Subcellular localisation and assembly of the RNase MRP complex

The RNase MRP and RNase P RNA are transcribed by RNA polymerase III. In-situ hybridisation experiments showed that RNase MRP and RNase P RNAs, like other RNA polymerase III products, can be detected in the so-called perinucleolar compartments (59). However, at these sites no protein subunits of the RNase MRP and RNase P complexes can be detected, suggesting that the RNase MRP and RNase P RNAs are not assembled into the mature ribonucleoproteins at these sites and that these RNAs are first relocalised in the nucleus before they are assembled (57).

It has been thought for a long time that transport of RNA-protein complexes to the nucleolus is a two-step process: first proteins are imported into the nucleoplasm, where they associate with their cognate RNA, followed by the actual transport to the nucleolus (107-109). In Chapter 4, we describe that RNase MRP/RNase P proteins are capable of entering the nucleolus independent of their association with RNA. In addition, we showed that clusters of basic residues in these proteins appear to be required for their nucleolar accumulation. Our data and recent work from other groups suggest that nucleolar localisation occurs by diffusion and retention in the nucleolus, the latter mediated by interactions with nucleolar components (Chapter 4, (188)). This idea is also supported by the observation that RNase MRP/RNase P protein subunits relocalise after shutdown of RNA polymerase I, which is responsible for the synthesis of rRNA, suggesting that the synthesis of substrate is coupled to the nucleolar accumulation of these enzymes (81). Chen and Huang showed that Rpp29/hPop4 and other factors involved in rRNA transcription and processing, shuttle between the nucleoplasm and nucleolus (188). In addition, they showed that these factors move faster when RNA polymerase I transcription in inhibited, suggesting that the lack of substrates leads to dissociation from the nucleolus and enhancement of their mobilities. The underlying mechanism of this dynamic process for the RNase MRP and other complexes is at present unclear and forms an interesting topic for future research.

Architecture of the RNase MRP complex

With the goal to identify the Th-40 autoantigen we studied the architecture of the RNase MRP complex. The Th-40 autoantigen was originally described as a 40 kDa protein that is immunoprecipitated from labelled cell extracts using patient sera that contain reactivity against RNase MRP and RNase P (68,72,73,135,136). Later, it was shown that proteins that are recognised by these patient sera bind the P3 domain of RNase MRP and RNase P RNA, suggesting that the Th-40 autoantigen is bound to the P3 domain (75,134). However, the identity of the Th-40 autoantigen was never elucidated. In Chapters 5 and 6 the identification of the Th-40 autoantigen is described and evidence that the immunoprecipitated 40 kDa protein is identical to the Rpp38 protein is presented. However, the Rpp38 protein does not bind to the P3 domain, but is associated with the central domain of the RNase MRP RNA. Recently, it was shown that Rpp38 is homologous to a ribosomal protein called L7AE, which was shown to bind a so-called Kink-turn motif present in rRNA. The observation that a Kink-turn motif is present in the central domain of RNase MRP RNA strongly suggests that this motif is involved in the association with Rpp38 (141).

This raised the question why previous data suggested that Th-40 binds to the P3 domain (75). Our data showed that two proteins associate with the P3 domain: Rpp20 and Rpp25. In addition, we obtained evidence that the Rpp20 protein interacts with the central domain as well and that the hPop1 protein needs both RNA domains to associate with the RNase MRP complex, indicating that Rpp20 and hPop1 form a molecular bridge between these two RNA domains. The observation that almost all patient sera with reactivity against RNase MRP and RNase P contain autoantibodies directed to Rpp25, strongly suggested that Rpp25 is the autoantigenic component bound to the P3 domain. The paradoxical appearance of a 40-kDa species in UV-crosslinking with the P3 domain appeared to be due to the choice of the ribonuclease applied in these experiments. RNase T1, which was applied by Yuan and coworkers, did not degrade the crosslinked RNA efficiently, thereby increasing the apparent molecular weight of the cross-linked proteins (75).

More data on the architecture of the RNase MRP complex were provided by yeast two-hybrid experiments using Rpp14, Rpp20, Rpp21, Rpp29, Rpp30, Rpp38, Rpp40 and hPop1 (82). These experiments identified two strong interactions: Rpp30 interacts with Rpp14 and Rpp40 with Rpp21. In addition, multiple weaker interactions (for example between hPop1 and Rpp38, and between Rpp20 and hPop1) were observed between the other proteins. However some of the observed interactions could not be confirmed when DNA binding and activation-domains in the yeast two-hybrid experiments were swapped, thus complicating the interpretation of these observations. Finally, preliminary results indicate that hPop5 interacts with Rpp30 (our unpublished observations). In Figure 2 a model for the RNase MRP complex based on the described RNA-protein and protein-protein interactions is presented (82).

Recently, the RNA-protein interactions in the RNase P complex were studied using a

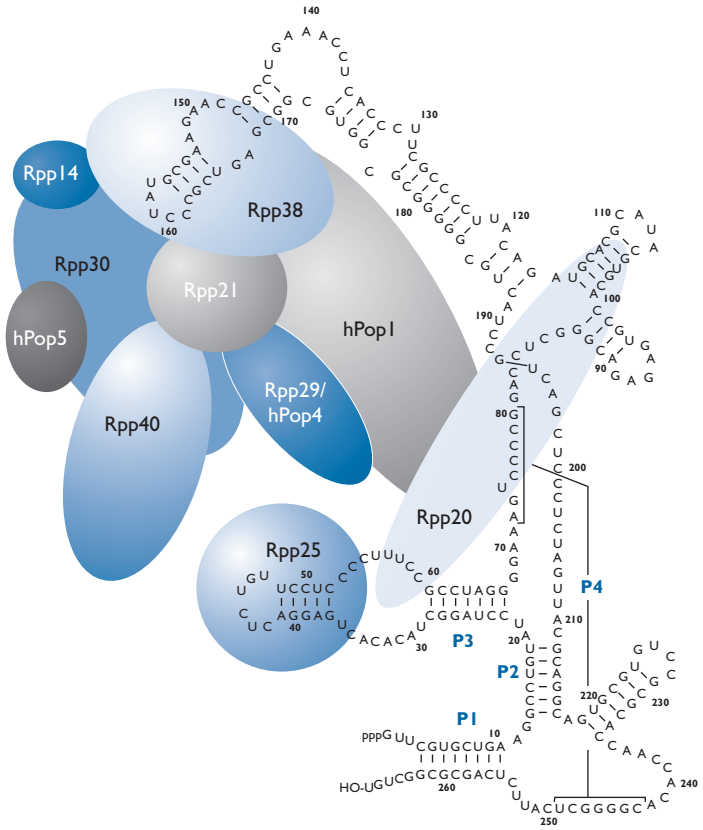

Figure 2. Structural model for the RNase MRP complex. Schematic representation of the binding of hPop1, Rpp38, Rpp25 and Rpp20 to the RNase MRP RNA. The Rpp25 and Rpp20 were shown to bind directly to the P3 domain of RNase MRP RNA (Chapter 6). The Rpp38 protein has been demonstrated to bind to the centrally located domain (Chapter 5 and 6), which was also shown for the Rpp20. The observation that hPop1 binds these two RNA domains as well, strongly suggests that the hPop1 and Rpp20 proteins form a molecular bridge between these two RNA domains. To generate this model the protein-protein interactions observed by yeast two-hybrid analyses (82) are included as well. Only interactions that were confirmed when DNA binding and activation domains were swapped were taken into account. The exact manner in which these proteins interact with each other or with the RNA is still unclear and the model depicted is just one of various possibilities.

yeast three-hybrid assay and UV-crosslinking analysis. This work shows that Rpp29/hPop4, Rpp30, Rpp21 and Rpp25 interact with the P3 domain, whereas the Rpp38 protein interacts with another part of the RNase P RNA ((86), Guerrier-Takada personal communication). How these data relate to the data obtained for the RNase MRP complex is not clear yet. The latter interactions might be typical for the human RNase P complex, although these proteins have been shown to associate with both complexes (see above).

At this moment, three proteins have been proposed to be involved in substrate binding by RNase P: hPop1, Rpp14 and Rpp21 (81,189). These proteins are the first to be implicated in actual substrate binding and/or catalysis of pre-tRNA cleavage.

RNase MRP in human disease

RNase MRP in systemic autoimmune diseases

Patients suffering from systemic autoimmune diseases frequently produce autoantibodies, which are directed to a large variety of cytoplasmic, nuclear and nucleolar autoantigens. The occurrence of these autoantibodies can be helpful in diagnosis and prognosis of the different autoimmune diseases (190). For example, anti-nucleolar reactivity has been demonstrated to occur frequently in patients suffering from systemic sclerosis ((68), reviewed in ref. (139,143,190)). Among the identified autoantigens targeted by patient sera displaying anti-nucleolar reactivity are the RNase MRP and RNase P complexes. This reactivity is referred to as anti-Th/To-specificity (61,62,64,65,68,73,136,191). Although the occurrence of anti-nucleolar reactivities including anti-Th/To autoantibodies have been reported to be specific for patients with systemic sclerosis, our analyses of 172 anti-nucleolar patients sera showed that these reactivities are also found in patients suffering from other systemic autoimmune disease like systemic lupus erythematosus and polymyositis (Chapter 7). These observations reduce the relevance of this autoantibody system for diagnostic purposes.

The Th/To autoantigen has been studied in more detail during the past decade and it has been demonstrated that a protein of 40 kDa (designated as Th-40) is the most frequently recognised autoantigenic protein (68,72,73,135,136). In Chapter 6, evidence is presented that the Th-40 autoantigen is identical to Rpp38. However, immunoprecipitations of *in vitro* translated recombinant proteins and western blot analyses showed that not Rpp38, but hPop1 and Rpp25 are the most frequently recognised Th/To autoantigens (Chapter 6). In addition, we demonstrated that some anti-Th/To patient sera (also) contained autoantibodies reactive with hPop5, Rpp14 and Rpp30. Based upon these findings, I suggest that the term Th-40 to refer to the most frequently recognised Th/To autoantigen should not be used anymore, because this is misleading. In fact, six of the ten known RNase MRP/RNase P associated proteins are frequently targeted by anti-Th/To positive patient sera. All together, these represent the Th/To autoantigen.

Although the etiology of systemic autoimmune diseases is at present unclear, it is hypothesised that modification of proteins during cell death contributes to the bypass of tolerance to 'self antigens' (reviewed in ref. (192,193)). During apoptotic or necrotic cell death most key enzymes and complexes essential for cell survival are post-translationally modified or cleaved. These modified "self" proteins translocate to the cell surface of the apoptotic cell or leak from the necrotic cell and become accessible for the immune system. Because of the modification, which may lead to a change in the tertiary structure, these antigens are not longer recognised as "self" and may trigger an autoimmune response (reviewed in ref. (192,193)). Whether the hPop1, Rpp38, Rpp30, Rpp25, hPop5 and Rpp14 proteins are modified during apoptotic or necrotic cell death remains to be determined.

RNase MRP in cartilage-hair hypoplasia

While the anti-Th/To autoantibodies proved to be extremely helpful in determining the

architecture of the RNase MRP complex, the genetic defect in the RNase MRP RNA may aid in elucidating the function(s) of the human RNase MRP. In Chapter 8 we describe the identification of mutations found in the gene encoding the RNase MRP RNA, which was shown to cause a pleiotropic disease called cartilage-hair hypoplasia (CHH). For the first time it was found that mutations in a nuclear gene encoding an untranslated RNA molecule could cause a disease. Recently, mutations in the nuclear gene encoding the telomerase RNA component were shown to cause dyskeratosis congenita, indicating that disease-causing mutations in genes encoding structural RNAs may be a more widespread phenomenon than initially thought (194).

The absence of patients homozygous for a so-called null mutation strongly suggests that RNase MRP RNA is essential for viability, as has been reported previously for yeast RNase MRP (28,29,98). The disease causing mutations in CHH are most likely leading to a (partial) functional impairment of the RNase MRP complex. A yet unresolved question is which function is impaired.

The RNase MRP complex has been implicated to function in two processes: the cleavage of a mitochondrial transcript to RNA primers that function in mitochondrial DNA replication and the cleavage of precursor rRNA at the 5'-end of 5.8S rRNA (reviewed in ref. (118)). To detect whether the mutations in the RNase MRP RNA associated with CHH had any effect on the maturation of the 5.8S rRNA, total RNA was analysed from cell lines derived from CHH patients. Analysis of the 5.8S rRNA using northern blot hybridisation did not reveal any difference in the relative abundance of 5.8S(S) and 5.8S(L) rRNA, suggesting that the maturation of 5.8S rRNA is not or hardly affected (our unpublished observations). It is unclear whether the processing of rRNA is not affected by the mutations in RNase MRP RNA or whether there is another control mechanism that regulates the relative steady-state levels of the short and long forms of 5.8S rRNA. Evidence for a direct role of RNase MRP in rRNA processing in human cells is not available, but the evolutionary conservation of the rRNA processing machinery as well as its nucleolar accumulation strongly support such a role. Therefore, it is more likely that the apparently normal expression levels of both forms of 5.8S rRNA in patient cells are due to a sufficient overall RNase MRP activity in the nucleoli of these cells, in spite of the possibly reduced activity per particle, or to a compensatory change that maintains normal expression levels. In addition to the processing of the 5.8S rRNA the mitochondrial function of the RNase MRP complex was studied in cells of patients suffering from CHH.

A first attempt to study the mitochondrial function in CHH and control cells was made by assaying the ability of the RNase MRP complex to cleave a mitochondrial RNA, spanning the mitochondrial origin of DNA replication (22,24,135). Unfortunately, these experiments did not result in conclusive data, which is probably due to the limited amount of CHH cell extracts available.

A reduction of the RNase MRP activity might decrease the efficiency of mitochondrial DNA replication, and as a result might lead to a reduced amount of mitochondrial DNA in CHH patients. However, Southern blotting analysis of total DNA showed that no significant decrease in the amount of mitochondrial DNA could be detected in CHH cells. In agreement with these observations western blotting analyses using extracts from isolated mitochondria demonstrated that proteins encoded by mitochondrial DNA were expressed to normal levels, using nuclear encoded mitochondrial proteins as an internal reference (our unpublished observations). Taken together, our preliminary data suggest that in CHH patients no obvious biochemical mitochondrial defect can be observed.

The third function that has been described for the RNase MRP complex in yeast is its involvement in the breakdown of the mitotic spindle and the closing steps of mitosis (41). As suggested before, the inhibition of such a function would negatively affect cell proliferation and thus might very well explain the growth defects and T-cell deficiencies observed in CHH patients (Chapter 8, (195)). Interestingly, the cell division rates of the available CHH patient derived cell lines are significantly lower than those of control cells. The establishment of new (better defined) cell lines of CHH patients will enable the further study of the role of RNase MRP in the cell cycle.

It should be noted that studies on the function of the RNase MRP complex using cells derived from CHH patients may be suboptimal in view of another aspect. Cartilage-hair hypoplasia is a disease that already manifests at birth, indicating that during embryogenesis a RNase MRP defect is already evident. The RNase MRP dependent process that is inhibited in the embryo can be any of the processes described above or another yet unidentified process. For example, in yeast it has been shown that depletion of RNase MRP RNA results in a different protein expression pattern, suggesting that RNase MRP somehow regulates the expression of certain proteins (29). Differential expression, mediated by RNase MRP, may in higher eukaryotes be important during embryogenesis and when abrogated by mutation in the RNA component may cause CHH.

Future perspectives

In this thesis studies on the composition and assembly of the RNase MRP complex are described. Its relevance as an autoantigen in systemic autoimmune diseases was also addressed and its functional importance was substantiated by the identification of its role in cartilage-hair hypoplasia.

Although many questions asked at the start of this project were answered, many more questions were raised by these answers.

Because the present data suggest that the RNA component is the only difference between the human RNase MRP and RNase P complexes, it will be a challenging and important task to purify the RNase MRP complex by introducing an RNA tag in the RNase MRP RNA. This may enable the selective isolation of the single RNase MRP complex and will provide information on whether the RNase MRP and RNase P complexes form one large complex or exist as two separate complexes. This approach can be also used to further explore the existence of complex specific proteins.

Another interesting area of research is the identification of protein-protein interactions in the RNase MRP complex. Although some information on this subject has been obtained using the yeast two-hybrid system, more reliable data may be generated in a mammalian two-hybrid system as well as by co-immunoprecipitation studies with recombinant proteins.

The involvement of the RNase MRP RNA in the genetic disease called cartilage-hair hypoplasia raises numerous interesting questions. New cell-lines derived from CHH patients will be essential tools before we can answer them. Such well-defined cell lines could for example be used to study proliferation rates of CHH cells and compare them with control cells. In addition, *in vivo* cell labelling followed by RNA analysis could generate information as to which RNAs are substrates for the RNase MRP complex. Identification of these substrates and developing new *in vitro* assays may contribute to the understanding of the molecular mechanism of the enzymatic activity of the RNase MRP complex.

Another approach to study the mechanism underlying cartilage-hair hypoplasia is the generation of mice in which CHH-specific mutations are introduced in the RNase MRP RNA genes and study the effects of these changes.

Samenvatting
Summary
References
List of publications
Dankwoord
Acknowledgements
Curriculum vitae

Samenvatting

Eukaryotische cellen bevatten verschillende soorten RNA, onder andere messenger RNA, transfer RNA en ribosomaal RNA. Direct na synthese van voorlopers van deze RNAs (de zgn. pre-RNAs) worden deze gekliefd en gemodificeerd. Klieving en modificatie van pre-transfer RNA en pre-ribosomaal RNA wordt gereguleerd door RNA-eiwit complexen die in de nucleolus voorkomen, de zogenaamde small nucleolar ribonucleoprotein complexes (of snoRNPs). SnoRNPs kunnen ruwweg worden ingedeeld in drie groepen: box C/D snoRNPs, box H/ACA snoRNPs en RNase MRP/RNase P.

Het RNase MRP complex is geïdentificeerd door haar betrokkenheid bij de klieving van een mitochondrieel RNA tot kleine RNA moleculen, die nodig zijn bij de synthese van het mitochondrieel DNA. Later bleek het RNase MRP complex ook betrokken te zijn bij de rijping van het nucleolaire 5.8S ribosomaal RNA.

Het RNase MRP complex bestaat uit één RNA molecuul en meerdere eiwit componenten. De RNA component van het RNase MRP complex vertoont structurele gelijkenis met de RNA component van het RNase P complex, waarvan is aangetoond dat het betrokken is bij de rijping van transfer RNA. Verder weten we dat de meeste eiwit componenten van het RNase MRP complex ook onderdeel zijn van het RNase P complex en dat patiënten die lijden aan bepaalde systemische auto-immuunziekten een afweerreactie ontwikkelen tegen een aantal van deze eiwitten.

Het doel van het onderzoek beschreven in dit proefschrift was de identificatie van nieuwe eiwit componenten van het RNase MRP complex (Deel I), het bestuderen van de opbouw van het RNase MRP complex (Deel II) en het bestuderen van de rol in humane ziekten van het RNase MRP complex (Deel III).

De algemene inleiding, Hoofdstuk 1, geeft een overzicht van de huidige kennis over de snoRNPs, met speciale aandacht voor de RNase MRP en RNase P complexen.

In Deel I worden enkele nieuwe eiwit componenten van het RNase MRP complex gepresenteerd. De Hoofdstukken 2 en 3 behandelen de identificatie en karakterisatie van de humane homologen van de gist Pop4 en Pop5 eiwitten. Beide eiwitten blijken zowel in het RNase MRP als het RNase P complex aanwezig te zijn.

Deel II bevat enkele studies over de assemblage van het RNase MRP complex. In Hoofdstuk 4 is met behulp van mutagenese en transfectie studies de subcellulaire lokalisatie van drie eiwitten geanalyseerd. Positief geladen domeinen in deze eiwitten blijken belangrijk te zijn voor hun accumulatie in de nucleolus. Deze eiwitten blijken ook onafhankelijk van associatie met het RNase MRP complex naar de nucleolus te kunnen migreren. Onze resultaten suggereren dat nucleolaire accumulatie van deze eiwitten via diffusie en retentie plaatsvindt. In de Hoofdstukken 5 en 6 worden data beschreven die de basis vormen voor een model van de architectuur van het RNase MRP

complex. Het Rpp38 eiwit blijkt een centraal domein van het RNase MRP RNA te binden, terwijl Rpp25 associeert met het zogenaamde P3 domein van het RNase MRP RNA. De hPop1 en Rpp20 eiwitten blijken beide domeinen nodig te hebben. Verder werd bestudeerd welke RNase MRP/P eiwitten herkend worden door patiënten sera die reactiviteit tegen de RNase MRP/RNase P complexen bevatten. Hieruit bleek dat Rpp25 en hPop1 het meest frequent herkend worden door patienten auto-antlichamen. We konden ook aantonen dat Rpp38 identiek is aan het zgn. Th-40 auto-antigen.

In Deel III is de relatie tussen het RNase MRP complex en bepaalde humane ziekten bestudeerd. In Hoofdstuk 7 wordt de klinische relevantie van auto-antilichamen tegen snoRNPs bestudeerd. Analyses van patiënten sera die reactiviteit tegen nucleolaire componenten vertonen, tonen aan dat anti-nucleolaire auto-antilichamen niet alleen voorkomen bij sclerodermie, zoals voorheen gedacht werd. Deze analyses hebben tevens tot identificatie van nieuwe auto-antilichaam specificiteiten geleid, gericht tegen ofwel box C/D ofwel box H/ACA snoRNPs in het algemeen of exclusief tegen de U3 of U8 snoRNPs. In Hoofdstuk 8 wordt de relatie van het RNase MRP RNA met een genetische ziekte, cartilage-hair hypoplasie genaamd, beschreven. Voor het eerst blijkt een genetische ziekte te worden veroorzaakt door een mutatie in een niet getransleerd gen dat door DNA in de kern gecodeerd wordt. Twee soorten mutaties zijn gevonden in patiënten die lijden aan cartilage-hair hypoplasie: een insertie/duplicatie in de promoter van het gen, wat een uitschakeling van dat gen tot gevolg heeft, of een substitutie in de coderende sequentie, wat tot de productie van een gemuteerd RNase MRP RNA leidt.

In het laatste hoofdstuk (Hoofdstuk 9) worden de resultaten verkregen binnen dit project bediscussieerd.

Summary

Eukaryotic cells contain several classes of RNA: messenger RNA, transfer RNA and ribosomal RNA. After transcription of these RNAs, cleavages and modifications have to occur to generate the mature RNAs. The cleavage and modification of transfer RNA and ribosomal RNA is mediated by RNA-protein complexes that are primarily found in the nucleolus. These complexes which are designated small nucleolar ribonucleoprotein particles (snoRNPs). SnoRNPs can roughly be divided into three groups: box C/D snoRNPs, box H/ACA snoRNPs and RNase MRP/RNase P.

Originally, the RNase MRP complex has been identified by virtue of its capacity to cleave a mitochondrial transcript to small RNA molecules that function in the priming of mitochondrial DNA synthesis. However, the RNase MRP complex also functions in the maturation of the 5'-end of the 5.8S ribosomal RNA, which occurs in the nucleolus.

The RNase MRP complex contains one RNA molecule and several protein components. The RNA component of the RNase MRP complex displays structural similarity to the RNA component of the RNase P complex, which has been shown to function in the cleavage of precursor transfer RNAs. In addition, it has been demonstrated that most of the protein subunits associated with the RNase MRP complex are also present in the RNase P complex and that patients suffering from certain systemic autoimmune diseases develop an autoimmune response directed to some of these proteins.

The goal of the research underlying this thesis was to identify new protein components of the RNase MRP complex (Part I), to obtain information on the architecture of the RNase MRP complex (Part II) and to study the autoantigenicity of the RNase MRP complex in systemic autoimmune diseases (Part III).

The general introduction presented in Chapter 1 reviews our current knowledge on snoRNPs with emphasis on the RNase MRP and RNase P complexes.

In Part I the identification of new protein subunits of the human RNase MRP and RNase P complexes is presented. In Chapters 2 and 3 the identification and characterisation of the human homologues of the yeast Pop4 and Pop5 proteins is described. These proteins are associated with both the RNase MRP and RNase P complexes.

Part II contains various data on the assembly of the RNase MRP complex. First (Chapter 4) the subcellular localisation was studied by mutagenesis and transfection studies of three protein components of the RNase MRP complex. Basic domains of these proteins appeared to be important for their nucleolar accumulation, which appeared to proceed independently of complex association. These data led to the hypothesis that proteins are accumulating in the nucleolus by a mechanism of diffusion and retention. In Chapters 5 and 6 data are described that provide the basis for a model of the architecture of the RNase MRP complex. It was found that Rpp38 binds to a centrally

located domain, that Rpp25 binds to the P3 domain, whereas hPop1 and Rpp20 are associated with both domains of the RNase MRP RNA. In addition, the reactivity of patient sera that recognise the RNase MRP and RNase P complexes with individual proteins was tested. The results indicated that the Rpp25 and hPop1 proteins are most frequently targeted by the autoantibodies of these patients. We also showed that Rpp38 is identical to the so-called Th-40 autoantigen

In Part III we studied relations between the RNase MRP complex and some human diseases. In Chapter 7 the clinical relevance of the detection of autoantibodies directed to snoRNPs was studied. Analyses of patient sera showing antinucleolar reactivity showed that this reactivity is not specifically associated with systemic sclerosis, as has been thought before, but can also be found in other systemic autoimmune diseases. Novel autoantibody reactivities specifically directed against either box C/D or box H/ACA snoRNPs or exclusively against the U3 or U8 snoRNPs were identified. In Chapter 8 the intriguing role of the RNase MRP RNA in a genetic disorder, called cartilage-hair hypoplasia, is described. For the first time it was found that mutations in a nuclear gene encoding an untranslated RNA molecule can cause a disease. Patients suffering from cartilage-hair hypoplasia may contain two types of mutations in this gene: an insertion/duplication in the promoter region, leading to abrogation of transcription, or substitutions in the coding region, leading to the expression of a mutated RNase MRP RNA. The latter mutations impair an as yet unidentified function of the RNase MRP complex.

In the last chapter (Chapter 9) of this thesis the results obtained in this project are discussed.

References

1. Eichler DC, Craig N (1994) Processing of eukaryotic ribosomal RNA. *Prog. Nucleic Acid Res. Mol. Biol.* **49**: 197-239.
2. Maden BE (1990) The numerous modified nucleotides in eukaryotic ribosomal RNA. *Prog. Nucleic Acid Res. Mol. Biol.* **39**: 241-303.
3. Balakin AG, Smith L, Fournier MJ (1996) The RNA world of the nucleolus: two major families of small RNAs defined by different box elements with related functions. *Cell* **86**: 823-834.
4. Tollervey D (1996) Trans-acting factors in ribosome synthesis. *Exp. Cell Res.* **229**: 226-232.
5. Tollervey D, Kiss T (1997) Function and synthesis of small nucleolar RNAs. *Current Opinion In Cell Biology* **9**: 337-342.
6. Kiss-Laszlo Z, Henry Y, Bachellerie JP, Caizergues-Ferrer M, Kiss T (1996) Site-specific ribose methylation of preribosomal RNA: a novel function for small nucleolar RNAs. *Cell* **85**: 1077-1088.
7. Kiss-Laszlo Z, Henry Y, Kiss T (1998) Sequence and structural elements of methylation guide snoRNAs essential for site-specific ribose methylation of pre-rRNA. *EMBO J* **17**: 797-807.
8. Tycowski KT, Shu MD, Steitz JA (1996) A mammalian gene with introns instead of exons generating stable RNA products. *Nature* **379**: 464-466.
9. Cavaille J, Nicoloso M, Bachellerie JP (1996) Targeted ribose methylation of RNA *in vivo* directed by tailored antisense RNA guides. *Nature* 383: 732-735.
10. Lowe TM, Eddy SR (1999) A computational screen for methylation guide snoRNAs in yeast. *Science* **283**: 1168-1171.
11. Huttenhofer A, Kiefmann M, Meier-Ewert S, O'Brien J, Lehrach H, Bachellerie JP, Brosius J (2001) RNomics: an experimental approach that identifies 201 candidates for novel, small, non-messenger RNAs in mouse. *EMBO J* **20**: 2943-2953.
12. Maxwell ES, Fournier MJ (1995) The small nucleolar RNAs. *Annu. Rev. Biochem.* **64**: 897-934.
13. Aris JP, Blobel G (1991) cDNA cloning and sequencing of human fibrillarin, a conserved nucleolar protein recognized by autoimmune antisera. *Proc. Natl. Acad. Sci. USA* **88**: 931-935.
14. Newman DR, Kuhn JF, Shanab GM, Maxwell ES (2000) Box C/D snoRNA-associated proteins: two pairs of evolutionarily ancient proteins and possible links to replication and transcription. *RNA* **6**: 861-879.
15. Lyman SK, Gerace L, Baserga SJ (1999) Human Nop5/Nop58 is a component common to the box C/D small nucleolar ribonucleoproteins. *RNA* **5**: 1597-1604.
16. Wang H, Boisvert D, Kim KK, Kim R, Kim SH (2000) Crystal structure of a fibrillarin homologue from *Methanococcus jannaschii*, a hyperthermophile, at 1.6 Å resolution. *EMBO J* **19**: 317-323.
17. Ganot P, Caizergues-Ferrer M, Kiss T (1997) The family of box ACA small nucleolar RNAs is defined by an evolutionarily conserved secondary structure and ubiquitous sequence elements essential for RNA accumulation. *Genes Dev.* **11**: 941-956.
18. Meier UT, Blobel G (1994) NAP57, a mammalian nucleolar protein with a putative homolog in yeast and bacteria. *J Cell Biol.* **127**: 1505-1514.
19. Dragon F, Pogacic V, Filipowicz W (2000) *In vitro* assembly of human H/ACA small nucleolar RNPs reveals unique features of U17 and telomerase RNAs. *Mol. Cell Biol.* **20**: 3037-3048.
20. Pogacic V, Dragon F, Filipowicz W (2000) Human H/ACA small nucleolar RNPs and telomerase share evolutionarily conserved proteins NHP2 and NOP10. *Mol. Cell Biol.* **20**: 9028-9040.
21. Lafontaine DL, Bousquet-Antonelli C, Henry Y, Caizergues-Ferrer M, Tollervey D (1998) The box H + ACA snoRNAs carry Cbf5p, the putative rRNA pseudouridine synthase. *Genes Dev.* **12**: 527-537.
22. Chang DD, Clayton DA (1987) A novel endoribonuclease cleaves at a priming site of mouse mitochondrial DNA replication. *EMBO J.* **6**: 409-417.
23. Lecrenier N, Foury F (2000) New features of mitochondrial DNA replication system in yeast and man. *Gene* **246**: 37-48.
24. Lee DY, Clayton DA (1997) RNase mitochondrial RNA processing correctly cleaves a novel R loop at the mitochondrial DNA leading-strand origin of replication. *Genes Dev.* **11**: 582-592.
25. Lee DY, Clayton DA (1998) Initiation of mitochondrial DNA replication by transcription and R-loop processing. *J Biol. Chem.* **273**: 30614-30621.
26. Chang DD, Clayton DA (1987) A mammalian mitochondrial RNA processing activity contains nucleus-encoded RNA. *Science* **235**: 1178-1184.
27. Chang DD, Clayton DA (1989) Mouse RNAase MRP RNA is encoded by a nuclear gene and contains a decamer sequence complementary to a conserved region of mitochondrial RNA substrate. *Cell* **56**: 131-139.

28. Chu S, Archer RH, Zengel JM, Lindahl L (1994) The RNA of RNase MRP is required for normal processing of ribosomal RNA. *Proc. Natl. Acad. Sci. USA*. **91**: 659-663.
29. Schmitt ME, Clayton DA (1993) Nuclear RNase MRP is required for correct processing of pre-5.8S rRNA in *Saccharomyces cerevisiae*. *Mol. Cell Biol*. **13**: 7935-7941.
30. Lygerou Z, Allmang C, Tollervey D, Seraphin B (1996) Accurate processing of a eukaryotic precursor ribosomal RNA by ribonuclease MRP in vitro. *Science* **272**: 268-270.
31. Shadel GS, Buckenmeyer GA, Clayton DA, Schmitt ME (2000) Mutational analysis of the RNA component of *Saccharomyces cerevisiae* RNase MRP reveals distinct nuclear phenotypes. *Gene* **245**: 175-184.
32. Schmitt ME, Clayton DA (1994) Characterization of a unique protein component of yeast RNase MRP: an RNA-binding protein with a zinc-cluster domain. *Genes Dev*. **8**: 2617-2628.
33. Stolc V, Altman S (1997) Rpp1, an essential protein subunit of nuclear RNase P required for processing of precursor tRNA and 35S precursor rRNA in *Saccharomyces cerevisiae*. *Genes Dev*. **11**: 2926-2937.
34. Chu S, Zengel JM, Lindahl L (1997) A novel protein shared by RNase MRP and RNase P. RNA **3**: 382-391.
35. Dichtl B, Tollervey D (1997) Pop3p is essential for the activity of the RNase MRP and RNase P ribonucleoproteins *in vivo*. *EMBO J*. **16**: 417-429.
36. Stolc V, Katz A, Altman S (1998) Rpp2, an essential protein subunit of nuclear RNase P, is required for processing of precursor tRNAs and 35S precursor rRNA in *Saccharomyces cerevisiae*. *Proc. Natl. Acad. Sci. USA*. **95**: 6716-6721.
37. Lygerou Z, Mitchell P, Petfalski E, Seraphin B, Tollervey D (1994) The POP1 gene encodes a protein component common to the RNase MRP and RNase P ribonucleoproteins. *Genes Dev*. **8**: 1423-1433.
38. Chamberlain JR, Lee Y, Lane WS, Engelke DR (1998) Purification and characterization of the nuclear RNase P holoenzyme complex reveals extensive subunit overlap with RNase MRP. *Genes Dev*. **12**: 1678-1690.
39. Henry Y, Wood H, Morrissey JP, Petfalski E, Kearsey S, Tollervey (1994) The 5′ end of yeast 5.8S rRNA is generated by exonucleases from an upstream cleavage site. *EMBO J* **13**: 2452-2463.
40. Chen XJ, Clark-Walker GD (2000) The *petite* mutation in yeasts: 50 years on. *Int. Rev. Cytol*. **194**: 197-238.
41. Cai T, Reilly TR, Cerio M, Schmitt ME (1999) Mutagenesis of SNM1, which encodes a protein component of the yeast RNase MRP, reveals a role for this ribonucleoprotein endoribonuclease in plasmid segregation. *Mol. Cell Biol*. **19**: 7857-7869.
42. Li K, Smagula CS, Parsons WJ, Richardson JA, Gonzalez M, Hagler HK, Williams RS (1994) Subcellular partitioning of MRP RNA assessed by ultrastructural and biochemical analysis. *J Cell Biol*. **124**: 871-882.
43. Puranam RS, Attardi G (2001) The RNase P associated with HeLa cell mitochondria contains an essential RNA component identical in sequence to that of the nuclear RNase P. *Mol. Cell Biol*. **21**: 548-561.
44. Jacobson MR, Cao LG, Wang YL, Pederson T (1995) Dynamic localization of RNase MRP RNA in the nucleolus observed by fluorescent RNA cytochemistry in living cells. *J Cell Biol*. **131**: 1649-1658.
45. Robertson HD, Altman S, Smith JD (1972) Purification and properties of a specific Escherichia coli ribonuclease which cleaves a tyrosine transfer ribonucleic acid presursor. *J Biol.Chem*. **247**: 5243-5251.
46. Stark BC, Kole R, Bowman EJ, Altman S (1978) Ribonuclease P: an enzyme with an essential RNA component. *Proc. Natl. Acad. Sci. USA*. **75**: 3717-3721.
47. Reed RE, Baer MF, Guerrier TC, Donis KH, Altman S (1982) Nucleotide sequence of the gene encoding the RNA subunit (M1 RNA) of ribonuclease P from *Escherichia coli*. *Cell* **30**: 627-636.
48. Hansen FG, Hansen EB, Atlung T (1985) Physical mapping and nucleotide sequence of the rnpA gene that encodes the protein component of ribonuclease P in Escherichia coli. *Gene* **38**: 85-93.
49. Kole R, Baer MF, Stark BC, Altman S (1980) *E. coli* RNAase P has a required RNA component. *Cell* **19**: 881-887.
50. Guerrier-Takada C, Gardiner K, Marsh T, Pace N, Altman S (1983) The RNA moiety of ribonuclease P is the catalytic subunit of the enzyme. *Cell* **35**: 849-857.
51. Altman S, Gopalan V, Vioque A (2000) Varieties of RNase P: a nomenclature problem? *RNA* **6**: 1689-1694.
52. Xiao S, Houser-Scott F, Engelke DR (2001) Eukaryotic ribonuclease P: increased complexity to cope with the nuclear pre-tRNA pathway. *J Cell Physiol*. **187**: 11-20.
53. Wolin SL, Matera AG (1999) The trials and travels of tRNA. *Genes Dev*. **13**:1-10.
54. Rossmanith W, Tullo A, Potuschak T, Karwan R, Sbisa E (1995) Human mitochondrial tRNA processing. *J. Biol. Chem*. **270**: 12885-12891.
55. Rossmanith W, Karwan RM (1998) Characterization of human mitochondrial RNase P: novel aspects in tRNA processing. *Biochem. Biophys. Res. Commun*. **247**: 234-241.
56. Chamberlain JR, Pagan Ramos, Kindelberger DW, Engelke DR (1996) An RNase P RNA subunit mutation affects ribosomal RNA processing. *Nucleic Acids Res*. **24:** 3158-3166.
57. Lee B, Matera AG, Ward DC, Craft J (1996) Association of RNase mitochondrial RNA processing enzyme with ribonuclease P in higher ordered structures in the nucleolus: a possible coordinate role in ribosome biogenesis. *Proc. Natl. Acad. Sci. USA*. **93**: 11471-11476.
58. Jacobson MR, Cao LG, Taneja K, Singer RH, Wang YL, Pederson T (1997) Nuclear domains of the RNA subunit of RNase P. *J. Cell Sci*. **110**: 829-837.
59. Matera AG, Frey MR, Margelot K, Wolin SL (1995) A perinucleolar compartment contains several RNA polymerase III transcripts as well as the polypyrimidine tract-binding protein, hnRNP I. *J Cell Biol*. **129**: 1181-1193.
60. Bertrand E, Houser Scott F, Kendall A, Singer RH, Engelke DR (1998) Nucleolar localization of early tRNA processing. *Genes Dev*. **12**: 2463-2468.
61. Gold HA, Craft J, Hardin JA, Bartkiewicz M, Altman S (1988) Antibodies in human serum that precipitate ribonuclease P. *Proc. Natl. Acad. Sci. USA*. **85**: 5483-5487.
62. Reddy R, Tan EM, Henning D, Nohga K, Busch H (1983) Detection of a nucleolar 7-2 ribonucleoprotein and a cytoplasmic 8-2 ribonucleoprotein with autoantibodies from patients with scleroderma. *J Biol. Chem*. **258**: 1383-1386.
63. Bartkiewicz M, Gold H, Altman S (1989) Identification and characterization of an RNA molecule that copurifies with RNase P activity from HeLa cells. *Genes Dev*. **3**: 488-499.
64. Gold HA, Topper JN, Clayton DA, Craft J (1989) The RNA processing enzyme RNase MRP is identical to the Th RNP and related to RNase P. *Science* **245**: 1377-1380.
65. Hashimoto C, Steitz JA (1983) Sequential association of nucleolar 7-2 RNA with two different autoantigens. *J Biol. Chem*. **258**: 1379-1382.
66. Topper JN, Clayton DA (1990) Characterization of human MRP/Th RNA and its nuclear gene: full length MRP/Th RNA is an active endoribonuclease when assembled as an RNP. *Nucleic Acids Res*. **18**: 793-799.
67. Okano Y, Medsger TAJ (1990) Autoantibody to Th ribonucleoprotein (nucleolar 7-2 RNA protein particle) in patients with systemic sclerosis. *Arthritis Rheum*. **33**: 1822-1828.
68. Kipnis RJ, Craft J, Hardin JA (1990) The analysis of antinuclear and antinucleolar autoantibodies of scleroderma by radioimmunoprecipitation assays. *Arthritis Rheum*. **33**: 1431-1437.
69. Forster AC, Altman S (1990) Similar cage-shaped structures for the RNA components of all ribonuclease P and ribonuclease MRP enzymes. *Cell* **62**: 407-409.
70. Schmitt ME, Bennett JL, Dairaghi DJ, Clayton DA (1993) Secondary structure of RNase MRP RNA as predicted by phylogenetic comparison. *FASEB J* **7**: 208-213.
71. Lindahl L, Fretz S, Epps N, Zengel JM (2000) Functional equivalence of hairpins in the RNA subunits of RNase MRP and RNase P in *Saccharomyces cerevisiae*. *RNA* **6**: 653-658.
72. Reimer G, Raska I, Scheer U, Tan EM (1988) Immunolocalization of 7-2-ribonucleoprotein in the granular component of the nucleolus. *Exp. Cell Res*. **176**: 117-128.
73. Karwan RM (1998) Further characterization of human RNase MRP/RNase P and related autoantibodies. *Mol. Biol. Rep*. **25**: 95-101.
74. Mamula MJ, Baer M, Craft J, Altman S (1989) An immunological determinant of RNase P protein is conserved between *Escherichia coli* and humans. *Proc. Natl. Acad. Sci. USA*. **86**: 8717-8721.
75. Yuan Y, Tan E, Reddy R (1991) The 40-kilodalton to autoantigen associates with nucleotides 21 to 64 of human mitochondrial RNA processing/7-2 RNA in vitro. *Mol. Cell Biol*. **11**: 5266-5274.
76. Reddy R, Shimba S (1995) Structural and functional similarities between MRP and RNase P. *Mol. Biol. Rep*. **22**: 81-85.
77. Lygerou Z, Pluk H, van Venrooij WJ, Seraphin B (1996) hPop1: an autoantigenic protein subunit shared by the human RNase P and RNase MRP ribonucleoproteins. *EMBO J*. **15**: 5936-5948.
78. Eder PS, Kekuda R, Stolc V, Altman S (1997) Characterization of two scleroderma autoimmune antigens that copurify with human Ribonuclease P. *Proc. Natl. Acad. Sci. USA*. **94**: 1101-1106.
79. Jarrous N, Eder PS, Wesolowski D, Altman S (1999) Rpp14 and Rpp29, two protein subunits of human ribonuclease P. *RNA* **5**: 153-157.
80. Jarrous N, Eder PS, Guerrier Takada C, Hoog C, Altman S (1998) Autoantigenic properties of some protein subunits of catalytically active complexes of human ribonuclease P. *RNA* **4**: 407-417.
81. Jarrous N, Reiner R, Wesolowski D, Mann H, Guerrier-Takada C, Altman S (2001) Function and subnuclear distribution of Rpp21, a protein subunit of the human ribonucleoprotein ribonuclease P. *RNA* **7**: 1153-1164.
82. Jiang T, Altman S (2001) Protein-protein interactions with subunits of human nuclear RNase P. *Proc. Natl. Acad. Sci. USA*. **98**: 920-925.
83. Jarrous N, Wolenski JS, Wesolowski D, Lee C, Altman S (1999) Localization in the nucleolus and coiled bodies of protein subunits of the ribonucleoprotein ribonuclease P. *J Cell Biol*. **146**: 559-571.
84. Li Y, Altman S (2001) A subunit of human nuclear RNase P has ATPase activity. *Proc. Natl. Acad. Sci. USA*. **98**: 441-444.
85. Ziehler WA, Morris J, Scott FH, Millikin C, Engelke DR (2001) An essential protein-binding domain of nuclear RNase P RNA. *RNA* **7**: 565-575.
86. Jiang T, Guerrier-Takada C, Altman S (2001) Protein-RNA interactions in the subunits of human nuclear RNase P. *RNA* **7**: 937-941.
87. Weinstein LB, Steitz JA (1999) Guided tours: from precursor snoRNA to functional snoRNP. *Curr. Opin. Cell Biol*. **11**: 378-384.
88. Shadel GS, Clayton DA (1997) Mitochondrial DNA maintenance in vertebrates. *Annu. Rev. Biochem* **66**: 409-435.
89. Venema J, Tollervey D (1999) Ribosome synthesis in *Saccharomyces cerevisiae*. *Annu. Rev. Genet*. **33**: 261-311.
90. Pitulle C, Garcia-Paris M, Zamudio KR, Pace NR (1998) Comparative structure analysis of vertebrate ribonuclease P RNA. *Nucleic Acids Res*. **26**: 3333-3339.

91. Frank DN, Adamidi C, Ehringer MA, Pitulle C, Pace NR (2000) Phylogenetic-comparative analysis of the eukaryal ribonuclease P RNA. *RNA* **6**: 1895-1904.
92. Bachellerie JP, Cavaille J (1997) Guiding ribose methylation of rRNA. *Trends Biochem. Sci.* **22**: 257-261.
93. Peculis B (1997) RNA processing: pocket guides to ribosomal RNA. *Curr. Biol.* **7**: 480-482.
94. Tollervey D (1996) Genetic and biochemical analyses of yeast RNase MRP. *Mol. Biol. Rep.* **22**: 75-79.
95. Yuan Y, Singh R, Reddy R (1989) Rat nucleolar 7-2 RNA is homologous to mouse mitochondrial RNase mitochondrial RNA-processing RNA. *J Biol. Chem.* **264**: 14835-14839.
96. Dairaghi DJ, Clayton DA (1993) Bovine RNase MRP cleaves the divergent bovine mitochondrial RNA sequence at the displacement-loop region. *J Mol. Evol.* **37**: 338-346.
97. Bennett JL, Jeong Yu S, Clayton DA (1992) Characterization of a *Xenopus laevis* ribonucleoprotein endoribonuclease. Isolation of the RNA component and its expression during development. *J Biol. Chem.* **267**: 21765-21772.
98. Schmitt ME, Clayton DA (1992) Yeast site-specific ribonucleoprotein endoribonuclease MRP contains an RNA component homologous to mammalian RNase MRP RNA and essential for cell viability. *Genes Dev.* **6**: 1975-1985.
99. Kiss T, Marshallsay C, Filipowicz W (1992) 7-2/MRP RNAs in plant and mammalian cells: association with higher order structures in the nucleolus. *EMBO J* **11**: 3737-3746.
100. Altman S, Kirsebom L, Talbot S (1993) Recent studies of ribonuclease P. *FASEB J.* **7**: 7-14.
101. Chamberlain JR, Tranguch AJ, Pagan Ramos E, Engelke DR (1996) Eukaryotic nuclear RNase P: structures and functions. Prog. *Nucleic Acid Res. Mol. Biol.* **55**: 87-119.
102. Morrissey JP, Tollervey D (1995) Birth of the snoRNPs: the evolution of RNase MRP and the eukaryotic pre-rRNA-processing system. *Trends Biochem. Sci.* **20**: 78-82.
103. Reilly TH, Schmitt ME (1995) The yeast, *Saccharomyces cerevisiae*, RNase P/MRP ribonucleoprotein endoribonuclease family. *Mol. Biol. Rep.* **22**: 87-93.
104. Hardin JA, Rahn DR, Shen C, Lerner MR, Wolin SL, Rosa MD, Steitz JA (1982) Antibodies from patients with connective tissue diseases bind specific subsets of cellular RNA-protein particles. *J Clin. Invest.* **70**: 141-147.
105. Pluk, H., van Eenennaam, H., Rutjes, S. A., Pruijn, G. J. M., and van Venrooij, W. J. (1999) RNA-protein interactions in the human RNase MRP Ribonucleoprotein complex. *RNA* **5**: 512-524.
106. Kreis TE (1986) Microinjected antibodies against the cytoplasmic domain of vesicular stomatitis virus glycoprotein block its transport to the cell surface. *EMBO J* **5**: 931-941.
107. Girard JP, Bagni C, Caizergues Ferrer M, Amalric F, Lapeyre B (1994) Identification of a segment of the small nucleolar ribonucleoprotein-associated protein GAR1 that is sufficient for nucleolar accumulation. *J Biol. Chem.* **269**: 18499-18506.
108. Schmidt Zachmann MS, Nigg EA (1993) Protein localization to the nucleolus: a search for targeting domains in nucleolin. *J Cell Sci.* **105**: 799-806.
109. Yan C, Melese T (1993) Multiple regions of NSR1 are sufficient for accumulation of a fusion protein within the nucleolus. *J Cell Biol.* **123**:1081-1091
110. Li K, Smagula CS, Parsons WJ, Richardson JA, Gonzalez M, Hagler HK, Williams RS (1994) Subcellular partitioning of MRP RNA assessed by ultrastructural and biochemical analysis. *J Cell Biol.* **124**: 871-882.
111. Altschul SF, Madden TL, Schaffer AA, Zhang J, Zhang Z, Miller W, Lipman DJ (1997) Gapped BLAST and PSI-BLAST: a new generation of protein database search programs. *Nucleic Acids Res.* **25**: 3389-3402.
112. Sillekens PT, Habets WJ, Beijer RP, van Venrooij WJ (1987) cDNA cloning of the human U1 snRNA-associated A protein: extensive homology between U1 and U2 snRNP-specific proteins. *EMBO J* **6**: 3841-3848.
113. Pluk H, Soffner J, Luhrmann R, van Venrooij WJ (1998) cDNA cloning and characterization of the human U3 small nucleolar ribonucleoprotein complex-associated 55-kilodalton protein. *Mol. Cell Biol.* **18**: 488-498.
114. Frangioni JV, Neel BG (1993) Solubilization and purification of enzymatically active glutathione S-transferase (pGEX) fusion proteins. *Anal. Biochem.* **210**: 179-187.
115. Harlow E, Lane D (1988) Antibodies: A laboratory manual. *Cold Spring Harbor Laboratory Press, Cold Spring Harbor, New York.*
116. Verheijen R, Wiik A, De Jong BA, Hoier Madsen M, Ullman S, Halberg P, van Venrooij WJ (1994) Screening for autoantibodies to the nucleolar U3- and Th(7-2) ribonucleoproteins in patients' sera using antisense riboprobes. *J Immunol. Methods* **169**: 173-182.
117. Krupp G, Cherayil B, Frendewey D, Nishikawa S, Soll D (1986) Two RNA species co-purify with RNase P from the fission yeast *Schizosaccharomyces pombe*. *EMBO J* **5**: 1697-1703.
118. van Eenennaam H, Jarrous N, van Venrooij WJ, Pruijn GJM (2000) Architecture and function of the human endonucleases RNase P and RNase MRP. *IUBMB LIFE* **49**: 265-272.
119. Ridanpää M, van Eenennaam H, Pelin K, Chadwick R, Johnson C, Yuan B, vanVenrooij W, Pruijn G, Salmela R, Rockas S, Makitie O, Kaitila I, de la Chapelle A (2001) Mutations in the RNA Component of RNase MRP Cause a Pleiotropic Human Disease, Cartilage-Hair Hypoplasia. *Cell* **104**: 195-203.
120. van Eenennaam H, Pruijn GJ, van Venrooij WJ (1999) hPop4: a new protein subunit of the human RNase MRP and RNase P ribonucleoprotein complexes. *Nucleic Acids Res.* **27**: 2465-2472.
121. Koonin EV, Wolf YI, Aravind L (2001) Prediction of the archaeal exosome and its connections with the proteasome and the translation and transcription machineries by a comparative-genomic approach. *Genome Res.* **11**: 240-252.
122. Collins LJ, Moulton V, Penny D (2000) Use of RNA secondary structure for studying the evolution of RNase P and RNase MRP. *J Mol. Evol.* **51**: 194-204.
123. van Eenennaam H, van der Heijden A, Janssen RJ, van Venrooij WJ, Pruijn GJ (2001) Basic domains target protein subunits of the RNase MRP complex to the nucleolus independently of complex association. *Mol. Biol. Cell* **12**: 3680-3689.
124. Gall JG (2000) Cajal bodies: the first 100 years. *Annu. Rev. Cell Dev. Biol.* **16**: 273-300.
125. Calado A, Kutay U, Kuhn U, Wahle E, Carmo-Fonseca M (2000) Deciphering the cellular pathway for transport of poly(A)-binding protein II. *RNA* **6**: 245-256.
126. Hebert MD, Matera AG (2000) Self-association of coilin reveals a common theme in nuclear body localization. *Mol. Biol. Cell* **11**: 4159-4171.
127. Liu JL, Lee LF, Ye Y, Qian Z, Kung HJ (1997) Nucleolar and nuclear localization properties of a herpesvirus bZIP oncoprotein, MEQ. *J Virol.* **71**: 3188-3196.
128. Rowland RR, Kervin R, Kuckleburg C, Sperlich A, Benfield DA (1999) The localization of porcine reproductive and respiratory syndrome virus nucleocapsid protein to the nucleolus of infected cells and identification of a potential nucleolar localization signal sequence. *Virus Res.* **64**:1-12.
129. Meetei AR, Ullas KS, Rao MR (2000) Identification of two novel zinc finger modules and nuclear localization signal in rat spermatidal protein TP2 by site-directed mutagenesis. *J Biol. Chem.* **275**: 38500-38507.
130. Thebault S, Basbous J, Gay B, Devaux C, Mesnard JM (2000) Sequence requirement for the nucleolar localization of human I-mfa domain-containing protein (HIC p40). *Eur. J Cell. Biol.* **79**: 834-838.
131. Smith CM, Steitz JA (1997) Sno storm in the nucleolus: new roles for myriad small RNPs. *Cell* **89**: 669-672.
132. Lindahl L, Zengel JM (1996) RNase MRP and rRNA processing. *Mol. Biol. Rep.* **22**: 69-73.
133. Frank DN, Pace NR (1998) Ribonuclease P: unity and diversity in a tRNA processing ribozyme. *Annu. Rev. Biochem.* **67**: 153-180.
134. Liu MH, Yuan Y, Reddy R (1994) Human RNaseP RNA and nucleolar 7-2 RNA share conserved 'To' antigen-binding domains. *Mol. Cell Biochem.* **130**: 75-82.
135. Karwan R, Bennett JL, Clayton DA (1991) Nuclear RNase MRP processes RNA at multiple discrete sites: interaction with an upstream G box is required for subsequent downstream cleavages. *Genes Dev.* **5**: 1264-1276.
136. Rossmanith W, Karwan R (1993) Definition of the Th/To ribonucleoprotein by RNase P and RNase MRP. *Mol. Biol. Rep.* **18**: 29-35.
137. Liu ZR, Wilkie AM, Clemens MJ, Smith CW (1996) Detection of double-stranded RNA-protein interactions by methylene blue-mediated photo-crosslinking. *RNA* **2**: 611-621.
138. Ricchiuti V, Pruijn GJ, Thijssen JP, van Venrooij WJ, Muller S (1997) Accessibility of epitopes on the 52-kD Ro/SSA protein (Ro52) and on the RoRNP associated Ro52 protein as determined by anti-peptide antibodies. *J Autoimmun.* **10**: 181-191.
139. Fritzler MJ (1993) Autoantibodies in scleroderma. *J Dermatol.* **20**: 257-268.
140. van Eenennaam H, Lugtenberg D, Vogelzangs JH, van Venrooij WJ, Pruijn GJ (2001) hPop5, a protein subunit of the human RNase MRP and RNase P endoribonucleases. *J Biol. Chem.* **276**: 31635-31641.
141. Klein DJ, Schmeing TM, Moore PB, Steitz TA (2001) The kink-turn: a new RNA secondary structure motif. *EMBO J* **20**: 4214-4221.
142. Watkins NJ, Segault V, Charpentier B, Nottrott S, Fabrizio P, Bachi A, Wilm M, Rosbash M, Branlant C, Luhrmann R (2000) A common core RNP structure shared between the small nucleoar box C/D RNPs and the spliceosomal U4 snRNP. *Cell* **103**: 457-466.
143. Pollard KM, Reimer G, Tan EM (1989) Autoantibodies in scleroderma. *Clin. Exp. Rheumatol.* **7** 3: S57-S62.
144. Fimiani, C (2001) Systemic Sclerosis: a woman disease. *Mod. Asp. Immunobiol.* **1**: 233-237.
145. Arnett FC, Reveille JD, Goldstein R, Pollard KM, Leaird K, Smith EA, Leroy EC, Fritzler MJ (1996) Autoantibodies to fibrillarin in systemic sclerosis (scleroderma). An immunogenetic, serologic, and clinical analysis. *Arthritis Rheum.* **39**: 1151-1160.
146. Humbel, RL (1993) Detection of antinuclear antibodies by immunofluorescence, A2, 1-16. IN: van Venrooij, WJ and Maini, RN. *Manual of biological markers of disease, Dordrecht, Kluwer Academic Publishers.*
147. Kasturi KN, Hatakeyama A, Spiera H, Bona CA (1995) Antifibrillarin autoantibodies present in systemic sclerosis and other connective tissue diseases interact with similar epitopes. *J Exp. Med.* **181**: 1027-1036.
148. Yamane K, Ihn H, Kubo M, Kuwana M, Asano Y, Yazawa N, Tamaki K (2001) Antibodies to Th/To ribonucleoprotein in patients with localized scleroderma. *Rheumatology* **40**: 683-686.
149. Brouwer R, Hengstman GJ, Vree EW, Ehrfeld H, Bozic B, Ghirardello A, Grondal G, Hietarinta M, Isenberg D, Kalden JR, Lundberg I, Moutsopoulos H, Roux-Lombard P, Vencovsky J, Wikman A, Seelig HP, van Engelen BG, van Venrooij WJ (2001) Autoantibody profiles in the sera of European patients with myositis. *Ann. Rheum. Dis.* **60**: 116-123.
150. Lee SJ, Baserga SJ (1999) Imp3p and Imp4p, two specific components of the U3 small nucleolar ribonucleoprotein that are essential for pre-18S rRNA processing. *Mol. Cell Biol.* **19**: 5441-5452.

151. Westendorf JM, Konstantinov KN, Wormsley S, Shu MD, Matsumoto-Taniura N, Pirollet F, Klier FG, Gerace L, Baserga SJ (1998) M phase phosphoprotein 10 is a human U3 small nucleolar ribonucleoprotein component. *Mol. Biol. Cell* **9**: 437-449.
152. Tomasevic N, Peculis B (1999) Identification of a U8 snoRNA-specific binding protein. *J Biol. Chem.* **274**: 35914-35920.
153. Brahms H, Raymackers J, Union A, de Keyser F, Meheus L, Luhrmann R (2000) The C-terminal RG dipeptide repeats of the spliceosomal Sm proteins D1 and D3 contain symmetrical dimethylarginines, which form a major B-cell epitope for anti-Sm autoantibodies. *J Biol. Chem.* **275**: 17122-17129.
154. Schellekens GA, De Jong BA, van den Hoogen FH, van de Putte LB, van Venrooij WJ (1998) Citrulline is an essential constituent of antigenic determinants recognized by rheumatoid arthritis-specific autoantibodies. *J Clin. Invest.* **101**: 273-281.
155. Arnett FC, Edworthy SM, Bloch DA, McShane DJ, Fries JF, Cooper NS, Healey LA, Kaplan SR, Liang MH, Luthra HS (1988) The American Rheumatism Association 1987 revised criteria for the classification of rheumatoid arthritis. *Arthritis Rheum.* **31**: 315-324.
156. Tan EM, Cohen AS, Fries JF, Masi AT, McShane DJ, Rothfield NF, Schaller JG, Talal N, Winchester RJ (1982) The 1982 revised criteria for the classification of systemic lupus erythematosus. *Arthritis Rheum.* **25**: 1271-1277.
157. Masi AT (1980) Preliminary criteria for the classification of systemic sclerosis (scleroderma). Subcommittee for scleroderma criteria of the American Rheumatism Association Diagnostic and Therapeutic Criteria Committee. *Arthritis Rheum.* **23**: 581-590.
158. Vitali C, Bombardieri S, Moutsopoulos HM, Balestrieri G, Bencivelli W, Bernstein RM, Bjerrum KB, Braga S, Coll J, de Vita S (1993) Preliminary criteria for the classification of Sjogren's syndrome. Results of a prospective concerted action supported by the European Community. *Arthritis Rheum* **36**: 340-347.
159. Bohan A, Peter JB (1975) Polymyositis and dermatomyositis (first of two parts). *N. Engl. J Med.* **292**: 344-347.
160. Bohan A, Peter JB (1975) Polymyositis and dermatomyositis (second of two parts). *N. Engl. J Med.* **292**: 403-407.
161. Sambrook J, Fritsch EF, Maniates T (1989) Molecular Cloning: a laboratory manual. *Cold Spring Harbor Laboratory Press, New York*
162. Kiss T (2001) New EMBO member's review: Small nucleolar RNA-guided post-transcriptional modification of cellular RNAs. *EMBO J* **20**: 3617-3622.
163. McKusick, VA, Eldridge, R, Hostetler, JA, Ruangwit, U, Egeland, JA (1965) Dwarfism in the Amish. II. Cartilage-hair hypoplasia. *Bull. Johns Hopkins Hosp.* **116**: 231-272.
164. Mäkitie, O. (1992) Cartilage-Hair Hypoplasia. *Dissertation thesis, University of Helsinki*, 1-65.
165. Makitie O, Kaitila I (1993) Cartilage-hair hypoplasia - clinical manifestations in 108 Finnish patients. *Eur. J Pediatr.* **152**: 211-217.
166. McKusick VA (2000) Ellis-van Creveld syndrome and the Amish. *Nat. Genet.* **24**: 203-204.
167. Sulisalo T, Francomano CA, Sistonen P, Maher JF, McKusick VA, de la Chapelle A, Kaitila I (1994) High-resolution genetic mapping of the cartilage-hair hypoplasia (CHH) gene in Amish and Finnish families. *Genomics* **20**: 347-353.
168. Sulisalo T, Sistonen P, Hastbacka J, Wadelius C, Makitie O, de la Chapelle A, Kaitila I (1993) Cartilage-hair hypoplasia gene assigned to chromosome 9 by linkage analysis. *Nat. Genet.* **3**: 338-341.
169. Sulisalo T, van dB, I, Rimoin DL, Bonaventure J, Sillence D, Campbell JB, Chitayat D, Scott CI, de la Chapelle A, Sistonen P (1995) Genetic homogeneity of cartilage-hair hypoplasia. *Hum. Genet.* **95**: 157-160.
170. Sulisalo T, Klockars J, Makitie O, Francomano CA, de la Chapelle A, Kaitila I, Sistonen P (1994) High-resolution linkage-disequilibrium mapping of the cartilage-hair hypoplasia gene. *Am. J Hum. Genet.* **55**: 937-945.
171. Vakkilainen T, Kivipensas P, Kaitila I, de le Chapelle A, Ridanpää M (1999) Integrated high-resolution BAC, P1, and transcript map of the CHH region in chromosome 9p13. *Genomics* **59**: 319-325.
172. Ben-Yosef T, Francomano CA (1999) Characterization of the human talin (TLN) gene: genomic structure, chromosomal localization, and expression pattern. *Genomics* **62**: 316-319.
173. Hsieh CL, Donlon TA, Darras BT, Chang DD, Topper JN, Clayton DA, Francke U (1990) The gene for the RNA component of the mitochondrial RNA-processing endoribonuclease is located on human chromosome 9p and on mouse chromosome 4. *Genomics* **6**: 540-544.
174. Clayton DA (1994) A nuclear function for RNase MRP. *Proc. Natl. Acad. Sci. USA* **91**: 4615-4617.
175. Hastbacka J, de la Chapelle A, Kaitila I, Sistonen P, Weaver A, Lander E (1992) Linkage disequilibrium mapping in isolated founder populations: diastrophic dysplasia in Finland. *Nat. Genet.* **2**: 204-211.
176. de la Chapelle A, Wright FA (1998) Linkage disequilibrium mapping in isolated populations: the example of Finland revisited. *Proc. Natl. Acad. Sci. USA* **95**: 12416-12423.
177. Lehesjoki AE, Koskiniemi M, Norio R, Tirrito S, Sistonen P, Lander E, de la Chapelle A (1993) Localization of the EPM1 gene for progressive myoclonus epilepsy on chromosome 21: linkage disequilibrium allows high resolution mapping. *Hum. Mol. Genet.* **2**: 1229-1234.
178. Paule MR, White RJ (2000) Survey and summary: transcription by RNA polymerases I and III. *Nucleic Acids Res.* **28**: 1283-1298.
179. Murphy S, Di Liegro C, Melli M (1987) The *in vitro* transcription of the 7SK RNA gene by RNA polymerase III is dependent only on the presence of an upstream promoter. *Cell* **51**: 81-87.
180. Yuan Y, Reddy R (1991) 5′ flanking sequences of human MRP/7-2 RNA gene are required and sufficient for the transcription by RNA polymerase III. *Biochim. Biophys. Acta* **1089**: 33-39.
181. Sbisa E, Pesole G, Tullo A, Saccone C (1996) The evolution of the RNase P- and RNase MRP-associated RNAs: phylogenetic analysis and nucleotide substitution rate. *J Mol. Evol.* **43**: 46-57.
182. Lux SE, Johnston RBJ, August CS, Say B, Penchaszadeh VB, Rosen FS, McKusick VA (1970) Chronic neutropenia and abnormal cellular immunity in cartilage-hair hypoplasia. *N. Engl. J Med.* **282**: 231-236.
183. Virolainen M, Savilahti E, Kaitila I, Perheentupa J (1978) Cellular and humoral immmunity in cartilage-hair hypoplasia. *Pediatr. Res.* **12**: 961-966.
184. Pierce GF, Polmar SH (1982) Lymphocyte dysfunction in cartilage-hair hypoplasia: evidence for an intrinsic defect in cellular proliferation. *J Immunol.* **129**: 570-575.
185. Makitie O, Pukkala E, Teppo L, Kaitila I (1999) Increased incidence of cancer in patients with cartilage-hair hypoplasia. *J Pediatr.* **134**: 315-318.
186. Kurz JC, Fierke CA (2000) Ribonuclease P: a ribonucleoprotein enzyme. *Curr. Opin. Chem. Biol.* **4**: 553-558.
187. Pelin K, Hilpela P, Donner K, Sewry C, Akkari PA, Wilton SD, Wattanasirichaigoon D, Bang ML, Centner T, Hanefeld F, Odent S, Fardeau M, Urtizberea JA, Muntoni F, Dubowitz V, Beggs AH, Laing NG, Labeit S, de la Chapelle A, Wallgren-Pettersson C (1999) Mutations in the nebulin gene associated with autosomal recessive nemaline myopathy. *Proc. Natl. Acad. Sci. USA* **96**: 2305-2310.
188. Chen D, Huang S (2001) Nucleolar components involved in ribosome biogenesis cycle between the nucleolus and nucleoplasm in interphase cells. *J Cell. Biol.* **153**: 169-176.
189. True HL, Celander DW (1998) Protein components contribute to active site architecture for eukaryotic ribonuclease P. *J Biol. Chem.* **273**: 7193-7196.
190. von Muhlen CA, Tan EM (1995) Autoantibodies in the diagnosis of systemic rheumatic diseases. *Semin. Arthritis Rheum.* **24**: 323-358.
191. Reddy R, Li WY, Henning D, Choi YC, Nohga K, Busch H (1981) Characterization and subcellular localization of 7-8 S RNAs of Novikoff hepatoma. *J Biol. Chem.* **256**: 8452-8457.
192. Rodenburg RJ, Raats JM, Pruijn GJ, van Venrooij WJ (2000) Cell death: a trigger of autoimmunity? *Bioessays* **22**: 627-636.
193. Degen WG, Pruijn GJ, Raats JM, van Venrooij WJ (2000) Caspase-dependent cleavage of nucleic acids. *Cell Death Differ.* **7**: 616-627.
194. Vulliamy T, Marrone A, Goldman F, Dearlove A, Bessler M, Mason PJ and Dokal I (2001). The RNA component of telomerase is mutated in autosomal dominant dyskeratosis congenita. *Nature* **413**, 432-435.
195. Clayton DA (2001) A big development for a small RNA. *Nature* **410**: 29-31.

List of publications

Helma Pluk, **Hans van Eenennaam**, Saskia A. Rutjes, Ger J.M. Pruijn and Walther J. van Venrooij (1999). RNA-protein interactions in the human RNase MRP ribonucleoprotein complex. *RNA* **5**: 512-524

Hans van Eenennaam, Ger J.M. Pruijn and Walther J. van Venrooij (1999). hPop4: a new protein subunit of the human RNase MRP and RNase P ribonucleoprotein complexes. *Nucleic Acids Research* **12**: 2465-2472

Hans van Eenennaam, Nayef Jarrous, Walther J. van Venrooij and Ger J.M. Pruijn (2000). Architecture and function of the human endonucleases RNase P and RNase MRP. *IUBMB Life* **49**: 265-272

Maaret Ridanpää, **Hans van Eenennaam**, Katarina Pelin, Robert Chadwick, Cheryl Johnson, Bo Yuan, Walther van Venrooij, Ger Pruijn, Riika Salmela, Susanna Rockas, Outi Mäkitie, Ilkka Kaitila and Albert de la Chapelle (2001). Mutations in the RNA component of RNase MRP cause a pleiotropic human disease, Cartilage-Hair Hypoplasia. *Cell* **104**: 195-203.

Hans van Eenennaam, Dorien Lugtenberg, Judith H.P. Vogelzangs, Walther J. van Venrooij and Ger J.M. Pruijn (2001). hPop5, a protein subunit of the human RNase MRP and RNase P endoribonucleases. *Journal of Biological Chemistry* **276**: 31635-31641.

Hans van Eenennaam, Annemarie van der Heijden, Rolf J.R.J. Janssen, Walther J. van Venrooij and Ger J.M. Pruijn (2001). Basic domains target protein subunits of the RNase MRP complex to the nucleolus independently of complex association. *Molecular Biology of the Cell* **12**:3680-3689.

Hans van Eenennaam, Judith H.P. Vogelzangs, Laurens Bisschops, Liane C.J. te Boome, Hans P. Seelig, Manfred Renz, Dirk-Jan de Rooij, Rick Brouwer, Helma Pluk, Ger J.M. Pruijn, Walther J. van Venrooij and Frank H.J. van den Hoogen (2001). Autoantibodies against small nucleolar ribonucleoprotein complexes and their clinical associations. *Submitted for publication*.

Hans van Eenennaam, Judith H.P. Vogelzangs, Dorien Lugtenberg, Frank H.J. van den Hoogen, Walther J. van Venrooij and Ger J.M. Pruijn (2001). Identification of the RNase MRP and RNase P associated Th/To-autoantigen. *Submitted for publication*.

Dankwoord

Zoals Ronald Plasterk waarschijnlijk terecht opmerkte in zijn column "Gods baan in Leiden", zijn het dankwoord, het curriculum vitae en de stellingen het enige dat de jonge promovendus geheel op eigen kracht heeft geschreven. Het is ook zo. Want vele anderen hebben aan de rest van dit proefschrift een bijdrage gehad, die in dit dankwoord een plaats verdienen.

Als eerste wil ik Petra Bindels en Helma Pluk bedanken. Jullie enthousiasme voor de wetenschap, wat jullie op mij hebben overgedragen, heeft mij uiteindelijk overgehaald om na mijn studie verder te gaan in de wetenschap.

Mijn promotor, Walther van Venrooij, u wil ik bedanken voor het creëren van een mooie leerschool. Wie weet dat ik u later nog eens bijval dat "mijn promotietijd de mooiste tijd van mijn carrière" is geweest, ik sta nu nog aan het begin. U heeft me bijgebracht om te denken in artikelen en doelgericht te werken. Verder heeft u mij vertrouwen geschonken bij het opzetten van de verschillende samenwerkingen en bij het regelen van mijn verblijf bij Sidney Altman. Tenslotte dank voor de enorme kluif aan corrigeerwerk welke u heeft doorgewerkt voor mij, want het moest natuurlijk altijd snel…..

Mijn co-promotor, Ger Pruijn. Ik heb je al in één van mijn eerste weken bij mijn onderzoek betrokken. In het begin nog betrokken bij het bediscussiëren of alle geopperde ideeën van mijn promotor wel praktisch uitvoerbaar waren, later ben je uitgegroeid tot een grote steun binnen mijn project. Vele uren heb ik bij je op je kamer gezeten, over proefjes en over hoe het op het lab eraan toeging…. Een enorme waardering heb ik voor al het werk dat je voor me hebt gedaan, ook al heb ik misschien iets te vaak gezegd dat je liep te neuzelen. Wat betreft het hPop5 verhaal en mijn vakantie naar Banff, je hebt helemaal gelijk.

Zonder de hulp van 3 studenten en 2 analisten zou mijn proefschrift er een stuk dunner uit hebben gezien. Rolf, jij was mijn eerste student en jij kreeg een op het eerste gezicht makkelijk project. Niets bleek minder waar, moeder natuur had de dingen anders bedacht dan door mij verwacht. Jij hebt veel werk verzet, waarvan een deel de basis is geworden van hoofdstuk 4.

Judith, het toppertje van de klas. Dat heb je waar gemaakt! Je was een harde werker en je zei waar het op stond. Kortom dat klikte! Mijn lange afwezigheid heeft geen invloed op je afstuderen gehad en ik was dan ook blij te horen dat je na je afstuderen als collega terug zou komen. Misschien waren 172 immuunprecipitaties voor de eerste week in je nieuwe baan iets teveel van het goede, maar ze zagen er in ieder geval alle 172 prachtig uit! Bedankt voor al je steun bij de totstandkoming van hoofdstuk 3, 6 en 7. Ik ben blij dat je mij van-

daag als paranimf bij wilt staan, ook al vind je het maar een stom toneelstukje.

Dorien, jou heb ik in de Xenos gestrikt om bij mij je afstudeerproject te doen. Jij zou het two-hybrid werk van Rolf en het hPop5 werk van Judith afmaken. Met als gevolg dat je de eerste vrijdag direct tot 20:00 uur op het Trigon zat. Je hebt goed werk verricht en dat terwijl je liever thuis tussen de koeien zat. Twee co-auteurschappen (hoofdstuk 3 en 6) heeft jouw hoofdvak opgeleverd, niet slecht!

Annemarie, jij zou mijn proefjes, beschreven in hoofdstuk 4, even herhalen, terwijl ik in Amerika zat. Dat even, was wat te optimistisch, want het zat op alle fronten tegen. Uiteindelijk was toch alles af voor de grote verhuizing en hebben we beiden van elkaar geleerd.

Ben, jij hebt niet alleen proefjes voor mij gedaan, maar met jou heb ik ook 4 jaar lang op 1.87 gezeten, het lab, voorheen bekend als het vrijgezellen-lab, nou dat hebben we mooi eens even rechtgezet. Ups en downs hebben we daar meegemaakt, wel jammer dat jouw ups vaak kwamen als ik op vakantie ging. 149 ELISA platen heb jij voor mij er doorheen gejaagd, dus 7450 patiënten sera getest, helaas is dit nooit in een paper terechtgekomen.

Ook wil ik Frank van den Hoogen bedanken. Als reumatoloog begeleidde je mijn onderzoek naar de klinische relevantie van het bepalen van het anti-Th/To reactiviteit. Jij was meteen enthousiast voor dit onderzoek en wist dat enthousiasme ook telkens weer op mij over te dragen. Bovendien wist jij Laurens en Liane te motiveren meer dan 100 patiënten statussen door te werken. Frank, Laurens en Liane, Bedankt!

Onderzoekers buiten Nederland hebben ook aan dit onderzoek bijgedragen: Dr. S. Altman, Dr. C. Guerrier-Takada, Dr. N. Jarrous, Dr. A. de la Chapelle, Dr. M. Ridanpää en Dr. I. Kaitila, bedankt voor deze samenwerkingen.

En dan de mensen die niet hebben meeonderzocht, maar op een andere wijze bij hebben gedragen aan dit onderzoek.

Erik en Michael, wij vormden samen de drie musketiers van het Trigon. Na onze studie zijn we alle drie bij de VRT als aio begonnen, samen niet lunchen in het Trigon. Heerlijk afblazen, zeiken over dingen en 'dat het niet leuk is als experimenten in één keer lukken'. Maar vooral ook veel lachen, 'errrruuug bedankt' voor een geweldige vriendschap en grote collegialiteit.

Erik, jou wil ik nog in het bijzonder noemen. Jij bent hartstikke gek! Eerst heb je me overgehaald mijn proefschrift toch te gaan lay-outen. Vervolgens ben jij helemaal uit je dak gegaan en heb je alle figuren die niet aan jouw lay-out eisen voldeden (lees ALLE figuren) aangepast. Ook heb je me gekker gemaakt dan dat ik al was, wat uitvoering van dit proefschrift betreft, maar goed het ziet er dan nu ook echt prachtig uit! Bedankt, bedankt, bedankt!

Alle andere collega's en ex-collega's wil ik verder bedanken voor de hand-en-span diensten, maar vooral eigenlijk de gezelligheid en discussies. In het bijzonder wil ik de volgende mensen noemen: Rick, ex- en huidige collega, bedankt voor de steun als 'oudere aio', maar vooral voor de leuke tijd op het Trigon en in Schotland. Reinout, jij was de 'jongere aio', bedankt voor de gezelligheid op onze Banff trip. De oudere ex-collega's: Frank, Saskia, Helma, Jacqueline, Christel, Yvonne, jullie bedankt voor de mooie verhalen (over het blauwe zeiltje etc.) en jullie vermogen mijn gevoelens een beetje te relativeren.

De secretaresse-met-pit, Els, jij verdient hier ook een plaats! Jij vond dat het af en toe meer op een gesticht leek dan op een universitaire instelling en voor mij was het in ieder geval duidelijk dat jij fungeerde als de Biochemie-psychotherapeut. We hebben dus ook heel wat afgekletst, over de organisatie, werktijden, attitude, Marktzicht en andere dingen daaromheen. Maar je was er ook om me te vertellen dat ik "liep te fluimen", dat ik te snel met mijn mening klaarstond of om me mijn schoenen na te brengen als ik daar naast dreigde te gaan lopen. En wat dit proefschrift betreft, je hebt helemaal gelijk, uiteindelijk is dat van mij ook gelayout!

Arjan, Ernest, Max en Sander voor jullie ligt het resultaat van 4 jaar met blauwe vloeistof schudden, wat je daar allemaal niet over kunt schrijven! Jullie hebben ook heel wat te horen gekregen over mijn promotie. Jullie steun en jullie "poep, lekker belangrijk" had ik zo af en toe nodig en jullie zorgden er ook voor dat ik me ondanks mijn werkend bestaan nog student voelde. Ernest, jij staat vandaag symbool voor mijn vriendschap met de Bundi's. Ik ben blij dat je mijn paranimf wilt zijn, vooral omdat onze vriendschap teruggaat naar 1976 in Nieuw- en Sint Joosland en is blijven bestaan op de C.S.W. te Middelburg en tijdens onze studie aan de K.U.N.. Voor jou is een promotie not-done, toch wil ik op deze manier samen met jou mijn opleiding afsluiten.

Ton en Ria, jullie wil ik bedanken voor alle steun die ik vooral in het vervolg van mijn promotie heb gekregen. De gesprekken over welke kant ik op wilde, het commentaar op mijn sollicitatiebrieven en natuurlijk de correcties van een aantal nederlandse stukken van dit proefschrift.

Marieke, jij hebt bijna mijn gehele aio-tijd meegemaakt en je hebt van dichtbij gezien dat het niet altijd even makkelijk was. "Want jij gelooft in mij, jij ziet toekomst in ons allebei". Onder dat motto accepteerde je dat mijn werk na 18:00 uur of op vrijdag niet ophield. En: "Zou je me laten gaan, als het nodig was," ik weet dat dat zo is. Jij hebt mijn trip naar Amerika alleen maar aangemoedigd en dat heeft bij ons alleen maar bevestigd wat we eigenlijk al wisten.

En nu mijn ouders, Leo en Jannie, aan jullie heb ik dit proefschrift opgedragen. Voor jullie is gaan studeren en promoveren altijd een beetje een zwarte doos geweest. Dankzij de waarden en normen, die jullie aan mij hebben overgedragen en de familietrekjes die kennelijk in mijn genen gecodeerd liggen heb ik mijn studie en deze promotie succesvol kunnen afronden. Mijn opleiding zit erop, bedankt voor hoe ik nu de wereld in kan. Voor jullie dit proefschrift!

Tenslotte dank aan alle belastingbetalers. Bedankt voor 4 jaar salaris, voor het uitbetalen van mijn resterende vakantiedagen en voor *fl*. 21703,- aan genoten subsidies, waardoor ik een bezoek heb kunnen brengen aan Wye (UK), Edinburgh (UK), New Haven (USA) en Banff (Canada).

Acknowledgements

Dear Nayef, with you I started my collaboration with the Altman group. Although in the beginning our collaboration was difficult, as we were working on highly related subjects, trust grew in time. Thanks for the trust you put in me, for all the materials you sent us and all the information you shared with us. I will never forget meeting you in person and still hold good memories to the talks we had over a glass of beer. I wish you all the best with your own group in Jerusalem. Finally, I would like to thank you for introducing to Sid my idea to work for some time in New Haven. Which brings me to you, Sid. I would like to thank you for the opportunity you have created for me to come and work in your lab for 4 months. You and your group gave me a warm welcome in a snow-covered New Haven. You taught me biochemical purifications, to be an enzymologist and to think in terms of functionality. More importantly, you have learned me to keep an open mind and not to think in dogmas, but to look at the experimental data every time. To my surprise, you also told me that life is more than working in the lab and that gave me the opportunity to visit much of New York's beauty. Cecilia and Donna, you two were my lab-mothers. You both took care of me and taught me everything about biochemical purifications. Cecilia, special thanks to you, you supervised my work and encouraged me daily. You and Sid made me a better scientist!!

Finally, I would like to thank Albert, Ilkka and Maaret. You contacted us and explained you had found a genetic defect, but needed biochemical help to understand your findings. I would like to thank you for all the trust you put in me and for the things you learned me about genetics. I enjoyed our collaboration very much.

Curriculum vitae

Hans van Eenennaam is geboren op 3 november 1973 te Nieuw- en Sint Joosland, gemeente Middelburg, als zoon van Jannetje Johanna Baas en Leendert van Eenennaam. In 1992 behaalde hij zijn V.W.O. diploma aan de Christelijke Scholengemeenschap Walcheren te Middelburg en begon hij aan zijn studie scheikunde aan de Katholieke Universiteit Nijmegen (KUN). Tijdens deze studie heeft hij een bijvakstage doorlopen op de afdeling Moleculaire- en Ontwikkelingsgenetica (Drs. P. Bindels en Prof. Dr. W.H.G. Hennig) van de KUN. Zijn hoofdvak-stage heeft hij doorlopen op de afdeling Biochemie van de KUN onder begeleiding van Dr. H. Pluk en Prof. Dr. W.J. van Venrooij. Het doctoraal examen Scheikunde is cum laude behaald in augustus 1997. Hij ontving voor zijn afstudeeronderzoek bij de afdeling Biochemie in 1998 de Universitaire scriptieprijs op het gebied van de Natuurwetenschappen.

Tijdens zijn studie is hij lid geweest van de Nijmeegse Studenten Roei Vereniging Phocas en is hij politiek commissaris geweest in het Bestuurlijk Overleg Studentenverenigingen. Verder is hij van 1996 tot 2001 lid van de Raad van Toezicht van de Stichting Studenten Huisvesting Nijmegen geweest.

Vanaf oktober 1997 tot oktober 2001 was hij werkzaam als Onderzoeker in Opleiding op de afdeling Biochemie van de KUN onder begeleiding van Dr. G.J.M. Pruijn en Prof. Dr. W.J. van Venrooij. Tijdens deze periode werd het onderzoek verricht dat is beschreven in dit proefschrift. Hij heeft gedurende deze periode drie studenten begeleid en een bijdrage geleverd aan het praktisch biochemie-onderwijs voor tweedejaars scheikunde studenten. Voor zijn onderzoek heeft hij een 4 maanden durend werkbezoek gebracht aan de groep van Prof. Dr. S. Altman (Yale University, New Haven, USA).

Hij heeft zijn onderzoeksresultaten gepresenteerd tijdens 'the fourth annual meeting of the RNA Society' in Edinburgh (1999) en 'the sixth annual meeting of the RNA society' in Banff (2001).

Sinds 1 januari 2002 is hij werkzaam bij de sectie Fertility van de Target Discovery Unit, Organon N.V. te Oss.

ontwerp & opmaak... Erik Vossenaar